Investigation into Phase Transformation of Yttria Stabilized Zirconia Femoral Heads

By:

Adrian Hohls

Under the guidance of:

Professor NDL Burger

Submitted in fulfilment of part of the requirements for the degree of Master's in engineering (Mechanical Engineering) in the faculty of Engineering, Building Environment and Information Technology,

University of Pretoria,

Pretoria

17 August 2010

Executive summary

27 Retrieved Yttria Stabilised Tetragonal Zirconia (Y-TZP) femoral heads were studied for the occurrence of tetragonal to monoclinic phase transformation and the effects that such transformation has on the bearing surface. The mean monoclinic percentage found is 53.6% with 25 of the samples having transformed more than 20%. This finding nullifies earlier predictions that it would take 25 to 30 years to transform to a monoclinic content of 30 to 40% inside the human body (Chevalier, Drouin & Calés 1997). It was however shown that Hot Isostatic Pressed (HIP'ed) Y-TZP femoral heads have a better, though still not adequate, resistance to phase transformation in the human body than non-HIP'ed femoral heads.

Results of various investigations show that this transformation degrades the surface condition of the femoral heads, which in turn increases wear and subsequently decreases the survival rate of the prosthesis due to a greater risk of aseptic loosening.

It is postulated that a great contributing factor to the phase transformation is increased temperatures inside the bearing couple, due to inadequate lubrication between the two bearing surfaces.

Tetragonal to monoclinic phase transformation and its associated effects renders Y-TZP femoral heads less attractive for hip replacements.

Table of contents

List of figures

List of tables

Glossary

Acetabular cup	Part of a hip prosthesis that is implanted in the acetabulum.
Arthritis	Inflammation of a joint, causing pain in and limiting movement of the joint. Usually associated with old age.
Articulate	The movement between the femoral head and the acetabulum.
Alumina	Ceramic material, Aluminium oxide – Al_2O_3.
Arthroplasty	Comes from the Greek words, *arthros* (joint) and *plassein* (to form or shape). It is a medical term used for surgery that is performed to reconstruct or replace a joint.
Aseptic loosening	Loosening of any part of the prosthesis due to osteolysis.
Avascular necrosis	Temporary or permanent loss of blood flow to the bones, causing the bone tissue to die and resulting in fracture or collapse of the bone, or parts thereof.
Calcar lysis	Destruction of the bone tissue at the spur shaped protrusion at the top of the femur, under the influence of a foreign agent. As shown in Figure 26.
Crosslink	A process that normally employs radiation to link long carbon string molecules to produce a stronger polymer (In this study UHMWPE).
DDH	Developmental displacement of the hip. A syndrome where the development of the hip was disrupted by displacement of the femoral head from the acetabulum.
Dysplasia	An abnormality of development.

FEEM	Field emission electron microscope, as shown in Figure 19.
Femur	Thigh bone. It is the bone that connects the knee to the hip.
Femoral stem	Part of the hip prosthesis that is implanted in the femur of the patient.
Femoral head	Part of the hip prosthesis; it is a spherical ball which fits on the femoral stem and forms a bearing with the acetabular cup.
FII	Fabrique D\'Implants et D\'Instruments Chirurg. A French manufacturer of Zirconia femoral heads.
HDPE	High density polyethylene.
HIP	Hot isostatic pressing. A process where a Zirconia femoral head is subjected to increased pressure and elevated temperature in an inert gas to increase the density of the Zirconia.
Impingement	A case where the femoral stem impacts with the rim of the acetabular cup.
In vivo	In the human body.
LTD	Low temperature degrading. In this study it refers to the degradation of tetragonal phase Zirconia to the monoclinic phase.
MAJ	Mehl-Avrami-Johnson law. It governs the shape of s-curves.
NMISA	National Metrology Institute of South Africa.
Osteoarthritis	Degenerative joint disease. A progressive joint disorder, caused by the gradual loss of cartilage, which causes the growth of bony spurs and cysts at the joint interface.

Osteolysis	A foreign body reaction caused by wear debris in the tissues surrounding a replacement.
PMMA	Poly(methyl methacrylate). Also known as 'bone cement'. Used as a grouting agent in orthopaedics.
Polycrystal	A material that is made of many smaller crystallites with varying orientation, similar to grains of metals.
Ra	Arithmetic surface mean. Used to quantify the roughness of a surface.
Rheumatoid arthritis	A chronic, systematic disease of the joints. Usually accompanied by general ill health, and not associated with age.
SEM	Scanning electron microscope.
UHMWPE	Ultra high molecular weight polyethylene
Yttria	Yttrium oxide, used as crystal stabiliser in ceramic materials – Y_2O_3
Y-TZP	Yttria stabilised tetragonal Zirconia polycrystal.
Zirconia	Ceramic material, Zirconium dioxide – ZrO_2.

1 Introduction

1.1 Background

Hip replacement surgery has grown to be a world-wide, multi-billion dollar industry, with great amounts of money and time being spent in search of better materials, designs and surgical techniques. The topic of hip replacement surgery has inspired countless PhD's and even more research articles from every corner of the world. What is the driving force behind all of this?

The answer in its simplest form could be: pain and self-worth.

The hip joint is only one of the miracles that make up the human body and in its healthy state it can be illustrated as in Figure 1. The three main components of interest in this study are; the femoral head, the acetabulum and the articular cartilage.

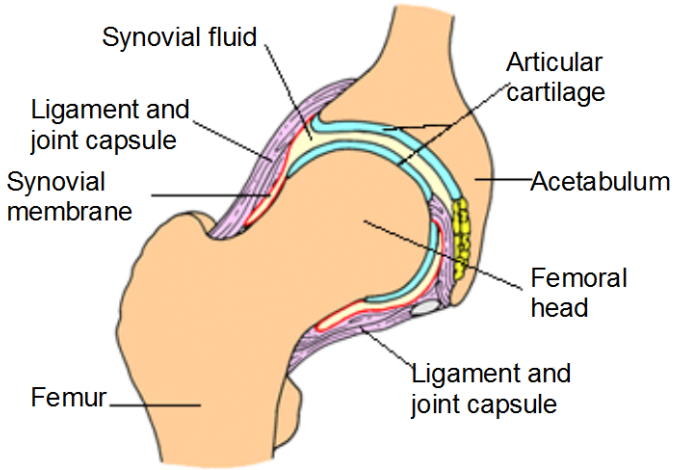

Figure 1: Hip joint

(Adapted from: http://www.childrenshospital.org)

When a person is walking, the femoral head rotates relative to the acetabulum (articulates). The acetabulum can therefore be regarded as the stationary part of the bearing (socket) and the femoral head the moving part of the bearing (ball). The articular cartilage forms the bearing surfaces of the two bearing parts and the synovial fluid provides the lubrication between the two articular cartilages.

The main cause of failure of the bearing formed by the natural hip is osteoarthritis. According to the Australian hip register, 88% of first time hip replacements are a result of osteoarthritis. Other countries, which also keep such registers, are Norway, who attributes 70% and Sweden who attributes 75% of first time hip replacements to osteoarthritis (Burger 2005:6). Other contributors to failure of the bearing are: Avascular necrosis, fractured neck of the femur, rheumatoid arthritis and developmental dysplasia (Burger 2005:6).

Osteoarthritis, also known more descriptively as degenerative joint disease, affects the synovium, articular cartilage and the bony plates that support the articular cartilage of either or both the femoral head and the acetabulum. As the descriptive name indicates, ostearthritis is a slow and progressive disease that affects the articular cartilage's ability to withstand the forces inside the hip joint, as well as the cartilage's ability to heal. The end result of osteoarthritis is that the articular cartilage is worn away, exposing the bone underneath, as is illustrated in Figure 2. Just outside the normal wear area, the joint still tries to heal and forms bony protrusions, which alters the shape of the joint. Symptoms of osteoarthritis are severe joint pain and difficulty in moving the joint (Smeltzer and Bare 2000:1428-1429).

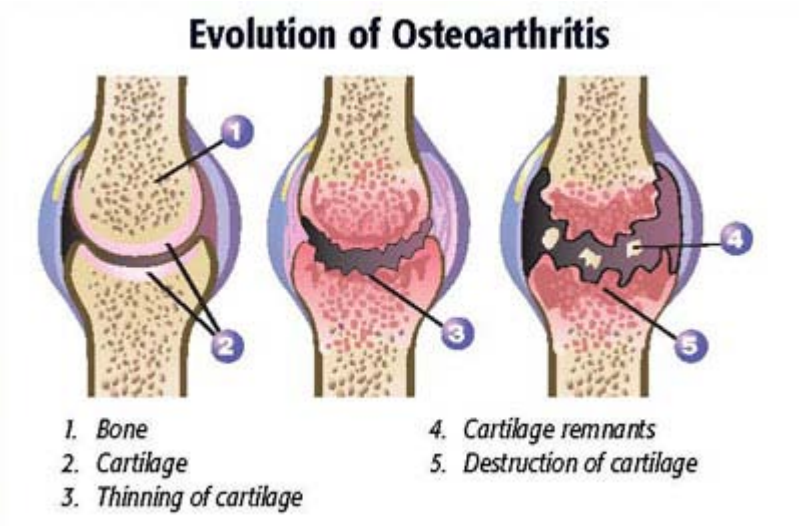

Figure 2: Osteoarthritis

(http://www.cvtechnologies.com)

There is no definite cause of osteoarthritis, but there are a number of factors that increase a person's risk of this disease, which include: increased age, genetic disposition, gender and hormonal factors, obesity, mechanical factors and prior inflammatory diseases. The factor which contributes the most is increased age. Osteoarthritis often starts at the age of 30 and peaks between the ages of 50 and 60 years. It is also postulated that by the age of 75, 85% of the population has evidence of osteoarthritis, but only 15% to 25% of these people experience significant symptoms of osteoarthritis. (Smeltzer and Bare 2000:1428-1429; Nettina 1996:879).

The modern day solution to the crippling and painful effects of, amongst others, osteoarthritis is hip replacement. During total hip replacement surgery, the femoral head is removed, the inside of the femur is broached to the form of the femoral stem and the acetabulum is reamed to receive the acetabular cup (see Figure 3). The femoral stem and acetabular cup are then inserted into the prepared cavities and the femoral stem receives a femoral head. There are numerous types of implants and techniques, which will be discussed at a later stage.

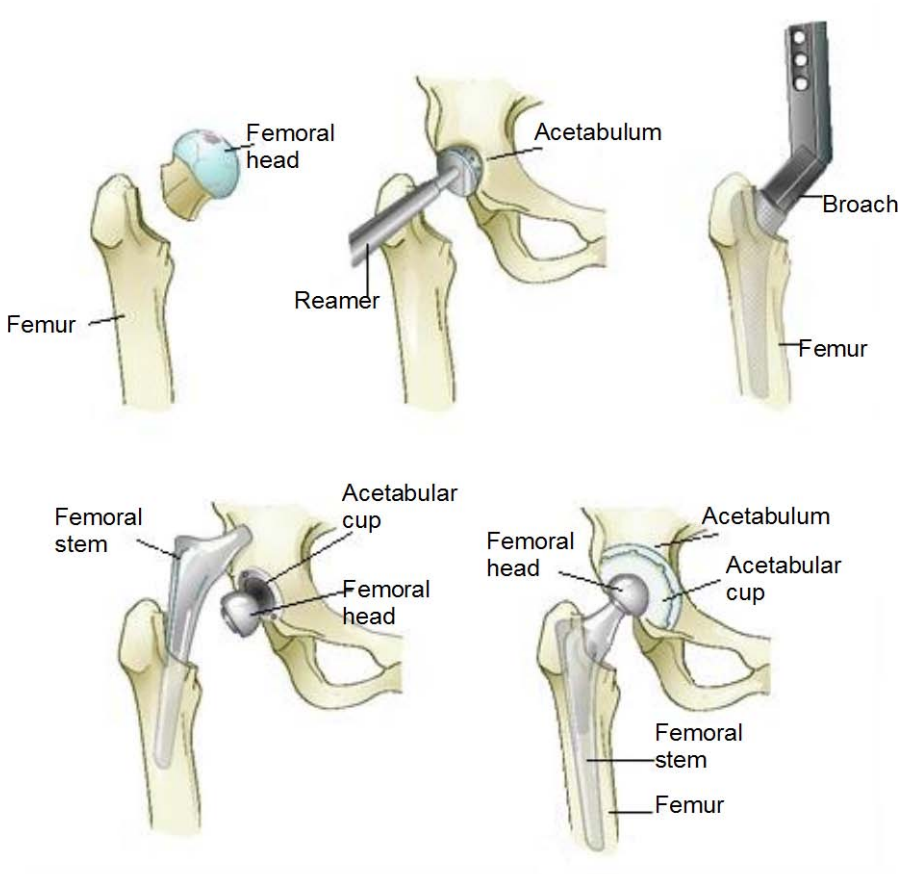

Figure 3: Hip replacement procedure

(Adapted from: http://www.answers.com)

1.2 History

Osteoarthritis and its likes are by no means a modern day phenomenon, as signs of joint disease have been found in Saxon, Medieval and Roman excavations (University of Leicester Archaeological Services 2007; Gomez and Morcuende, 2005:25). Advances in the field of surgery in the late 1700s made surgery a viable treatment for joint disorders. These first surgeries consisted of removing parts of, or whole joints, smoothing of the joint surfaces and even fixation of the joint, which all provided partial relief from

pain and short term increased patient mobility (Gomez and Morcuende 2005:25).

The first total hip replacement is attributed to Professor Themistocles Glück who implanted an ivory ball and socket in 1891. For his first attempt he used nickel plated screws to fix the joint to the bone, but he later experimented with a mixture of plaster of Paris and powdered pumice with resin for better fixation (Gomez and Morcuende 2005:26).

The ivory implants used by Glück did not have great results and apparently the medical profession at that time did not think that it was a promising option. The focus of research in the next 30 odd years focussed on putting a layer of material between the two articulating surfaces of the hip joint. Various materials were used, like: muscle, pig bladder, gold, celluloid, glass, bakelite, Pyrex, magnesium and zinc, none of which showed good consistent results (Gomez and Morcuende 2005:26; Burger 2005:1). The first good, consistent results with the technique of putting material between the two articulating surfaces of a hip joint was achieved in 1937 by Dr. Marius Smith-Petersen with a material called Vitallium®, which he moulded around the femoral head. Vitallium® is a cobalt chromium alloy, originally intended for dentistry and was recommended to Smith-Petersen by his dentist. Smith-Petersen implanted about 500 Vitallium® moulds over the next ten years with what was considered at that time as good results (Gomez and Morcuende 2005:28).

From the early 1920s several attempts were made to replace the whole hip joint, or parts thereof, employing various materials such as: rubber, acrylic, ivory and even stainless steel, but none proved to be successful (Gomez and Morcuende 2005:28). These previous attempts were perfected in part by Thomson and Moore in the 1950s, who, independent of each other,

developed a replacement for the femoral head of a hip joint. These designs consisted of a ball attached to a shank that is inserted into the top of the femur. Combined with modern cementing techniques this type of replacement is still used today to treat fractured femoral heads and is known as the Austin-Moore prosthesis, a picture of which is shown in Figure 4 (Burger 2005:2).

Figure 4: Austin-Moore prosthesis

(http://wavessurgicals.tradeindia.com)

The Austin-Moore prosthesis only solves problems pertaining to the femoral head of the hip joint and not the acetabulum. In the early 1950s Kenneth McKee used the femoral implant of Thompson with a metal three-claw type cup that was screwed into the acetabulum of the hip, but loosening of the prosthesis damped his success. It was Peter Ring who got the first successful results (97% of implants surviving at 17 years) using cementless metal femoral heads and acetabular cup implants, which he started to test clinically in 1964 (Gomez and Morcuende, 2005, p28).

The limelight was however stolen by Dr. John Charnley who revolutionised the orthopaedic world in November 1962 with the first truly successful hip replacement, which, incidentally, is still one of the most successful hip replacements up to date (Wroblewski 2002:825). Figure 5 shows the system, including the installation equipment needed, developed by Charnley. Charnley's hip replacement consisted of a (monoblock) stainless steel femoral implant, with a Ø 22 mm head and a first of its kind, High Density Polyethylene (HDPE) acetubular cup. His success was not purely because of the prostheses he developed, but because he used bone cement (PMMA) to fix the prostheses to the bone. Charnley's prostheses exhibited much lower friction and a higher success rate - in other words his patients experienced much better mobility and longer prosthesis lifetime (Burger 2005:3).

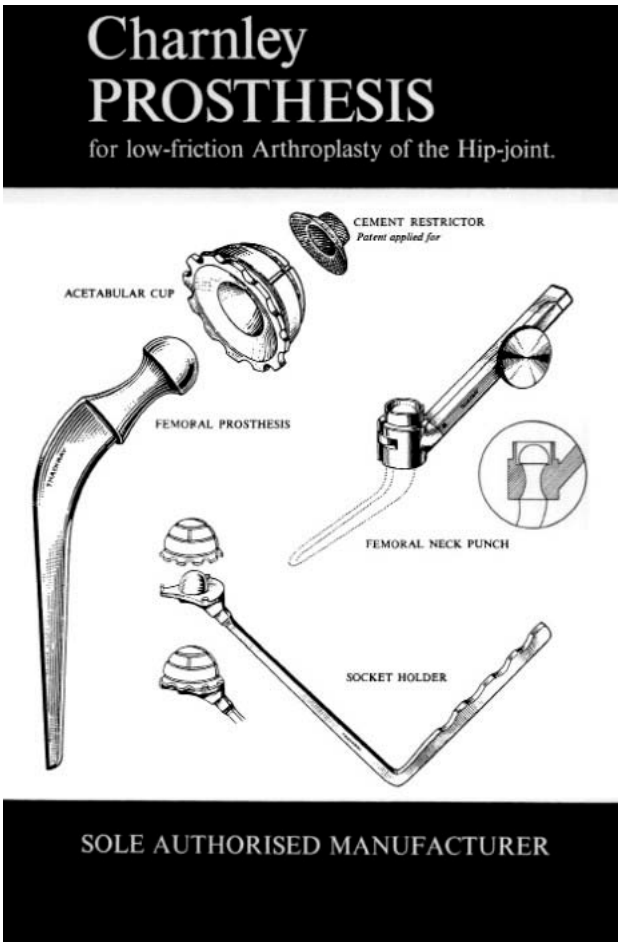

Figure 5: Charnley Hip System

(http://www.aaos75th.org)

1.3 Problem statement

The introduction of UHMWPE as acetabular cup material improved the quality of hip prostheses dramatically, but UHMWPE still has a finite lifetime and the only option when a prosthesis has reached the end of its life is to replace it – a procedure called revision surgery. There are many reasons for revision surgery, but by far the greatest reason is aseptic loosening, which according to the Australian hip register, is the cause of 63% of revision surgeries. The Norwegian register attributes 68% and the Swedish register 75% of revision surgeries to aseptic loosening (Burger 2005:8).

Even though UHMWPE in bulk form exhibits very good biocompatibility, it is the source of aseptic loosening: small wear particles of UHMWPE are produced when the joint articulates. Some of these wear particles find their way to the bone in which the prosthesis is implanted and at these locations the body's immune system attacks the bone tissue surrounding the wear particles and the bone degenerates (see Figure 6). As more wear particles are generated over time, the process accelerates until the bone that is left cannot support the prosthesis anymore, which then starts to loosen under the prevailing load.

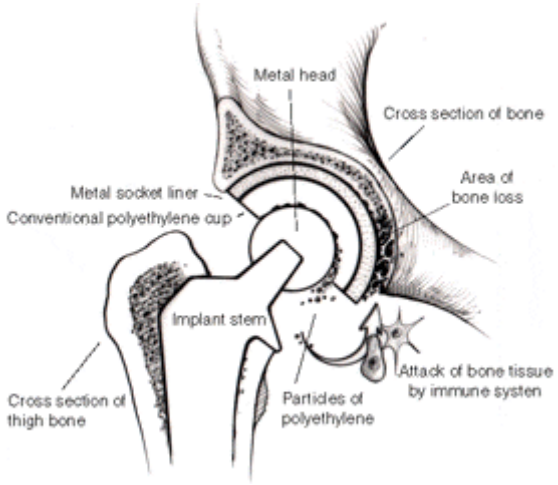

Figure 6: Mechanism of osteolysis

(http://www.zimmerindia.com)

In cases where the patient is not suffering from aseptic loosening the acetabular cup wears away, which can cause impingement, and subsequent prosthesis dislocation. In the most fortunate cases the acetabular cup can wear through completely, causing the femoral head to protrude into the PMMA or metal backing of the cup, depending on the type used.

The benefits of decreasing the amount of wear of UHMWPE acetabular cups are obvious and it was the drive for lower wear rates that led to the implementation of ceramic materials into orthopaedics in the early 1970's (Allain et al. 1999:835). Ceramic materials can be very hard, (about 9 on the Mohs scale, with diamond being 10) can be polished to a much finer surface finish than metal and are normally chemically inert. Due to its hardness, ceramics exhibit a good resistance to wear and because of the very fine surface finish, ceramics exhibit a very low friction coefficient against UHMWPE, all of which makes it a very promising material for femoral head implants. The only drawback of ceramic materials, combined with plastics in bearing applications, is the inability of both materials to dissipate the heat that is generated in the bearing during activity.

The first ceramic to be successfully used as femoral head was Alumina (Al_2O_3). Alumina however exhibits a low resistance to brittle fracture, which limits its design possibilities, for instance, to prevent failures the diameter of earlier alumina femoral heads were limited to 32 mm (Allain et al. 1999:835).

Zirconia offers an attractive solution to the problem of brittle fracture by possessing the same excellent bearing properties as well as a fracture toughness of roughly twice that of Alumina. With these properties in mind Zirconia was introduced into orthopaedics in 1985 (Skyrme et al. 2005:63).

Femoral heads as small as 22 mm are manufactured from Zirconia, which allows surgeons to implant a ceramic material for developmental displacement of the hip (DDH) patients. The fracture toughness is achieved by a mechanism called stress induced phase transformation, which is illustrated in Figure 7 and can be described as follows: at the root of a crack the material is in tension stress, this stress causes the tetragonal phase Zirconia at the root to change into monoclinic phase Zirconia. When transforming from the tetragonal to monoclinic phase, Zirconia undergoes an increase in volume. This increase in volume decreases the tension stress at the root of the crack, which slows down the crack growth, resulting in the improved fracture strength (French et al. 1994:5133; Piconi and Maccauro, 1997).

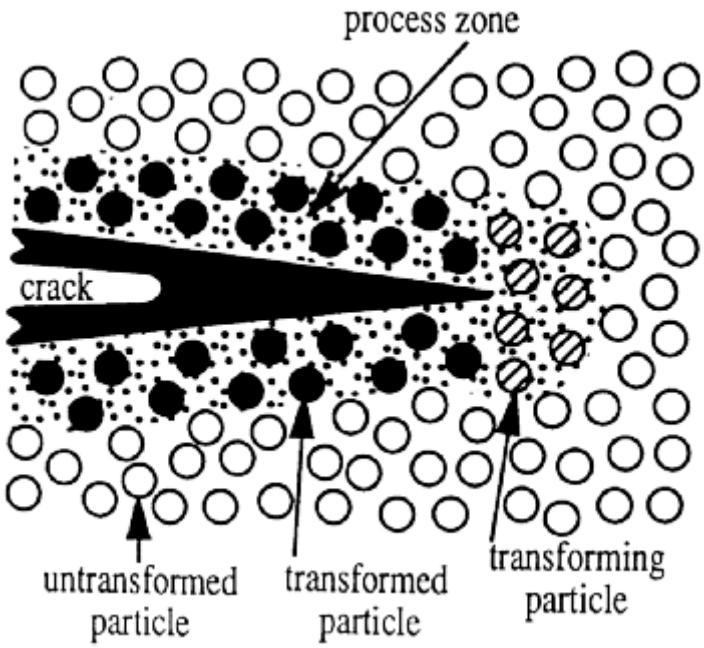

Figure 7: Mechanism of transformation toughening

(Piconi and Maccauro, 1997)

Ironically it is this slow phase transformation inside the human body that could lead to the downfall of Zirconia femoral heads.

The purpose of this study is to investigate the occurrence of tetragonal to monoclinic phase transformation in Zirconia femoral heads, together with the associated deterioration of the surface of the femoral head, which can result in degraded surface finish, decreased hardness, micro cracks and shape change.

2 Literature survey

2.1 Current concepts

With the vast amounts of research being done all over the world it is not surprising that there are currently numerous different designs, with many different permutations, employing many different materials. The aim of this part of the study is to summarise the main characteristics of the modern day hip replacement, as perceived by the author.

A typical modern day modular hip implant, as it has evolved from the groundbreaking prosthesis developed by Dr. Charnley, is shown in Figure 8 and consists of a femoral stem, a femoral head, acetabular cup and, with or without a metal backing. The femoral stem shown in Figure 8 is a revision stem and is therefore about twice as long as a normal stem.

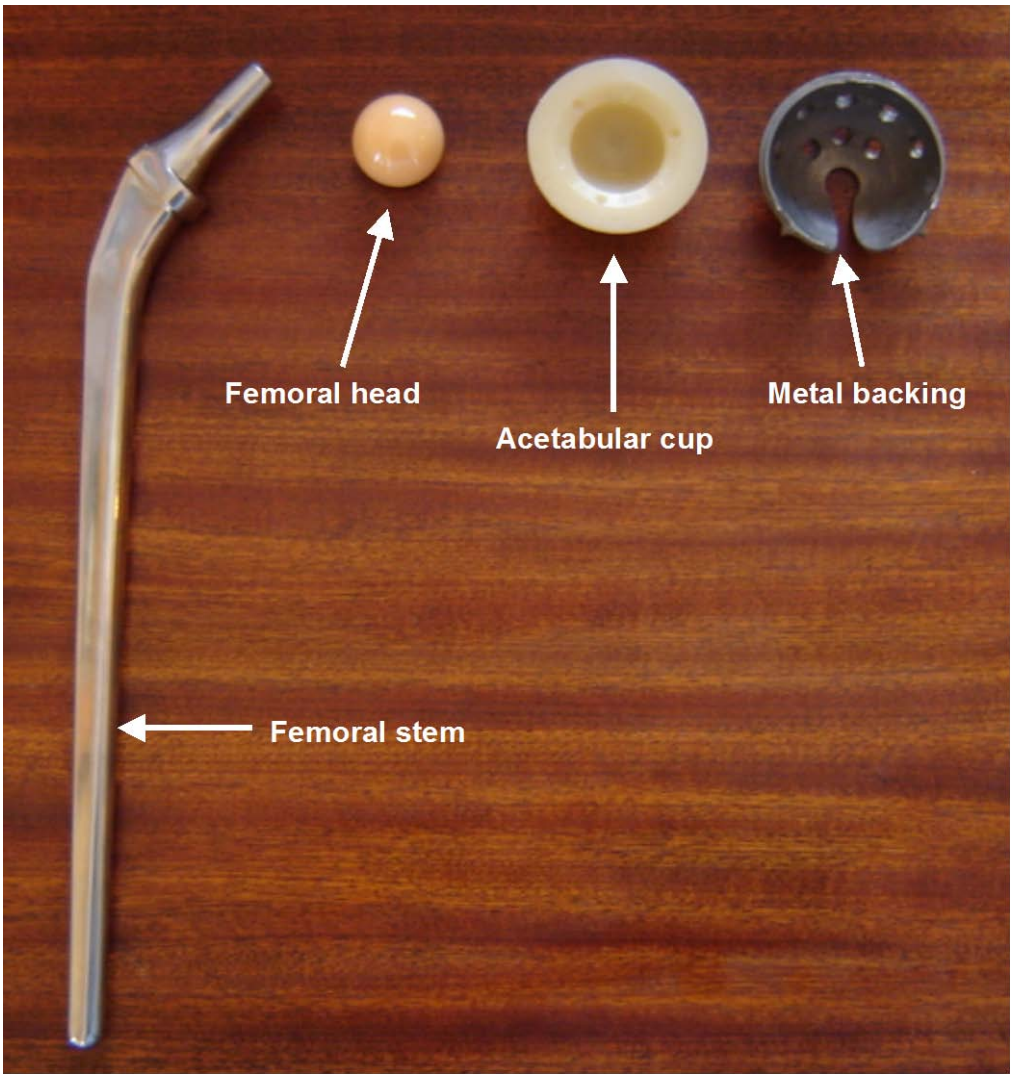

Figure 8: Typical modern day modular hip replacement

The separate femoral stem and femoral head, shown in Figure 8, have a couple of major advantages over the monoblock type used by Dr. Charnley, shown in Figure 5: it allows the surgeon to fine tune the distance between the femur and the hip, because the femoral heads are manufactured with different depth of tapers. By fine-tuning the distance between the femur and the hip joint, the surgeon increases the patient's likelihood of walking normally and decreases the chance of dislocation. Another advantage is that different material femoral heads can be fitted to femoral stems – the correct material can be used for the structural strength needed for the femoral stem and the correct material with the bearing properties needed for the femoral head. Another main advantage of the separate femoral stem and head is the

option of only replacing the femoral head upon revision surgery. This prevents unnecessary disturbance to a well-fixed, healthy femoral stem. Monoblocks are still being used, although to a lesser extent and mostly in partial hip replacement, an example of which is the Austin-Moore prosthesis shown in Figure 4.

Femoral stems are mostly manufactured from cobalt chrome, 316L stainless steel, Titanium (90-6Al-4Va) and Vitallium®, of which the last is the least common. The shape of the femoral stem depends greatly on the technique used to fix it to the femur, the size and strength of the femur and the weight and activity of the patient. The two most common ways to fixate the femoral implant is with PMMA (cemented implant), or to let natural bone growth fixate the femoral stem (cementless implant). There are countless ways and means to achieve both types of fixation, but it will not be discussed in this report, as it bears no influence on the results of this study.

The femoral head and acetabular cup form the bearing couple of the joint and it is here where the most considerable differences in designs are found. Different bearing couples being used are: metal on UHMWPE, metal on metal, metal on ceramic, ceramic on UHMWPE and ceramic on ceramic.

The femoral heads are manufactured in different sizes: Ø 22 mm, Ø 26 mm, Ø 28 mm, Ø 30 mm, Ø 32 mm and Ø 34 mm, of which the Ø 28 mm and Ø 32 mm are the most common. As mentioned previously, the depth of the taper inside femoral heads varies to give the surgeon more options when operating. The most common materials used for femoral heads are: Zirconia, Alumina, Cobalt Chromium and 316L stainless steel. Figure 9 shows femoral heads made from Alumina, 316L stainless steel and Zirconia. Note the finely polished surfaces of each of these femoral heads. A Cobalt Chrome femoral head would have a very similar appearance to the 316L stainless steel

femoral head. Permutations of these materials exist, like alumina-coated stainless steel and Zirconia strengthened Alumina, but these are currently not very common.

Figure 9: Different femoral heads

Most acetabular cups are manufactured from UHMWPE and are normally classified as cemented or metal backed. Charnley's design was an HDPE cup that was cemented to the acetabulum with PMMA, but many modern designs employ a metal backing, like the one shown in Figure 8, to support the UHMWPE cup. The metal backing can be cemented, but in most cases it is implanted so that natural bone-growth can fixate the acetabular cup. There are advantages and disadvantages to both methods and it has been the topic of many heated debates and a great deal of research. These methods will not be discussed further in this report, as they bear no relevance to the results of this study.

UHMWPE acetabular cups can be crosslinked to increase its wear characteristics. Crosslinking employs radiation to link the long carbon string molecules of the UHMWPE together to produce a stronger, but more brittle material. As all the UHMWPE acetabular cups in this study are non-

crosslinked, this topic does not hold relevance to this study and is not investigated further.

Other materials used to manufacture acetabular cups are Alumina, 316L stainless steel, Cobalt Chrome or even Cobalt Chrome covered with alumina.

Acetabular cups are manufactured with inside diameters to conform to the various sized femoral heads. Each cup is available in a variety of outside diameters, as illustrated by the two UHMWPE acetabular cups in Figure 10. In most cases when an acetabular cup is replaced, the cavity in the acetabulum needs to be reamed bigger; therefore the surgeon normally implants an acetabular cup with the smallest outside diameter possible, but still keeps in mind that the cup must not wear through.

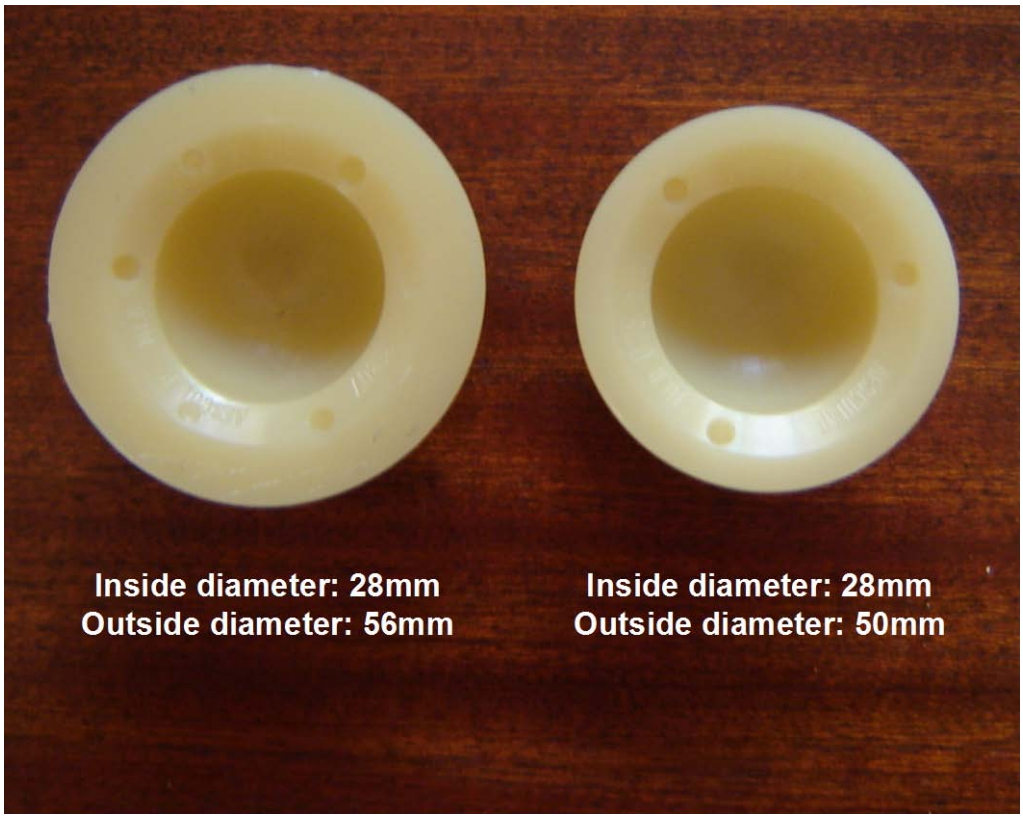

Figure 10: Different outside diameter acetabular cups

2.2 Material properties of Zirconia

Zirconia can exist in three phases, namely cubic, tetragonal and monoclinic. The most commonly known of the three phases is probably cubic Zirconia, which is grown as a flawless crystal at temperatures exceeding 1500°C (Dambreville et al. 1999:59), and used as a replacement for diamond, as is evident in Figure 11. The cubic phase of Zirconia is too brittle to use in hip replacements.

Figure 11: A Round-brilliant cut cubic Zirconia
(http://en.wikipedia.org/wiki/Cubic_zirconia)

The two phases that are of importance in this study are the tetragonal and monoclinic phases, whose crystalline structures are shown in Figure 12. Unlike the grown cubic Zirconia crystal shown in Figure 11, the Zirconia used in femoral heads is sintered from fine powder not to form a flawless crystal, but a polycrystalline structure, which gives it the less impressive appearance shown in Figure 9.

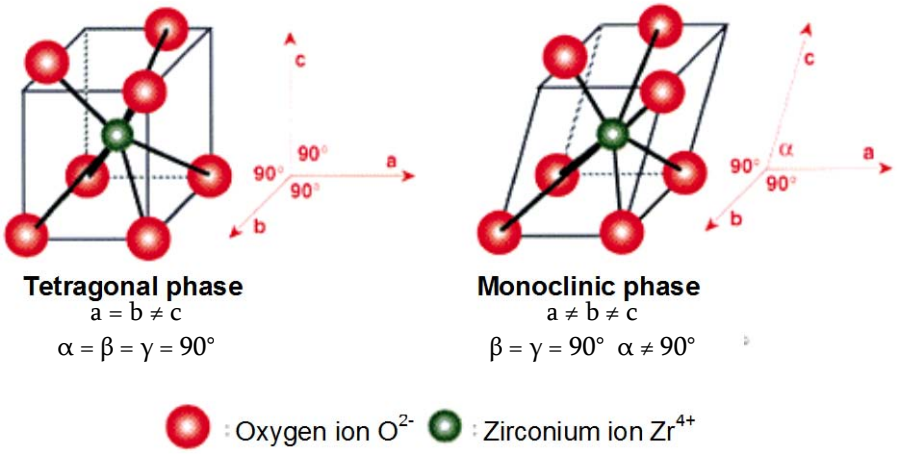

Figure 12: Tetragonal and monoclinic structures

(Adapted from: Dambreville et al. 1999:58)

Zirconia in its tetragonal phase possesses the mechanical properties needed for applying it as a femoral head in hip replacement, but this phase exists in pure Zirconia at about 1 000°C, with the monoclinic phase being the dominant phase at room temperature (Chevalier et al. 2007:2-3). To keep tetragonal Zirconia from transforming to the monoclinic phase at room temperature, about 5% Yttria (Y_2O_3) is added per weight to the Zirconia as stabilising agent, therefore the name Yttria stabilised tetragonal Zirconia polycrystal (Y-TZP) (Chevalier et al. 2007:2-3). Y-TZP is only metastable, allowing it to still have stress induced phase transformation toughening, which gives Zirconia its superior mechanical properties, but also allows tetragonal to monoclinic transformation over extended periods of time. This phase transformation is often referred to as low temperature degradation (LTD) (Chevalier et al. 2007:2-3).

Elevated temperatures (100°C to 500°C) and the presence of water (including water vapour) accelerate the transformation of Y-TZP to the monoclinic phase, with a maximum transformation rate at 250°C (Chevalier et al.

1997:9). The conditions inside an autoclave are exactly as described for accelerated tetragonal to monoclinic transformation, therefore Y-TZP femoral heads should not be sterilised in an autoclave.

Chevalier et al. (1997) performed accelerated phase transformation experiments on Y-TZP in humid environments (steam and ringers solution) at temperatures of 70°C to 130°C and projected these results to the normal body temperature of 37°C. The study by Chevalier et al. (1997) concluded that at 37°C in the human body (in vivo) it would take about 10 years to start considerable tetragonal to monoclinic phase transformation, and another 25 to 30 years to transform to a monoclinic content of 30% to 40%. It will be shown in this study that in reality phase transformation in vivo occurs at much faster rates.

The resistance of Yttria stabilised Tetragonal Zirconia (Y-TZP) to low temperature degrading is dependent on its micro structure and composition (Calés and Stefani 1994:376), therefore the properties of such Y-TZP are governed by specifications such as ISO 13356:1997 and ASTM F1873. A comparison between these two standards and the standard maintained by Norton Desmarquest (Saint Gobain Ceramiques Avancees Desmarquest) in their Prozyr® – Inceral range of Y-TZP femoral heads are shown in Table 1. This clearly shows that the Prozyr® range exceeds the requirements of both of these specifications. Note the specification on monoclinic content, as this will become especially relevant when the results are offered during the course of this study.

Table 1: Properties of Yttria stabilised Zirconia

Property	Y-TZP*	ISO 13356	ASTM F1873
Chemical composition			
ZrO_2+HfO_2+ Y_2O	>99.0	>99.0	>99.0
Y_2O	4.5-5.4	4.5-5.4	4.5-5.4
Al_2O_3	<0.5	<0.5	<0.5
Other total oxides	<0.5	<0.5	<0.5
Physical properties			
Bulk density (g/cm^3)	6.05	>6.00	>6.00
Grain size (μm)	0.2	<0.6	<0.6
Monoclinic phase (%)	**1**	**-**	**<5**
Mechanical properties			
Flexural strength - 4 point bend (MPa)	1666	>800	>800
Elastic modulus (GPa)	201	-	>200
Vickers hardness (HV)	1270	-	>1200
Fracture toughness (Kgf/mm$^{2/3}$)	16.8	-	-
Compressive strength (MPa)	4900	-	-
Impact strength (MPa)	137	-	-

*Values from Prozyr® – Inceral, Norton Desmarquest (Haraguchi et al. 2001:997; Dambreville et al. 1999:57)

2.3 Manufacturing process of Y-TZP

The manufacturing process of Y-TZP femoral heads can be summarized, like all ceramic materials, as the sintering of a fine powder. Because the material properties of the end product are greatly dependant on the manufacturing process, the manufacturing process needs to be researched.

Saint Gobain Ceramiques Avancees Desmarquest (France), also known as Norton Desmarquest, manufactures most of the Y-TZP femoral heads in the world. Prozyr® is the brand manufactured and distributed by Norton Desmarquest, not only does Norton Desmarquest have its own brand, but it also manufactures femoral heads for many other brands. The manufacturing process research will therefore be focussed towards the process used by Norton Desmarquest.

Dambreville et al. 1999, describes the manufacturing process, without surrendering trade secrets, in a publication by Norton Desmarquest as the following:

The base material used is a powder with particles smaller than 0.6μm and of very high purity, governed by the standards given in Table 1. The powder is then compressed at high pressure, typically 100 bar, to initiate adhesion.

Sintering is carried out at a temperature of between 1400°C and 1500°C. Above 1500°C there is a risk of forming the cubic phase and below 1400°C there is a risk of poor density. The lower the temperature is between 1400°C and 1500°C the smaller the crystallites. The smaller the crystallites are, the better the mechanical properties are for the Zirconia. The material shrinks by 20% to 30% during sintering, which means that the initial size of the ball must be substantially larger. For example: a Ø 40 mm ball is required before sintering to produce a Ø 28 mm femoral head after sintering.

After sintering a process called Hot isostatic pressing (HIP) is followed to increase the density of the material even further. During HIP'ing the sintered femoral head is heated to between 1400°C and 1500°C in an inert gas, usually Argon, at a pressure exceeding 1000 bar, for a period of time.

During the HIP'ing process oxygen is depleted from the surface of the femoral head, resulting in a grey coloured Zirconia. To restore the normal white colour the femoral heads are heated in air.

The femoral heads are then grinded and polished with the help of diamond paste and finally the taper where the femoral stem is inserted is machined.

From literature two of the process steps have been found to be of significance: the sintering and HIP'ing steps:

The Australian government (2001) recalled certain batches of femoral heads manufactured by Saint Gobain Ceramiques Avancees Desmarquest (France) in August 2001, due to an uncommon spontaneous fracture. According to the information supplied in the hazard alert, the affected batches were manufactured in January and February 1998, with a new through-oven sintering process, instead of the traditional batch sintering process. The exact cause of this fracture could not be found in literature, but because only certain batches were affected it is assumed that Norton Desmarquest rectified the problem.

Norton Desmarquest introduced the process of HIP'ing in 1995 (Skyrme et al. 2005:69) to further increase the density of the Zirconia (Chevalier et al. 1999:2150; Dambreville et al. 1999:59). This means that non-HIP'ed femoral heads have lower density than HIP'ed femoral heads and could affect the resistance of Y-TZP femoral heads against phase transformation. Many of the authors whose work is quoted in this report suggest that this could indeed be the case, but none produced evidence to prove this theory.

2.4 Incidents of failure

The human body never seizes to amaze and even though theoretical phase stability lifetimes of 25 to 30 years have been determined, the following authors reported premature tetragonal to monoclinic phase transformation on explanted Y-TZP femoral heads: Erick et al. (2004), Haraguchi et al. (2001), Hernigou & Bahrami (2003), Skyrme et al. (2005) and Stewart et al. (2003).

Erick et al. (2004) found a mean monoclinic content of 21% on the surfaces of 18 retrieved Y-TZP femoral heads articulating against UHMWPE, with a mean in vivo time of 64 months. Even with the lack of proper clinical data Erick et al. (2004) was able to illustrate a general trend of increased monoclinic content with increased time in vivo.

Haraguchi et al. (2001) reported on two Y-TZP femoral heads articulating against UHMWPE and found 20% monoclinic content after five years in vivo in the first sample and 30% monoclinic content after three years in vivo in the other sample, resulting in a mean of 25% monoclinic content for a mean in vivo time of four years.

Hernigou et al. (2003) retrieved three Zirconia femoral heads that articulated against UHMWPE and reported that the surfaces of all three samples had considerable monoclinic content. Unfortunately Hernigou et al. (2003) did not mention precise figures.

Skyrme et al. (2005) reported significant monoclinic content on a single explanted Y-TZP femoral head, articulating against UHMWPE, but did not mention precise figures either.

Stewart et al. (2003) reported up to 35% monoclinic content inside the wear areas of three Y-TZP femoral heads, articulating against Alumina acetabular cups in a hip simulator, employing micro separation. Again exact figures were not mentioned. This work by Stewart et al. (2005) is significant because it indicates that phase transformation does not only occur in Y-TZP/UHMWPE prostheses, but also in hard on hard bearings. In this case it was in a simulator where the femoral head is exposed for a much shorter time than it would be in vivo. This study however does not cover hard on hard prostheses.

Erick et al. (2004), is the only study mentioned in this section, that investigated trends pertaining to the monoclinic content and even this study lacks good clinical data, which leaves many questions unanswered, for example: the relationship between in vivo time and monoclinic content and the effect of HIP'ing on monoclinic content.

2.5 Extent of failures

2.5.1 Sphericity

In the cases mentioned in the previous section the monoclinic content was in each case a percentage value of the surface area, which means that phase transformation on the surface of Y-TZP femoral heads is non-uniform, a phenomenon shown by Chevalier et al. (2007) as well. The non-uniform occurrence of tetragonal to monoclinic transformation, combined with a volume increase of about 4%, associated with such transformation (French et al. 1994:5133), would adversely affect the sphericity of the femoral head.

Hernigou and Bahrami (2003) reported a spherical deviation as high as 100μm, on three explanted Y-TZP femoral heads, which had between 19% and 30% monoclinic content. These femoral heads had a spherical deviation smaller than 5μm before implantation.

None of the other authors that reported the incidence of monoclinic content researched the deviation of sphericity and the sample size of Hernigou and Bahrami (2003) is too small to reveal conclusive results.

2.5.2 Surface micro cracks

The same irregular increase in volume due to phase transformation that causes deterioration of sphericity of a femoral head also causes residual stresses in the femoral head, especially on the surface, which could lead to surface micro cracks. Erick et al. (2004) and Haraguchi et al. (2001) reported evidence of such surface micro cracks, after scanning electron microscope (SEM) investigations on retrieved Y-TZP femoral heads, which had significant monoclinic content.

A SEM image by Haraguchi et al. (2001), shown in Figure 13, shows a surface crack, as well as the effect that surface cracks may have on the surface of a Y-TZP femoral head. The way in which the areas of grain pull-out in Figure 13 is delineated by the remnants of surface cracks indicates that the grain pull-out started with micro cracks, which had sharp, probably protruding (because of sphericity changes) edges. The sharp edges have resistance against the UHMWPE when the patient is walking, which in turn generates forces on the sharp edges, subsequently the edges start to break down, or whole parts of the surface may even flake off. An interesting observation is that the direction of crack edge destruction is more or less the same for all the craters, meaning that this is most probably the direction of relative movement between the femoral head and acetabular cup during the patient's weight bearing cycle of walking. The joint fluid that is present between the two bearing surfaces may accelerate the process of crack edge destruction, by means of hydraulic pressure. The micro crack fills up with fluid that pressurises during the high load cycle of walking because the UHMWPE seals off the crack. The pressurised fluid then forces the crack tip open which accelerates the crack growth.

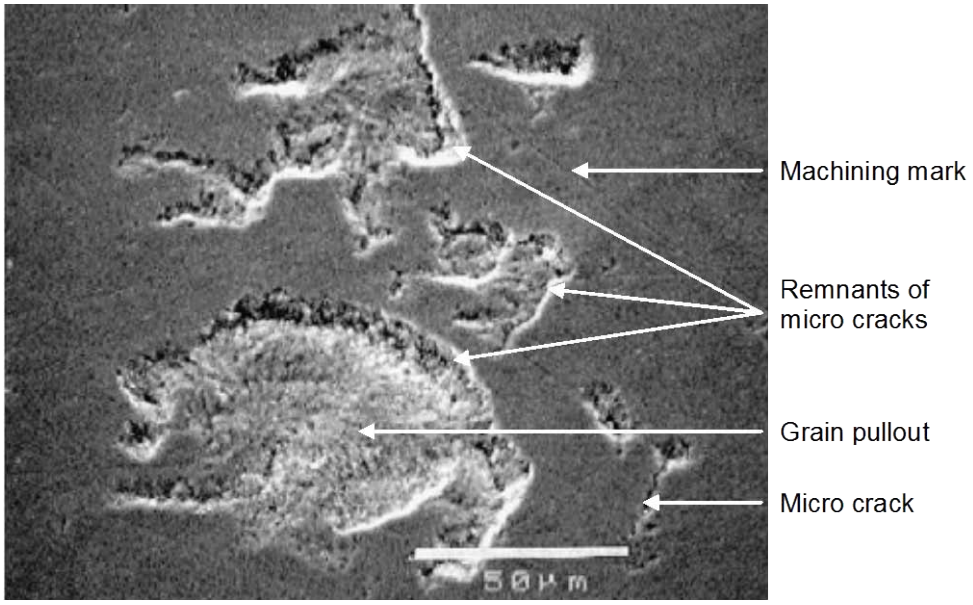

Figure 13: Surface destruction on Y-TZP femoral head

(Monoclinic content of about 30%)

(Adapted from Haraguchi et al. 2001:998)

The existence of micro surface cracks immediately raises the concern of possible femoral head fractures due to significant phase transformation of Y-TZP femoral heads. Erick et al. (2004) reported that the ultimate compressive load strength decreases from 1 253 MPa with a standard deviation of 850 MPa to 561 MPa with a standard deviation of 344 MPa, because of surface cracks. The method of determining the ultimate compressive load strength used by Erick et al. (2004) does not allow for the elimination of influencing factors such as stress concentrations and the shortcomings of the method is evident from the large amount of scatter present in the data for the two sample groups. If the mechanism of transformation toughening and the fact that Haraguchi et al. (2001) reported phase transformation of Y-TZP femoral heads being a surface phenomenon that does not extend into the inner bulk of the femoral heads, doubt exists over the significance of the ultimate compressive load tests done by Erick et al. (2004). It is agreed that surface micro cracks would adversely affect the strength of a femoral head, but the question to ask is the relevance of this

and as far as could be determined from literature non-autoclaved Y-TZP femoral head fracture is a very rare occurrence. (Cases of Y-TZP femoral head fracture were reported on specimens that were sterilised in steam/autoclaved, which led to a hazard alert being published on this topic by: amongst others, the Australian Government (Australian Government, 2001)).

The effect of surface micro cracks on the wear rate of the acetabular cup could not be found in literature. The edges of surface micro cracks can accelerate wear of the UHMWPE acetabular cup. Wear of the UHMWPE acetabular cup is an important parameter, as the wear particles cause aseptic loosening, which is by far the biggest cause of implant failure (See Figure 6 and accompanying discussion).

2.5.3 Surface finish

In the literature surveyed all parties seem to agree that phase transformation of tetragonal Zirconia to the monoclinic phase adversely affects the surface finish of femoral heads. It is no wonder that the surface finish would deteriorate when viewing the SEM image by Haraguchi et al. (2001), shown in Figure 13. Erick et al. (2004), Hernigou and Bahrami (2003) and Skyrme et al. (2005), also reported grain pullout on Y-TZP femoral heads, which had significant monoclinic content.

Erick et al. (2004) examined the surface finish of 18 retrieved samples and found an average surface finish of about 0.15 μm with a standard deviation of about 0.075 μm. The sample group was also big enough for Erick et al. (2004) to investigate trends and it was found that surface finish roughly (r^2 = 0.04) increases with increase in monoclinic content and that surface finish deteriorates with time in vivo with a much stronger relationship (r^2 = 0.44).

The sample group studied by Erick et al. (2004) comprised of Y-TZP femoral heads from several different manufacturers. The study lacked clinical data, therefore the work done serves as a measure of general trend, but does not separate factors that could prove to have significant effects on the data, for example HIP'ing. During this study clinical and mechanical data will be combined to be able to separate as many factors possible.

Haraguchi et al. (2001) reported an average deterioration in surface finish from 0.006 μm to 0.12 μm, on the surfaces of only two explanted femoral heads with an average monoclinic content of 25% and an average in vivo life of 4.5 years.

Hernigou and Bahrami (2003) reported a deterioration of surface finish to between 0.2 μm and 0.5 μm, compared to the finish of non-implanted heads of 0.005 μm. The average in vivo life and monoclinic content for the three samples analysed by Hernigou and Bahrami (2003) was 9.5 years and 25% respectively.

The research of surface finish by the abovementioned authors indicates that surface finish deteriorates because of tetragonal to monoclinic phase transformation on Y-TZP femoral heads, but the lack of clinical data and small sample sizes creates the opportunity for more in depth research into this phenomenon, which will be addressed during this study. The deterioration in surface finish is especially significant because one of the biggest motivations for the use of ceramic materials for femoral heads is the fine surface finish to which it can be polished (0.005 μm Ra as opposed to 0.07 μm Ra for stainless steel - Hernigou & Bahrami 2003:505 & 507).

2.5.4 Wear rate

The deterioration of the bearing surface of Y-TZP femoral heads due to phase transformation must have an influence on the performance of the hip replacement. Most probably the single most significant parameter of performance must be the amount of UHMWPE wear, because of the highly increased risk of osteolysis associated with an increase of wear particles. Hernigou and Bahrami (2003), as well as Skyrme et al. (2005), compared the in vivo wear rate of Y-TZP femoral heads with other femoral heads also articulating against UHMWPE.

Two parameters are normally used to describe the amount of acetabular cup wear i.e. linear wear (also called linear penetration) and volumetric wear. In most cases the volumetric wear is determined mathematically using linear wear data, but it can be calculated using telemetry measurements, or in the case of simulators the acetabular cup is often weighed. The last method has provoked some discussion as to its accuracy, but this method is not used in this study and will not be discussed in further detail.

The way by which Hernigou and Bahrami (2003) compared the UHMWPE wear rate of Y-TZP femoral heads with that of Alumina, is actually a very creative method, which not only gives the comparison between these two materials, but also gives UHMWPE wear data on stainless steel femoral heads. The Alumina group comprised of Ø 32 mm femoral heads and the Zirconia of Ø 28 mm non-HIP'ed femoral heads, which Hernigou and Bahrami (2003) overcame by comparing each of these groups with a stainless steel group comprising of the same sized femoral head. Hernigou and Bahrami (2003) used radiographic methods to determine the amount of wear, in vivo, on a yearly basis, with a minimum time of 10 years and a maximum of 12 years. Figure 14 is a good summary of the work done by

Hernigou and Bahrami (2003) and shows a general increase in wear rate from year 5 to year 12, which is severe for the Zirconia group, with a wear rate increase of 0.4 mm/year, as opposed to 0.13 mm/year for both stainless steel groups and 0.07 mm/year for the alumina group. Note that the peak on the left-hand side of the graph is the bedding-in wear caused by the acetabular component conforming to the shape and movement of the femoral head.

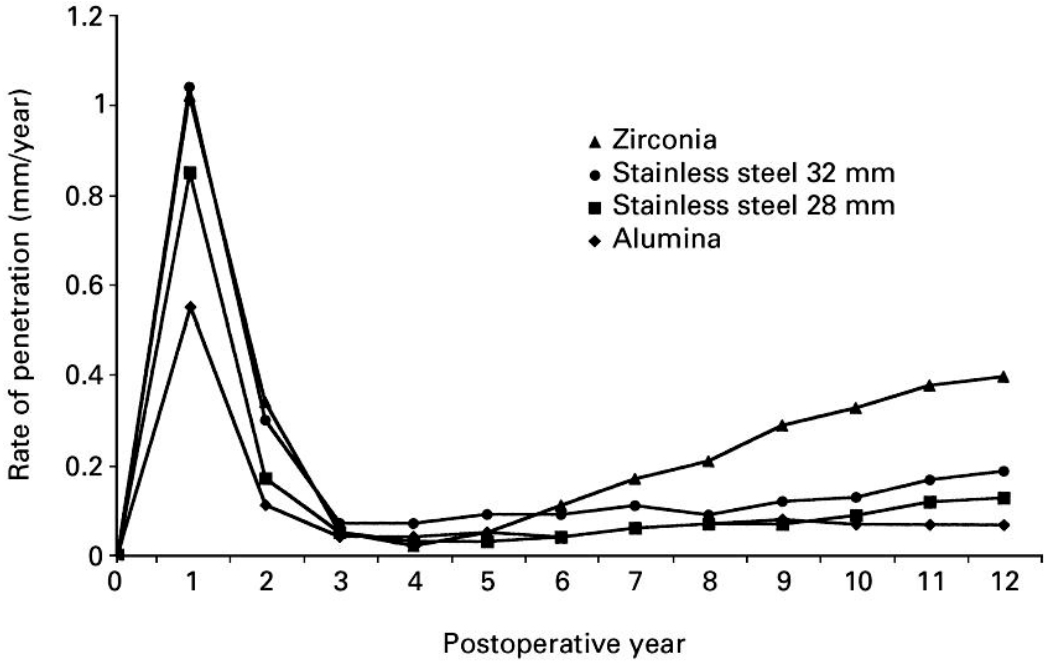

Figure 14: Comparison of wear rates

(Hernigou and Bahrami 2003:506)

After the final follow-up, (12 years after implantation) Hernigou and Bahrami (2003) report the mean amounts of volumetric wear as the following: 1360 mm^3 for the Ø 28 mm Zirconia group, 683mm^3 for the 28mm stainless steel group, 755 mm^3 for the Ø 32mm Alumina group and 1314 mm^3 for the Ø 32 mm stainless steel group. Investigation of three explanted Y-TZP femoral heads, revealed phase transformation and associated surface deterioration, therefore Hernigou and Bahrami (2003)

concluded by postulating that the increase in wear rate observed in the Zirconia group can be attributed to the long term, gradual phase transformation and associated surface deterioration of the femoral heads.

Skyrme et al. (2005) compared the wear rates of non-HIP'ed Y-TZP on UHMWPE hip replacements with Cobalt Chrome against UHMWPE hip replacements, based on radiographic data collected at a mean follow-up time of 78 months. The study by Skyrme et al. (2005) comprised of a total of 281 primary cementless total hip replacements, from the mentioned materials and of different sizes. The most conclusive results were found by Skyrme et al. (2005), when 31 patients with Ø 28 mm Zirconia heads were matched with 31 patients with Ø 28 mm Cobalt Chrome heads for gender and age, resulting in a mean linear wear rate for Zirconia of 0.19 mm/year and 0.14 mm/year for Cobalt Chrome. Skyrme et al. (2005) concluded that the higher wear rate found with the Y-TZP femoral heads could be attributed to the surface deterioration present on 19 explanted femoral heads, caused by phase transformation. Because this study only involved non-HIP'ed Y-TZP femoral heads, Skyrme et al. (2005) postulates that HIP'ed Y-TZP femoral heads would show better results.

The radiographic methods used by the abovementioned researchers, as well as the fact that only non-HIP'ed Y-TZP femoral heads were studied, leaves the opportunity to confirm these results with a retrieval study and to answer the question of whether HIP'ed Y-TZP femoral heads would perform better than non-HIP'ed femoral heads.

2.5.5 Implant survival

Implant survival is what matters the most to patients, because of the pain and distress that is gone through with a hip replacement. From the literature studied, the future for Zirconia femoral heads is bleak.

Allain et al. (1999) investigated the poor survival of 78 non-HIP'ed Y-TZP femoral heads (63% at eight years) as opposed to 156 Alumina femoral heads (93% at nine years), implanted at the same hospital, by the same doctors, using the same femoral stem, cement, and UHMWPE cup. Subsequently, Allain et al. (1999) abandoned the use of Zirconia Femoral heads. It must be noted that Allain et al. (1999) did not use revision surgery, as the measure of failure, but rather by means of clinical assessment, meaning that the results obtained are a bit harsh.

Skyrme et al. (2005) reported that 19 of 250 (7.6%) non-HIP'ed Y-TZP hip replacements had to be revised due to osteolysis at a mean follow up time of 78 months, and that no revisions had to be done on 31 Cobalt Chrome femoral heads, of the same mean follow-up time. The higher incidence of osteolysis found by Skyrme et al. (2005) in the Zirconia group of patients, was attributed to the higher UHMWPE wear rate of Zirconia group (0.19 mm/year), compared to that of the Cobalt Chrome group (0.14 mm/year), because of the surface deterioration associated with Y-TZP phase transformation.

The poor survival results of Y-TZP femoral heads, confirm what can be anticipated from the bearing surface condition results, as well as the wear results that were found in the literature surveyed for this study. There is however room for improvement on the results found in the literature surveyed, by a retrieval study, which incorporates clinical data, includes

HIP'ed and non-HIP'ed Y-TZP femoral heads and uses measured data to explain observations.

3 Experimental methods

For this study, the surgeon retrieved 27 Y-TZP femoral heads during normal revision surgery. All the implants had reached the end of their useful in vivo life, as the patients experienced excessive pain. Severe pain is a clear indication of a failed implant, whether it can be attributed to the acetabular or the femoral component. The failures were radiologically confirmed and assessed prior to revision surgery. The femoral heads were from different suppliers, and all the acetabular cups were non-crosslinked UHMWPE. All the explanted samples used during this study were documented, including: Available patient details, radiology and histology. Each femoral head and acetabular cup was photo documented for reference purposes.

3.1 Background

The wear area on the femoral head is of great significance, as this gives an indication of how the surface of the Y-TZP femoral head reacted to the specific conditions that occurred in the bearing couple. Due to the nature and complexity of revision surgery, during which the samples were collected, it was not possible to keep the system in-tact and the position of the femoral heads relative to the acetabular cups were not documented; therefore the position of wear is not known, apart from the samples that exhibited dulling of the very finely polished surface (See Figure 29 and accompanying discussion). The dulling phenomenon will be shown to be a visible sign of surface degradation, which would be on the wear area, because this is the area exposed to the harshest conditions inside the bearing couple. Special precaution was taken to insure that the analysis that was done incorporated the actual wear area on the femoral head.

Figure 15 is a two dimensional representation of a total hip replacement in an anatomical position, illustrating the main features of a hip replacement that is relevant to this study. The acetabular cup is fixed to the acetabulum and the femoral stem is inserted into the femur of the patient. The pole of the femoral head is defined as the top point of the sphere, opposite the tapered hole in which the femoral stem fits and is illustrated in Figure 16. The equator is a fictional line in the middle of the femoral head, exactly as its name describes. The theoretical wear area is shown in Figure 15, with its apex in the centre of the wear area, as denoted.

In the majority of the samples that were retrieved during revision surgery the femoral stems were still stable and only the acetabular cups and femoral heads were replaced.

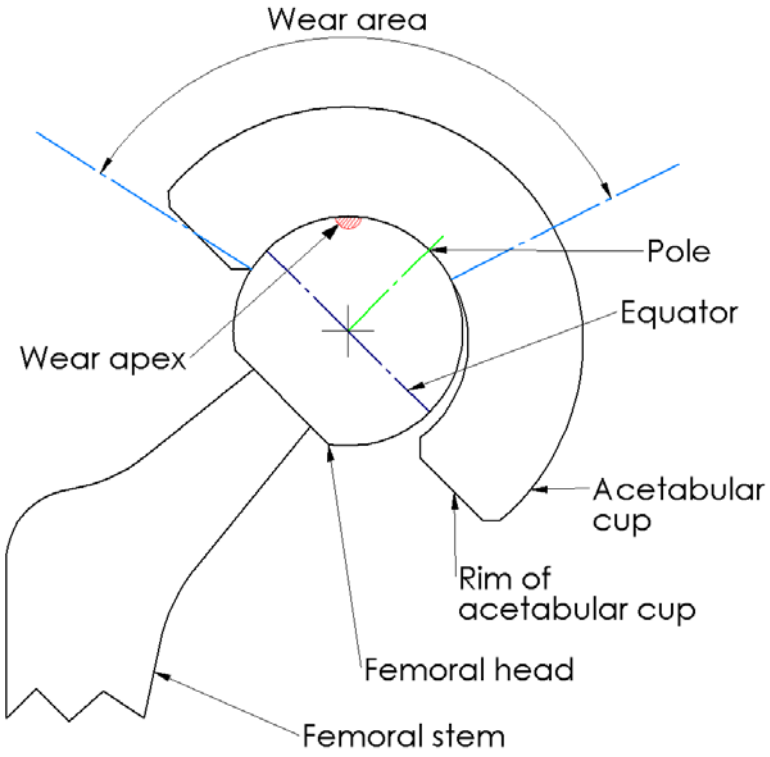

Figure 15: Features of a hip replacement

Figure 16 shows the typical wear area on femoral heads as seen during revision surgery. In the top view the pole is shown as well as the greater wear area and its apex. The apex is shown in greater detail in the front view and is on a line that is drawn from the centre of the femoral head at a 45° angle from the equator. The shape of the apex does not depict the real shape of the wear area, it depicts only the apex's position. The wear area as well as its apex is different in every implant due to the manufacturing tolerances of the femoral head and acetabular cup, the orientation of the cup due to the surgical procedure and the patient's mobility and weight.

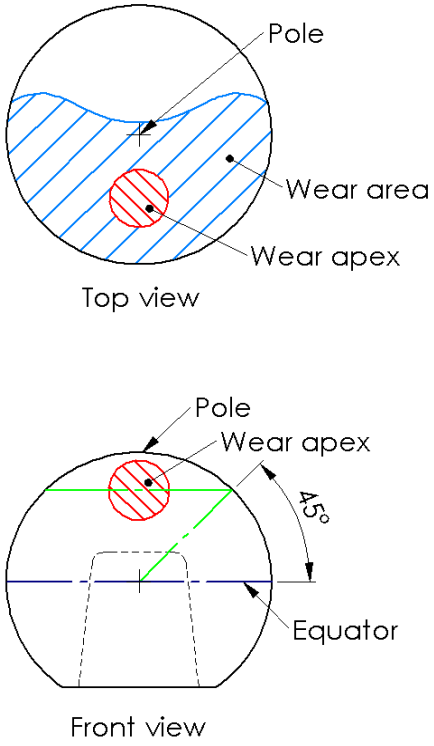

Figure 16: Typical location of wear area on femoral head

3.2 Sample composition

In this study 30 Y-TZP femoral heads were studied in total, of which 3 were new and 27 were retrieved with their acetabular cups, during revision surgery. The retrieved group can be summarised as follows:

- 27 Explanted Y-TZP femoral heads and their corresponding UHMWPE acetabular cups, as shown in Table 2.
    - Average patient age: 66.4 years, ranging from 41 years to 84 years.
    - 7 Male patients.
    - 20 Female patients.
    - Average in vivo life: 10.3 years ranging from 7 years to 15 years.
    - 5 FII femoral heads and 22 Prozyr® femoral heads.
    - The femoral head sizes were as follows:
      1 x Ø 22 mm, 2 x Ø 26 mm, 21 x Ø 28 mm and 3 x Ø 32 mm.
    - 23 Cemented cups from various manufacturers.
    - 4 Cups with Mont Blanc® metal backings.
    - All cups are non-crosslinked UHMWPE.
    - The cup inner diameters matched that of the femoral heads, with varying outer diameters, ranging from 44 mm to 56 mm.
- Three new Ø 28 mm Prozyr® Y-TZP femoral heads (HIP'ed) were used as control.

Table 2: Explanted samples' summary

Nr.	Gender	Age [yrs]	Year implanted	In vivo [yrs]	Cup manufact.	Head manufact.	Serial nr	Size [mm]
2	Male	77	1996	10.4	BARC	Prozyr	211123	28
3	Female	65	1997	9.0	Sferi	Prozyr	260352	28
4	Female	57	1994	7.8	Sferi	Prozyr	094567	28
5	Male	58	1996	9.1	Sferi	Prozyr	131585	32
6	Male	67	1993	7.7	Aesculap	Prozyr	..3087	28
7	Female	68	1991	14.0	Mont	Prozyr	25883	28
8	Female	40	1996	10.0	BARC	Prozyr	186873	28
9	Male	70	1993	14.0	Aesculap	FII	s8734-5348	32
10	Female	84	1995	10.3	BARC	Prozyr	170735	28
11	Female	61	1991	14.0	Mont	FII	s8730-5206	28
12	Male	43	1993	9.2	Aesculap	Prozyr	121661	28
13	Female	68	1996	9.8	BARC	Prozyr	121632	28
14	Female	70	1991	15.0	BARC	FII	s8650-4735	28
15	Female	71	1997	9.0	BARC	Prozyr	260373	28
16	Female	71	1995	10.0	Sferi	Prozyr	51082	32
17	Female	66	1992	14.0	BARC	FII	s8931-5640	28
18	Female	62	1997	9.0	Aesculap	Prozyr	266768	28
19	Female	58	1995	11.0	Aesculap	Prozyr	140167	28
20	Male	84	1997	9.0	Aesculap	Prozyr	271705	28
21	Male	73	1998	8.0	Aesculap	Prozyr	283859	28
22	Female	66	1998	8.5	Aesculap	Prozyr	104928	26
23	Female	64	1999	7.0	Aesculap	Prozyr	104863	26
24	Female	73	1995	10.5	BARC	Prozyr	186805	28
25	Female	69	1993	13.0	BARC	FII	s…..-…...	28
26	Female	82	1995	10.0	BARC	Prozyr	186845	28
27	Female	58	1995	10.0	Mont	Prozyr	209803	28
28	Female	67	1998	8.8	Aesculap	Prozyr	257075	22
29	Control					Prozyr	353771	28
30	Control					Prozyr	330926	28
31	Control					Prozyr	255830	28

The sample consists of femoral heads and acetabular cups from different manufacturers and of different sizes, which need to be incorporated in the analysis of the data in order to eliminate possible influencing factors.

All of the acetabular cups are non-crosslinked UHMWPE and therefore the base material can, within reasonable limits, be accepted as similar.

The differences in femoral head diameter give rise to differences of the kinetics inside the bearing couple, for example:

- The relative surface speed between the femoral head and acetabular cup surfaces differs and is governed by Equation 1.

$$\nu = \omega r \qquad (1)$$

ν = Linear speed [m/s]

ω = Rotational speed [rad/s]

r = Radius of femoral head [m]

If a person is walking at a constant pace, with two different diameter hip replacements, the rotational speed would be similar for both hip replacements, but because the radiuses differ, the linear speed between the acetabular cup surfaces and femoral head surfaces would differ. The bigger the diameter of the femoral head is, the greater the surface speed is between the femoral head and acetabular cup.

- The contact pressure differs between different sized femoral heads, governed by Equation 2.

$$P = F/A \qquad (2)$$

P = Pressure [MPa]

F = Force [N]

A = Projected Area [m^2]

If a person is walking with two different diameter hip replacements, the force exerted on the two hip replacements would be similar, but because the diameters differ, the area over which the force is exerted differs, resulting in a difference between the pressures inside the two respective hip replacements. The bigger the femoral head diameter is, the lower the pressure inside the bearing is.

The differences in surface speed and pressure results in differences in lubrication, heat development and dissipation, UHMWPE behaviour and wear rate.

A difference in UHMWPE acetabular cup wear rate associated with a difference in femoral head diameter is a common phenomenon in hip replacement surgery and is illustrated by the results of Skyrme et al. (2005) and Hernigou and Bahrami (2003). The Ø 32 mm and Ø 28 mm Zirconia groups of Skyrme et al. (2005) showed similar linear penetration rates, which means that the Ø 32 mm group had greater volumetric wear rates. Hernigou and Bahrami (2003) showed a significant difference in wear rate (both penetration and volumetric) between Ø 32 mm and Ø 28 mm Cobalt Chrome femoral heads on UHMWPE. Surgeons tend to implant Ø 32 mm femoral heads into younger, more active patients, which introduces a further uncertainty, which is very difficult to quantify into the wear rate comparison, as was the case with Skyrme et al. (2005).

A difference in the kinetics inside the bearing couple formed by the hip replacement could lead to differences in femoral head surface temperatures and subsequently the rate of Y-TZP phase transformation, because of the dependence of Y-TZP phase transformation on temperature, illustrated by Chevalier et al. (1999).

To eliminate the possible factors that a difference in femoral head diameter can introduce, the samples will be divided into Ø 26 mm, Ø 28 mm and Ø 32 mm size groups.

The difference in outer diameter, as well as the implantation technique has an influence on the elasticity of the hip replacement, which could affect the results of this study. The effect that elasticity has on the performance of hip

replacements will not be taken into account during analysis of the data, because no definite indication of this could be found in the literature surveyed for this study and researching such effects would consist of a study on its own.

As mentioned in Section 2.3, Norton Desmarquest introduced the process of hot isostatic pressing (HIP'ing) in 1995 (Skyrme et al. 2005:69). HIP'ing increases the density and associated material properties of Y-TZP femoral heads. Norton Desmarquest is the manufacturer of the Prozyr® brand of femoral heads, which forms the largest part of this study group, therefore the data will be divided into HIP'ed and non-HIP'ed groups.

The FII femoral heads are from a French manufacturer called: Fabrique D\'Implants et D\'Instruments Chirurg. Norton Desmarquest acquired FII in the mid 1990's; subsequently there is very little information available on the FII femoral heads. The FII femoral heads were all implanted before 1995 and are most probably not HIP'ed. Due to the amount of uncertainty the five FII femoral heads will be treated, according to their size, as separate sample groups.

The serial numbers for samples nr 6 and 25 could not be retrieved fully. Sample nr. 6 is a Prozyr® femoral head and will be added to the non-HIP'ed Prozyr® sample group, because it was implanted prior to 1995. Sample nr. 25 was implanted in the same time window as the other FII femoral heads and has the same serial number structure as the FII femoral heads, therefore it would be added to the FII sample group. The lack of serial numbers will be taken into account in the data analysis, so that an artificial trend is not produced, or a wrong conclusion reached.

Another possible influential manufacturing feature is the re-oxidation of the femoral heads after sintering and HIP'ing, which returns oxygen to the surface of the femoral head and changes its colour from black to a white or even pink colour. All of the femoral heads were whitish in colour, indicating that all of the HIP'ed femoral heads were re-oxidised, but none were pink or a brilliant white, indicating that none were re-oxidised to an extreme extent. The colour of the HIP'ed and non-HIP'ed groups corresponded within each group, with the non-HIP'ed group being off-white in colour and the HIP'ed group being cream in colour with a dark, almost black, reflective undertone. From this it was concluded that the re-oxidation was done similarly for all the heads in the HIP'ed group. Any difference occurring due to re-oxidation will be incorporated in the differences and relations found between the HIP'ed and non-HIP'ed groups.

The Australian government (2001) recalled femoral heads manufactured by Saint Gobain Ceramiques Avancees Desmarquest (France) in August 2001, due to an uncommon spontaneous fracture. The cause of this spontaneous fracture was not known at the time of the recall, but it indicates a difference in material properties, which could affect the results of this study. According to the information supplied by the Australian government (2001) the affected batches were manufactured in January and February 1998, using a new through-oven sintering process, instead of the traditional batch sintering process. Only four of the retrieved samples in this study were not implanted before 1998. Three of which (Sample 21, 22 & 28) was implanted in February and early March of 1998, which makes it unlikely to be of the affected batches, especially when considering that it was manufactured in France, had to be imported into South Africa and work its way through the importer's stock levels. The other femoral head's serial number (Sample 23) indicates that it was manufactured before the femoral head of sample 22, which was implanted in February 1998. According to the serial numbers of

the three control samples one was manufactured prior to 1998 and the other two long after the affected batches, but still with the through oven sintering process. It is therefore concluded that the retrieved femoral heads investigated in this study were not from the through-oven sintering process, which could affect the results of this study.

Another issue raised in the previous paragraph is the time that elapses between manufacture and the implantation of the femoral heads. Even though the exact date of manufacture could not be determined, comparing the (consecutive) serial numbers with implantation dates did not produce any irregularities, meaning that as far as can be determined none of the samples had an excessive shelf life, compared to the sample mean. From the work done by Chevalier et al. (1999) it is evident that Y-TZP has a very slow phase transformation rate at room temperature, especially if the humidity is low, as would be expected in a storing facility. This is confirmed by control sample 31, which according to its serial number was probably manufactured in 1996 and after ten years in storage it only has 1.6% monoclinic content. It is therefore judged that the time between manufacture and implantation would not cause significant Y-TZP transformation prior to implantation and would therefore not significantly affect the results of this study.

All the femoral heads were sterilised by Gamma irradiation and not in an autoclave, which would have started phase transformation and affected the results of this study considerably.

Dividing the sample group into smaller groups eliminates possible influencing factors, but results in groups that are too small to be meaningfully analysed which subsequently results in the loss of data. To alleviate this, the data will be analysed in bulk, small groups and even in different levels of break down, so that all possible data can be meaningfully

incorporated into this study. The abovementioned factors will however be kept in mind when doing this so that the wrong conclusions are not derived from the presented data. The advantage of treating the data in this manner is that it gives an indication of how Y-TZP femoral head implants would react to the conditions inside the body, of the average patient.

To conclude the samples collected will be treated in two ways: as bulk and as separate groups to eliminate certain influencing factors. These separate groups will be divided according to manufacturer, HIP'ed or non-HIP'ed and size.

3.3 General acetabular cup condition

The acetabular cups were investigated in general with the naked eye, as well as with a magnifying glass. Above and beyond the general impressions, three characteristics were noted: impingement, adhesive wear and abrasive wear.

Impingement is the term used for a case where the femoral stem collides with the acetabular cup. In hip replacements this is the most common form of mechanical damage (Burger 2005:89). This is a traumatic occurrence that can cause; severe pain to the patient, damage to the tissue surrounding the joint, dislocation and premature loosening of either the acetabular cup or the femoral implant. The relevance of impingement is evident in the shortening effect that it could have on the in vivo life of a hip prosthesis. It must also be noted that impingement is in most cases a first symptom of loosening of the acetabular cup and not the cause of it.

The most dominant wear type evident on the surface of the acetabular cup gives a good indication of the wear mechanism that prevailed inside the

bearing couple. According to studies by Burger (2005) adhesive wear is a more dominant occurrence in non-crosslinked UHMWPE, than abrasive wear. If abrasive wear is found to be more dominant than adhesive wear, it would indicate that the major wear mechanism inside the hip replacement has changed, due to surface deterioration associated with Y-TZP phase transformation.

Third body wear originates mainly from four sources: bone chippings created during implant, ceramic particles originating from the femoral head, particles of bone cement (PMMA and Zirconia) and UHMWPE wear particles, of which the most commonly found by Burger (2005) during a retrieval study was bone cement and UHMWPE wear particles. Zirconia, or Barium sulphide ($BaSO_4$) is added to PMMA when manufacturing bone cement as an opaque identifier for bone cement during X-rays (Sabokbar et al. 1997:129), therefore particles of Zirconia found inside the acetabular cup can be the remainders of bone cement and not necessarily from the femoral head. Third body wear, especially of particles trapped during implantation, can be a substantial contributor to the wear of the UHMWPE acetabular cup, because it starts influencing the wear process from day one. Because of the great effect of third body wear, it was not separated from the abrasive wear, which also made the results of this study comparable to the results found by Burger (2005), mentioned in the first paragraph of this section.

3.4 General femoral head condition

The surface conditions of the retrieved samples were investigated using electron microscopy at the University of Pretoria. To understand some of the results obtained from the electron microscopy, it is essential that the basics of electron microscopy be explained.

A scanning electron microscope operates on the principle of shooting a ray of electrons onto a specimen and detecting the electrons emitted from the specimen. Figure 17 is a diagram explaining the process. The electron source is normally a heated element and produces the electrons that the specimen is bombarded with. A voltage is created between the electron source and the specimen, which attracts the electrons towards the specimen. The electrons are focused with a lens and then directed with a magnetic beam deflector before going through another lens onto the specimen. The electrons from the beam excite a part of the specimen surface, causing the surface to emit electrons, which are then picked up with a detector and converted into an image. Each pixel on the image is formed by bombarding a small area of the specimen with the electron beam and detecting the electrons that are emitted. The more electrons that are detected, the brighter the colour of the pixel is. A scanning electron microscope employs the beam deflector to control the direction of the electron beam and scans the area of the specimen investigated, bit-by-bit, forming the image pixel by pixel.

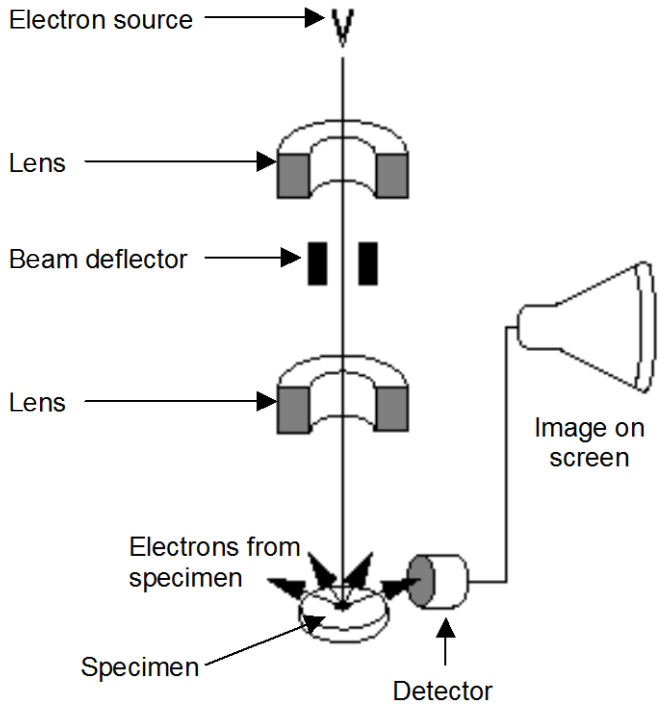

Figure 17: Diagram of scanning electron microscope

(Adapted from: http://www.nslc.wustl.edu)

The part of the electron microscope process that is of importance to this study is the way in which the specimen reacts to the electron beam. Figure 18 shows the way in which the surface of a specimen is excited. The measurements shown in Figure 18 are typical and vary with material density and excitation voltage. The electrons enter the specimen at the surface and cause the dispersion of electrons from the specimen from different depths beneath the surface.

Auger electrons are emitted from the surface and are generally used to study surface focussed topics such as corrosion and adhesion.

Secondary electrons are formed when electrons from the beam displace electrons from the material of the specimen. Secondary electrons have lower energy and are detected with a detector next to the sample.

Secondary electrons are used to form the normal SEM image because they originate from nearer to the surface and are sensitive to topography.

Backscatter electrons originate from deeper under the surface of the specimen and form when the electrons from the beam are deflected back up towards the beam, therefore the backscatter detector would be above the specimen with a hole to let the electron beam pass through onto the specimen. Backscatter electrons are generally less sensitive to topography, but can be used to obtain detail deeper into the surface of the specimen.

X-rays are formed when electrons are displaced from the outer spheres of atoms in the specimen. Each material emits a characteristic wavelength of X-ray; therefore these X-rays can be used to determine the elemental composition of materials. The depth and width of the excitation volume shown in Figure 18, varies with specimen material density and excitation voltage.

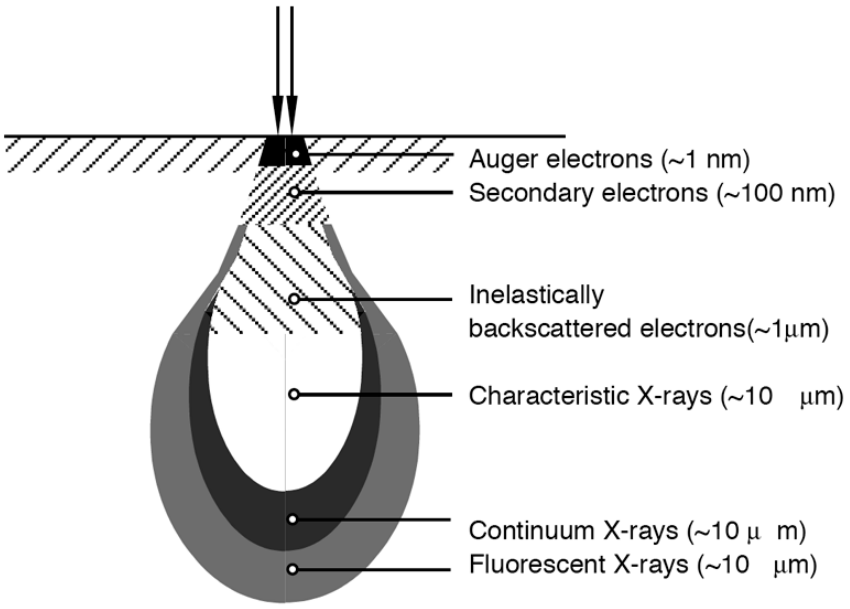

Figure 18: Excitation on specimen surface

(http://www.iap.tuwien.ac.at/~werner/qes_tut_interact.html)

The most important fact that arises from the discussion on electron microscopy is that the electrons that are used to form the various types of images arise from different depths beneath the surface of the specimen.

The surfaces of the femoral heads were investigated by use of a normal scanning electron microscope (SEM) as well as the latest field emission scanning electron microscope (FEEM), the Zeiss – Ultra 55, as shown in Figure 19. The Ultra 55 is a scanning electron microscope, but was the first of its kind in the world because it employs an electron beam emitted from a crystal instead of the normal heated filament and an inline electron backscatter detector. The electron beam is up to a thousand times more intense than the beam of a normal SEM, enabling the use of lower excitation voltages and magnifications of up to 1 000 000 times, which is far more than the magnification of a normal SEM which achieves about 300 000 times. With an ingenious way of manipulating the electron beam, the backscatter detector is placed directly above the specimen, which greatly increases the detection of backscatter electrons. The inline backscatter detector can detect a staggering 85% of backscatter electrons emitted from the specimen. The electron beam and detectors of the Ultra 55 create an image at a lower excitation voltage, which means that the excitation volume is smaller and subsequently the resolution is much better at extreme magnifications.

The backscatter detector of the Zeiss Ultra 55 is also fitted with a backscatter interference detector/filter, which allows for distinguishing between monoclinic and tetragonal phase of Zirconia, as will be illustrated when the results are offered.

In normal electron microscopes a process called Electron Backscatter Diffraction (EBSD) can be used to determine crystal orientations. This process involves bombarding the specimen at an angle of about 70° the

backscatter electrons that are emitted at an angle of 90° to the beam then hit a fluorescent screen, which in turn is recorded with a low light camera. This image that forms can be used to differentiate between crystalline orientations. (http://serc.carleton.edu, http://www.ebsd.com) The only information available on the Zeiss 55 is that it uses an Angle Selective Backscatter Electron Detector (http://www.zeiss.com) together with filters to distinguish between crystal orientations. Judging by the name of the detector it seems as though a similar process as the conventional one is followed, but because of the dedicated detector the sample does not need to be angled and that with the software images can be interpolated over each other to produce the results as shown in this report.

Figure 19: Zeiss Ultra 55 microscope

3.5 Amount of acetabular cup wear

The measure for acetabular cup wear employed was the amount of linear femoral head penetration and was measured using the following means: a hole was drilled through the acetabular cup in the apex of the wear region and the thickness of the acetabular cup was measured by putting the femoral head inside the cup and measuring with a vernier from the outside. The measured thickness was then subtracted from the original thickness, producing the amount of linear head penetration. (The original thickness is available on the markings of the cup.) An example of the hole drilled for measuring linear head penetration is shown in Figure 20 and a diagram illustrating the technique is shown in Figure 21.

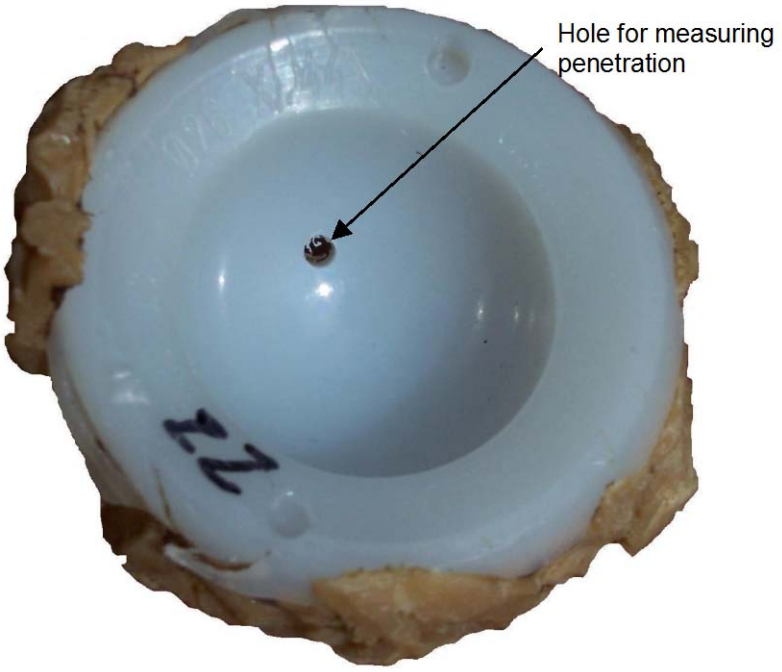

Figure 20: Hole for linear head penetration

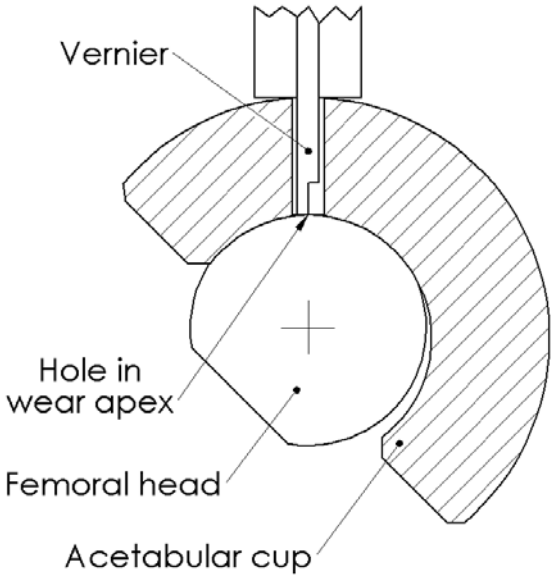

Figure 21: Penetration measurement

Great care was taken to ensure that the measurements are accurate and it is believed that the results of this are accurate within ±0.1 mm. The acetabular cups are typically manufactured with a tolerance of +0.1mm. (Burger, 2005), Therefore the measurement are believed to be within +0.2, -0.1mm accuracy.

The linear femoral head penetration can be used to calculate volumetric wear, which could theoretically be used to eliminate the effect of different head diameters on the amount of wear. As was argued in Section 3.2, different femoral head sizes create different kinetics in joints. It was therefore decided that the data would be treated in groups of similar femoral head size; subsequently the volumetric wear will not be calculated.

3.6 Sphericity

The measure used to express the sphericity of the femoral heads is the deviation in roundness (referred to as 'out of roundness' in this study) at a position of 45° between the pole and the equator of the femoral head, as is shown in Figure 22. Measurements at this position include a large part of the bearing area, as well as the wear apex as defined in Figure 16, irrespective of the rotational orientation of the specimen.

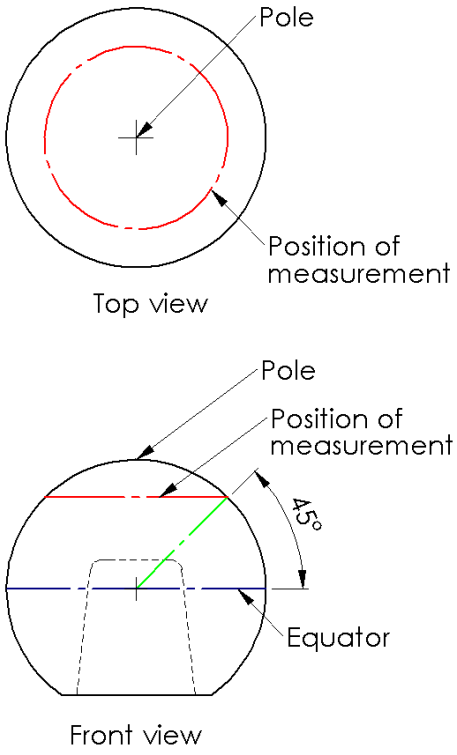

Figure 22: Roundness measurement position

The National Metrology Institute of South Africa (NMISA) took the measurements with a Taylor Hobson Talyround and provided the data in processed form as a graphical plot and a RONt value. An example of the format in which the measurements were received can be seen in Figure 37, with all the measurements attached in Section 9.

The RONt value is basically a peak to valley roundness deviation and is governed by ISO/TS 12181-1 (Thalmann and Spiller 2005). According to Thalmann and Spiller (2005), the RONt value alone is not enough to produce repeatable results, but when the study commenced it has been judged to be sufficient.

3.7 Surface finish

The surface finish was measured on the pole of each femoral head in three directions: 90°, 0° and 45°, with a sample length of 8mm, as is shown in Figure 23. The place and directions of measurement were chosen so that the wear area, as well as the wear direction can be incorporated into the data.

If the measurement positions shown in Figure 23 were imposed on the wear area shown in Figure 16, it is clear that the larger part of the measurements would be taken inside the wear area, irrespective of the in vivo rotational orientation of the specimen.

Because of the recurring movement of the joint whilst the patient is walking, the wear on the femoral head tends to be directional, as was observed by the author on similar stainless steel femoral heads. To get a good average, not influenced by the directional wear, the three positions of measurements showed in Figure 23 were chosen and the average of these three directional measurements will be used in the analysis. Only one measurement was taken for each of the control samples, as no irregularities were expected.

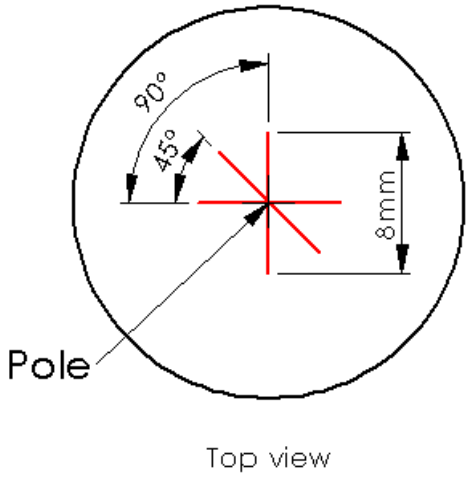

Figure 23: Surface finish measurement positions

NMISA took the measurements with a Taylor Hobson Talysurf series II and provided the data already processed in terms of a surface topography graph and the arithmetic surface mean, Ra. An example of the results received can be seen in Figure 39 with all the results attached in Section 10.

3.8 Phase transformation

The amount of phase transformation that has already taken place on the surface of each femoral head was measured by means of X-ray diffraction at the University of Pretoria. As indicated in Figure 24, a constant exposure area of 5 mm by 5 mm at the pole of the femoral head was used, with measurements taken from two directions 90° apart, as is denoted by measuring direction 1 and 2 in Figure 24.

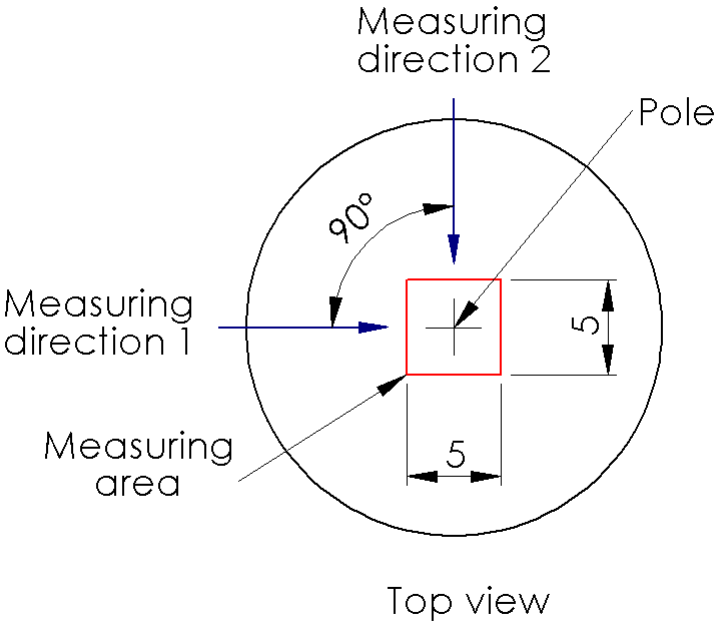

Figure 24: XRD analysis positions

The equipment used was a PANalytical X'Pert Pro Powder difractometer, shown in Figure 25, with X'Celerator detector and variable divergence- and receiving slits and Fe filtered Cu-Kα radiation. The different phases were identified by X'Pert Highscore plus software and in turn quantified with Autoquan/BGMN software form GE Inspection Technologies, using the Fundamental Parameter Approach. All of the equipment used resulted in a simple percentage value indicating the amount of monoclinic content present in the top layers of the surface of a femoral head, at the measured positions.

The X-rays used by the difractometer penetrates into the top layers of the surface (typically about 3 μm at an incidents angle of 35° in Zirconia), which means that the percentage of monoclinic content given as a result is the monoclinic content of the first couple of layers (about 6) of crystallites.

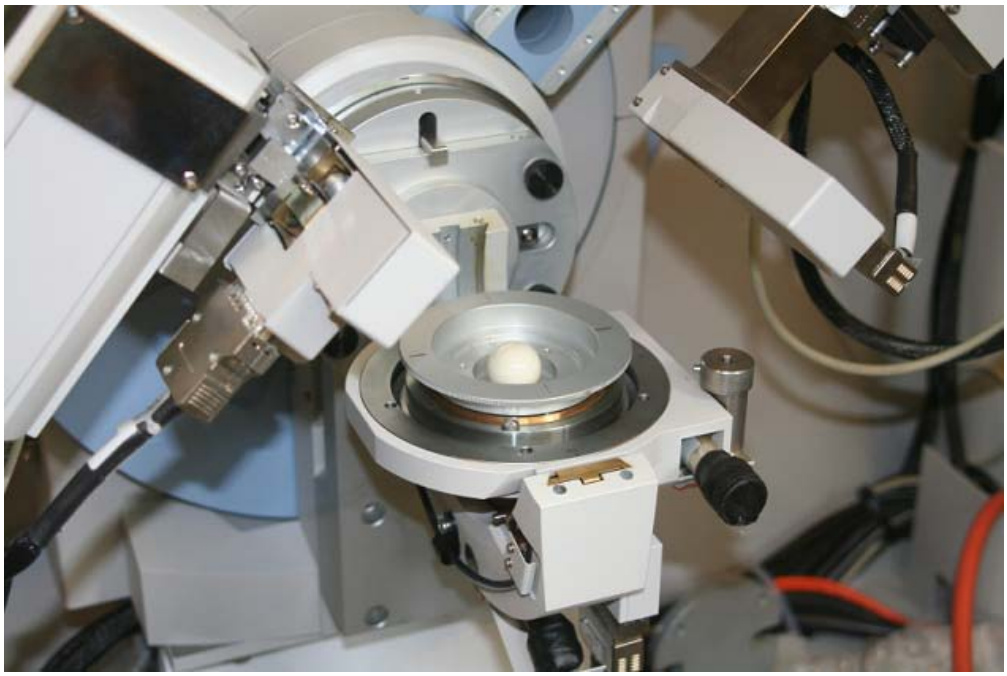

Figure 25: Specimen inside the difractometer

It would have been best to measure in the apex of the wear area, as this would give an indication of what happens at the harshest environment of the wear area, but these locations are not known, for reasons previously stated. The current measurement position shown in Figure 24 does encompass the wear area shown in Figure 16, irrespective of the in vivo rotational orientation of the femoral head and would get comparable results from each femoral head.

A diffraction graph of a couple of samples is shown in Figure 36, as part of the exemplary discussion of Section 4.1, but as the graphs are not of much practical use, the measurements were received in an already processed form, as a percentage and an error.

4 Analysis of results

The results will be offered in the following three sections:

1. An illustration of the data collection process, by using Sample 27 as a representative case.
2. The results of the whole sample group, with as many trends as can be made responsibly.
3. The results in the smaller groups, as described in Section 3.2, so that certain trends can be investigated.

4.1 Single example

Sample 27 will be elaborated to illustrate the process undergone as well as some of the observations made. The information on Sample 27 can be summarised as follows:

- Female patient, 57 years of age.
- In vivo life: 10 years.
- Clinical diagnosis: Loose cup due to aseptic loosening, significant femoral head penetration, calcar lysis of femur.
- Cup: Metal back Mont Blanc.
- Cup size: 28/54.
- Impingement: Yes.
- Adhesion wear in cup: No.
- Abrasive wear in cup: Yes.
- Femoral head penetration: 5.9 mm.
- Dull scuffing marks found on head.
- Monoclinic content: 37.3%.
- Out of roundness: 2.4 μm.
- Surface finish: Ra = 0.0757 μm.

Figure 26 is a good example of a double, total hip replacement, with one hip badly displaced and the other hip still in relatively good condition. The calcar lysis can be clearly seen, with the subsequent breakdown of the bone tissue evident by the higher transparency of the bone in that region, especially when compared to the other side. The calcar lysis was caused by a foreign body reaction to the femoral implant. The top of the femur with the calcar lysis can't support the femoral implant anymore; therefore the femoral head needs to be replaced with a longer femoral implant, similar to the one shown in Figure 8.

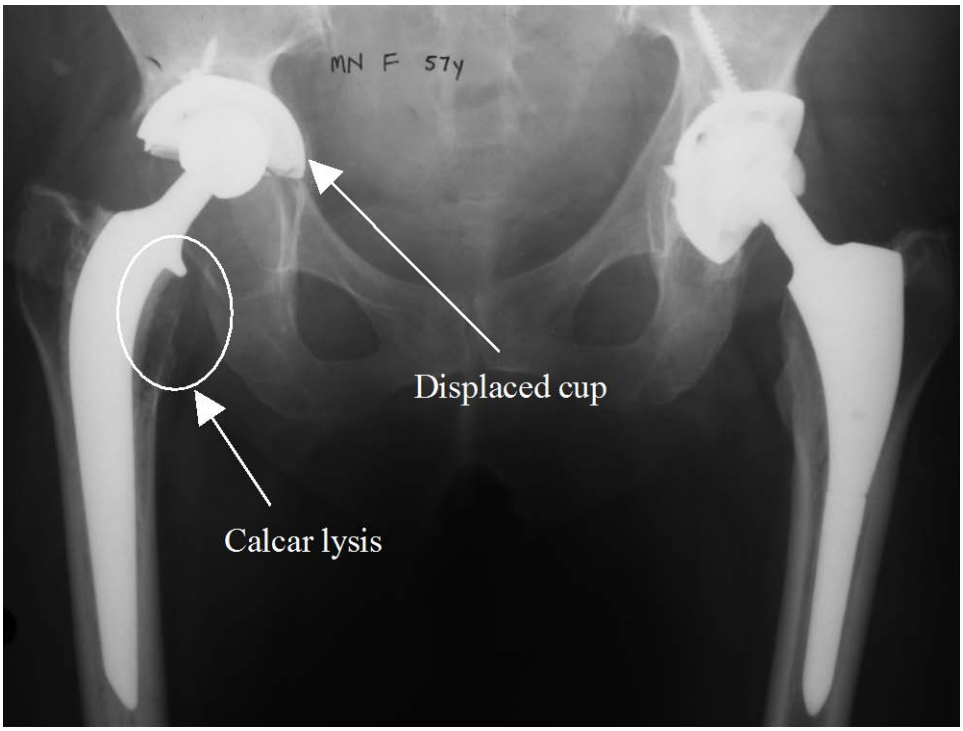

Figure 26: Patient X-ray

The difference in position between the two hip replacements, clearly illustrates the amount of displacement that the hip on the left hand side of Figure 26 underwent. This displaced hip must have caused the patient extreme discomfort. The displacement in this case is due to osteolysis, as described in the discussion pertaining to Figure 6.

Figure 27 shows the retrieved prosthesis, with the impingement caused when the cup displaced and the femoral stem impacted against the side of the acetabular cup. Judging by the size and condition of the impingement mark the patient must have walked with the displaced acetabular cup for some time before the surgery was done.

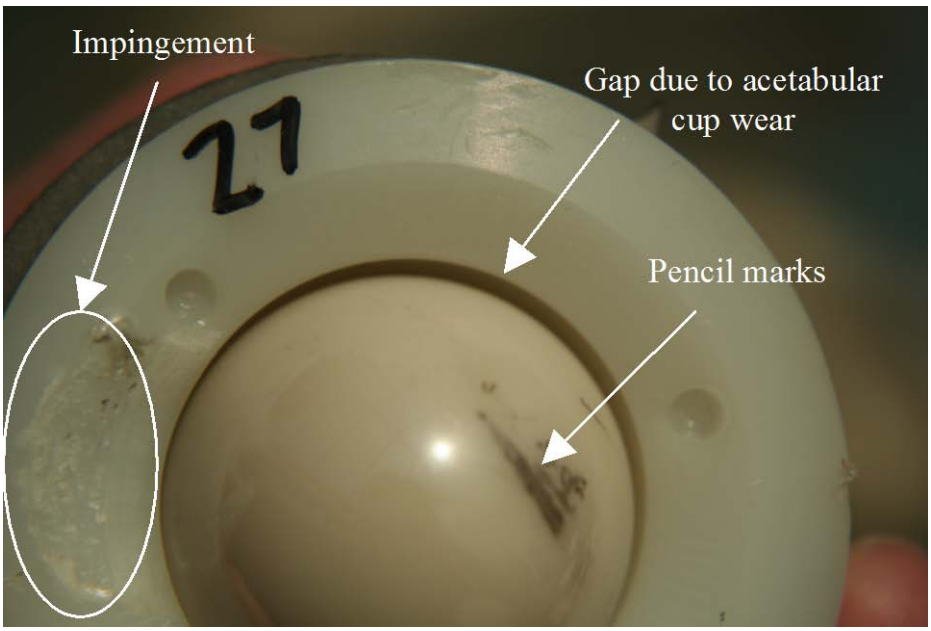

Figure 27: Sample 27, Head and Cup

The amount of wear is illustrated by the gap between the femoral head and the rim of the acetabular cup, shown in Figure 27. In new prostheses the clearance between the head and cup is about 0.2 mm. It must be kept in mind that the gap is not in the same direction as the amount of linear penetration (wear) and is therefore not 5.9 mm big.

The pencil marks, denoted in Figure 27, are areas where metal has been transferred onto the surface of the femoral head by the tools used by the surgeon when removing the femoral head from the femoral implant. Y-TZP is much harder than the stainless steel (normally 316L stainless steel) that

the tools are made of, resulting in the Y-TZP wearing away the tools, causing the metal deposit, observed as pencil marks.

The wear damage to the acetabular cup is shown in Figure 28 and clearly shows the abrasive wear, evident as scratch marks on the surface of the acetabular cup. No indications of adhesive wear, or large scale third body wear was found inside the cup. Third body wear by smaller particles could have also contributed to the abrasive wear, but separating it was not attempted due to reasons mentioned in Section 3.3.

Figure 28: Wear inside the cup

This study started when a dull patch, similar to the one shown in Figure 29 was discovered on the normally bright surface of a retrieved Y-TZP femoral head. Note the mirror like reflections on the bright surface of the femoral head. The dull patch shown in Figure 29 has the appearance of a scuffing (abrasive) mark, which immediately suggests the presence of very hard abrasive third particles inside the bearing couple, but considering the

hardness of the Zirconia used for Y-TZP femoral heads (9 on the Mohs scale), this is very unlikely.

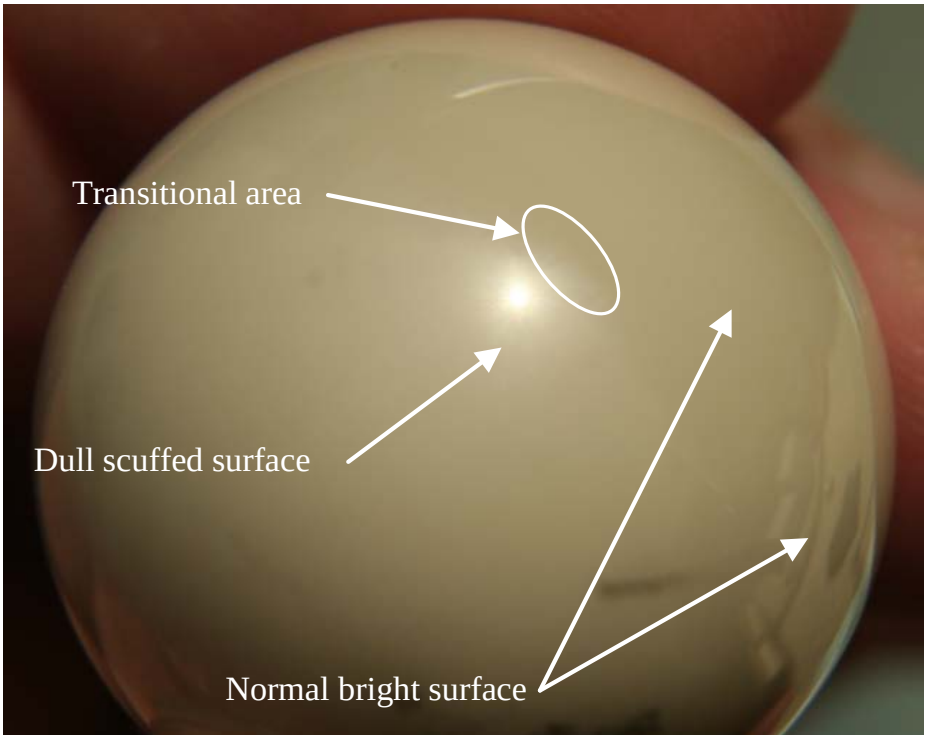

Figure 29: Dull scuffing on head

Closer investigation by means of scanning electron microscope (SEM) revealed the source of the dullness. Figure 30 shows a 3000 times magnification SEM image taken of the dull surface of the femoral head shown in Figure 29. The increased roughness of the destructed part of the surface causes the dullness. It must be noted that the same kind of surface destruction was found on the bright parts of the femoral head, shown in Figure 29 and that dull patches were evident on only four of the twenty seven retrieved Y-TZP femoral heads. It was however noticed that the amount of surface destruction appeared more on the dull parts of the femoral head, shown in Figure 29, than on its bright parts. This means that there must be a threshold of surface destruction that needs to be surpassed before it can be noticed by the naked eye.

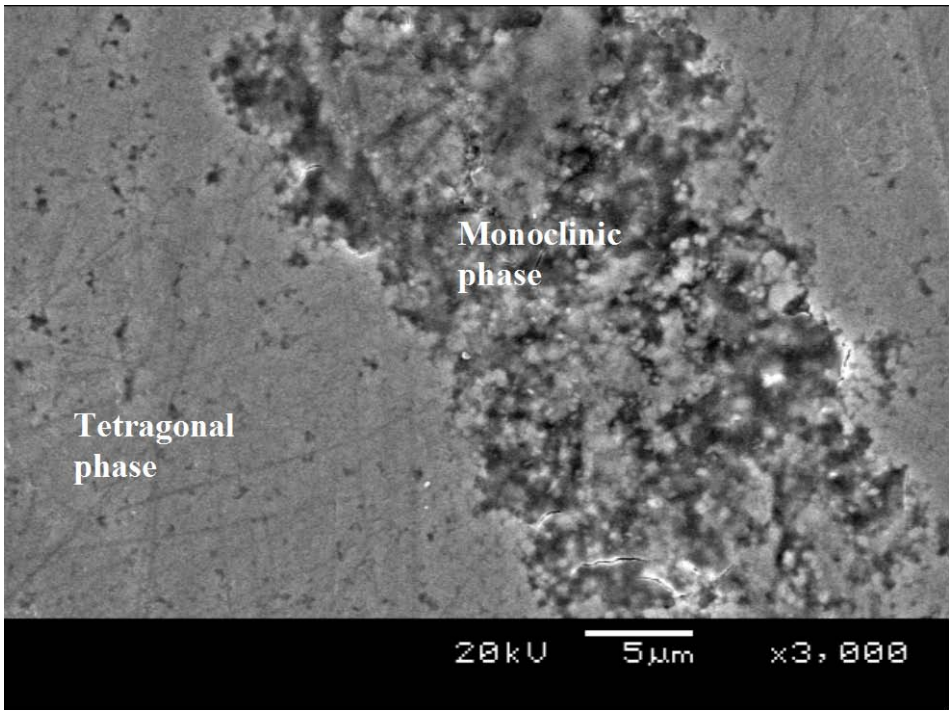

Figure 30: SEM image of surface

From the literature found on Y-TZP phase transformation and from the lesser material properties associated with the monoclinic phase of Zirconia, it can be concluded that the parts of the surface that were destructed, are largely monoclinic phase, whereas the non-damaged parts are still to a large extent tetragonal phase, as is indicated on Figure 30. An alarming fact is that the part of the surface that is still in good order is already showing signs of small craters. This would indicate that phase transformation is to some degree present in that region too.

By means of the interference filter on the backscatter detector of the Zeiss Ultra 55 microscope shown in Figure 19, the phase of the Zirconia can be determined and is visually presented as a colour difference. Figure 31 shows a normal field emission electron microscope (FEEM) image of the surface of the Y-TZP femoral head and Figure 32 shows a backscatter image of the same part of surface, whilst employing the interference filter. The polycrystalline structure of the Zirconia is well illustrated in Figure 31, by

the small crystallites, packed closely together to form the bulk material. The phase of the Zirconia refers to the phase of the small crystallites. Most of the tetragonal phase crystallites still have polished (flat) tops, whereas in the regions of monoclinic content the top layer of crystallites has been ripped out. The tetragonal crystallites are now higher than the surrounding area, still very hard and have sharp edges, which would wear away the UHMWPE like a very fine rasp.

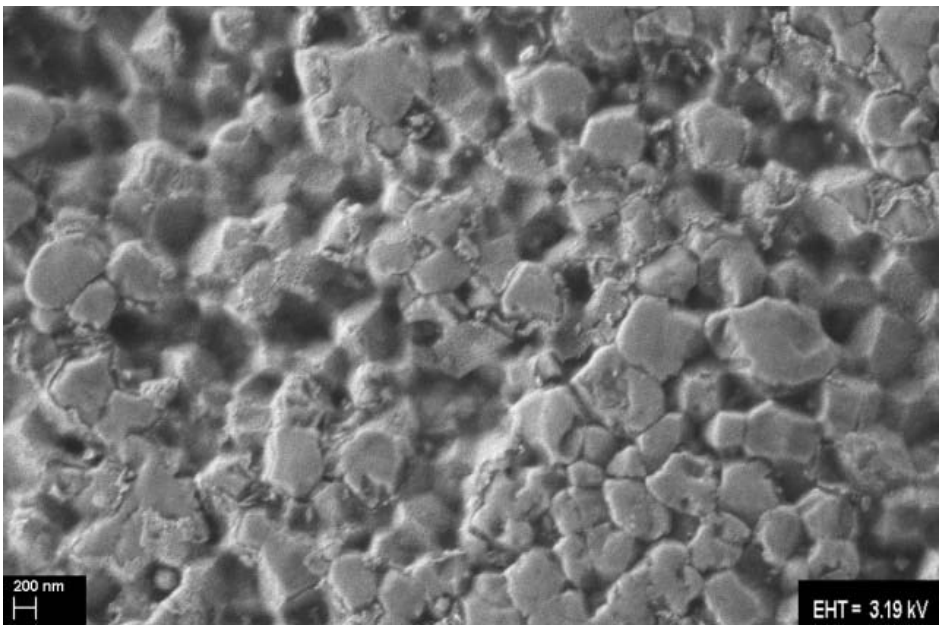

Figure 31: Field emission electron microscope image

Note that the scale bar in the bottom left hand corner of Figure 31 and Figure 32 is 200 nanometres in size, which gives an indication of how small the crystallites are that form the material.

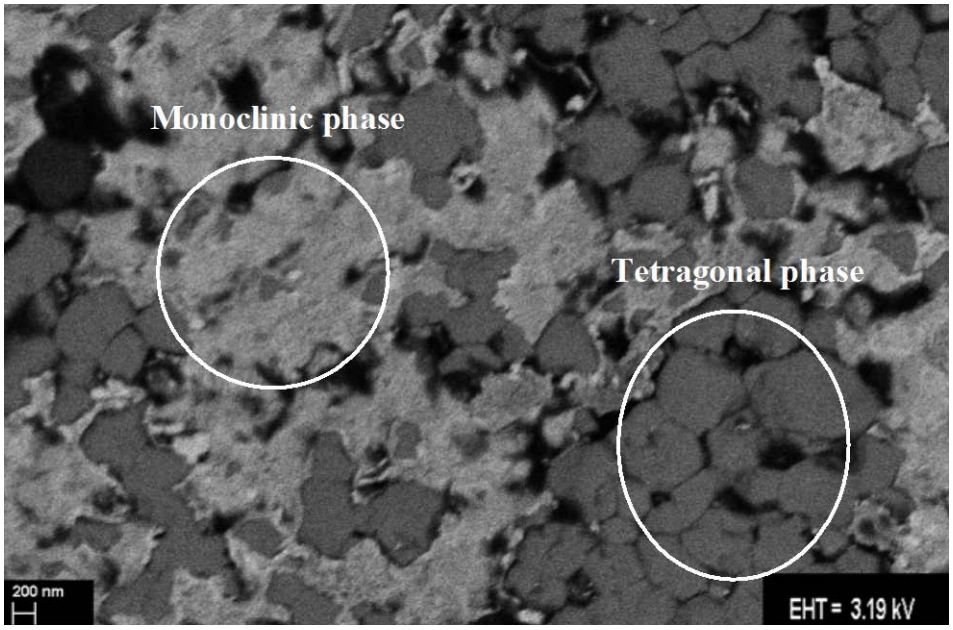

Figure 32: Backscatter image with diffraction filter

A FEEM image shown in Figure 33 is compared to a FEEM backscatter image shown in Figure 34. At first glance, Area 1 and Area 2 shown in Figure 33 seem to be abrasion marks from third body particles inside the bearing couple, or even machining marks, it is however evident from closer inspection and the different phases of each of the two areas, shown in Figure 34, that neither is the case. Due to its hard tetragonal phase and flat top surface, with small diagonal scratches (probably still machining marks), Area 1 is still part of the original top surface of the femoral head, and due to its soft monoclinic phase and much narrower shape, Area 2 is most probably an abrasion mark.

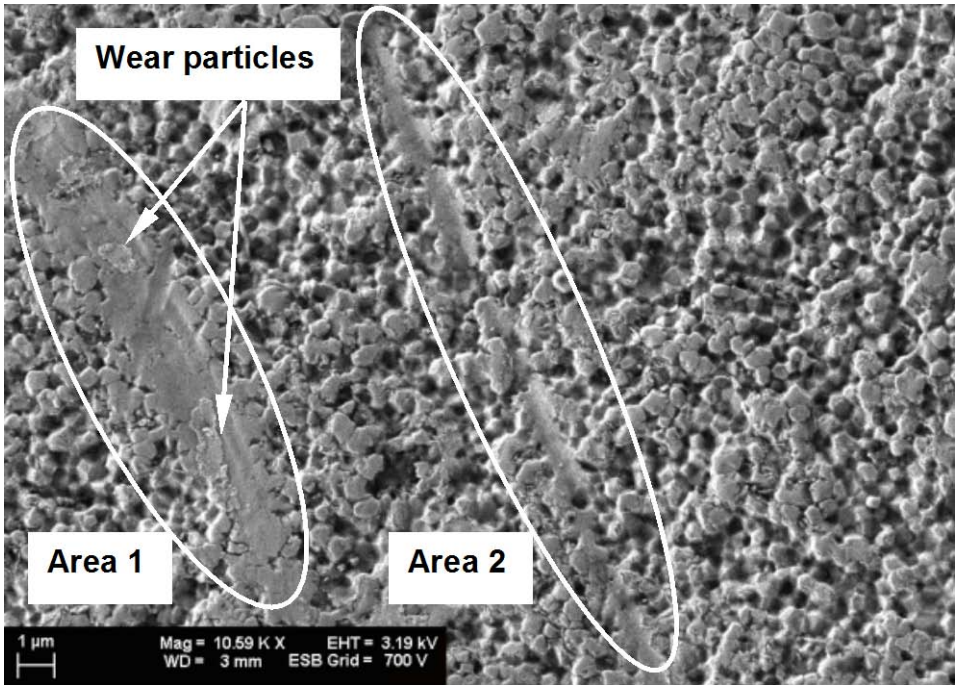

Figure 33: Normal FEEM image of wear/machining marks

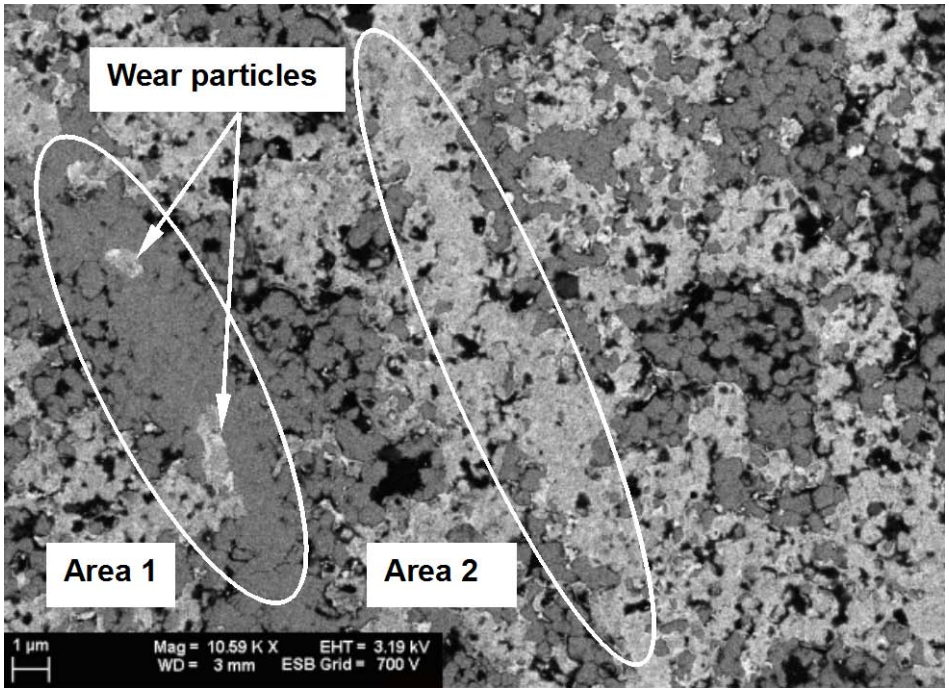

Figure 34: Backscatter image of wear/machining marks

The wear particles, denoted in Figure 33 and Figure 34, are UHMWPE that have been "welded" onto the Zirconia surface. The wear particles shown in

Figure 34 are just thick enough to disturb the backscatter electrons coming from the tetragonal Zirconia underneath and give it the appearance of the monoclinic phase. (Note that the wear particles shown in Figure 34 seem a little opaque). It must, at all times, be taken into account that the electron microscope does not construct its images from the surface, but from a very short distance (typically 1 nm to 5 nm) under the surface and that this distance increases when backscatter is employed, therefore the material under the wear particles have an influence on the image.

The wear particles as shown in Figure 33 and Figure 34, are indicative of adhesive wear (abrasive particles would tend to be long fibrous particles), yet it was recorded that no evidence of adhesive wear could be found. The wear mechanism recordings were made by investigating the condition of the acetabular cups with a magnifying glass, which accounts for macro scaled effects. The wear particles shown in Figure 33 and Figure 34 indicate micro scaled effects and therefore adhesive wear was not recorded in this case.

The SEM investigation revealed the existence of surface micro cracks, one of which is shown in Figure 35. The crack can be clearly distinguished from the machining marks by its shape: the machining marks all have very gradual, regular shapes, whereas the crack is wider, deeper and has a distinctive irregular kink, which is almost impossible to form with machining. The depth of the crack could not be determined, but if the SEM image by Haraguchi et al. (2001), shown in Figure 13, is considered, this crack does not extend beyond the first couple of crystallite layers. A crack like the one shown in Figure 35 causes a discontinuity on the surface of the femoral head, which is a starting point for surface destruction, especially in areas where monoclinic phase transformation has occurred. A surface micro crack would affect the UHMWPE wear rate depending on its width and orientation to movement. The sharp edges of the crack act like one of the

teeth on a file, albeit a very fine file. The micro crack seems so small (almost the same width as a machining mark) that it seems unlikely that it would have a considerable effect on the lifetime of the bearing, but it will be shown in the results that combining all the small surface defects does indeed have a negative effect on the amount of wear of the UHMWPE acetabular cup.

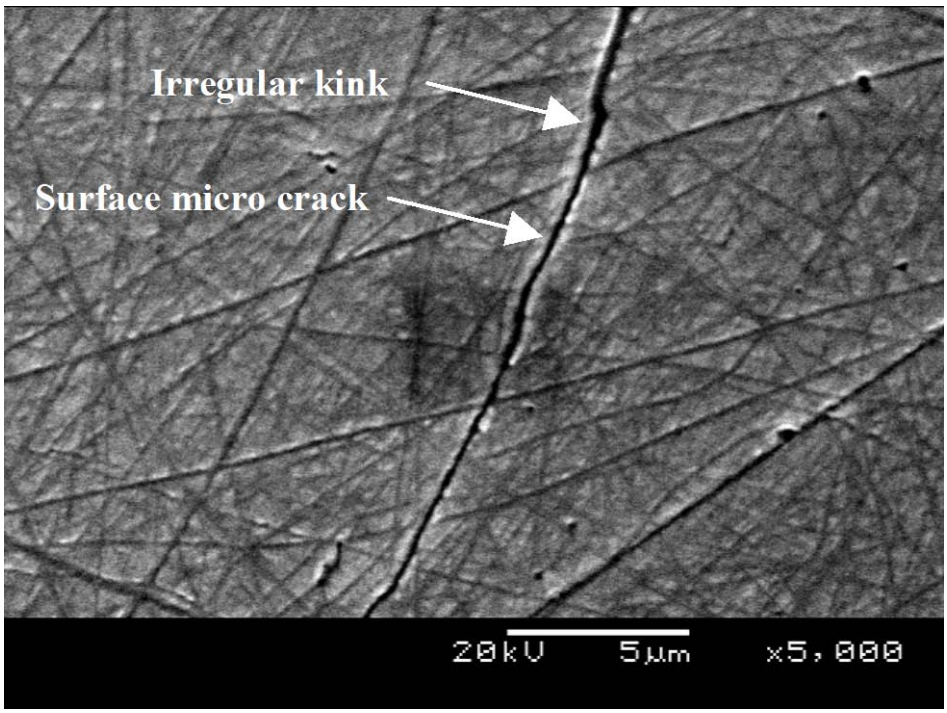

Figure 35: Surface micro crack on Y-TZP femoral head

The results of the XRD analysis are shown in Figure 36 and confirm the monoclinic content observed with the backscatter image of the FEEM. The graphical plots show the diffraction angle of the X-rays on the x-axis, with intensity on the y-axis (the figure is cropped to the right hand side for legibility's sake). The two peaks denoted in Figure 36, are processed into the percentage values of 37% monoclinic and 63% tetragonal, which will be used throughout the report. Note that the sample marked "Hip_Original" only has the slightest monoclinic peak, as expected.

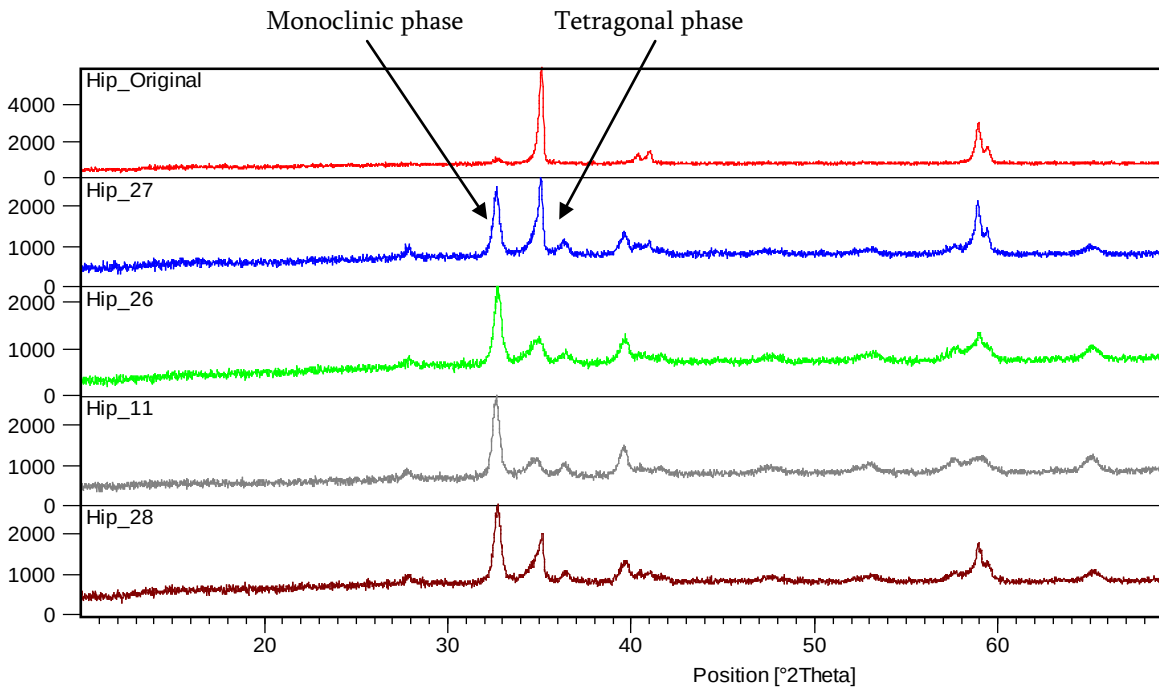

Figure 36: XRD results for various samples, including Sample 27

The roundness measurement for sample 27 is shown in Figure 37 and can be compared with the measurement for one of the control samples shown in Figure 38. The differences between the two samples are clear, but note the difference in scale between the two figures. The control sample is plotted at twice the scale of Sample 27. Therefore when Sample 27 is compared to the new femoral head, the roundness deviation seems less severe.

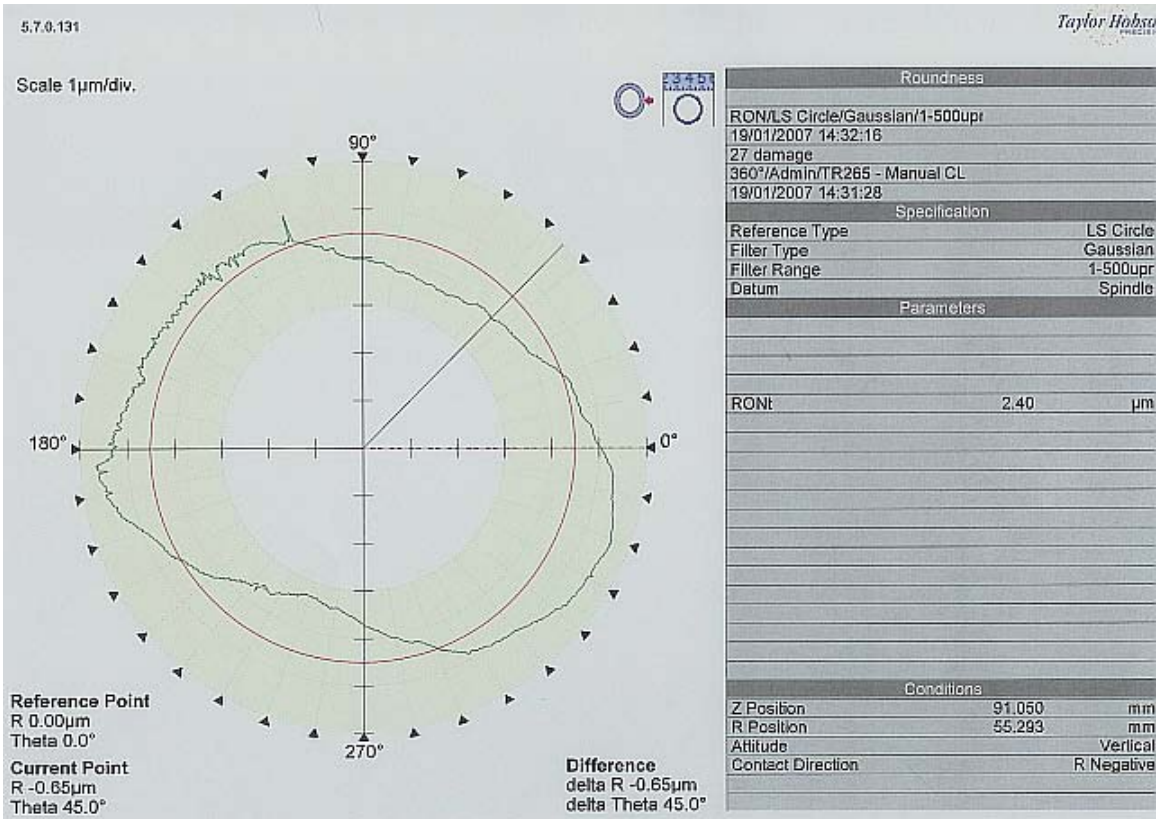

Figure 37: Roundness – Sample 27 (RONt 2.4µm)

The femoral head of Sample 27 is reshaped into an oval form, whereas the control sample has several (seven major) "protrusions". The oval shape of Sample 27 is most probably due to the effect of the wear area, which is encompassed in the measurements. As the position of the wear apex for Sample 27 is not known, it is uncertain whether it causes the bigger diameter parts due to volume increase during phase transformation, or the smaller diameter parts due to wear of the softer monoclinic phase. Note that the median circle is a calculated mean and not the original diameter before implantation. The reshaped oval shape of sample 27 is however not optimal for bearing performance.

Figure 38: Roundness – Control sample (RONt = 0.66µm)

The surface finish measurement for Sample 27 is shown in Figure 39, with the comparative measurement for a control sample shown in Figure 40. As with the roundness measurements, the differences are obvious, even with the control sample being plotted on a scale two times bigger than the scale of Sample 27.

The graphical plots illustrate the difference in Ra values (Ra = 0.0744µm for Sample 27 and Ra = 0.0187µm for the control sample) very well. The sharp peaks in Figure 39 indicate extremities on the surface, which would accelerate wear of the acetabular cup and cause higher friction, which is why a smooth, even surface, as shown in Figure 40, is essential to good bearing operation.

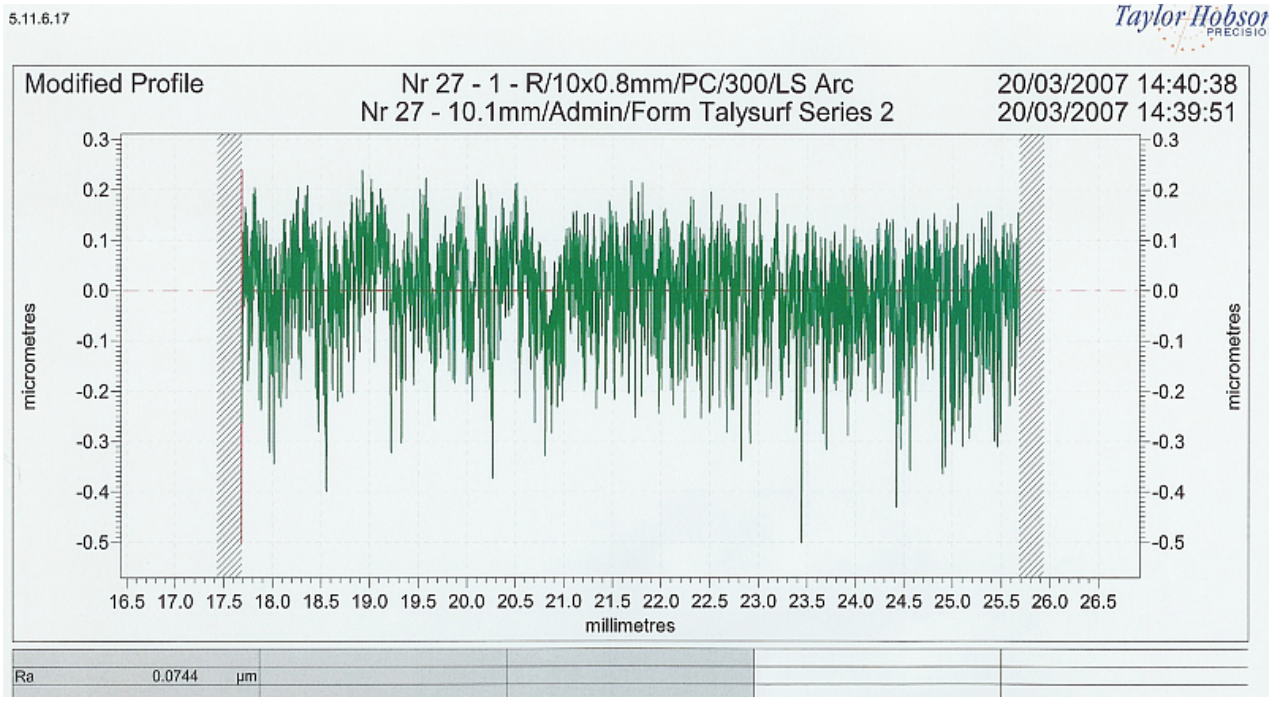

Figure 39: Surface finish – Sample 27 (Ra = 0.0744 µm)

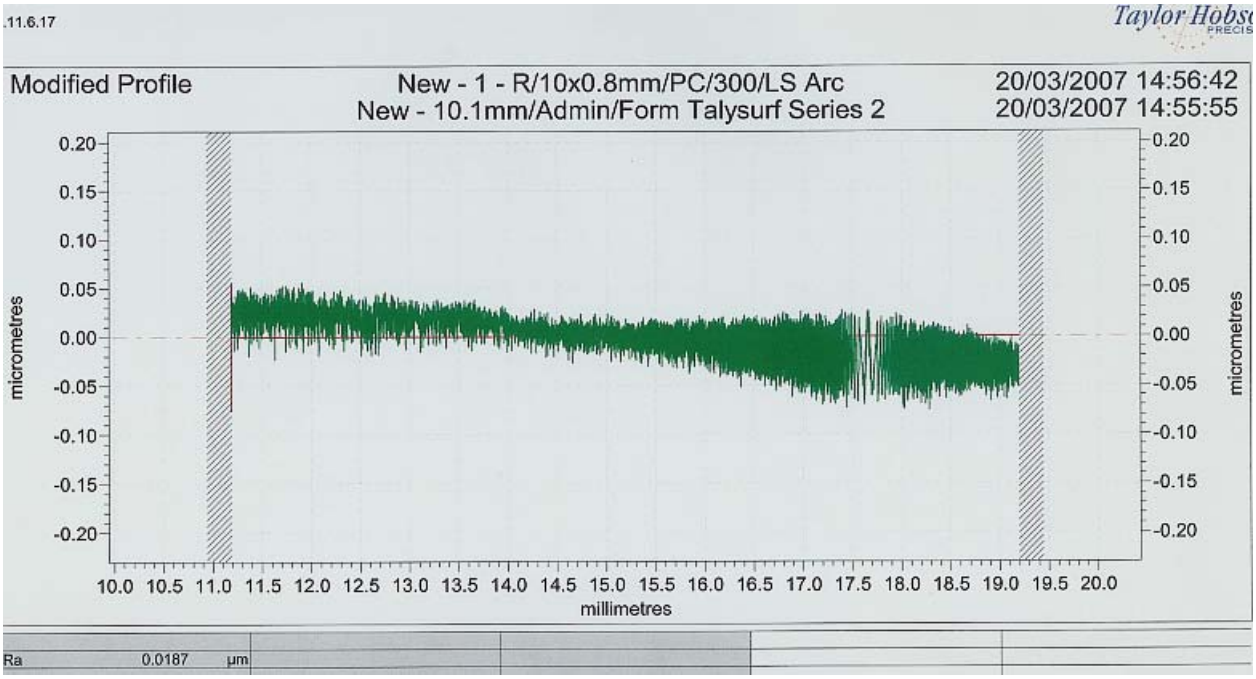

Figure 40: Surface finish – Control sample (Ra = 0.0187µm)

4.2 Whole sample

A total of 27 samples were retrieved from patients and three new femoral heads were used as controls. Sample number 18 had an in vivo life of 9 years, only transformed to a monoclinic content of 11%, only penetrated 2mm into the cup and exhibits very little surface degradation in terms of roundness and surface finish. This is uncommon and suggests that the patient was very inactive, which in turn is uncommon as the patient is only 62 years of age. Due to the lack of sufficient patient detail no judgement can be made on this issue and it was subsequently decided to omit the data for sample 18 in all of the data analysis, as it would introduce uncertainty into the data.

One of the three new femoral heads that were used in the control group (Sample 30) showed a monoclinic content of 9.61%, which is more than the ASTM F1873-98 standard of 5% and the 1% threshold of the manufacturer, as noted in Table 1. The high monoclinic content of this control specimen causes a misrepresentation of new femoral heads by the control group and was therefore not used in the analysis of the data, unless where it is specifically stated.

Table 3: Summary of data statistics

Property	Mean	Standard deviation
Patient age	66.5 years	10.4 years
In vivo life	10.4 years	2.3 years
Femoral head penetration	3.3 mm	1.8 mm
Femoral head penetration rate	0.32 mm/year	0.15 mm/year
Out of roundness - retrieved	3.23 μm	2.68 μm
Out of roundness - new	0.71 μm	0.07 μm
Surface finish - retrieved (Ra)	0.040 μm	0.036 μm
Surface finish - new (Ra)	0.021 μm	0.0009 μm
Monoclinic content - retrieved	53.6%	17.9%
Monoclinic content - new	1.45%	0.27%

*26 Retrieved samples, 2 control samples

According to the values given in Table 3, Y-TZP phase transformation seems to have a devastating effect on the parameters investigated, especially on the roundness and surface finish. The monoclinic content, amounting to 52.3%, is significant compared to the 5% maximum monoclinic content allowed by ASTM F1873 (See Table 1).

Figure 41 shows the worse than anticipated phase transformation on the investigated femoral heads. With the exception of sample 20, all the femoral heads have a monoclinic content of more than 20%, which creates doubt as to the findings of Chevalier et al. (1997), that concluded that at 37 °C in the human body (in vivo) Y-TZP femoral heads would take about 35 to 40 years to transform to a monoclinic content of 30 to 40%.

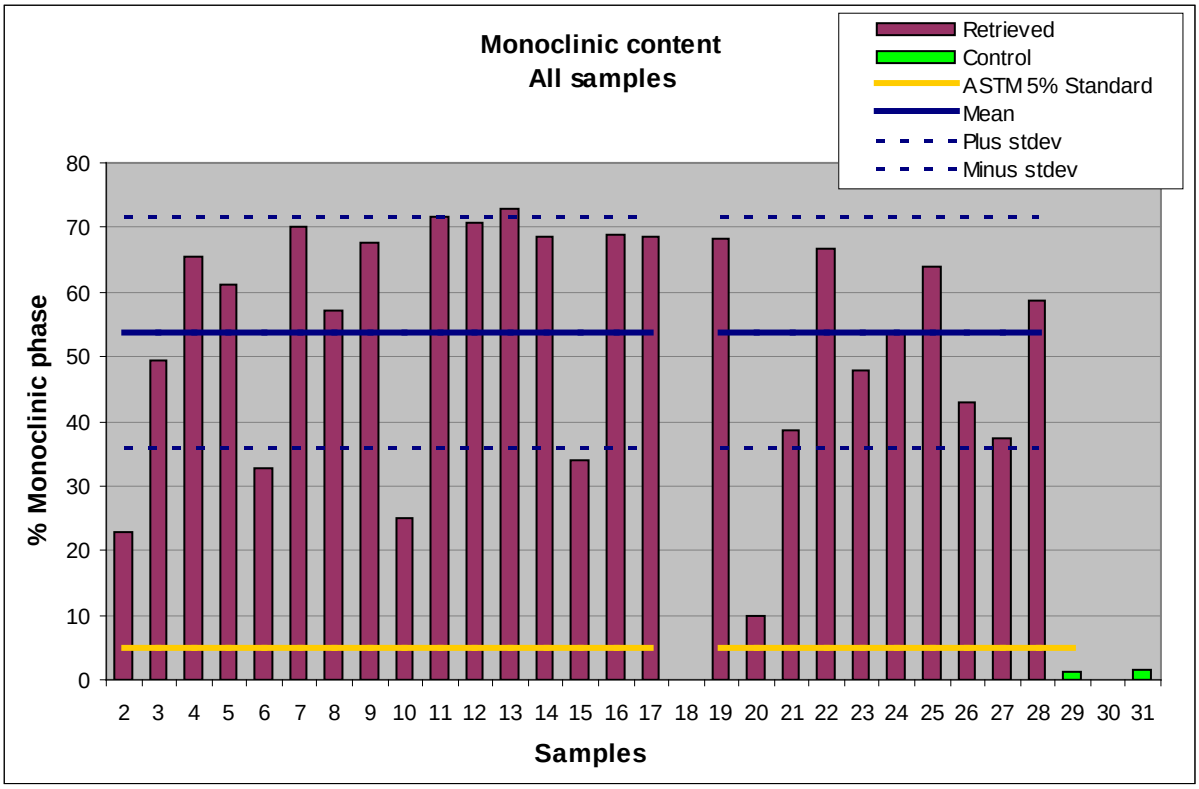

Figure 41: Monoclinic content – All samples

In Figure 42 the monoclinic content of each femoral head is compared to its in vivo life. At first glance it seems as though the values for samples 2, 10 and 20 are irregular, but patient 2 is 77 years of age and patients 10 and 20 are each 84 years of age. Therefore, these seemingly irregular samples come from much older, less active patients. It is expected that the transformation rate is slower for older, less active patients, as less activity would result in lower and less frequent high temperatures inside the bearing couple. This hypothesis will be further investigated in Section 4.3 with the data in logical groups.

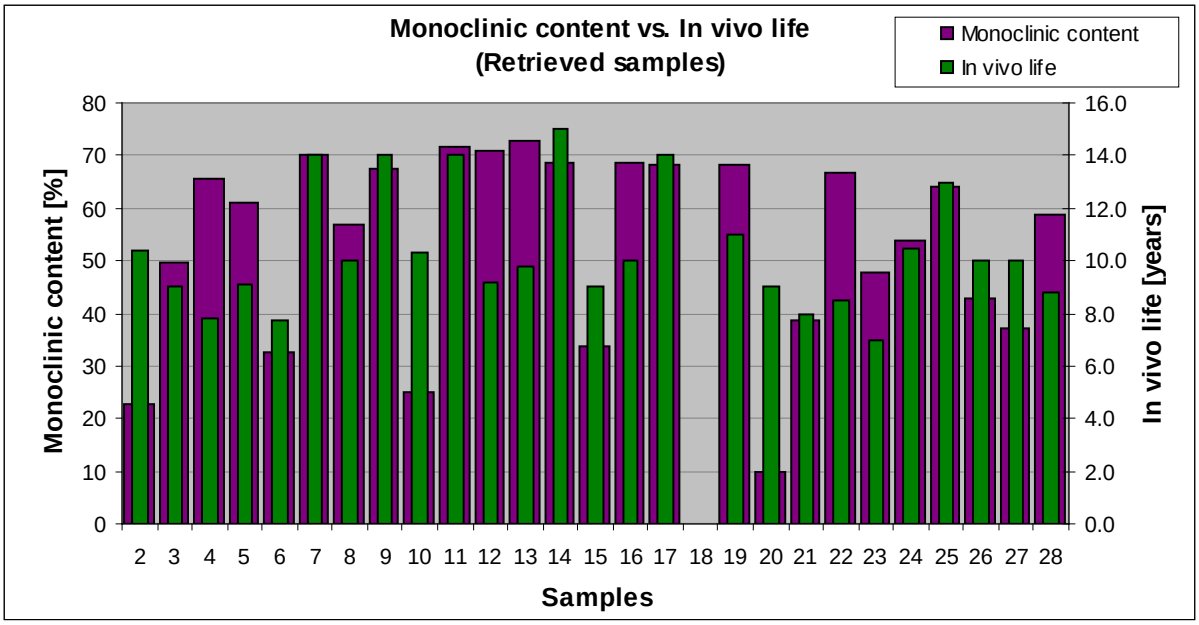

Figure 42: Monoclinic content vs. In vivo life – All samples

It seems as though the monoclinic content increases with in vivo life, which is what is expected, since the longer a Y-TZP femoral head is exposed, the more it would transform. However for reasons mentioned in Section 3.2, such a deduction cannot be made from this graph and will be further investigated with the logical groups of Section 4.3.

Out of roundness for the whole sample group is shown in Figure 43. Note that the horizontal lines denote the mean and one standard deviation, which does not include the data from the control samples 29, 30 and 31.

When the out of roundness of the retrieved samples are compared to the control samples, the literal "bad shape" of the retrieved femoral heads is evident.

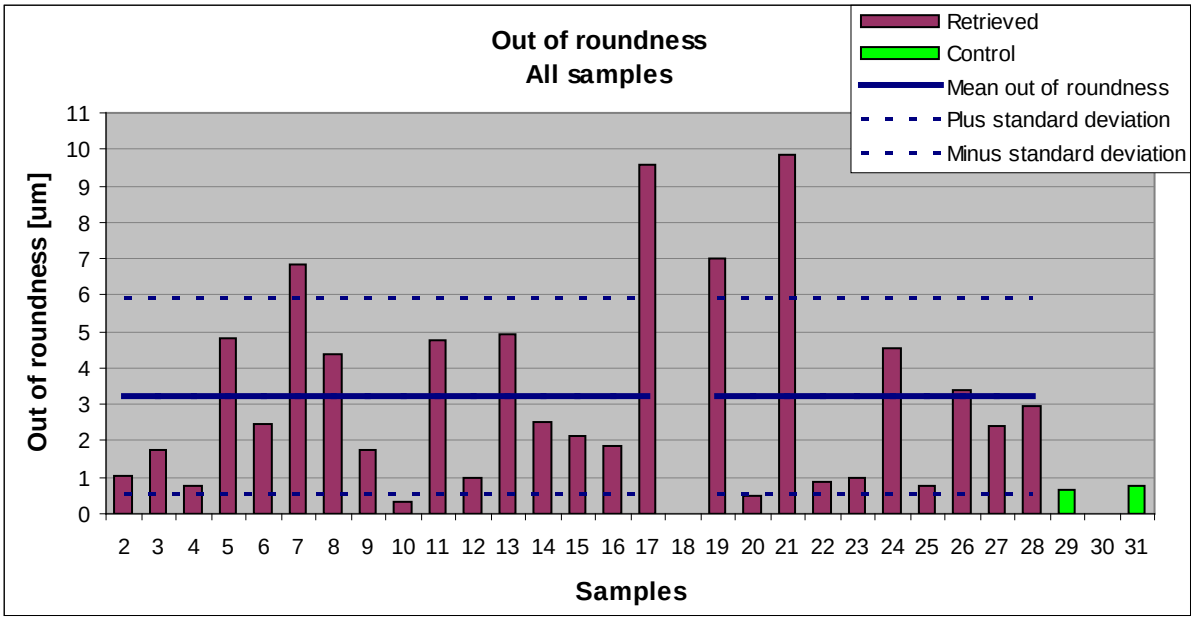

Figure 43: Out of roundness – All samples

In the above case, samples 10 and 20 show far less out of roundness than the other samples, which is consistent with the less monoclinic content associated with the high age of the two patients (77 and 84 respectively), as discussed in the paragraph relating to Figure 42.

The out of roundness data does show another alarming factor and that is that the RONt value is driven by the probabilistic occurrence of a scratch, or even a dust particle. This is evident when comparing the results of Sample 7 with Sample 19, given in Section 10. Sample 19 has a far worse shape than Sample 7, but both have similar RONt values, because Sample 7 has one large protrusion.

No quantitative comparison can be made between the roundness measurements and the measured data is not available in raw format to obtain more meaningful results.

To obtain some information from the roundness measurements, all the graphs are compared with each other and it can be concluded that the retrieved samples does indeed have a shape not suitable for bearing operation.

The surface finish for all the samples are shown in Figure 44, with the mean surface finish and associated standard deviation denoted by the horizontal lines. The mean minus one standard deviation line is at Ra = 0.005µm, which is incidentally the surface finish quoted by Hernigou and Bahrami (2003) for new femoral heads.

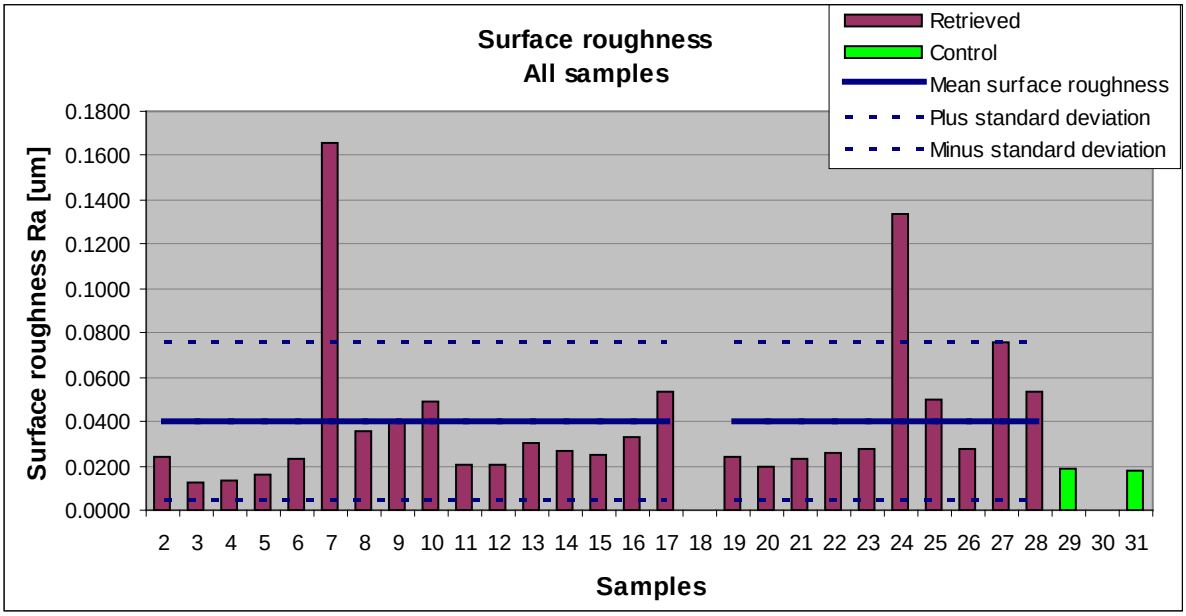

Figure 44: Surface finish – All samples

The surface finish for the two control samples appears to be excessively rough for new femoral heads (Ra of 0.0187µm opposed to the 0.005µm quoted by Hernigou and Bahrami (2003)). The surface measurements for Sample 29, shown in Figure 45, shows a difference between the measurement mean and the physical mean, as is denoted in the figure. This difference between means would have an exaggerating effect on the Ra

value, as the Ra value is the arithmetic mean of the absolute values of the data points collected. The amount by which the Ra value is exaggerated could not be determined, but judging by Figure 45, it is most probably not enough to account for the full difference between the measured amount and that of Hernigou and Bahrami (2003).

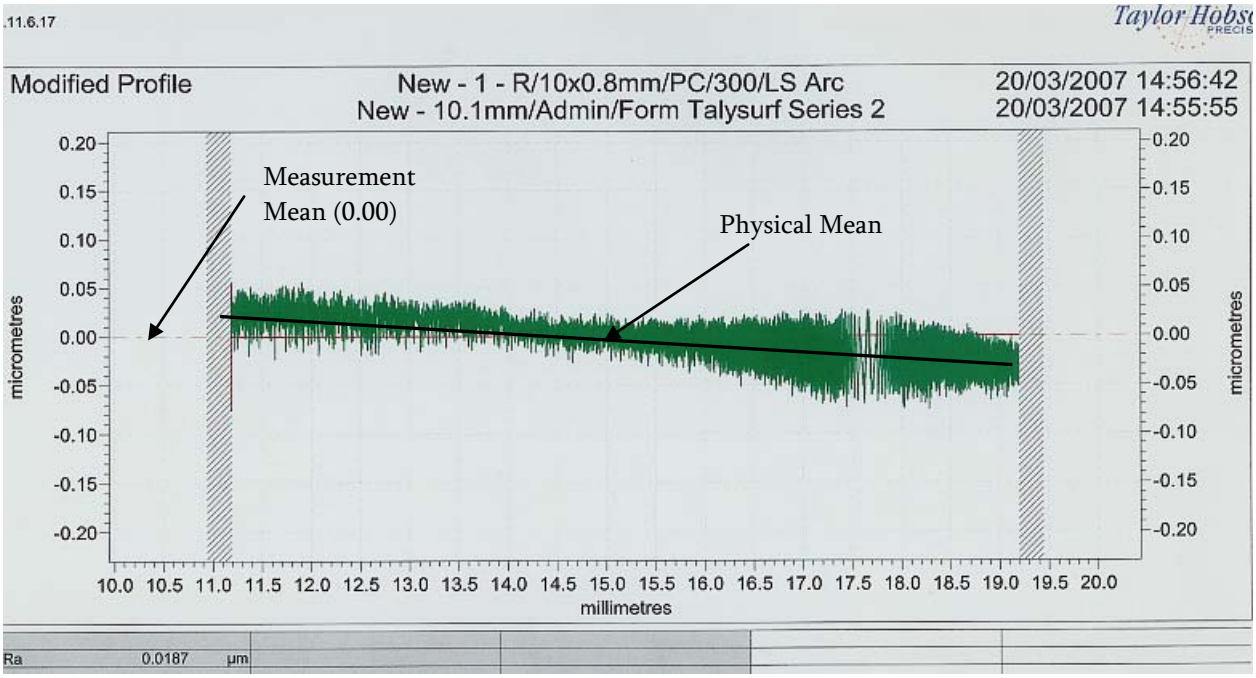

Figure 45: Surface finish measurement – Sample 29

The origin of the deviation between the two means is most probably because of an over or under estimation of the femoral head centre. The reference for all of the measurements is the taper hole in the femoral head, as the heads were put on a taper, which was gripped in the measuring device. In the case of the control samples, the taper was, most probably, not in the centre of the femoral head and caused the means deviation. This deviation could have been eliminated with the use of the post-processing software or with an algorithm. Unfortunately the data was received in processed form, without access to the raw data.

A manual method of taking the deviation was implemented in the following manner: A linear regression line was drawn on the graphical plot and its Ra value was calculated and subtracted from the given Ra value. This could be done because the Ra value is an arithmetic mean. This method resulted in values with a far larger margin of error, partly because of the y-axis scale on the graphical plots. All samples are not plotted on the same scale, therefore a sample that has some large indents/protrusions like Sample 9 is plotted on a much larger scale than the other samples, which make it difficult to capture an offset with the same magnitude as Sample 8 for instance. This method was subsequently abandoned.

A rational method of dealing with the means deviation was adopted to be able to salvage some information from the measurements taken. From Sample 5 to 31 the same means deviation is noticed, but is more prominent in the following samples: 5, 11, 12, 13, 14, 15, 19, 20, 21, 22, 23 and 26. These are all samples that are relatively less rough (low Ra values), hence the prominence of the means deviation phenomenon. From the plotted data shown in Section 10 it seems as though the means deviation is nearly the same for all the samples mentioned (Samples 5 to 31) and therefore these samples can, even though not completely accurate in terms of Ra values, be compared with each other. Samples 2, 3 and 4 do not exhibit the same amount of means deviation. These femoral heads are 28mm Prozyr® femoral heads and will be dealt with extreme caution when the data is analysed in logical groups, as the values of the other samples are higher in relation to these three than they should be. Further caution will be taken when analysing the data, as not to make unfounded claims.

The debate about the means deviation should not overshadow the fact that the surfaces measured are, by far, rougher than is needed for optimal bearing operation inside the hip joint.

Femoral head penetration gives an indication as to the amount of acetabular cup wear and is strongly dependant on the length of time that the prosthesis was inside the body, therefore femoral head penetration and in vivo time should always be considered together. For this reason the femoral head penetration is plotted against the in vivo life of the prosthesis in Figure 46.

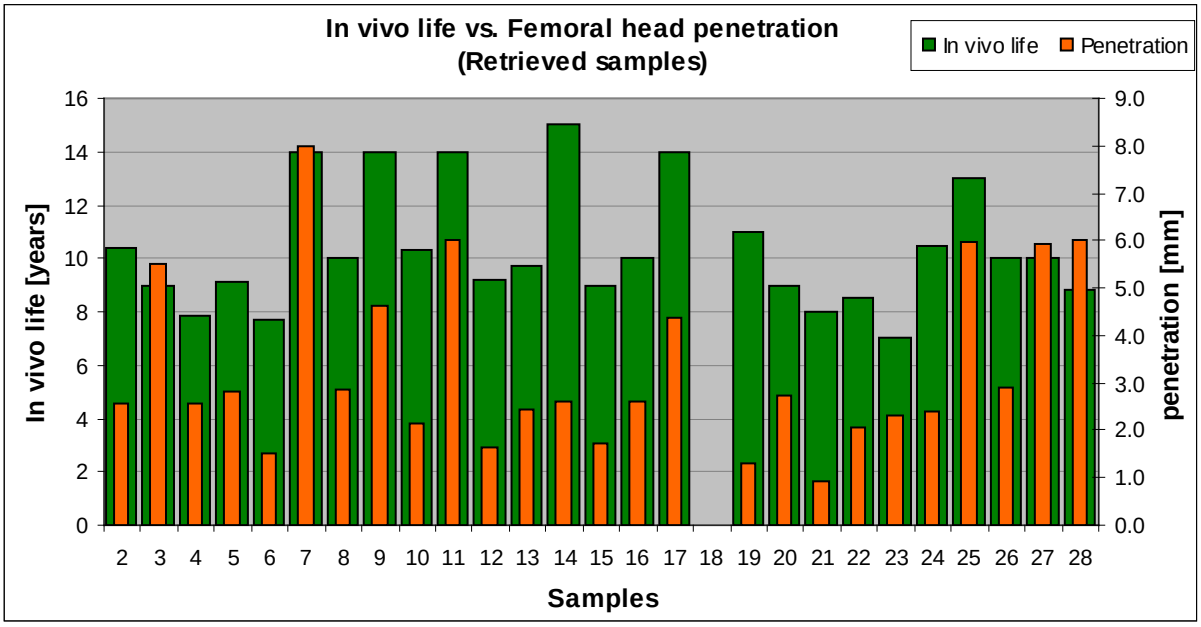

Figure 46: In vivo life vs. femoral head penetration

From Figure 46 it seems evident that femoral head penetration is dependent not only on the in vivo life, but also on age, as Samples 3, 7, 27 and 28 are much younger and probably more active patients. However as femoral head penetration is also dependent on other factors (like femoral head diameter etc.) mentioned in Section 3.2, these trends will be investigated with the data in logical groups.

The large amount of femoral head penetration of Sample 7 (14mm femoral head penetration) is an example of where the acetabular cup has worn through completely, as can be seen in Figure 47. The femoral head was in

this case, after wearing through the cup, articulating against the bone cement used to fixate the acetabular cup. A case where revision surgery is necessary due to a worn through acetabular cup can be considered to be ideal, as the acetabular cup was fully used. It must however be kept in mind that the UHMWPE wear particles that were created, remain in the body after surgery and will cause osteolysis when coming into contact with bone. In other words: the revision prosthesis may loosen due to osteolysis caused by wear particles created by the first prosthesis. Secondly, if the wear rate of the acetabular cup was reduced, the prosthesis would have lasted longer. It is therefore still important to reduce the amount of acetabular cup wear.

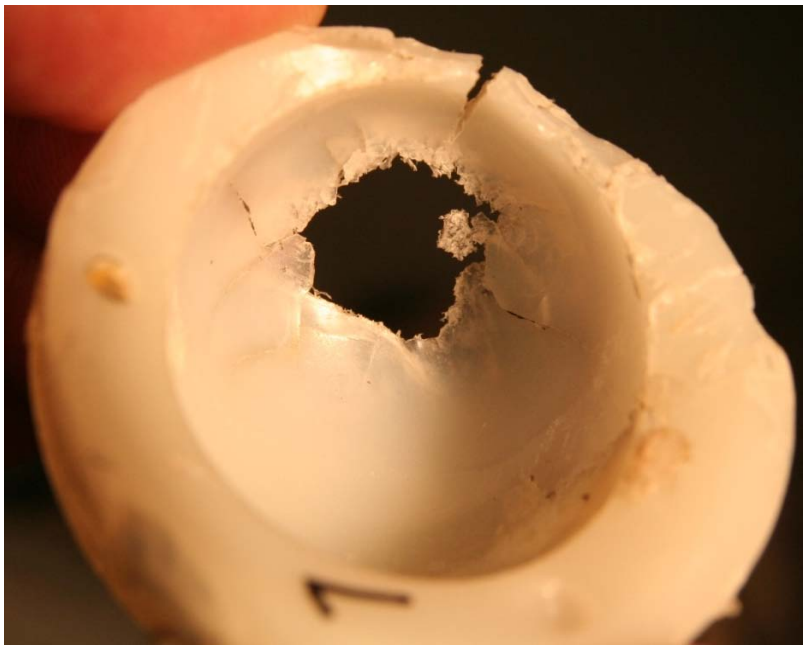

Figure 47: Sample 7 worn through

When compared to the monoclinic content, the surface finish and roundness are characteristics that would be relatively independent of femoral head size, manufacturer, process, age and activity.

A trend could be found by inspection that relates an increase in monoclinic content to degrading roundness. The three samples with the worst shape are Samples 19, 21 and 23, which has monoclinic contents of 68%, 38% and 47% respectively, which indicates, that monoclinic content adversely affects roundness of the femoral head.

Figure 49 shows the results for surface finish vs. monoclinic content, with Samples 2, 3 and 4 omitted due to the mean deviation mentioned in the discussions relating to Figure 45.

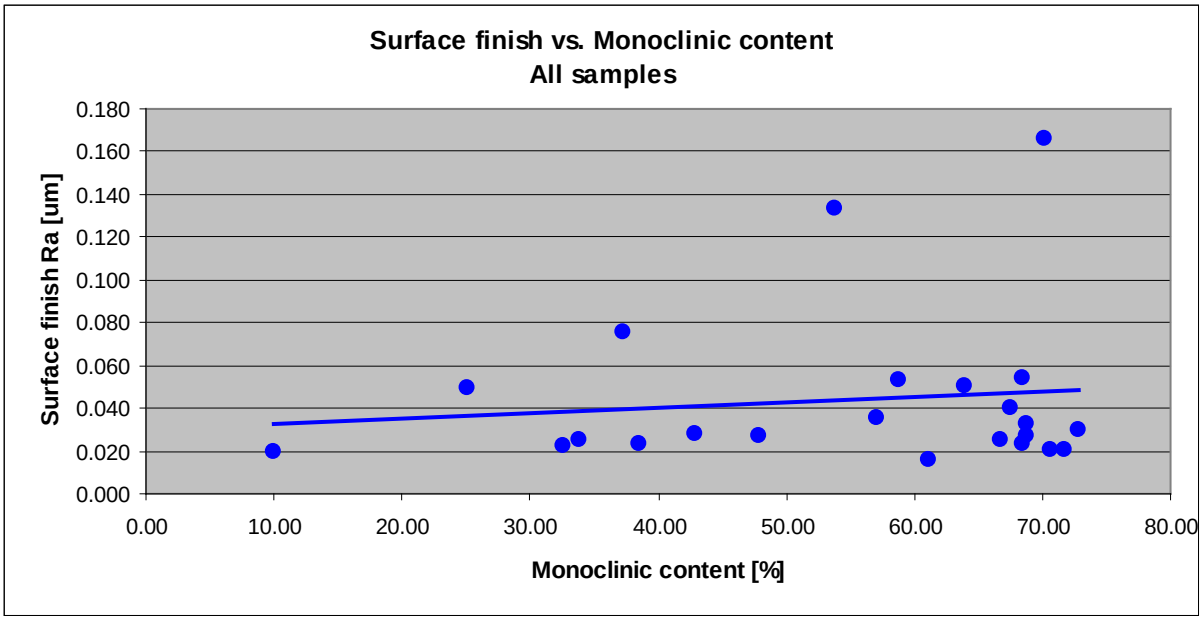

Figure 48: Surface finish vs. Monoclinic content – All samples

Figure 49 illustrates that the surface finish deteriorates as the monoclinic content increases. As there is doubt as to the accuracy of the surface measurements, as discussed on p86, this relationship cannot be taken as an absolute result, but if reasoned that the more monoclinic phase present the more defects as shown in Figure 30 would be present, this can actually be a fair result.

There is a large amount of scatter evident in the data shown in Figure 49, especially in the samples that have been significantly transformed. One factor that would influence the amount of scatter in the surface condition data is femoral head wear. Femoral head wear can either correct the surface damage caused by the ± 5% volume increase of phase transformation by wearing down asperities, or aggravate the surface damage by grain pull-out. The only way to establish the dominant mechanism is to compare the surface conditions on the exact same part or parts of the surface prior to implantation and after retrieval, which was not possible for this study.

The acetabular cups were investigated with a magnifying glass and the wear mechanisms evident in the cups were recorded and are shown in Table 4. From the results it is evident that abrasive wear is the dominant wear mechanism, as evidence of it was found in 100% of the acetabular cups, whereas evidence of adhesive wear was only found in 67% of the acetabular cups.

Table 4: Acetabular wear mechanisms

Sample Nr.	Adhesive wear	Abrasive wear
2	No	Yes
3	Yes	Yes
4	Yes	Yes
5	Yes	Yes
6	No	Yes
7	Yes	Yes
8	Yes	Yes
9	Yes	Yes
10	No	Yes
11	Yes	Yes
12	No	Yes
13	Yes	Yes
14	Yes	Yes
15	Yes	Yes
16	Yes	Yes
17	No	Yes
18	Yes	Yes
19	No	Yes
20	Yes	Yes
21	Yes	Yes
22	No	Yes
23	Yes	Yes
24	Yes	Yes
25	No	Yes
26	Yes	Yes
27	No	Yes
28	Yes	Yes

According to studies by Burger (2005), adhesive wear is a more dominant occurrence in non-crosslinked UHMWPE, than abrasive wear, which means that the results shown in Table 4 indicate a change in the major wear mechanism inside the bearing couple due to surface deterioration associated with Y-TZP phase transformation.

The lesser occurrence of adhesive wear could be attributed to more than just the deteriorated surfaces that physically scratch the acetabular cup. The deteriorated surface possesses more recesses were joint fluid is trapped, which forms a barrier layer between the two articulating surfaces that

prevents the UHMWPE from adhering to the femoral head. From the amount of abrasive wear, it is obvious that the trapped fluid does not provide lubrication that is sufficient enough to reduce abrasive wear.

4.3 Data in logical groups

For reasons discussed in Section 3.2 the Ø 28 mm femoral heads will be used in logical groups to analyse the data further and as an attempt to find relationships. Note that the data for Sample 18 will not be included in this part, because of uncertainty, as discussed in Section 4.2.

There are three Ø 28 mm femoral head size groups: HIP'ed Prozyr®, non-HIP'ed Prozyr® and the FII group. The general statistical results for these groups are shown in Table 5.

Table 5: Statistical summary of Ø 28 mm groups

	Non-HIP'ed		HIP'ed		FII	
Feature	Average	Standard deviation	Average	Standard deviation	Average	Standard deviation
In vivo life [years]	9.9	2.3	9.6	0.8	14.0	0.8
Patient age [years]	60.2	10.3	70.7	13.6	66.5	4.0
Monoclinic content [%]	63.4	2.7	37.1	1.5	68.2	3.2
Trans. rate [%/year]	6.5	1.3	3.9	1.5	4.9	0.2
Surf finish [µm Ra]*	0.046	0.065	0.043	0.037	0.038	0.016
Penetration [mm]	3.8	2.7	2.8	1.2	4.1	1.4
Penetration rate [mm/yr]	0.39	0.18	0.29	0.14	0.30	0.12

*Values are indicative only. See discussion on p85-86.

The first results to compare are from the the HIP'ed and non-HIP'ed groups. Figure 50 shows a scatter plot for the 28 mm Prozyr® group, which is divided into HIP'ed and non-HIP'ed groups. The serial numbers of the femoral heads are used as x-axis instead of implant date, because it orders the

data in manufacturing order. The implant date was however used to determine where the split is between the HIP'ed and non-HIP'ed groups.

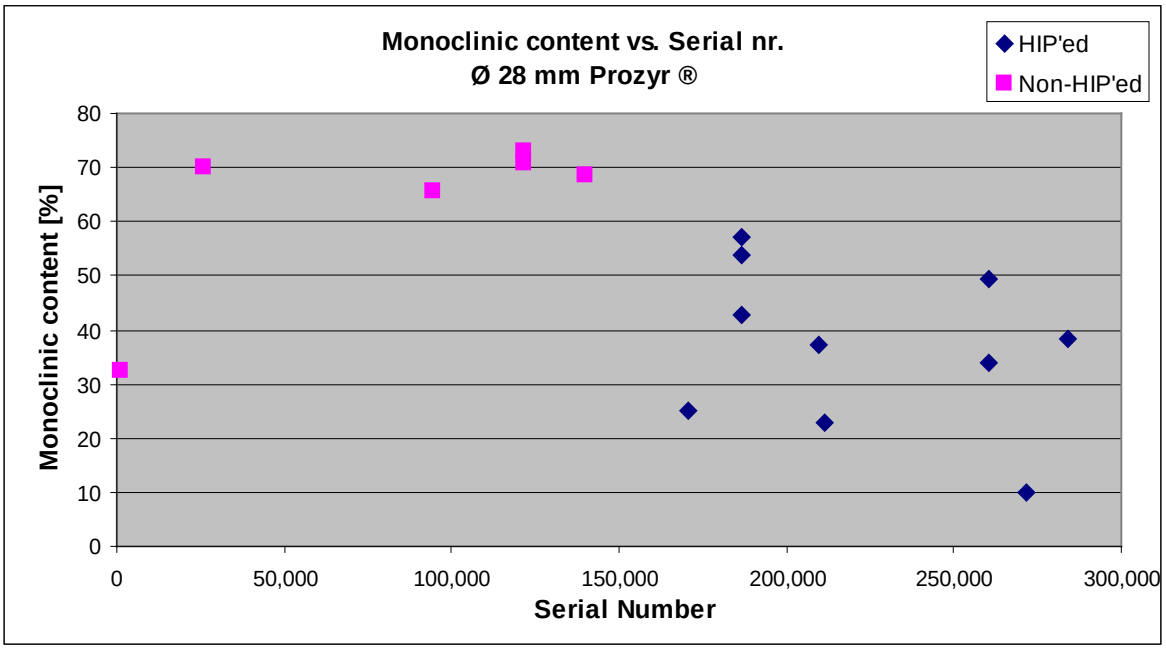

Figure 49: Monoclinic content - Ø 28mm Prozyr®

A major difference in the monoclinic content exists between the HIP'ed and non-HIP'ed groups (an average of 63% as opposed to 37%), but phase transformation is a time dependent phenomenon, as was illustrated by Chevallier et al. (1999:2151). Even though the average in vivo lifetime is similar for the non-Hipped and Hipped Prozyr® groups (9.9 years and 9.6 years respectively), the monoclinic content was normalised by dividing it with the in vivo lifetime of the hip replacement and naming it transformation rate. This is shown in Figure 51.

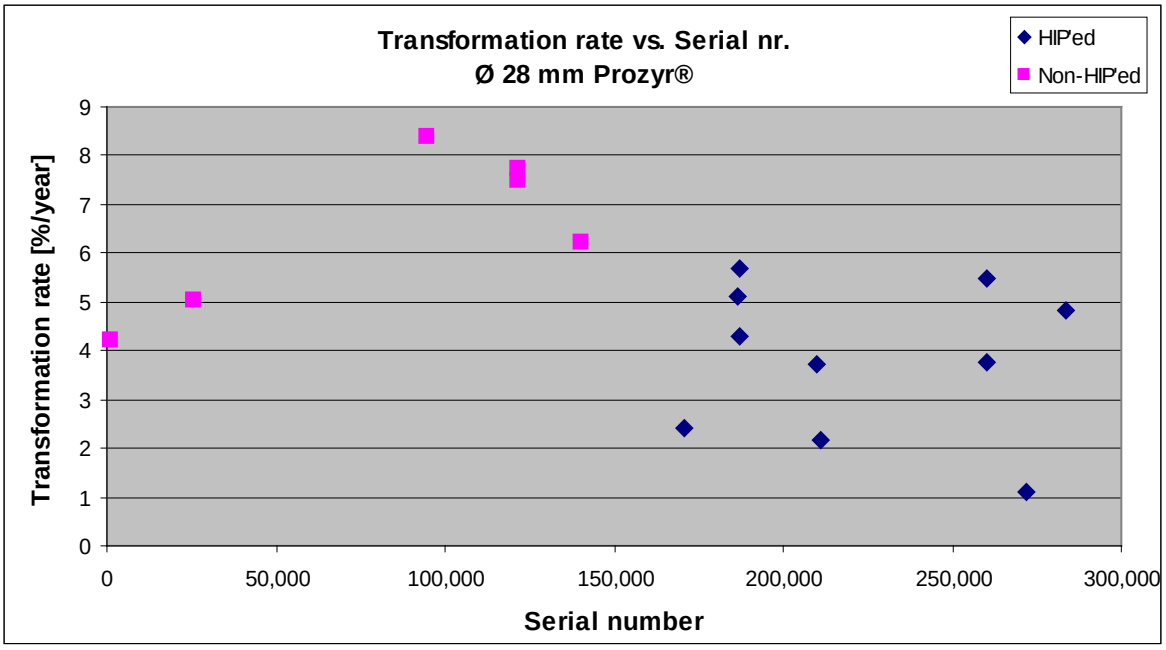

Figure 50: Transformation rate – Ø 28 mm Prozyr®

Again a considerable difference is obvious: 6.5% per year as opposed to 3.9% per year. The difference between the average patient age for the two groups is 9.7 years (non-HIP'ed = 60.2 and HIP'ed = 69.9), which means that the HIP'ed group of patients are most probably less active than the non-HIP'ed group. In order to compare the transformation rate of the HIP'ed and non-HIP'ed Prozyr® groups, the four youngest patients were taken from the HIP'ed group and compared with the six samples of the non-HIP'ed group. The average age of the four youngest patients of the HIP'ed group is 58.5 years, with a transformation rate of 4.7% per year, compared to the 60.2 years, with a transformation rate of 6.5% per year for the non-HIP'ed group. Therefore, if the monoclinic content of the two Prozyr® groups are normalised with respect to in vivo lifetime and to patient age, it can be concluded that the HIP'ed femoral heads have better phase stability than the non-HIP'ed femoral heads.

The time-dependency of Y-TZP phase transformation was deemed important enough to introduce the term transformation rate, therefore this

time-dependency should be tested within the data group. Figure 52 shows a graph of Monoclinic content versus in vivo life for the three different Ø 28 mm groups. The FII group of Ø 28 mm femoral heads consist of only four samples, therefore care should be taken when conclusions are made from this group.

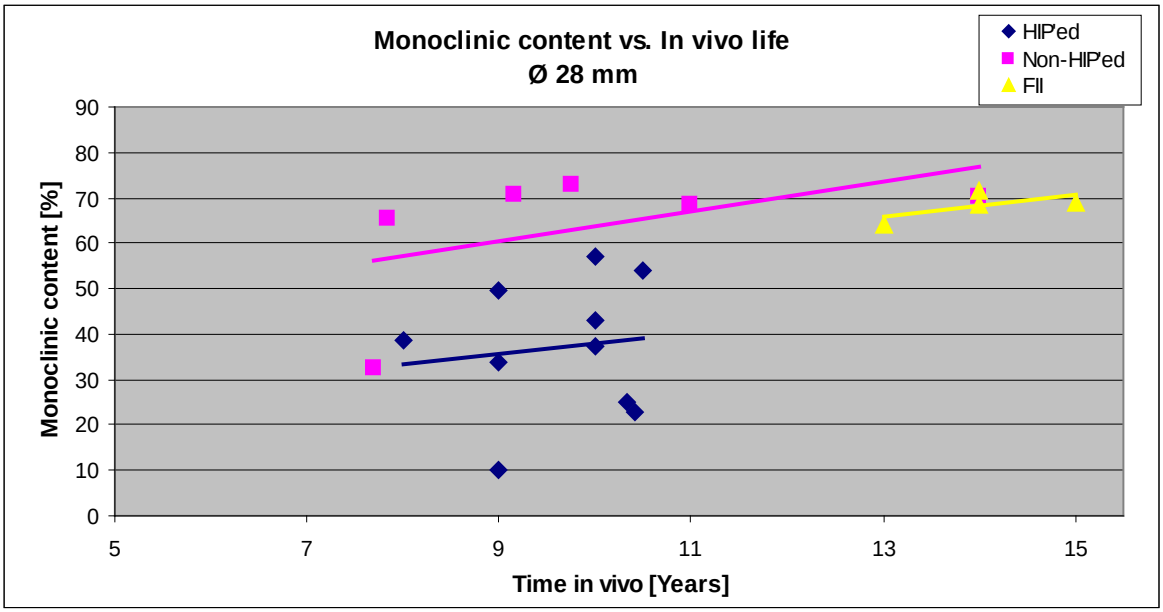

Figure 51: Monoclinic content vs. in vivo life – Ø 28 mm

The regression lines for the data points are included and each group shows that the monoclinic content on the surface of a femoral head does increase with time inside the human body.

Phase transformation is temperature dependent, as was shown by Chevalier et al. (1999:2151), which gives rise to the idea that phase transformation of Y-TZP in the human body would also be dependent on the activity of the patients. The more active a person, the more heat would be developed in the bearing couple, which would increase the femoral head surface temperature and expose the femoral head to longer periods of elevated temperature. The only measure available from the data gathered for patient

activity is the patient age; therefore it is used in Figure 53. For this graph the normalised entity of transformation rate is used, to eliminate the effect that in vivo life would have on the results.

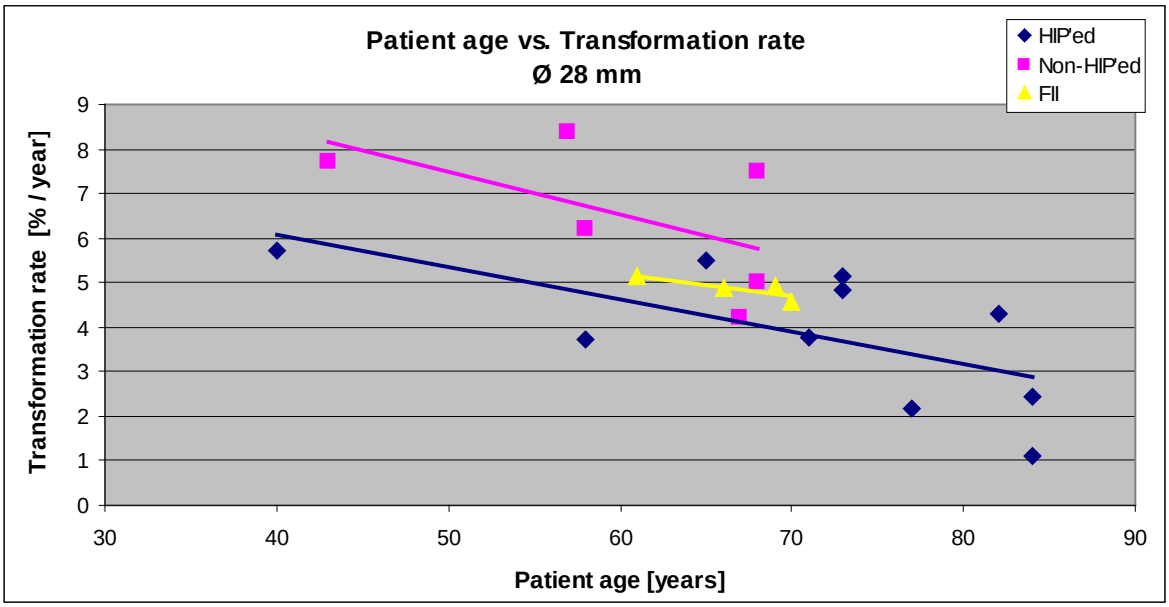

Figure 52: Patient age vs. transformation rate – Ø 28 mm

All three groups show a definite decrease in transformation rate with increase in patient age. Patient age is not in all cases a good measure of patient activity, but the results of Figure 53 are rather conclusive.

The data for Sample 30 was omitted from the results shown in Section 4.2, as it had already transformed more than the 5% allowed by ASTM F1873-98. The reason for the abnormal monoclinic content of Sample 30 could not be found, as it was in its standard package and had not been taken out of its packaging or put in an Autoclave. The upside of this phenomenon is that it gives the opportunity for comparing new femoral heads with different amounts of monoclinic content.

Since the amount of monoclinic content for Sample 29 and 31 (1.26% and 1.64% respectively) are very similar, the data for these two samples were averaged to form a "new femoral head baseline", to which the data of Sample 30 can be compared. The baseline approach is adopted to guard against false trends that can be formed because of having only three data points with two very close to each other.

The comparison of the new femoral heads is shown in Table 6, with the data for Sample 29 and 31 included as well.

Table 6: New femoral head comparison

Sample/property	Sample 29	Sample 31	Baseline [29 & 31 Averaged]	Sample 30
Monoclinic content [%]	1.26	1.64	1.45	9.61
Surface finish [μm]*	0.0187	0.0175	0.0181	0.0235

*Values are indicative only. See discussion on p85-86.

From Table 6 it is evident that the surface conditions for Sample 30 are worse than that of the baseline. Even though there are very few samples in this comparison, its results are significant, as it confirms the results obtained from the retrieved samples (degrading of surface properties with increase in monoclinic content) without the complicating factors like: patient age, weight, activity, in vivo life etc.

The relationship between acetabular cup wear and the monoclinic content of the Ø 28 mm femoral heads is shown in Figure 54. The measure for wear used is femoral head penetration, which is applicable because all of the femoral heads are of the same size.

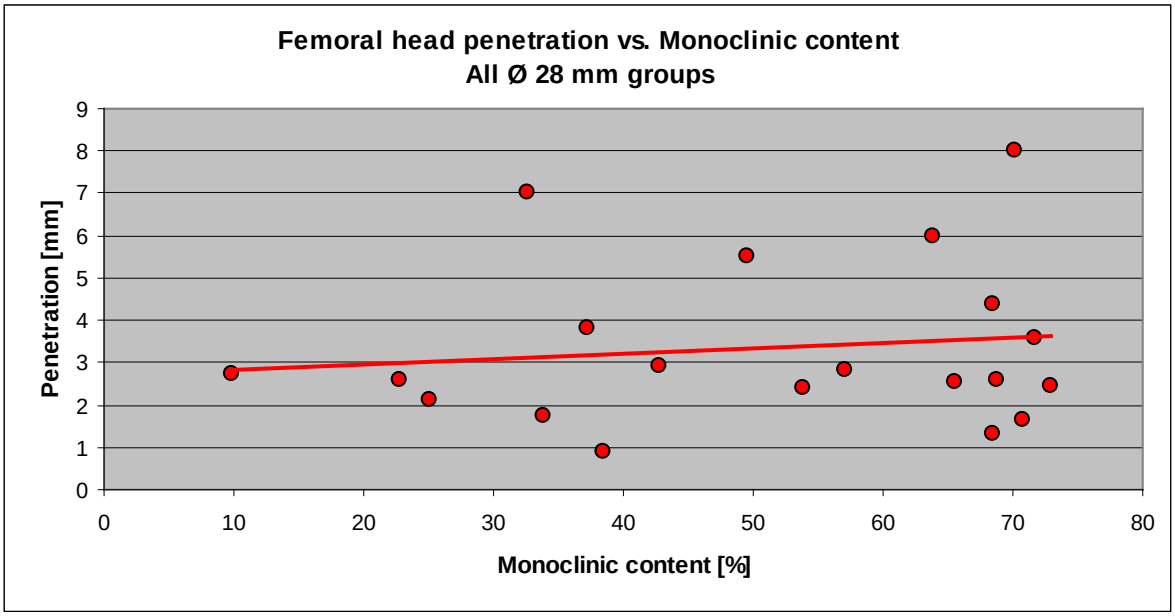

Figure 53: Femoral head penetration vs. monoclinic content – Ø 28 mm

A relationship of increased wear, with increase in monoclinic content is evident from the data. It cannot however be concluded outright that penetration is dependent on the monoclinic content, because the same factors influence both. For instance: the more active and heavier a patient, the more heat is generated in the hip, the more phase transformation is expected, but a more active, heavier patient would also be associated with higher wear rates. In this case the results shown in Figure 54 must be interpreted with the surface deterioration evident on the femoral head surface, as shown in Section 4.1, as well as the deterioration of shape and surface finish shown in Section 4.2. From all this evidence it can be concluded that an increase in monoclinic content indeed increases the amount of wear.

5 Discussion

The average 53.6% monoclinic content found in this study far exceeds the amounts found in literature: Erick et al. (2004) reported 21%, Haraguchi et al. (2001) reported 25% and Stewart et al. (2003) reported up to 35%. This is largely because the mentioned authors investigated femoral heads with lower in vivo lifetimes.

Chevalier et al. (1999:2151) reported that the phase transformation of Y-TZP follows the Mehl-Avrami-Johnson (MAJ) law with n=3.6. In other words: the phase transformation follows an s-curve with respect to time, as shown in Figure 55. The curve shown in Figure 55 is by Laurent, Chevalier, Epicier, Deville & Fantozzi (2004), who based it on the MAJ calculations by Chevalier et al. (1999), for accelerated phase transformation on a femoral head. The phase transformation process can be described as an initialization part with slow transformation, a growth part with rapid transformation and an end part where the monoclinic content asymptotically approaches a limit value. Chevalier et al. (1999:2151) found the limiting value of monoclinic content to be 88%.

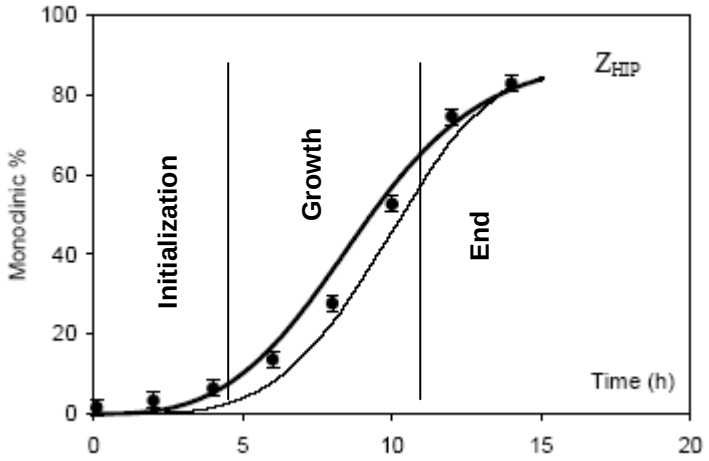

Figure 54: LTD S-curve

(Adapted from: Laurent et al. 2004:3484)

The data for monoclinic content, as shown in Figure 56 exhibits a non-uniform distribution with more samples above the mean, 15 to be exact, than the 11 samples below the mean. The non-uniformity is also evident by the fact that the monoclinic content for only one sample lies above the mean plus one standard deviation, whereas five samples lie below the mean minus one standard deviation. These observations can be explained by interpolating the mean plus one standard deviation range of 54% to 72% onto the s-curve of Figure 55 and noting that this data range is nearing the end range of phase transformation.

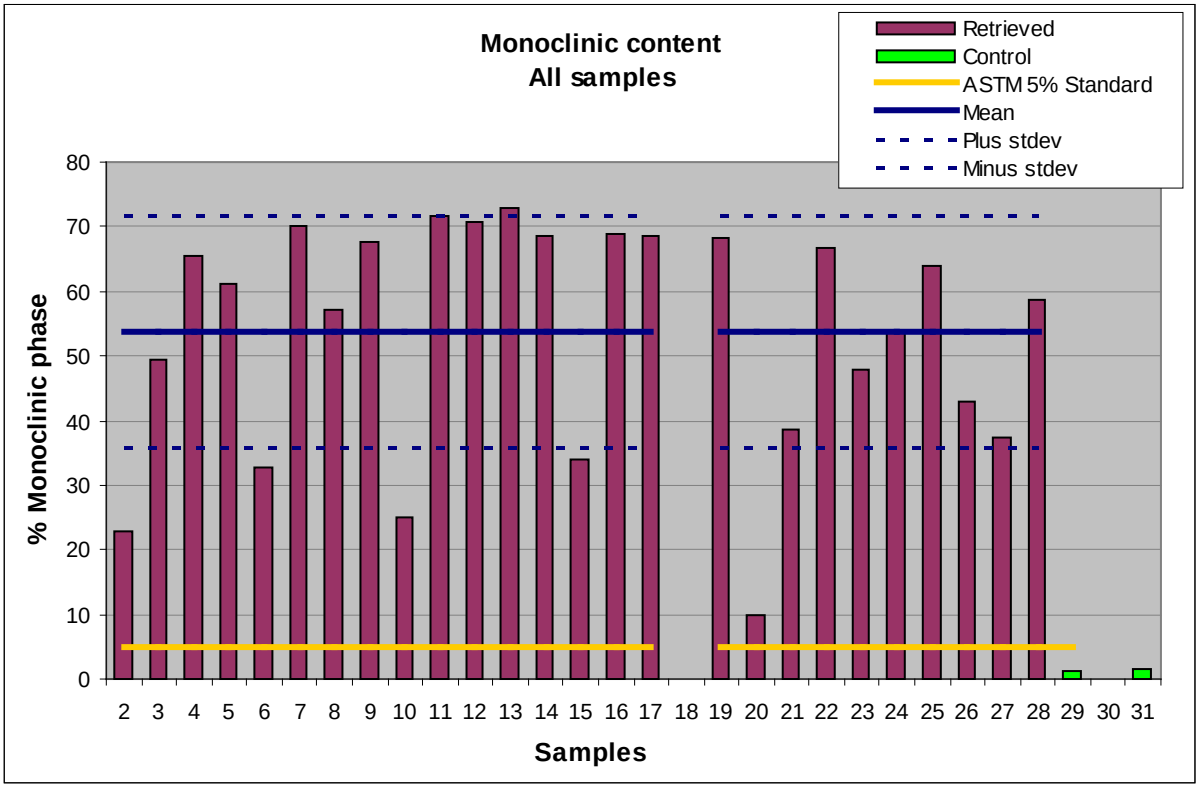

Figure 55: Monoclinic content for all samples

The maximum amount of monoclinic content recorded is 73% for Sample 13, which means that this sample has already entered a stage of decreasing transformation rate. This s-curve behaviour of transformation rate complicates any results containing this parameter, therefore the trend lines

in Figure 52 should be interpreted as only showing an upwards trend between in vivo life and monoclinic content and not a linear relationship.

No useful results were found by this study to be able to compare roundness with the measurements by Hernigou and Bahrami (2003). This study does suggest that roundness deteriorates with increase in monoclinic content, as was found by Hernigou and Bahrami (2003).

The surface finish data found in this study does not compare well to that of the authors surveyed in literature, as illustrated in Table 7.

Table 7: Surface finish measurement comparisons

	Retrieved Ra [μm]		New Ra [μm]	
Study	**Mean**	**Stdev.**	**Mean**	**Stdev.**
This study*	0.04	0.036	0.018	0.00085
Erick et al. (2004)	0.15	0.075	-	-
Haraguchi et al. (2001)	0.12	-	0.006	-
Hernigou and Bahrami (2003)	0.35	-	0.005	-

*Values are indicative only. See discussion on p85-86

Due to the mean deviation as discussed on p 85-86 a direct comparison cannot be made between the data of this study and that of the mentioned authors. Some factors might however enlighten the topic and will be discussed. The new femoral heads are far rougher than that found in literature. The mean surface finish for the retrieved samples is far better than found in literature, which is not as expected, if the mean deviation is taken into consideration. Because the samples of this study are far more transformed than the samples analysed by the different authors in the

literature, it was expected that the surface finish of this study would be worse than that found in literature. The maximum of Ra = 0.16 μm found in this study, barely reaches the amounts found in literature. Unfortunately very little is known about the techniques used by the different authors to reach their Ra values, so a detailed comparison is not possible.

Despite the debate about the numeric values of the surface finish measurements, this study did indicate that the surface finish does degrade with the increase of monoclinic content, and therefore this study agrees with the literature found.

The only penetration rate for this study that can be compared to that found in literature is that of the Non-HIP'ed groups and those results compare very well. This study found a mean of 0.39 mm/year for the Non-HIP'ed Prozyr® group and 0.30 mm/year for the FII group, which is also non-HIP'ed, whereas Hernigou and Bahrami (2003) found 0.28 mm/year and Skyrme et al. (2005) found 0.19 mm/year.

In analysing the data, there was no distinguishing between male and female patients. Male patients tend to be heavier than female patients, thereby putting more strain on the hip replacement, which could lead to greater amounts of wear, higher bearing surface temperature and subsequently more phase transformation. If the data was distinguished between male and female, the sample groups would have been even smaller: the Prozyr® non-HIP'ed group would have been three samples, the Prozyr® HIP'ed group would have been seven instead of ten. In this case the weight and activity level of the patients were not known, which could have influenced the data as well, especially when groups are small. It was therefore decided to rather not distinguish between genders for the sake of having bigger sample groups

that would give more realistic mean values, even though it might increase standard deviation in the data.

One shortfall of this study is the size of the sample group. To get even more reliable trends the small data groups would have to be divided into similar gender, age, weight, activity and lifestyle groups in order to eliminate as many influencing factors as possible. Such distinguishing would have led to the addition of more relationships to the results, as well as less deviation in the data.

This study proved that HIP'ed Y-TZP femoral heads exhibit better phase stability than non-HIP'ed Y-TZP femoral heads, even though it can still be considered as inadequate. It was also proved that an increase in monoclinic content is associated with an increase in the amount of acetabular cup wear. Both of these facts were only postulated in the literature.

6 Conclusion

It can be concluded that phase transformation in Y-TZP Zirconia femoral heads is a real occurrence and that it adversely affects the bearing couple by degrading surface conditions, ultimately increasing wear, which in turn decreases the survival rate of the hip prosthesis due to an elevated risk of aseptic loosening.

A great contributing factor to the phase transformation could be reasoned as follows: phase transformation occurs at a temperature ranging between 70°C and 130°C (Chevalier et al. 1997, Chevalier et al. 1999). The femoral surface of a Y-TZP UHMWPE hip replacement has been measured at a temperature of 90°C whilst running in a hip simulator (Lu & Mckellop 1997). Burger (2005), went a step further and proved that temperatures in excess of 90°C are reached inside the bearing couple of a Y-TZP UHMWPE hip replacement, inside the human body. These elevated temperatures mean that the surface transforms from tetragonal to monoclinic because of the heat produced by the prosthesis. The heat produced is in turn aggravated by insufficient lubrication that exists between the two bearing surfaces (Burger 2005:213). To make matters worse, the thermal conductivity of Y-TZP and UHMWPE is very low, therefore the heat generated cannot easily escape the bearing couple.

From all the data and literature gathered it can be concluded that because of tetragonal to monoclinic phase transformation, Y-TZP femoral heads are less suited for use in hip replacements.

7 Acknowledgements

The author would like to acknowledge the following persons for their contribution, without which, this research would not have been possible

- Prof. Danie Burger

  Department of Mechanical and Aeronautical Engineering, University of Pretoria.
- Prof. Frans Weber

  Sandton Medi Clinic & Department of Orthopaedic Surgery, University of Witwatersrand.
- Mr. Andre Botha

  Electron Microscopy, University of Pretoria.
- Dr. Sabine Verryn

  X-ray Diffraction, University of Pretoria.
- NMISA

  Metrology Department.

8 References

1. Allain, J, Le Mouel, S, Goutalier, D & Voisin, M 1999, 'Poor eight year survival of cemented zirconium-polyethylene total hip replacements', *Journal of Bone and Joint Surgery*, vol. 81-B, no. 5, p. 835-842.
2. ASTM F1873-98, 'Standard Specification for High-Purity Dense Yttria Tetragonal Zirconium Oxide Polycrystal (Y-TZP) for Surgical Implant Applications', (Withdrawn 2007), ASTM International, West Conshohocken, PA, www.astm.org.
3. Australian Government, 23 August 2001, 'Urgent information on spontaneous disintegration of zirconia femoral head hip prostheses' ,*Hazard alert ,* revision V1-2.
   http://www.tga.gov.au/alerts/devices/zirconia.htm
4. Burger, N 2005, 'Failure analysis of ultra high molecular weight polyethylene acetabular cups', *Faculty of engineering the build environment and information technology*, University of Pretoria.
5. Calés, B & Stefani, Y 1994, 'Mechanical properties and surface analysis of retrieved zirconia hip joint heads after an implantation time of two to three years', *Journal of Materials Science Materials in Medicine*, vol. 5, pp. 376-380.
6. Chevalier, J, Drouin, J & Calés, B 1997, 'Low temperature aging behaviour of Zirconium hip joint heads', *Saint-Gobain Ceramiques industrielles publications*, Rev.: 02/99, pp. 9-11. Also in: *Bioceramics*, vol. 10, 1997.
7. Chevalier, J, Drouin, J & Calés, 1999, 'Low temperature aging of Y-TZP ceramics', *Journal of the American Ceramic Society*, vol. 82, no. 8, pp. 2150 – 2154.
8. Chevalier, J, Gremillard, L & Deville, S 2007, 'Low temperature degredation of Zirconia and implications for biomedical implants' , *Annual Review of Materials Research*, vol. 37, pp. 1-32.

9. Dambreville, A Philippe, M Ray, A 1999, 'Zirconia Ceramics or "by night, all cats are grey"', *Saint-Gobain Ceramiques industrielles publications*, Rev.: 02/99, pp. 56-63. Also at: http://www.maitrise-orthop.com/corpusmaitri/orthopaedic/mo78_zircone/index.shtml – Last accessed July 2008.
10. Erick, M, Santos, M, Vohra, S, Catledge, A, McClenny, M, Lemons, J & Moore, D 2004, 'Examination of surface and material properties of explanted Zirconia femoral heads', *Journal of Arthroplasty*, vol. 19, no. 7, suppl. 2, pp. 30- 34.
11. French, R, Glass, S, Ohuchi, F, Xu, Y & Ching, W 1994, 'Experimental and theoretical determination of the electronic structure and optical properties of three phaes of ZrO_2' , *Physical Review B Condensed Matter*, 3rd series , vol. 49, no. 8, pp. 5133-5141.
12. Gomez, P & Morcuende, J 2005, 'Early attempts at hip arthroplasty 1700s to 1950s', *The IOWA Orthopeadic Journal*, vol. 25, pp. 25-29.
13. Haraguchi, K, Sugano, N, Nishii, T, Miki, H, Oka, K & Yoshikawa, H 2001, 'Phase transformation of a zirconium ceramic head after total hip arthroplasty', *Journal of Bone and Joint Surgery*, vol. 83-B, no. 7, pp. 996-1000.
14. Hernigou, P & Bahrami, T 2003, 'Zirconium and aluminina ceramics in comparison with stainless steel heads', *Journal of Bone and Joint Surgery*, vol. 85-B, no. 4, pp. 504-509.
15. http://en.wikipedia.org/wiki/Cubic_zirconia - Last accessed July 2008.
16. http://serc.carleton.edu/research_education/geochemsheets/ebsd.html - Last accessed December 2010.
17. http://wavessurgicals.tradeindia.com - Last accessed July 2008.
18. http://www.aaos75th.org/stories/physician_story.htm?id=12 - Last accessed July 2008.
19. http://www.answers.com/topic/hip-replacement-surgical-term?cat=health - Last accessed July 2008.

20. http://www.childrenshospital.org/clinicalservices/Site1163/mainpageS1163P6.html - Last accessed July 2008.
21. http://www.cvtechnologies.com/products/cellfx_mechanism.htm - Last accessed July 2008.
22. http://www.ebsd.com/ebsd-explained/ebsdexplained.htm (Oxford instruments) - Last accessed December 2010
23. http://www.iap.tuwien.ac.at/~werner/qes_tut_interact.html - Last accessed August 2008.
24. http://www.nslc.wustl.edu/courses/Bio2960/labs/04Microscopy/microscopy.html - Last accessed September 2009.
25. http://www.zeiss.com/c1256e4600305472/Contents-Frame/2b0e2152b5c764c7c1256e5f0039c1e7 - Last accessed December 2010.
26. http://www.zimmerindia.com/z/ctl/op/global/action/1/id/7888/template/MP - Last accessed July 2008.
27. ISO 13356: 1997, 'Implants for surgery – ceramic materials based on Yttria stabilized tetragonal Zirconia (Y-TZP)'.
28. Laurent, G Chevalier, J Epicier, T Deville, S Fantozzi, G 2004, 'Modeling the aging kinetics of zirconia ceramics', '*Journal of the European Ceramic Society',* No. 24, pp. 3483-3489.
29. Lu Z & Mckellop H, 'Frictional heating of bearing materials tested in a hip joint wear simulator', *Proc Instn Mech Engrs*, vol 211 (H), p101-107, 1997
30. Nettina, S 1996, The Lippincott manual of nursing practice, 6th edn., Lippincott, Philadelphia.
31. Piconi, C & Maccauro, G 1997, 'Zirconia as a ceramic biomaterial', *Biomaterials review*, vol. 20, pp. 1-25, Found on: http://www1.elsevier.com/homepage/sai/biomaterials/201/201.htm - Last accessed July 2008.
32. Skyrme, A, Richards, S, John, A, Chia, M, Walter, W & Zicat, B 2005, 'Polyethylene wear rates with Zirconia and Cobalt Chrome heads in the ABG hip', *Hip International*, vol. 15, no. 2, pp. 63-70.

33. Smeltzer, S & Bare, B 2000, Textbook of medical surgecal nursing, 9th edn., Lippincott, Philadelphia.
34. Stewart, T, Tipper, J, Insley, G, Streicher, R, Ingham, E & Fisher, J 2003, 'Severe wear and fracture of Zirconia heads against Almina inserts in hip simulator studies with microseperation', *Journal of Arthroplasty*, vol. 18, no. 6, pp. 726-734.
35. Thalmann, S and Spiller, J, 2005, 'A Primary Roundness Measuring Machine', *Recent Developments in Traceable Dimensional Measurements III Proceedings,* Vol. 5879.
36. Wroblewski, B 2002, 'Professor sir John Charnley (1911-1982)' , *Rheumatology*, vol. 41, pp. 824-825.
37. University of Leicester Archaeological Services, 2007, 'St. Peters Church and Cemetery: An insight into the health of the people of Medieval Leicester', http://www.le.ac.uk/ulas/services/human_remains.html - Last accessed July 2008.

9 Appendix A – Roundness measurements

5.7.0.131

Taylor Hobson PRECISION

Scale 0.5µm/div.

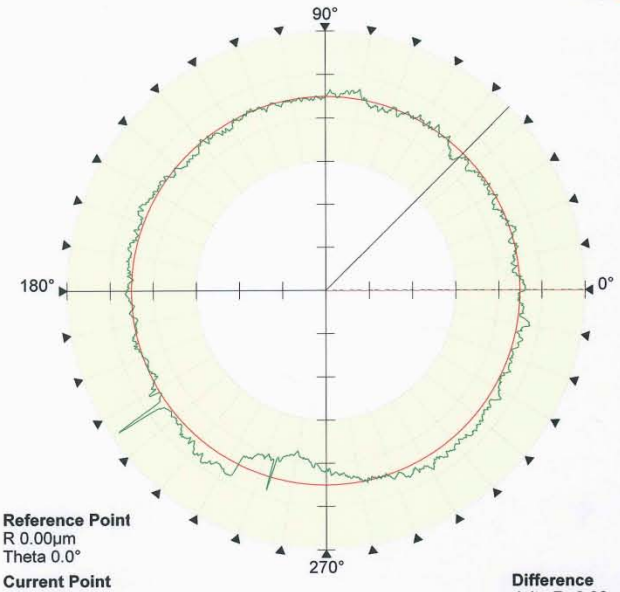

Reference Point
R 0.00µm
Theta 0.0°

Current Point
R -0.06µm
Theta 45.0°

Difference
delta R -0.06µm
delta Theta 45.0°

Roundness		
RON/LS Circle/Gaussian/1-500upr		
17/01/2007 16:07:06		
2		
360°/Admin/TR265 - Manual CL		
17/01/2007 16:06:16		
Specification		
Reference Type		LS Circle
Filter Type		Gaussian
Filter Range		1-500upr
Datum		Spindle
Parameters		
RONt	1.02	µm
Conditions		
Z Position	84.680	mm
R Position	55.990	mm
Attitude		Vertical
Contact Direction		R Negative

5.7.0.131

Taylor Hobson PRECISION

Scale 1µm/div.

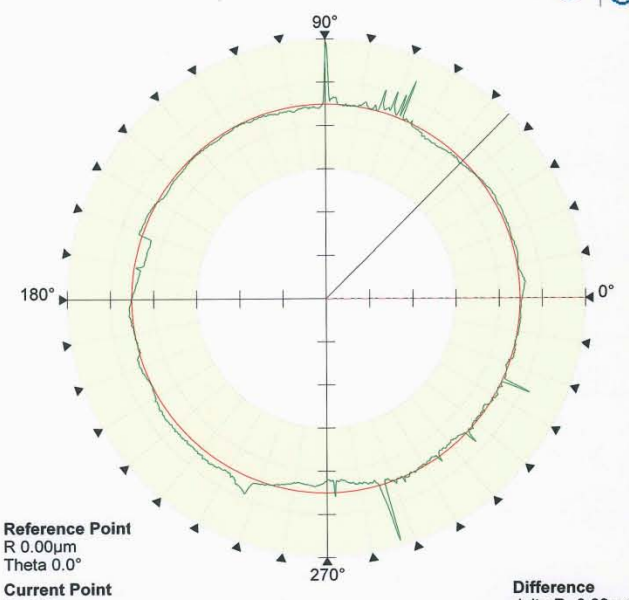

Reference Point
R 0.00µm
Theta 0.0°

Current Point
R -0.09µm
Theta 45.0°

Difference
delta R -0.09µm
delta Theta 45.0°

Roundness		
RON/LS Circle/Gaussian/1-500upr		
19/01/2007 09:42:30		
3		
360°/Admin/TR265 - Manual CL		
19/01/2007 09:41:55		
Specification		
Reference Type		LS Circle
Filter Type		Gaussian
Filter Range		1-500upr
Datum		Spindle
Parameters		
RONt	1.74	µm
Conditions		
Z Position	84.680	mm
R Position	56.024	mm
Attitude		Vertical
Contact Direction		R Negative

5.7.0.131

Taylor Hobson PRECISION

Scale 0.5µm/div.

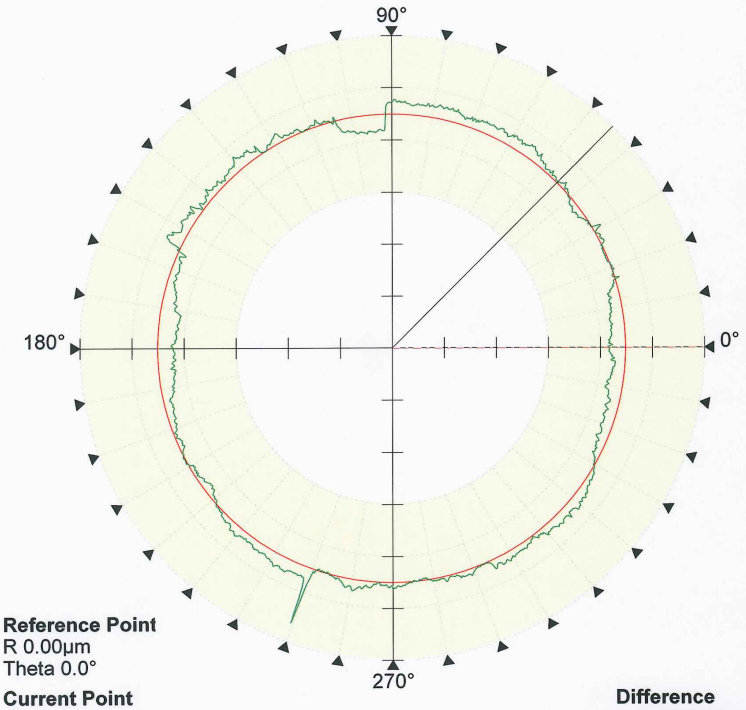

Reference Point
R 0.00µm
Theta 0.0°

Current Point
R 0.00µm
Theta 45.0°

Difference
delta R 0.00µm
delta Theta 45.0°

Roundness		
RON/LS Circle/Gaussian/1-500upr		
19/01/2007 09:44:03		
4		
360°/Admin/TR265 - Manual CL		
19/01/2007 09:43:35		
Specification		
Reference Type		LS Circle
Filter Type		Gaussian
Filter Range		1-500upr
Datum		Spindle
Parameters		
RONt	0.76	µm
Conditions		
Z Position	80.045	mm
R Position	56.125	mm
Attitude		Vertical
Contact Direction		R Negative

5.7.0.131

Taylor Hobson PRECISION

Scale 5µm/div.

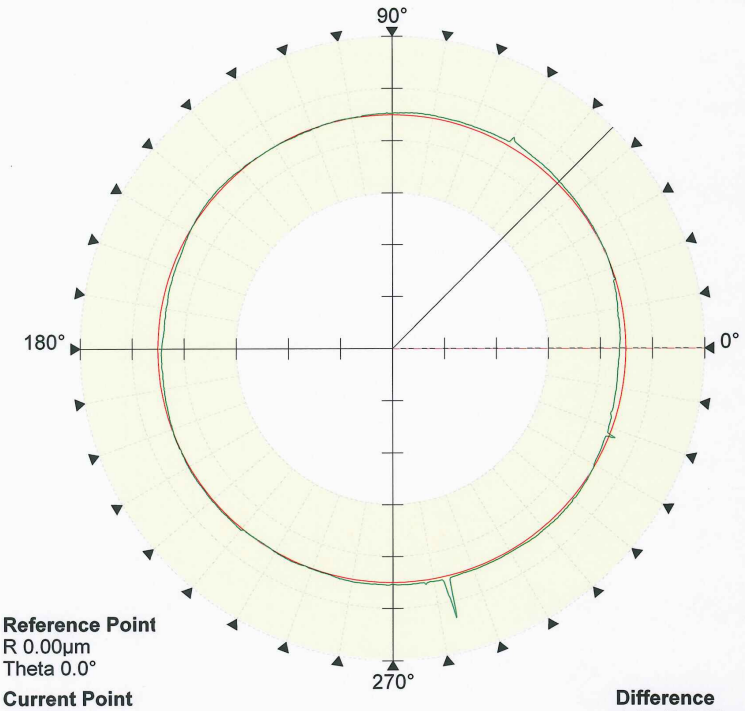

Reference Point
R 0.00µm
Theta 0.0°

Current Point
R 0.23µm
Theta 45.0°

Difference
delta R 0.23µm
delta Theta 45.0°

Roundness		
RON/LS Circle/Gaussian/1-500upr		
19/01/2007 09:45:37		
5		
360°/Admin/TR265 - Manual CL		
19/01/2007 09:45:13		
Specification		
Reference Type		LS Circle
Filter Type		Gaussian
Filter Range		1-500upr
Datum		Spindle
Parameters		
RONt	4.82	µm
Conditions		
Z Position	88.900	mm
R Position	58.163	mm
Attitude		Vertical
Contact Direction		R Negative

5.7.0.131

Taylor Hobson PRECISION

Scale 2µm/div.

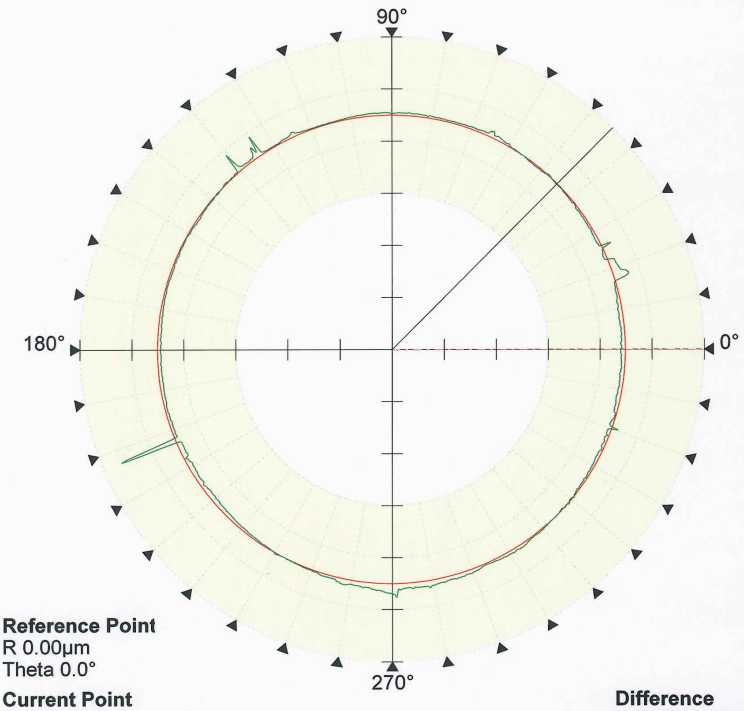

Reference Point
R 0.00µm
Theta 0.0°

Current Point
R -0.03µm
Theta 45.0°

Difference
delta R -0.03µm
delta Theta 45.0°

Roundness		
RON/LS Circle/Gaussian/1-500upr		
19/01/2007 09:47:19		
6		
360°/Admin/TR265 - Manual CL		
19/01/2007 09:46:51		
Specification		
Reference Type		LS Circle
Filter Type		Gaussian
Filter Range		1-500upr
Datum		Spindle
Parameters		
RONt	2.46	µm
Conditions		
Z Position	84.870	mm
R Position	56.062	mm
Attitude		Vertical
Contact Direction		R Negative

5.7.0.131

Taylor Hobson PRECISION

Scale 5µm/div.

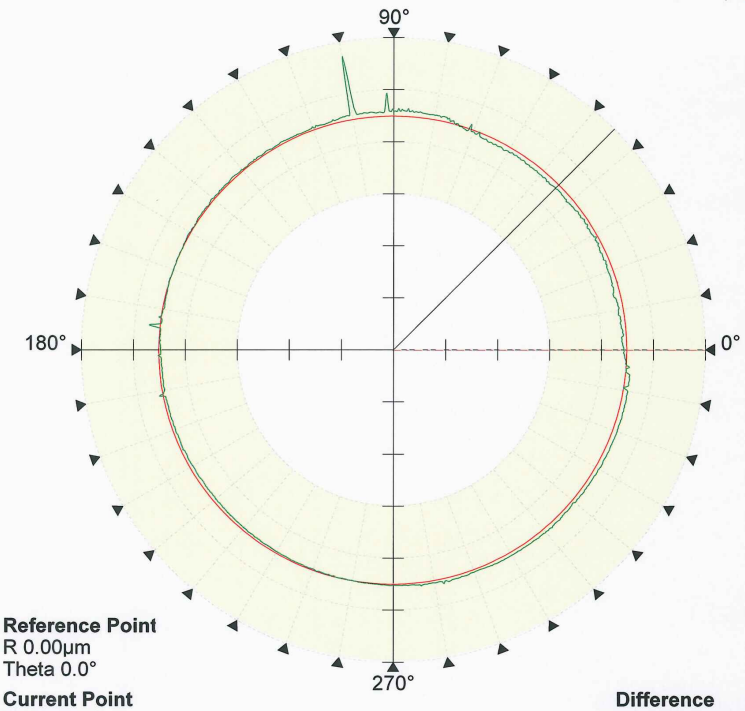

Reference Point
R 0.00µm
Theta 0.0°

Current Point
R -0.49µm
Theta 45.0°

Difference
delta R -0.49µm
delta Theta 45.0°

Roundness		
RON/LS Circle/Gaussian/1-500upr		
19/01/2007 09:51:14		
7		
360°/Admin/TR265 - Manual CL		
19/01/2007 09:50:47		
Specification		
Reference Type		LS Circle
Filter Type		Gaussian
Filter Range		1-500upr
Datum		Spindle
Parameters		
RONt	6.85	µm
Conditions		
Z Position	84.870	mm
R Position	55.336	mm
Attitude		Vertical
Contact Direction		R Negative

5.7.0.131

Taylor Hobson PRECISION

Scale 5µm/div.

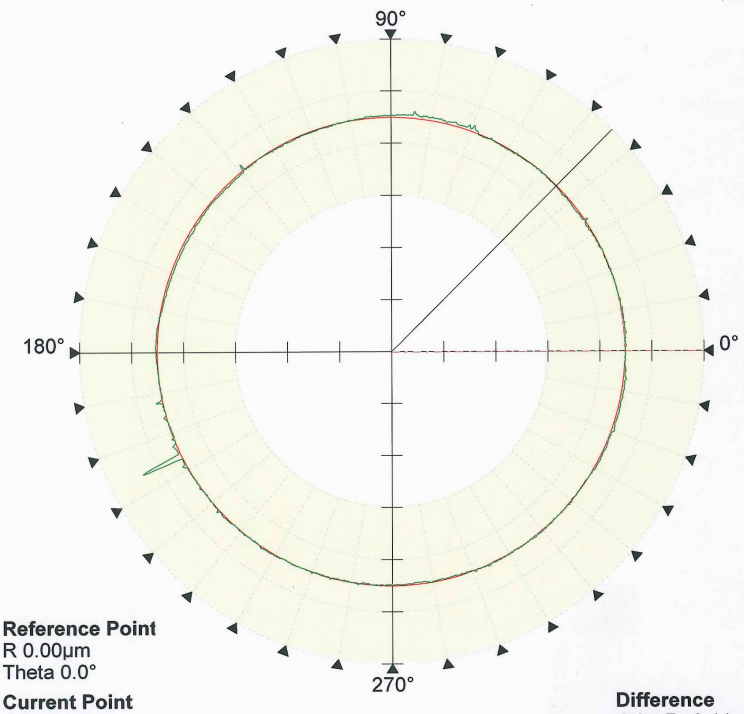

Reference Point
R 0.00µm
Theta 0.0°

Current Point
R -0.11µm
Theta 45.0°

Difference
delta R -0.11µm
delta Theta 45.0°

Roundness		
RON/LS Circle/Gaussian/1-500upr		
19/01/2007 09:53:08		
8		
360°/Admin/TR265 - Manual CL		
19/01/2007 09:52:04		
Specification		
Reference Type		LS Circle
Filter Type		Gaussian
Filter Range		1-500upr
Datum		Spindle
Parameters		
RONt	4.37	µm
Conditions		
Z Position	84.870	mm
R Position	55.324	mm
Attitude		Vertical
Contact Direction		R Negative

5.7.0.131

Taylor Hobson PRECISION

Scale 1µm/div.

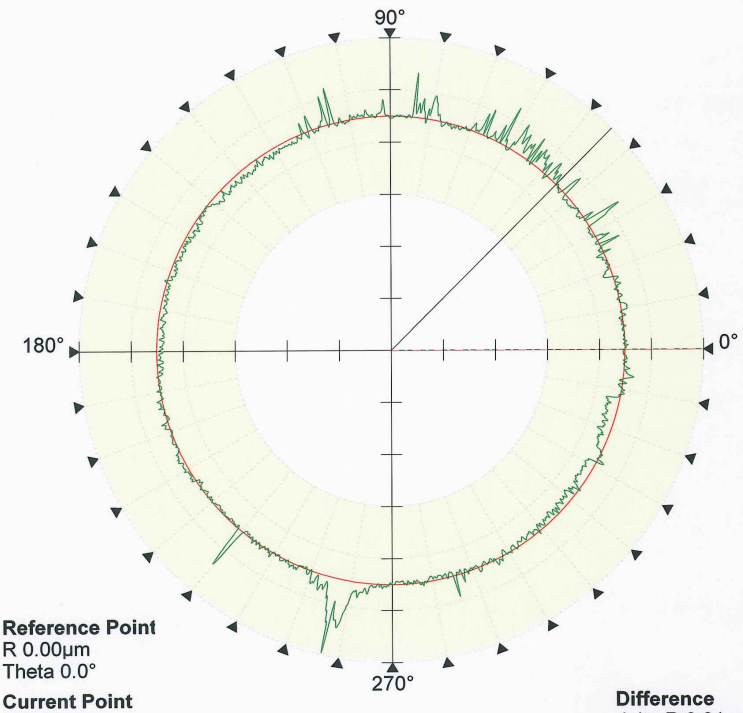

Reference Point
R 0.00µm
Theta 0.0°

Current Point
R 0.01µm
Theta 45.0°

Difference
delta R 0.01µm
delta Theta 45.0°

Roundness		
RON/LS Circle/Gaussian/1-500upr		
19/01/2007 09:55:07		
9		
360°/Admin/TR265 - Manual CL		
19/01/2007 09:54:42		
Specification		
Reference Type		LS Circle
Filter Type		Gaussian
Filter Range		1-500upr
Datum		Spindle
Parameters		
RONt	1.74	µm
Conditions		
Z Position	86.100	mm
R Position	57.230	mm
Attitude		Vertical
Contact Direction		R Negative

5.7.0.131

Taylor Hobson PRECISION

Scale 0.2µm/div.

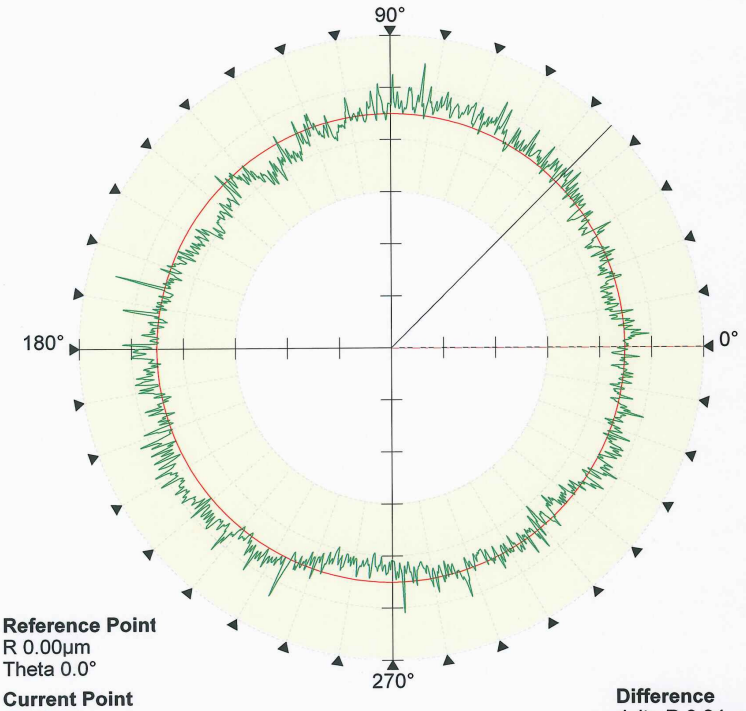

Reference Point
R 0.00µm
Theta 0.0°

Current Point
R 0.04µm
Theta 45.0°

Difference
delta R 0.04µm
delta Theta 45.0°

Roundness		
RON/LS Circle/Gaussian/1-500upr		
19/01/2007 09:57:10		
10		
360°/Admin/TR265 - Manual CL		
19/01/2007 09:55:57		
Specification		
Reference Type		LS Circle
Filter Type		Gaussian
Filter Range		1-500upr
Datum		Spindle
Parameters		
RONt	0.34	µm
Conditions		
Z Position	86.015	mm
R Position	55.250	mm
Attitude		Vertical
Contact Direction		R Negative

5.7.0.131

Taylor Hobson PRECISION

Scale 5µm/div.

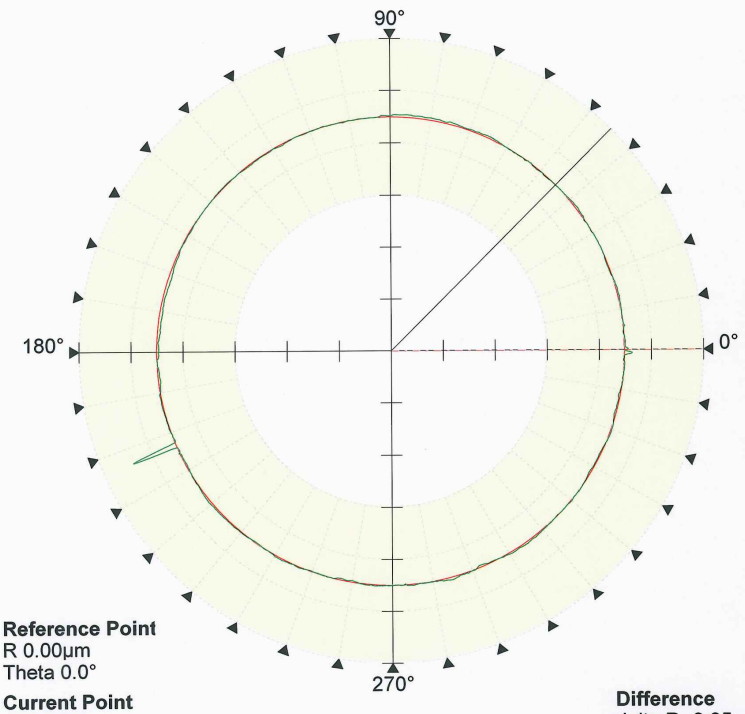

Reference Point
R 0.00µm
Theta 0.0°

Current Point
R -0.05µm
Theta 45.0°

Difference
delta R -0.05µm
delta Theta 45.0°

Roundness		
RON/LS Circle/Gaussian/1-500upr		
19/01/2007 09:58:47		
11		
360°/Admin/TR265 - Manual CL		
19/01/2007 09:58:21		
Specification		
Reference Type		LS Circle
Filter Type		Gaussian
Filter Range		1-500upr
Datum		Spindle
Parameters		
RONt	4.77	µm
Conditions		
Z Position	84.510	mm
R Position	55.368	mm
Attitude		Vertical
Contact Direction		R Negative

5.7.0.131

Taylor Hobson PRECISION

Scale 0.5µm/div.

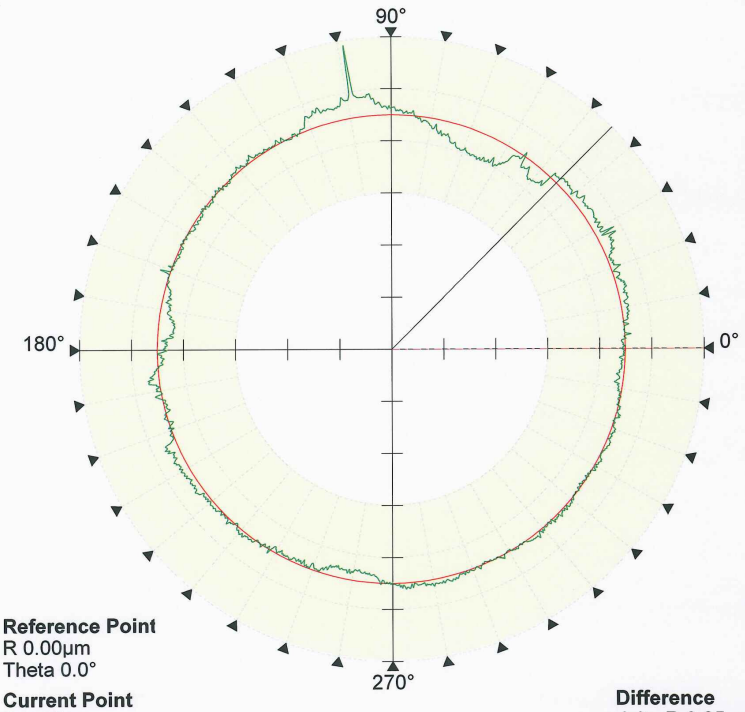

Reference Point
R 0.00µm
Theta 0.0°

Current Point
R 0.05µm
Theta 45.0°

Difference
delta R 0.05µm
delta Theta 45.0°

Roundness		
RON/LS Circle/Gaussian/1-500upr		
19/01/2007 14:00:45		
12		
360°/Admin/TR265 - Manual CL		
19/01/2007 13:59:28		
Specification		
Reference Type		LS Circle
Filter Type		Gaussian
Filter Range		1-500upr
Datum		Spindle
Parameters		
RONt	0.96	µm
Conditions		
Z Position	79.715	mm
R Position	55.356	mm
Attitude		Vertical
Contact Direction		R Negative

5.7.0.131

Taylor Hobson PRECISION

Scale 5µm/div.

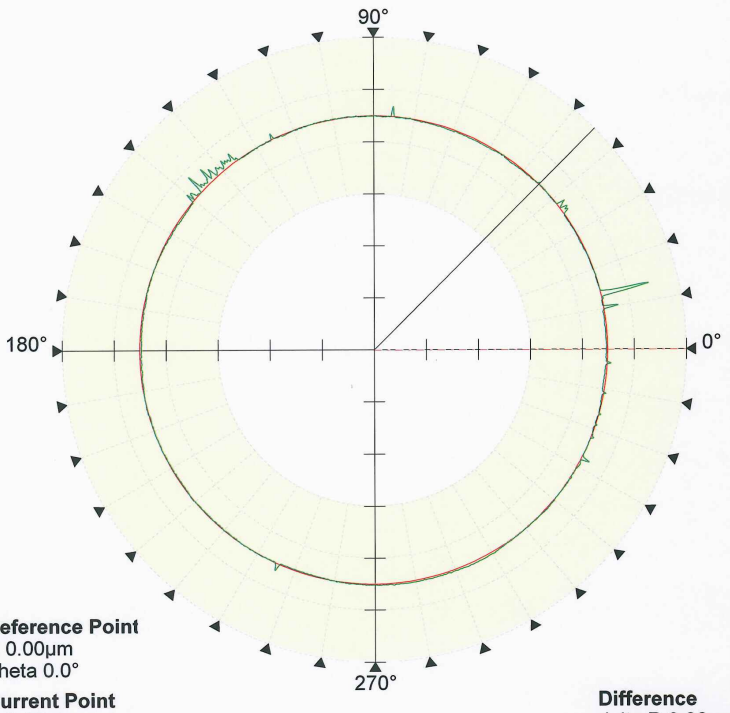

Reference Point
R 0.00µm
Theta 0.0°

Current Point
R 0.06µm
Theta 45.0°

Difference
delta R 0.06µm
delta Theta 45.0°

Roundness		
RON/LS Circle/Gaussian/1-500upr		
19/01/2007 14:02:05		
13		
360°/Admin/TR265 - Manual CL		
19/01/2007 14:01:38		
Specification		
Reference Type		LS Circle
Filter Type		Gaussian
Filter Range		1-500upr
Datum		Spindle
Parameters		
RONt	4.91	µm
Conditions		
Z Position	79.645	mm
R Position	55.444	mm
Attitude		Vertical
Contact Direction		R Negative

5.7.0.131

Taylor Hobson PRECISION

Scale 2µm/div.

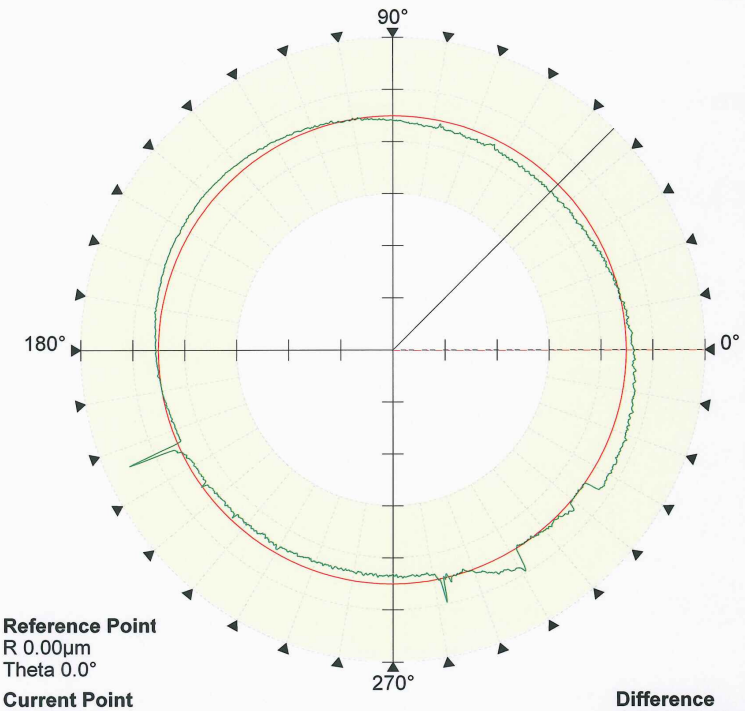

Reference Point
R 0.00µm
Theta 0.0°

Current Point
R -0.40µm
Theta 45.0°

Difference
delta R -0.40µm
delta Theta 45.0°

Roundness		
RON/LS Circle/Gaussian/1-500upr		
19/01/2007 14:03:34		
14		
360°/Admin/TR265 - Manual CL		
19/01/2007 14:03:05		
Specification		
Reference Type		LS Circle
Filter Type		Gaussian
Filter Range		1-500upr
Datum		Spindle
Parameters		
RONt	2.52	µm
Conditions		
Z Position	85.440	mm
R Position	55.333	mm
Attitude		Vertical
Contact Direction		R Negative

5.7.0.131

Taylor Hobson PRECISION

Scale 2µm/div.

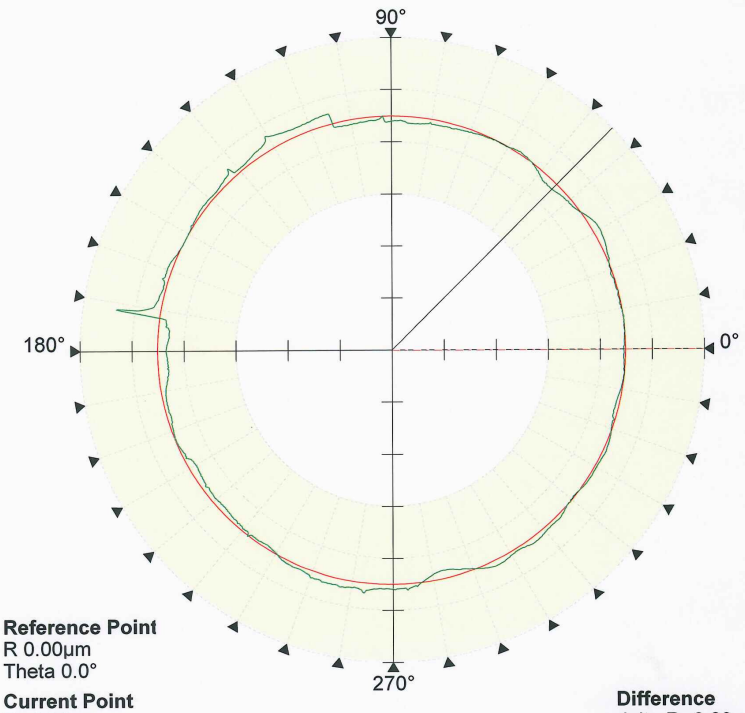

Reference Point
R 0.00µm
Theta 0.0°

Current Point
R -0.29µm
Theta 45.0°

Difference
delta R -0.29µm
delta Theta 45.0°

Roundness		
RON/LS Circle/Gaussian/1-500upr		
19/01/2007 14:04:32		
15		
360°/Admin/TR265 - Manual CL		
19/01/2007 14:04:07		
Specification		
Reference Type		LS Circle
Filter Type		Gaussian
Filter Range		1-500upr
Datum		Spindle
Parameters		
RONt	2.13	µm
Conditions		
Z Position	85.440	mm
R Position	55.332	mm
Attitude		Vertical
Contact Direction		R Negative

5.7.0.131

Taylor Hobson PRECISION

Scale 2µm/div.

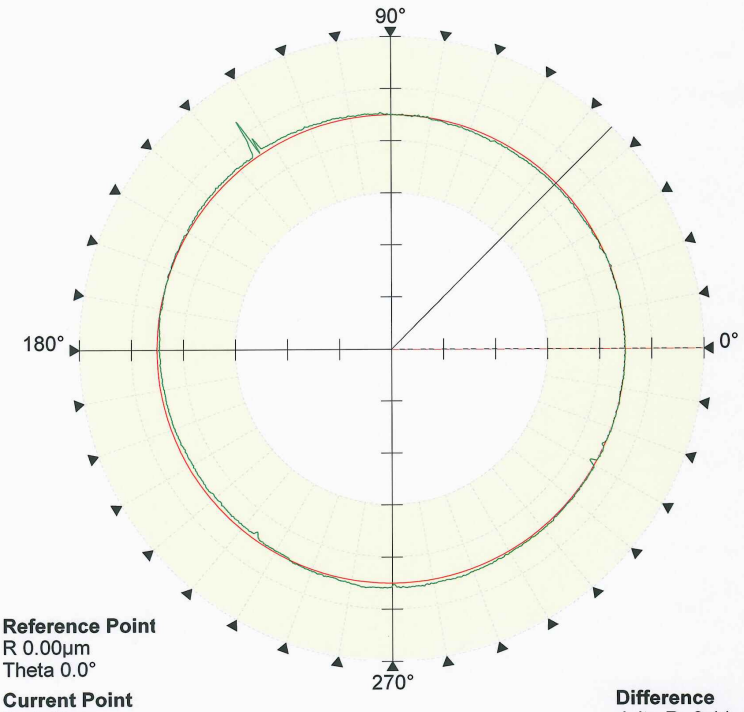

Reference Point
R 0.00µm
Theta 0.0°

Current Point
R -0.11µm
Theta 45.0°

Difference
delta R -0.11µm
delta Theta 45.0°

Roundness		
RON/LS Circle/Gaussian/1-500upr		
19/01/2007 14:05:36		
16		
360°/Admin/TR265 - Manual CL		
19/01/2007 14:05:12		
Specification		
Reference Type		LS Circle
Filter Type		Gaussian
Filter Range		1-500upr
Datum		Spindle
Parameters		
RONt	1.86	µm
Conditions		
Z Position	85.440	mm
R Position	57.125	mm
Attitude		Vertical
Contact Direction		R Negative

5.7.0.131

Taylor Hobson PRECISION

Scale 10µm/div.

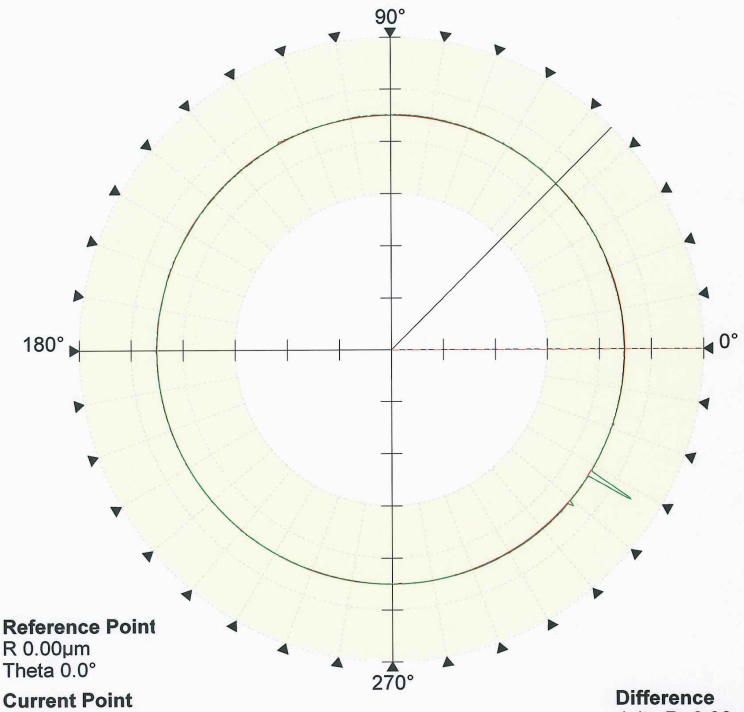

Reference Point
R 0.00µm
Theta 0.0°

Current Point
R -0.06µm
Theta 45.0°

Difference
delta R -0.06µm
delta Theta 45.0°

Roundness		
RON/LS Circle/Gaussian/1-500upr		
19/01/2007 14:06:49		
17		
360°/Admin/TR265 - Manual CL		
19/01/2007 14:06:21		
Specification		
Reference Type		LS Circle
Filter Type		Gaussian
Filter Range		1-500upr
Datum		Spindle
Parameters		
RONt	9.58	µm
Conditions		
Z Position	85.440	mm
R Position	55.267	mm
Attitude		Vertical
Contact Direction		R Negative

5.7.0.131

Taylor Hobson PRECISION

Scale 5µm/div.

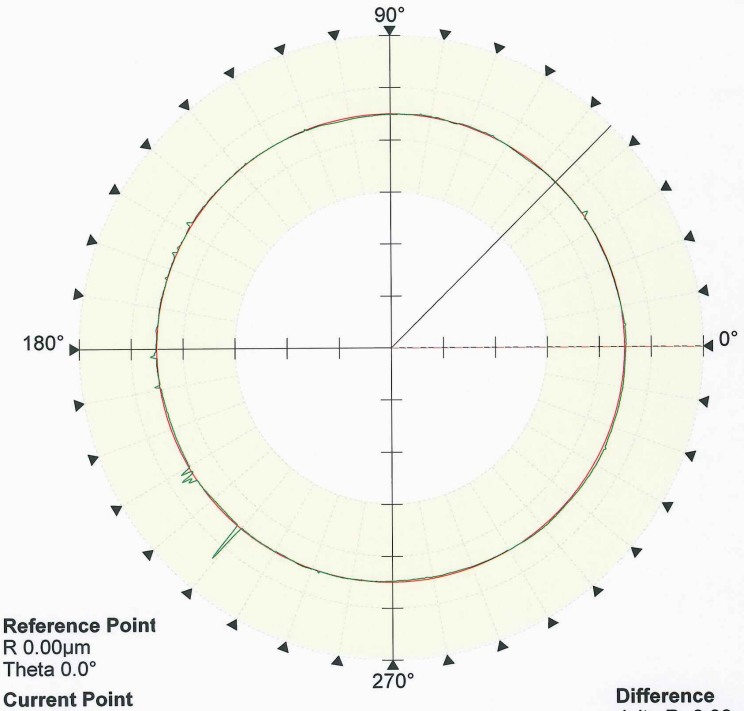

Reference Point
R 0.00µm
Theta 0.0°

Current Point
R -0.06µm
Theta 45.0°

Difference
delta R -0.06µm
delta Theta 45.0°

Roundness		
RON/LS Circle/Gaussian/1-500upr		
19/01/2007 14:08:31		
18		
360°/Admin/TR265 - Manual CL		
19/01/2007 14:08:07		
Specification		
Reference Type		LS Circle
Filter Type		Gaussian
Filter Range		1-500upr
Datum		Spindle
Parameters		
RONt	4.17	µm
Conditions		
Z Position	85.335	mm
R Position	55.427	mm
Attitude		Vertical
Contact Direction		R Negative

5.7.0.131

Taylor Hobson PRECISION

Scale 5µm/div.

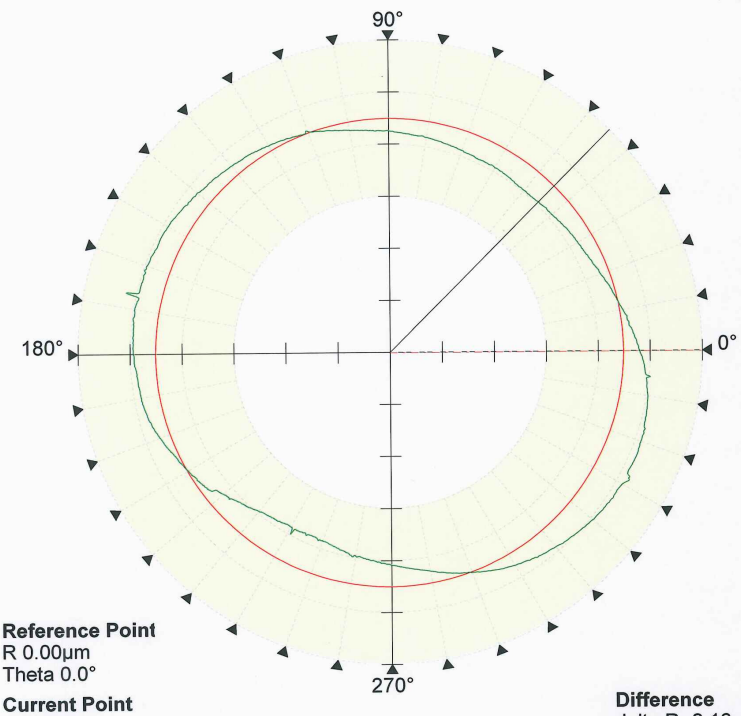

Reference Point
R 0.00µm
Theta 0.0°

Current Point
R -2.16µm
Theta 45.0°

Difference
delta R -2.16µm
delta Theta 45.0°

Roundness		
RON/LS Circle/Gaussian/1-500upr		
19/01/2007 14:10:24		
19		
360°/Admin/TR265 - Manual CL		
19/01/2007 14:09:57		
Specification		
Reference Type		LS Circle
Filter Type		Gaussian
Filter Range		1-500upr
Datum		Spindle
Parameters		
RONt	7.00	µm
Conditions		
Z Position	89.530	mm
R Position	54.411	mm
Attitude		Vertical
Contact Direction		R Negative

5.7.0.131

Taylor Hobson PRECISION

Scale 0.5µm/div.

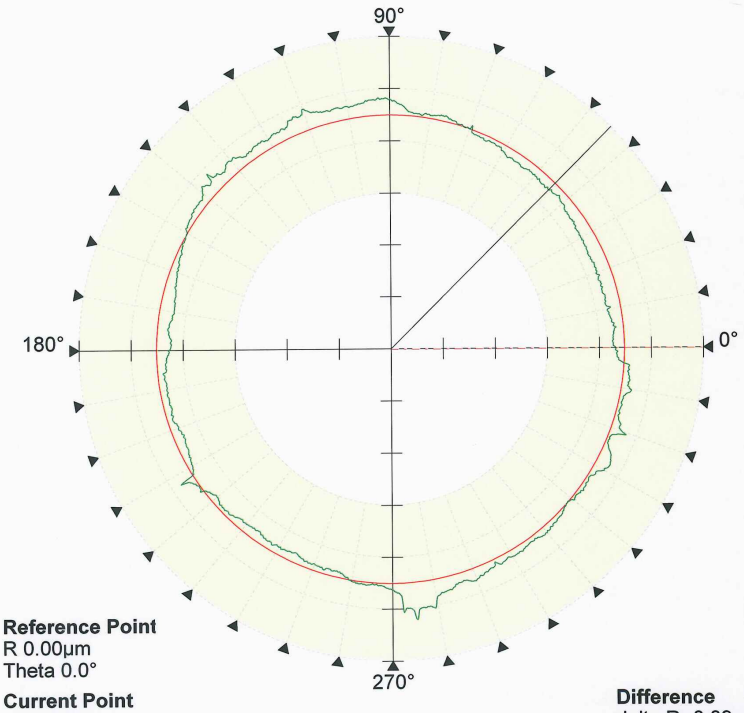

Reference Point
R 0.00µm
Theta 0.0°

Current Point
R -0.09µm
Theta 45.0°

Difference
delta R -0.09µm
delta Theta 45.0°

Roundness		
RON/LS Circle/Gaussian/1-500upr		
19/01/2007 14:11:46		
20		
360°/Admin/TR265 - Manual CL		
19/01/2007 14:11:19		
Specification		
Reference Type		LS Circle
Filter Type		Gaussian
Filter Range		1-500upr
Datum		Spindle
Parameters		
RONt	0.51	µm
Conditions		
Z Position	85.540	mm
R Position	55.408	mm
Attitude		Vertical
Contact Direction		R Negative

5.7.0.131

Taylor Hobson PRECISION

Scale 5µm/div.

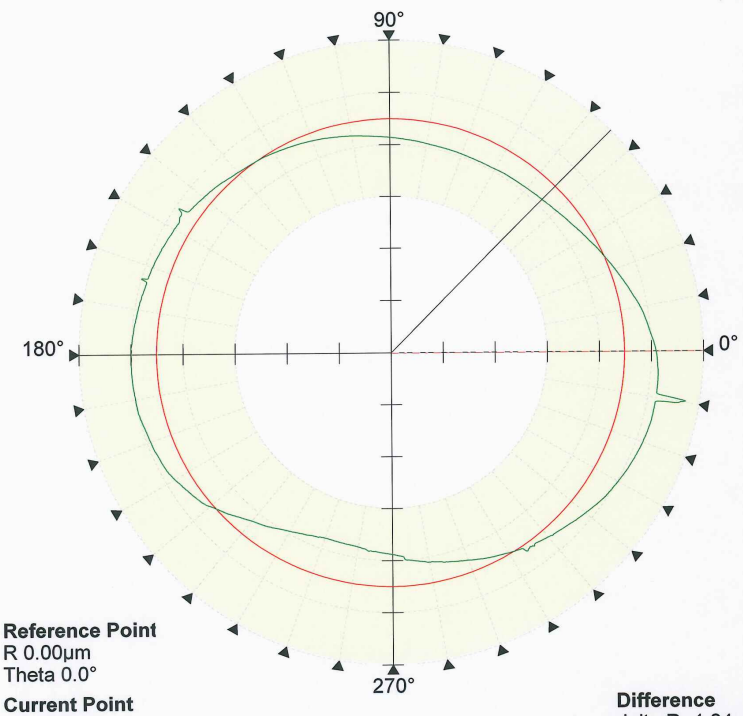

Reference Point
R 0.00µm
Theta 0.0°

Current Point
R -1.84µm
Theta 45.0°

Difference
delta R -1.84µm
delta Theta 45.0°

Roundness		
RON/LS Circle/Gaussian/1-500upr		
19/01/2007 14:14:22		
21		
360°/Admin/TR265 - Manual CL		
19/01/2007 14:13:59		
Specification		
Reference Type		LS Circle
Filter Type		Gaussian
Filter Range		1-500upr
Datum		Spindle
Parameters		
RONt	9.83	µm
Conditions		
Z Position	90.500	mm
R Position	55.203	mm
Attitude		Vertical
Contact Direction		R Negative

5.7.0.131

Taylor Hobson PRECISION

Scale 0.5µm/div.

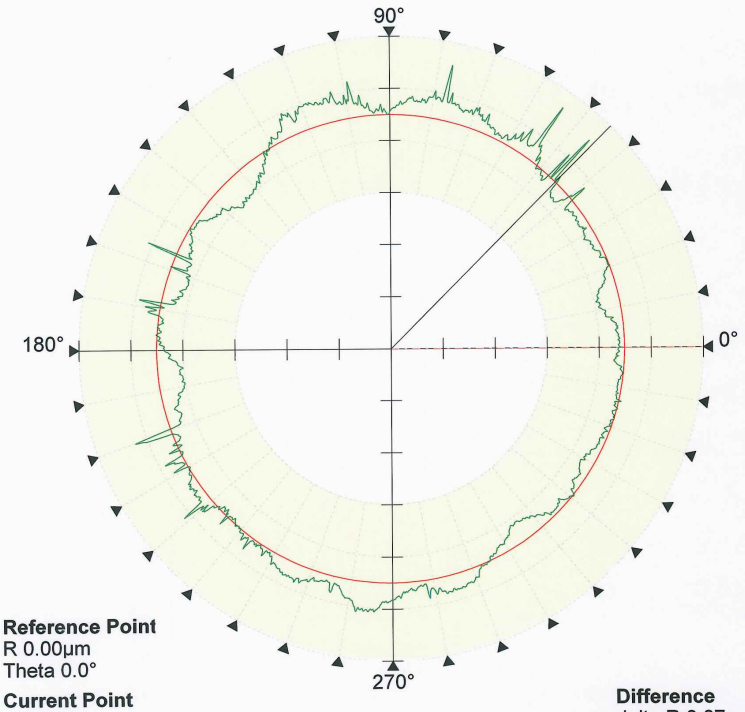

Reference Point
R 0.00µm
Theta 0.0°

Current Point
R 0.07µm
Theta 45.0°

Difference
delta R 0.07µm
delta Theta 45.0°

Roundness		
RON/LS Circle/Gaussian/1-500upr		
19/01/2007 14:15:38		
22		
360°/Admin/TR265 - Manual CL		
19/01/2007 14:15:13		
Specification		
Reference Type		LS Circle
Filter Type		Gaussian
Filter Range		1-500upr
Datum		Spindle
Parameters		
RONt	0.88	µm
Conditions		
Z Position	84.480	mm
R Position	54.427	mm
Attitude		Vertical
Contact Direction		R Negative

5.7.0.131

Taylor Hobson PRECISION

Scale 0.5µm/div.

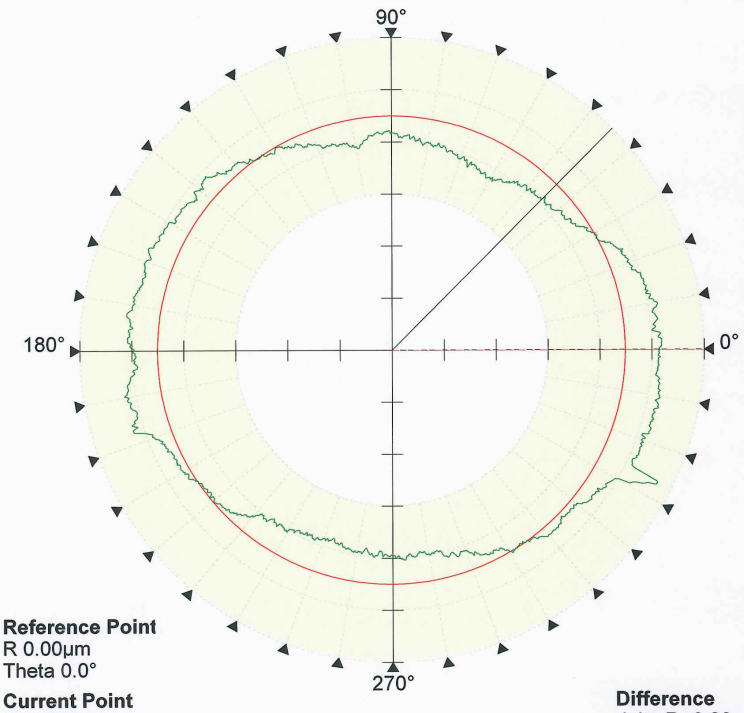

Reference Point
R 0.00µm
Theta 0.0°

Current Point
R -0.20µm
Theta 45.0°

Difference
delta R -0.20µm
delta Theta 45.0°

Roundness		
RON/LS Circle/Gaussian/1-500upr		
19/01/2007 14:18:08		
23		
360°/Admin/TR265 - Manual CL		
19/01/2007 14:17:21		
Specification		
Reference Type		LS Circle
Filter Type		Gaussian
Filter Range		1-500upr
Datum		Spindle
Parameters		
RONt	0.97	µm
Conditions		
Z Position	88.545	mm
R Position	54.393	mm
Attitude		Vertical
Contact Direction		R Negative

5.7.0.131

Taylor Hobson PRECISION

Scale 5µm/div.

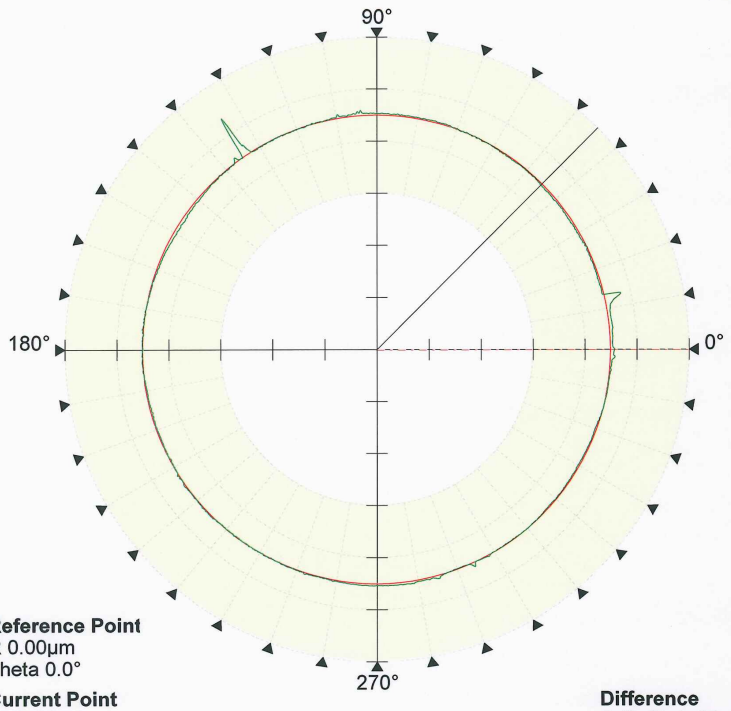

Reference Point
R 0.00µm
Theta 0.0°

Current Point
R -0.17µm
Theta 45.0°

Difference
delta R -0.17µm
delta Theta 45.0°

Roundness		
RON/LS Circle/Gaussian/1-500upr		
19/01/2007 14:19:07		
24		
360°/Admin/TR265 - Manual CL		
19/01/2007 14:18:45		
Specification		
Reference Type		LS Circle
Filter Type		Gaussian
Filter Range		1-500upr
Datum		Spindle
Parameters		
RONt	4.53	µm
Conditions		
Z Position	83.975	mm
R Position	55.333	mm
Attitude		Vertical
Contact Direction		R Negative

5.7.0.131

Taylor Hobson PRECISION

Scale 0.5µm/div.

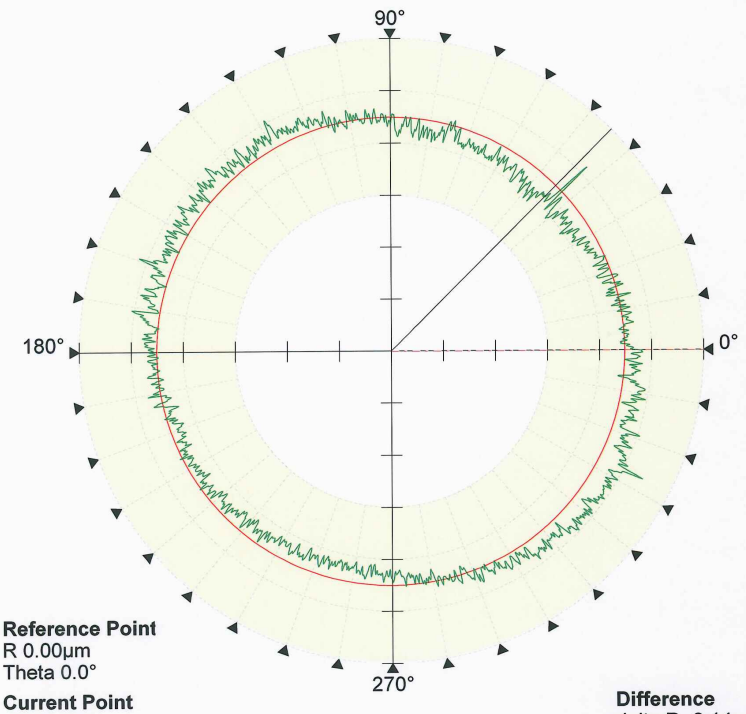

Reference Point
R 0.00µm
Theta 0.0°

Current Point
R -0.14µm
Theta 45.0°

Difference
delta R -0.14µm
delta Theta 45.0°

Roundness		
RON/LS Circle/Gaussian/1-500upr		
19/01/2007 14:20:54		
25		
360°/Admin/TR265 - Manual CL		
19/01/2007 14:20:27		
Specification		
Reference Type		LS Circle
Filter Type		Gaussian
Filter Range		1-500upr
Datum		Spindle
Parameters		
RONt	0.77	µm
Conditions		
Z Position	83.970	mm
R Position	55.415	mm
Attitude		Vertical
Contact Direction		R Negative

5.7.0.131

Taylor Hobson PRECISION

Scale 5µm/div.

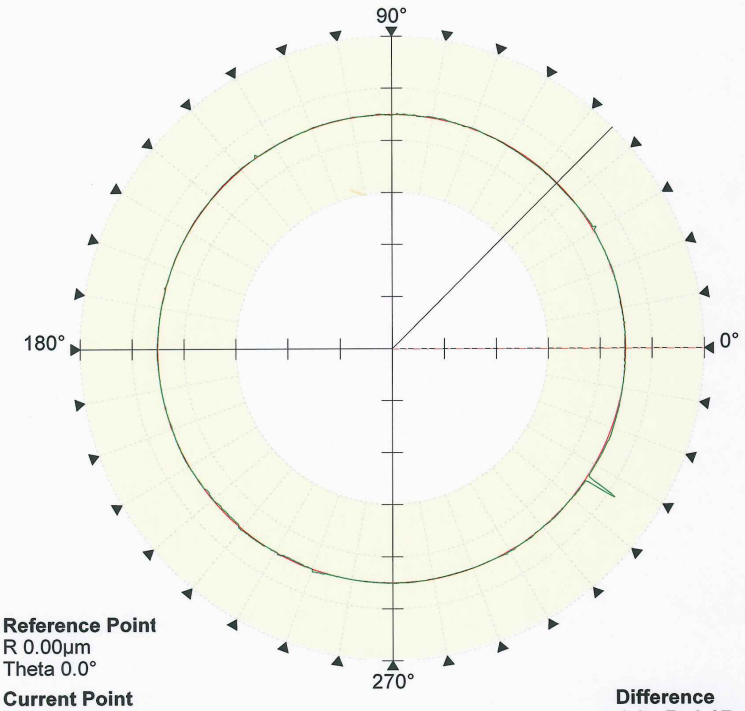

Reference Point
R 0.00µm
Theta 0.0°

Current Point
R -0.07µm
Theta 45.0°

Difference
delta R -0.07µm
delta Theta 45.0°

Roundness		
RON/LS Circle/Gaussian/1-500upr		
19/01/2007 14:30:16		
26 damage		
360°/Admin/TR265 - Manual CL		
19/01/2007 14:29:52		
Specification		
Reference Type		LS Circle
Filter Type		Gaussian
Filter Range		1-500upr
Datum		Spindle
Parameters		
RONt	3.41	µm
Conditions		
Z Position	84.010	mm
R Position	52.507	mm
Attitude		Vertical
Contact Direction		R Negative

5.7.0.131

Taylor Hobson PRECISION

Scale 1µm/div.

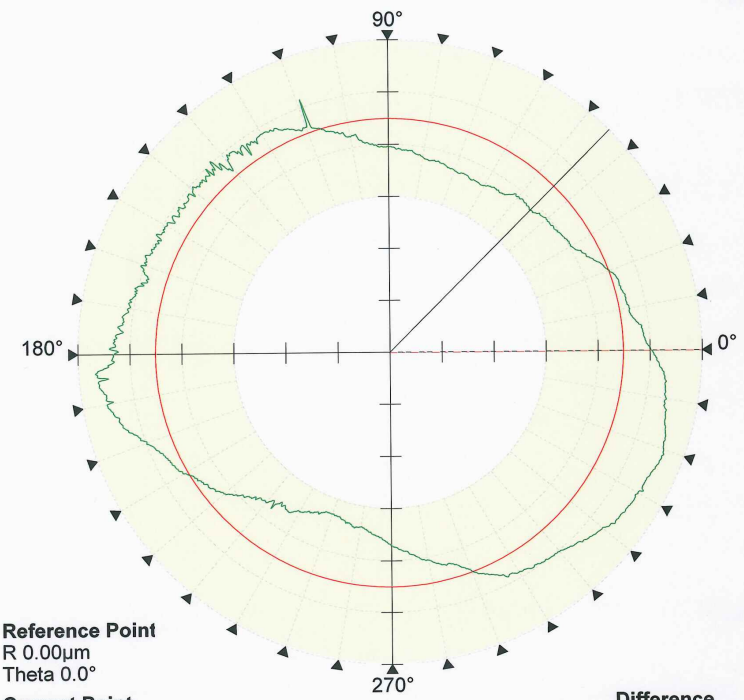

Reference Point
R 0.00µm
Theta 0.0°

Current Point
R -0.65µm
Theta 45.0°

Difference
delta R -0.65µm
delta Theta 45.0°

Roundness		
RON/LS Circle/Gaussian/1-500upr		
19/01/2007 14:32:16		
27 damage		
360°/Admin/TR265 - Manual CL		
19/01/2007 14:31:28		
Specification		
Reference Type		LS Circle
Filter Type		Gaussian
Filter Range		1-500upr
Datum		Spindle
Parameters		
RONt	2.40	µm
Conditions		
Z Position	91.050	mm
R Position	55.293	mm
Attitude		Vertical
Contact Direction		R Negative

5.7.0.131

Taylor Hobson PRECISION

Scale 2µm/div.

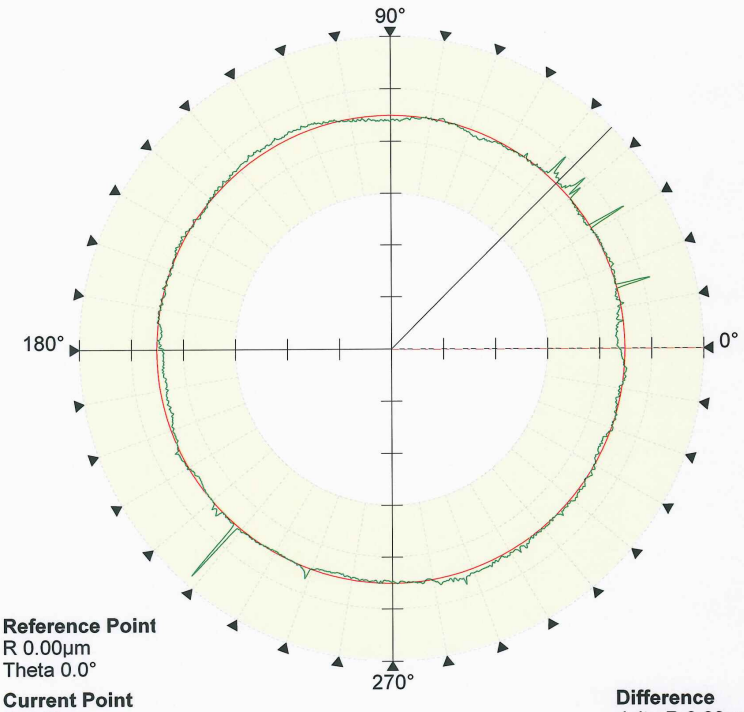

Reference Point
R 0.00µm
Theta 0.0°

Current Point
R 0.09µm
Theta 45.0°

Difference
delta R 0.09µm
delta Theta 45.0°

Roundness		
RON/LS Circle/Gaussian/1-500upr		
19/01/2007 14:34:09		
28 damage		
360°/Admin/TR265 - Manual CL		
19/01/2007 14:33:25		
Specification		
Reference Type		LS Circle
Filter Type		Gaussian
Filter Range		1-500upr
Datum		Spindle
Parameters		
RONt	2.96	µm
Conditions		
Z Position	84.895	mm
R Position	55.411	mm
Attitude		Vertical
Contact Direction		R Negative

5.7.0.131

Taylor Hobson PRECISION

Scale 0.5µm/div.

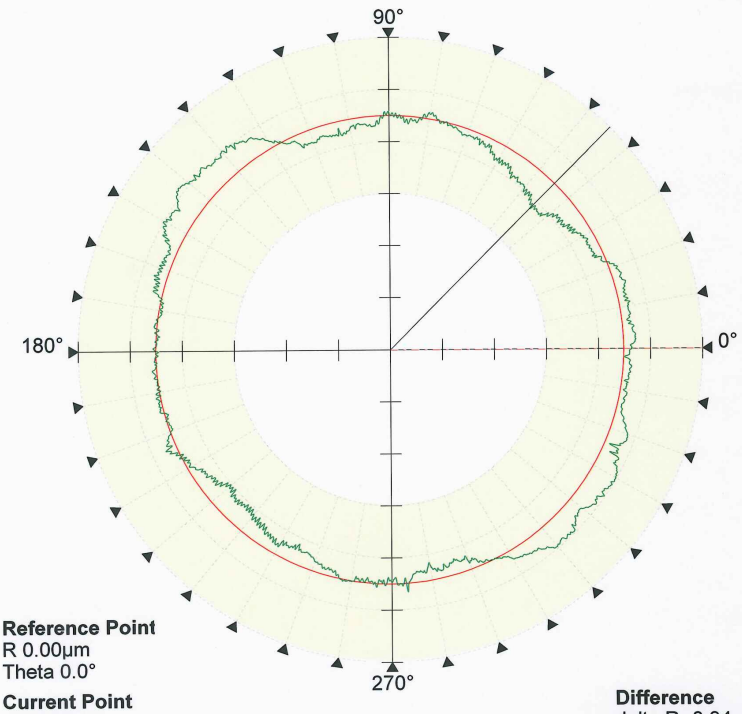

Reference Point
R 0.00µm
Theta 0.0°

Current Point
R -0.34µm
Theta 45.0°

Difference
delta R -0.34µm
delta Theta 45.0°

Roundness		
RON/LS Circle/Gaussian/1-500upr		
19/01/2007 14:41:33		
new 29		
360°/Admin/TR265 - Manual CL		
19/01/2007 14:41:06		
Specification		
Reference Type		LS Circle
Filter Type		Gaussian
Filter Range		1-500upr
Datum		Spindle
Parameters		
RONt	0.66	µm
Conditions		
Z Position	89.565	mm
R Position	54.377	mm
Attitude		Vertical
Contact Direction		R Negative

5.7.0.131

Taylor Hobson PRECISION

Scale 0.5µm/div.

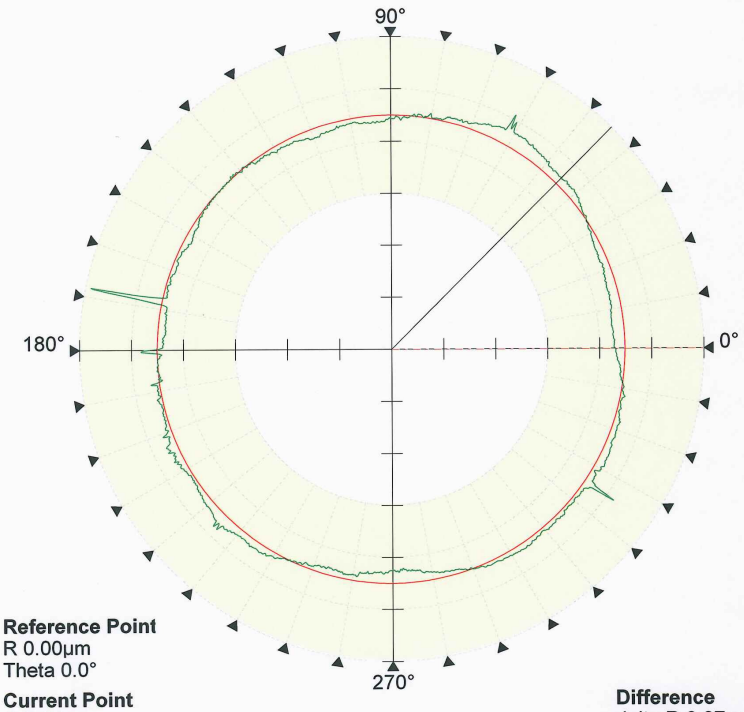

Reference Point
R 0.00µm
Theta 0.0°

Current Point
R 0.07µm
Theta 45.0°

Difference
delta R 0.07µm
delta Theta 45.0°

Roundness		
RON/LS Circle/Gaussian/1-500upr		
19/01/2007 14:43:14		
new 30		
360°/Admin/TR265 - Manual CL		
19/01/2007 14:42:50		
Specification		
Reference Type		LS Circle
Filter Type		Gaussian
Filter Range		1-500upr
Datum		Spindle
Parameters		
RONt	0.84	µm
Conditions		
Z Position	80.080	mm
R Position	55.314	mm
Attitude		Vertical
Contact Direction		R Negative

5.7.0.131

Taylor Hobson PRECISION

Scale 0.5µm/div.

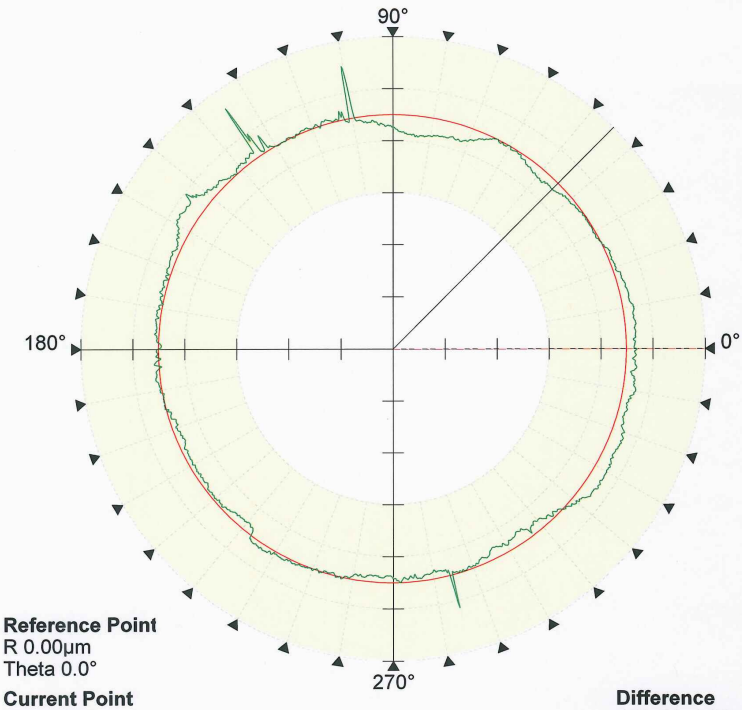

Reference Point
R 0.00µm
Theta 0.0°

Current Point
R -0.08µm
Theta 45.0°

Difference
delta R -0.08µm
delta Theta 45.0°

Roundness		
RON/LS Circle/Gaussian/1-500upr		
19/01/2007 14:45:23		
new 31		
360°/Admin/TR265 - Manual CL		
19/01/2007 14:44:59		
Specification		
Reference Type		LS Circle
Filter Type		Gaussian
Filter Range		1-500upr
Datum		Spindle
Parameters		
RONt	0.76	µm
Conditions		
Z Position	88.910	mm
R Position	55.279	mm
Attitude		Vertical
Contact Direction		R Negative

10 Appendix B– Surface finish measurements

5.11.6.17

Taylor Hobson PRECISION

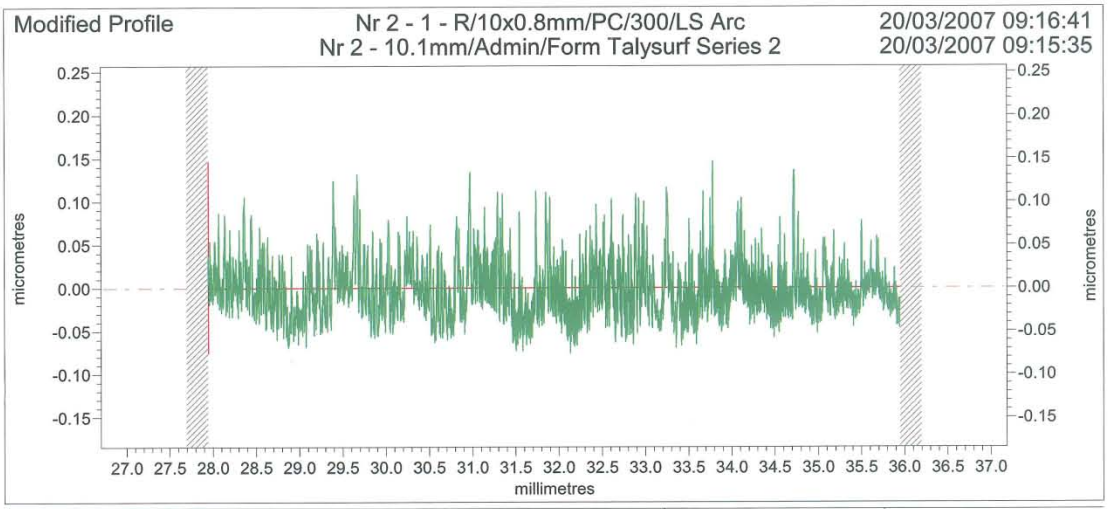

Radius	13.9604	mm
Ra	0.0251	µm

5.11.6.17

Taylor Hobson PRECISION

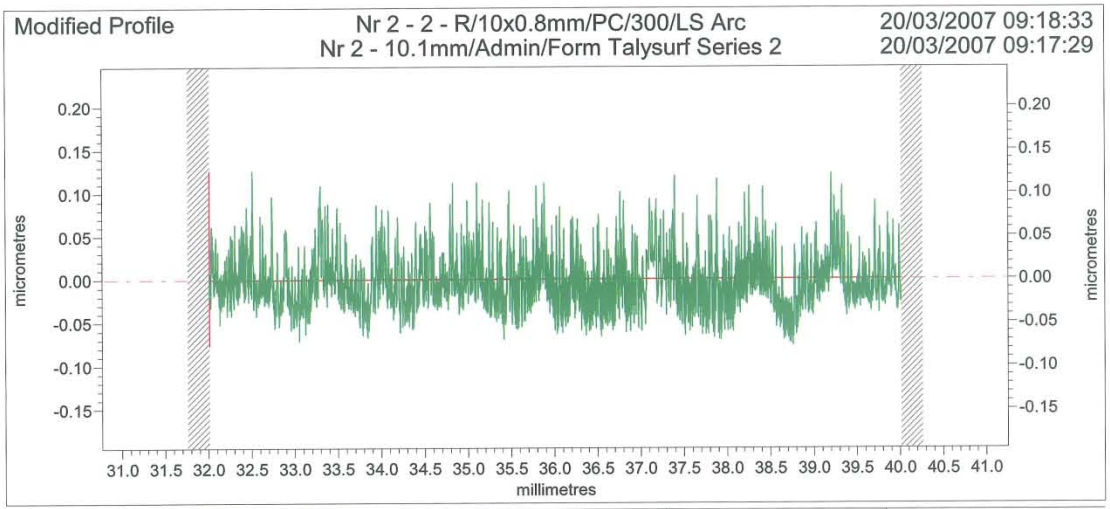

Radius	13.9794	mm
Ra	0.0245	µm

5.11.6.17

Taylor Hobson PRECISION

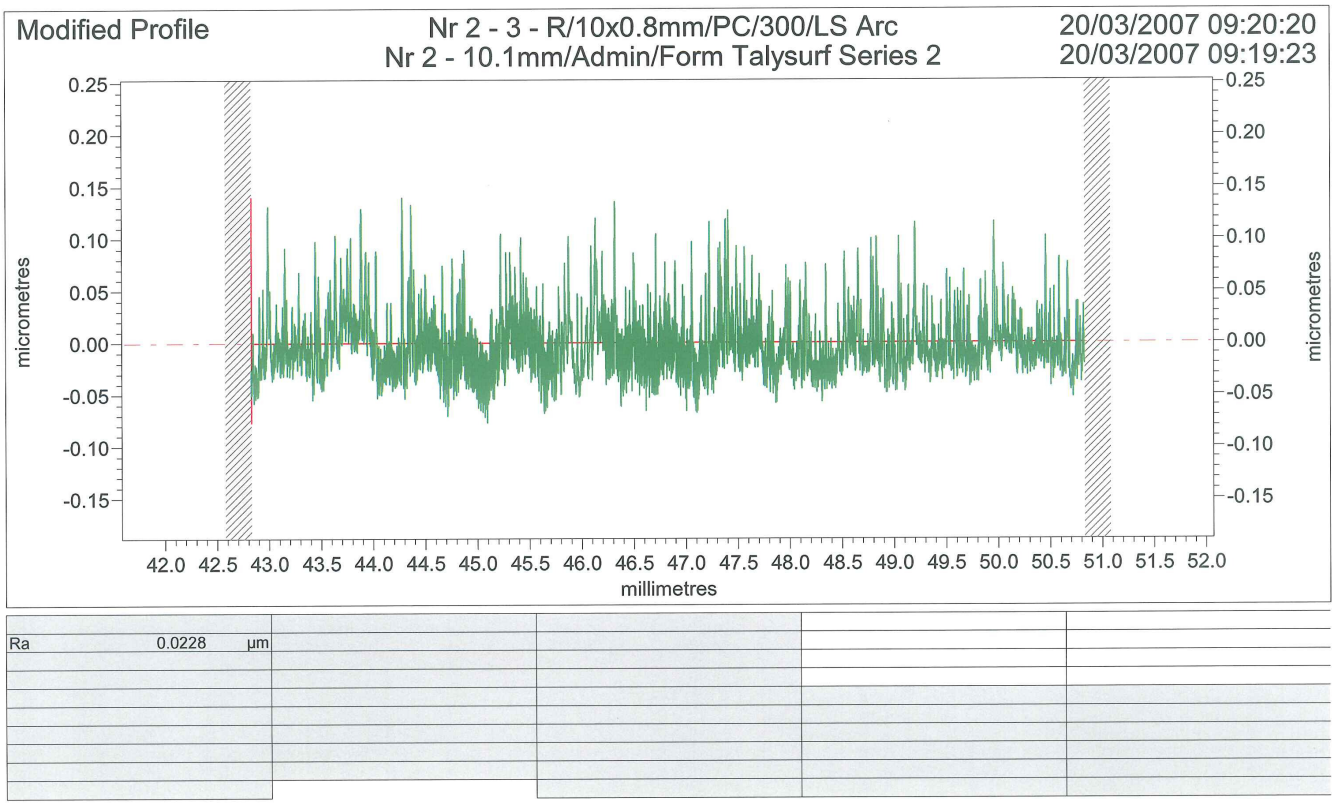

Ra	0.0228	µm

5.11.6.17

Taylor Hobson PRECISION

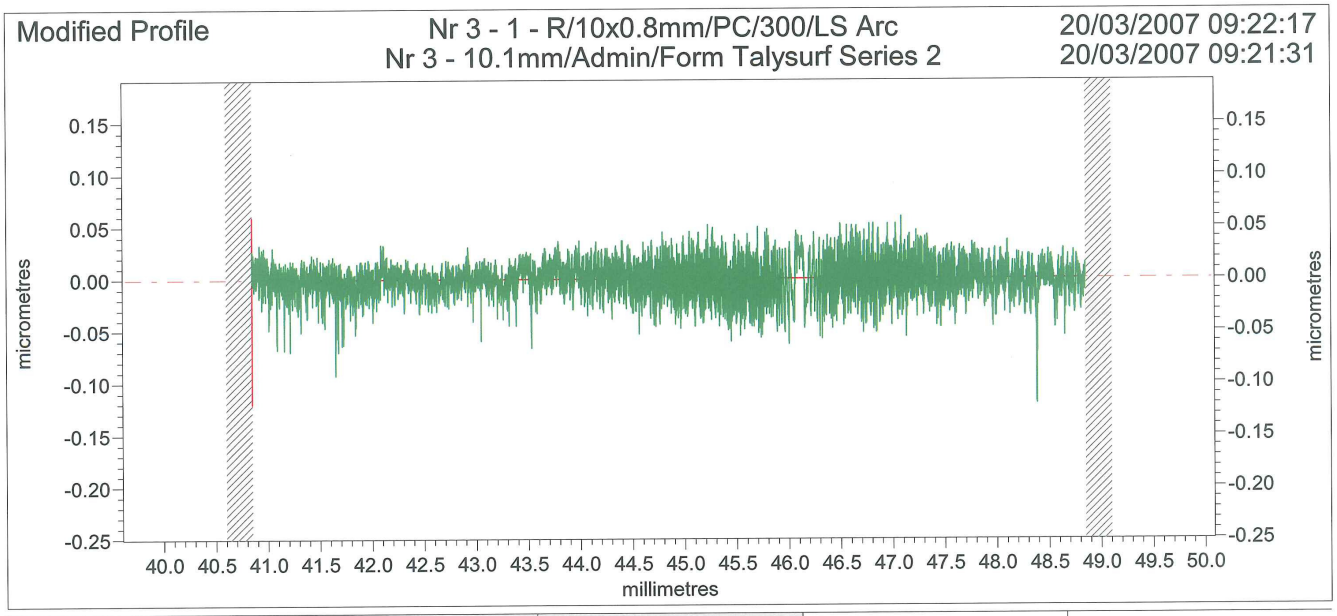

Ra	0.0128	µm

5.11.6.17

Taylor Hobson PRECISION

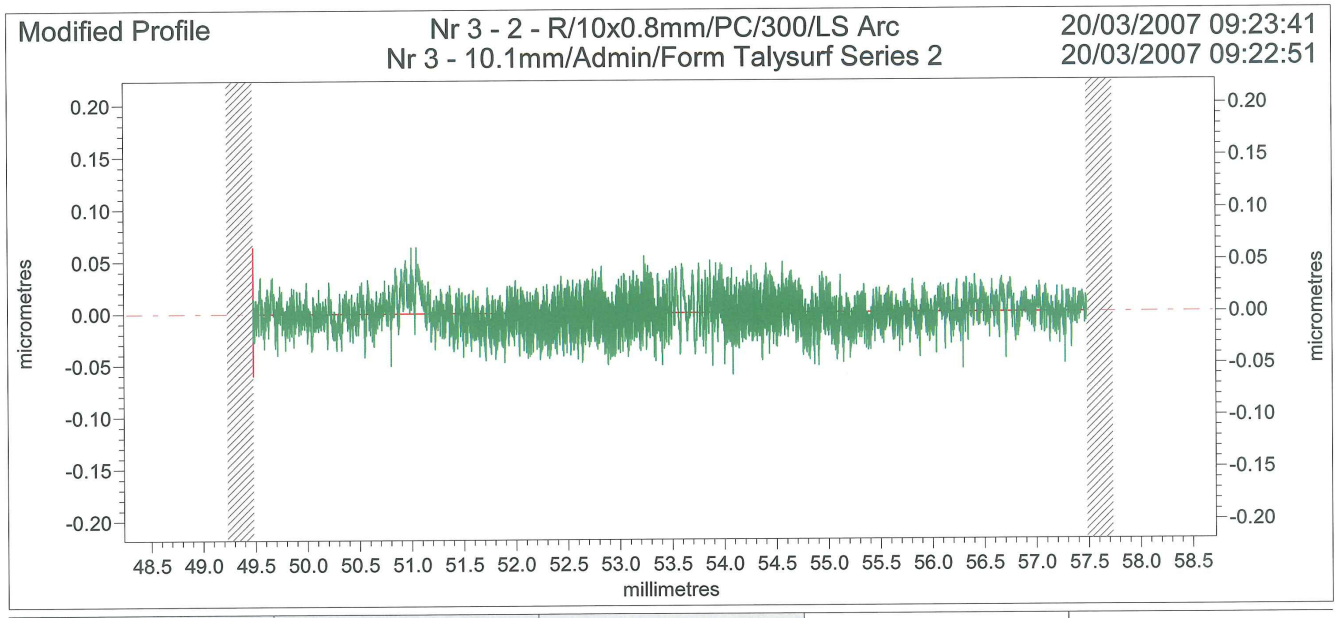

Ra	0.0130	µm

5.11.6.17

Taylor Hobson PRECISION

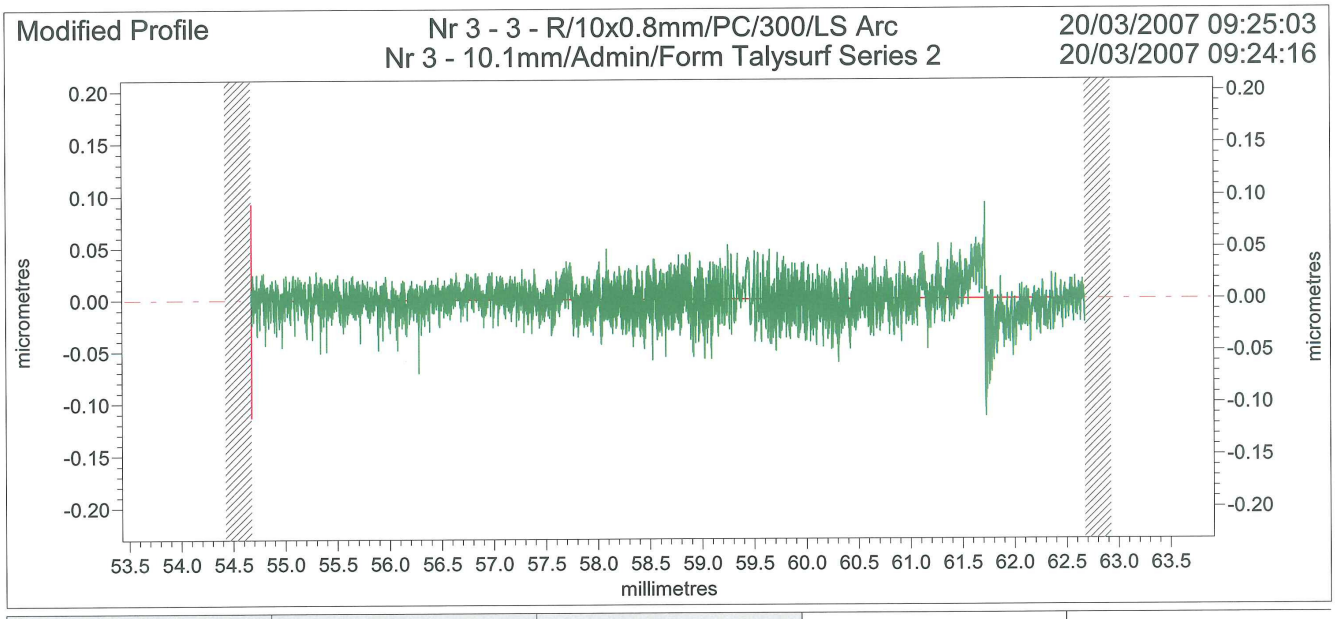

Ra	0.0126	µm

5.11.6.17

Taylor Hobson PRECISION

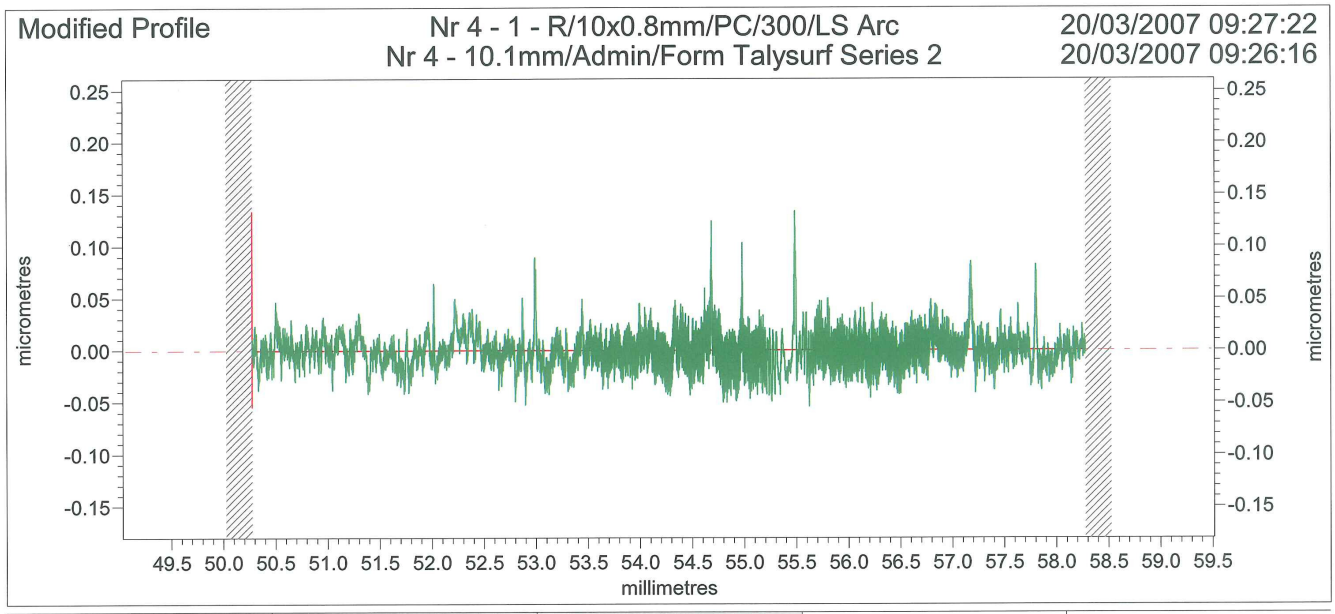

Ra	0.0135	µm

5.11.6.17

Taylor Hobson PRECISION

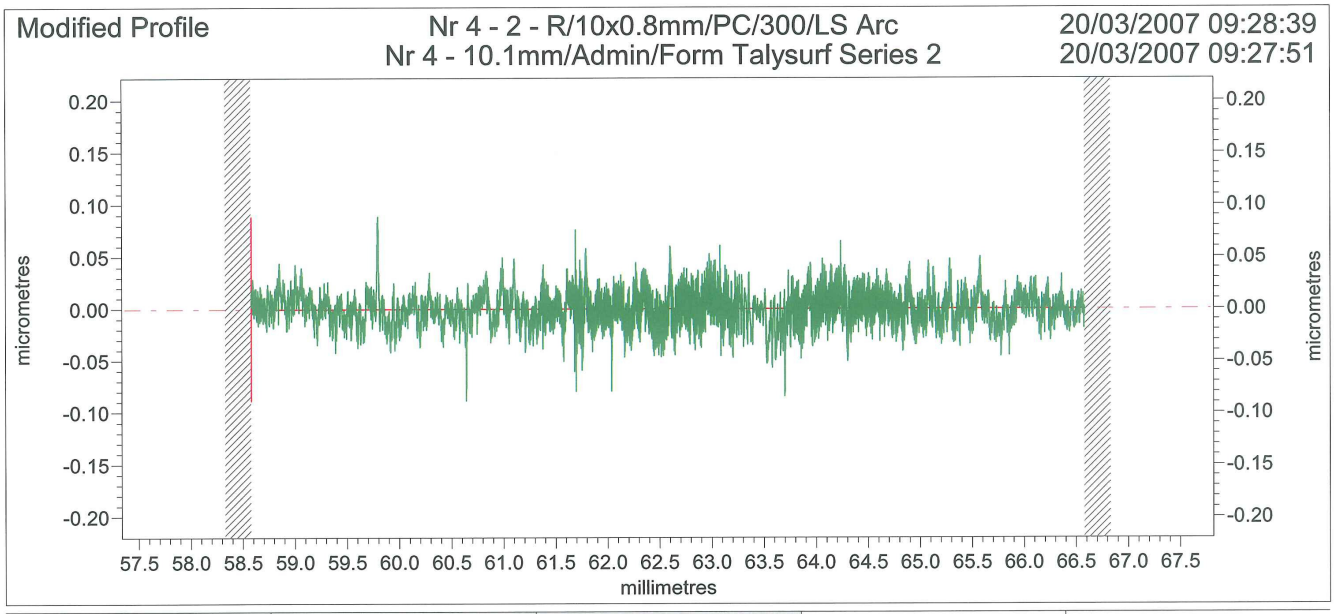

Ra	0.0128	µm

5.11.6.17

Taylor Hobson PRECISION

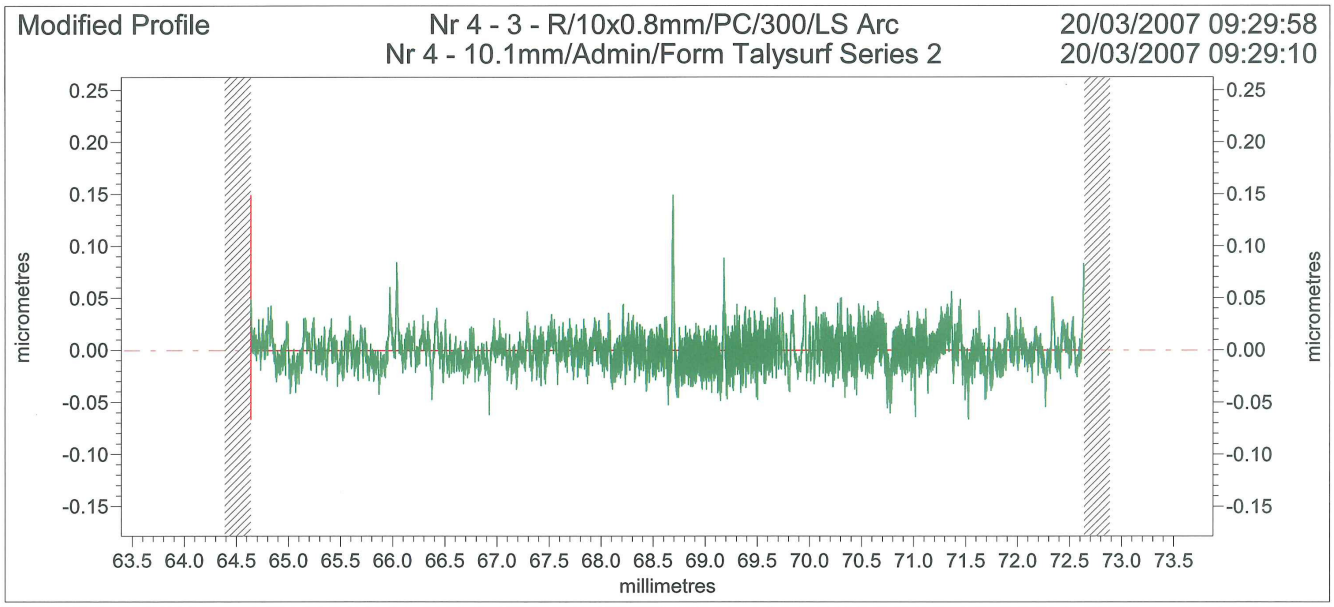

Ra	0.0130	µm

5.11.6.17

Taylor Hobson PRECISION

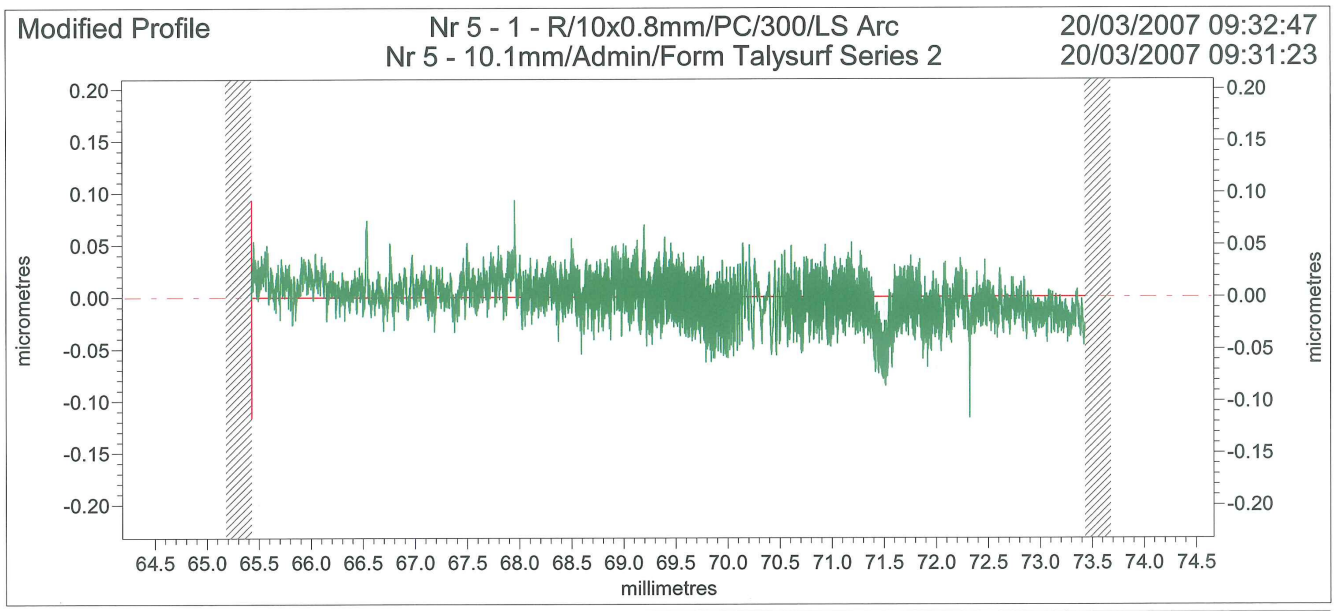

Ra	0.0163	µm

5.11.6.17

Taylor Hobson PRECISION

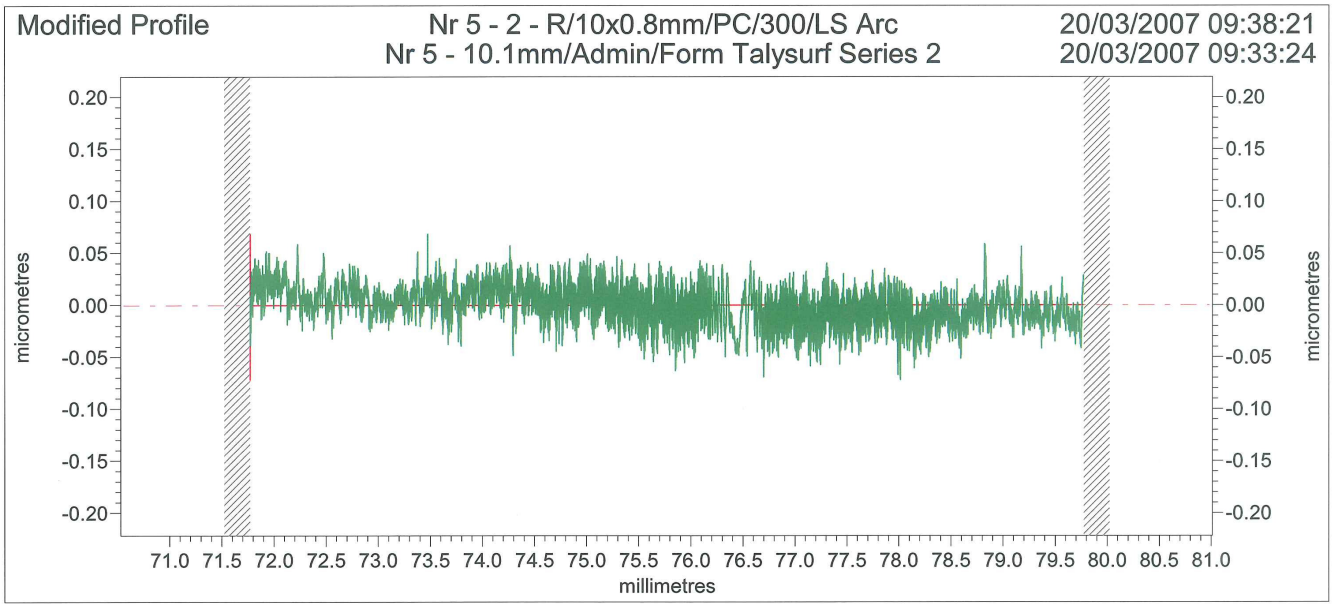

Ra	0.0149	µm

5.11.6.17

Taylor Hobson PRECISION

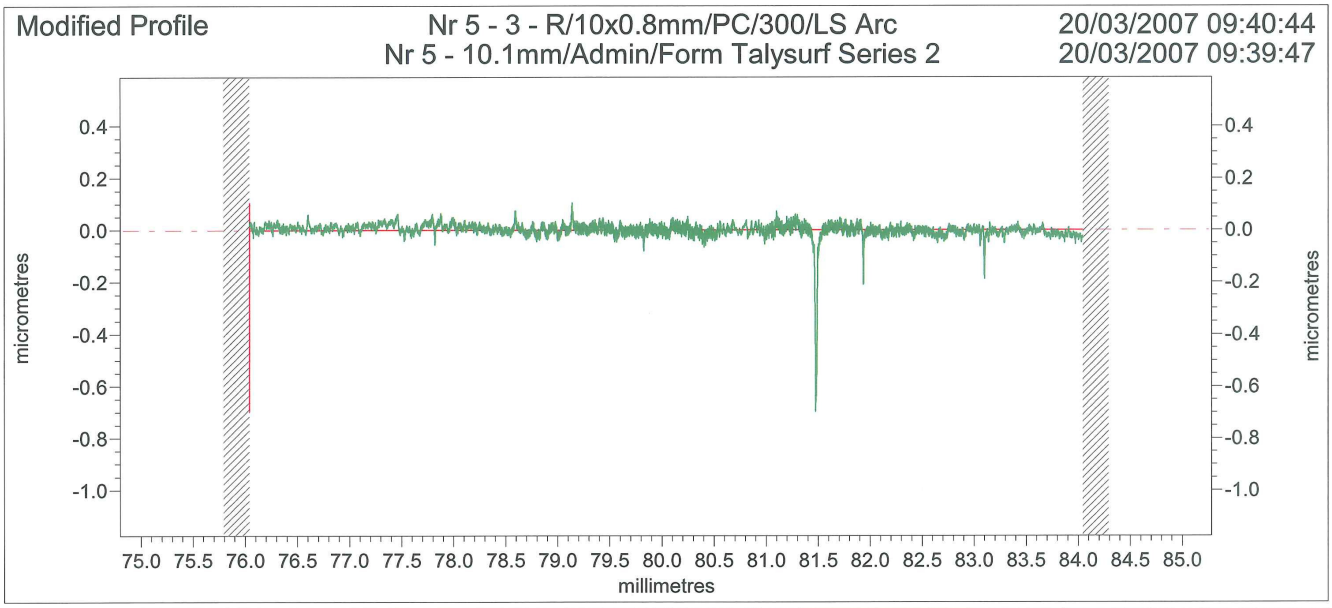

Ra	0.0167	µm

5.11.6.17

Taylor Hobson PRECISION

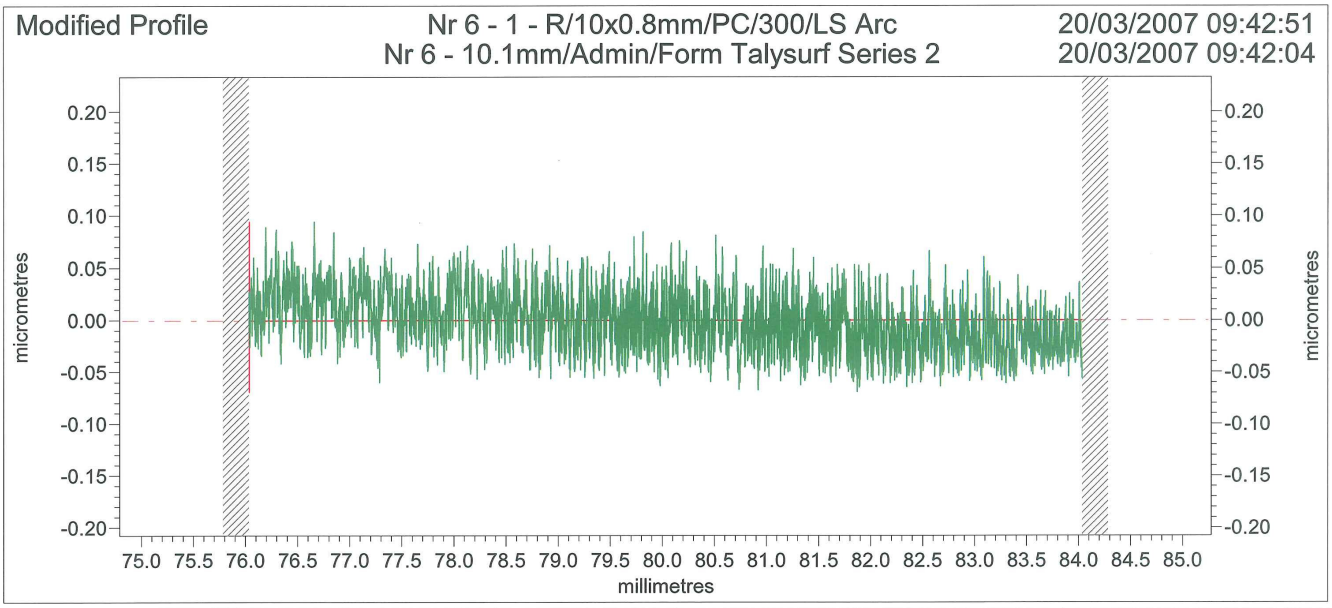

Ra	0.0225	µm

5.11.6.17

Taylor Hobson PRECISION

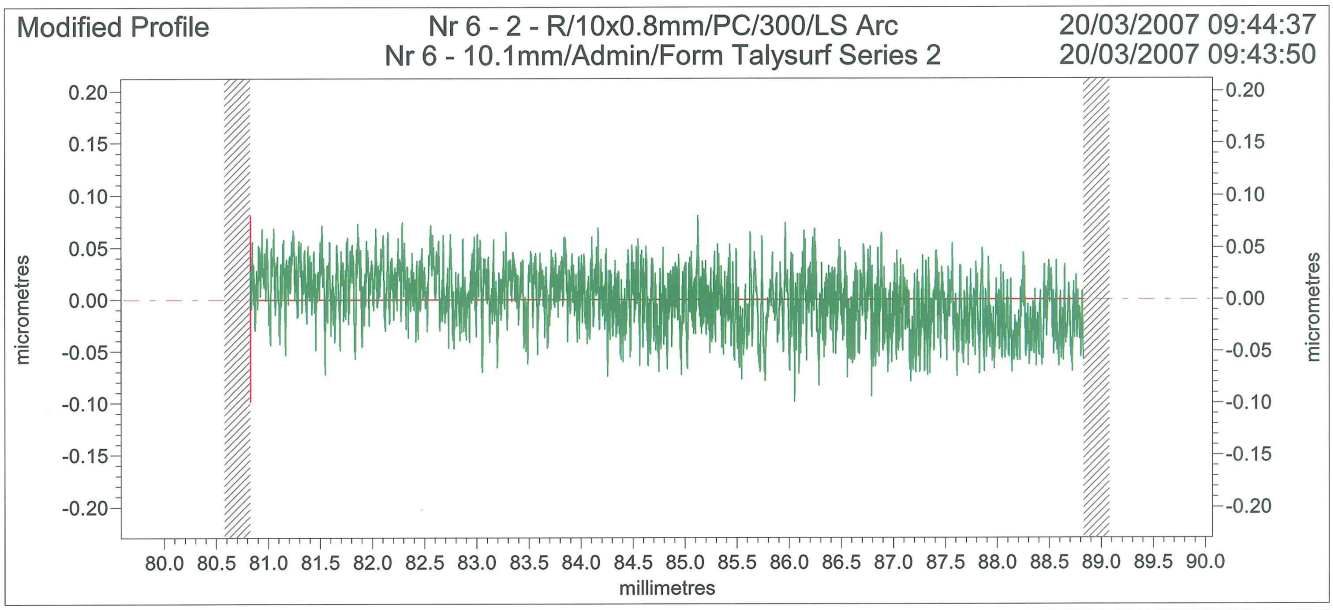

Ra	0.0228	µm

5.11.6.17

Taylor Hobson PRECISION

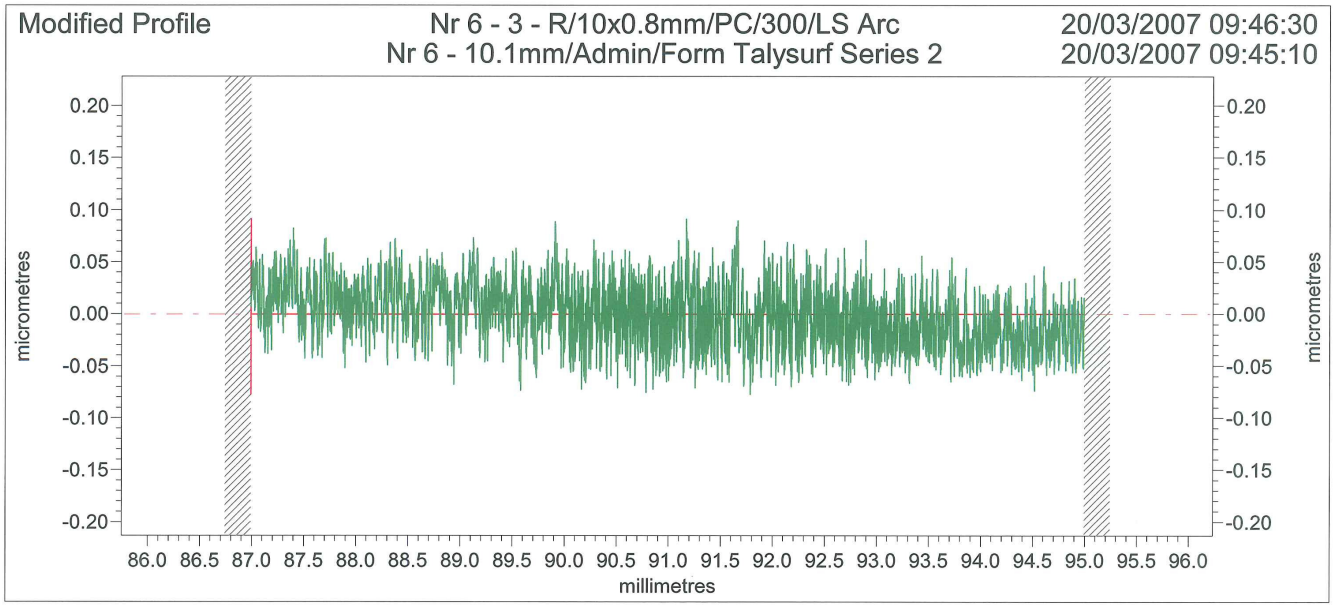

Ra	0.0232	µm

5.11.6.17

Taylor Hobson PRECISION

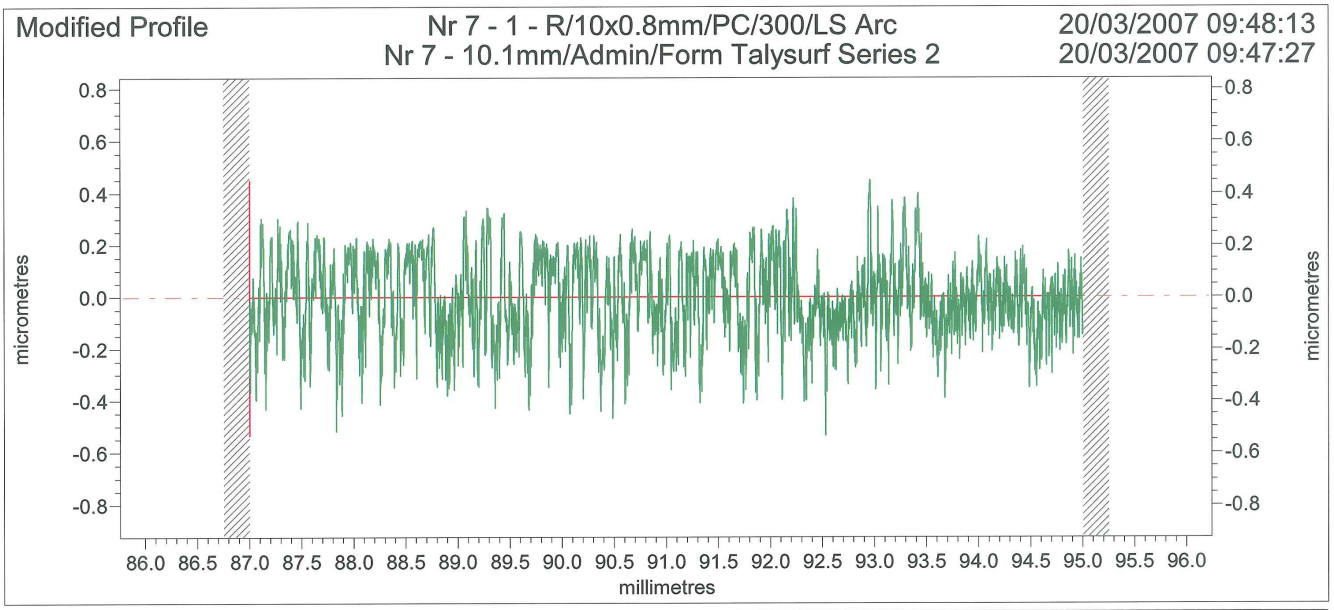

Ra	0.1256	µm

5.11.6.17

Taylor Hobson PRECISION

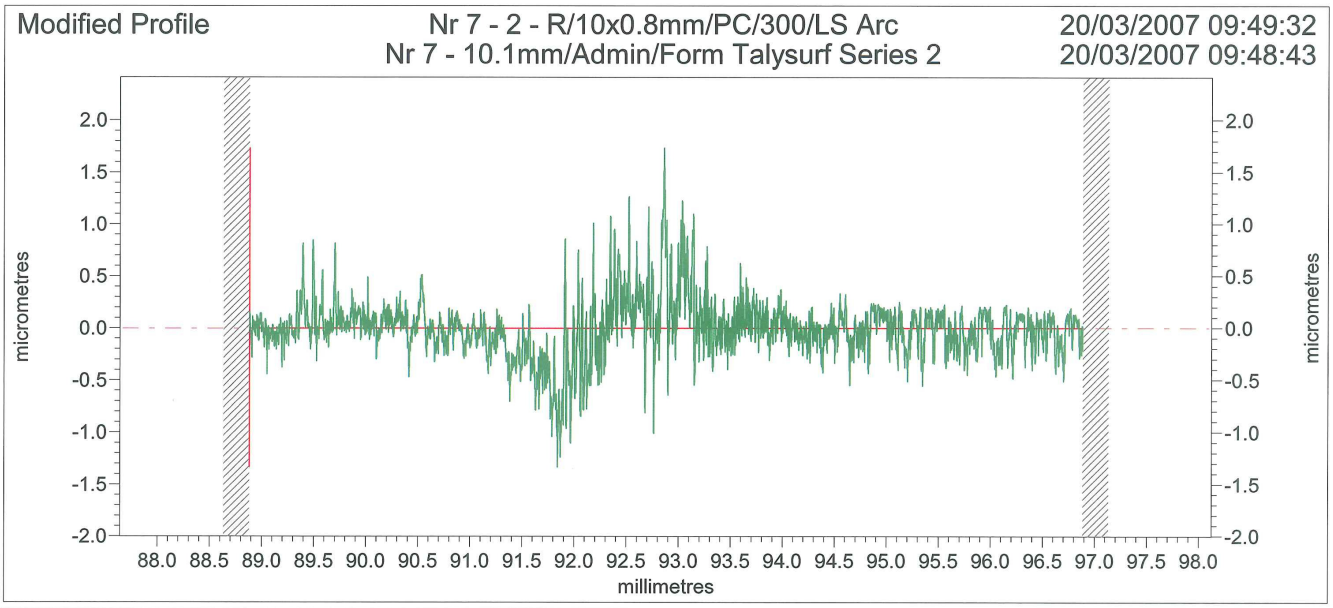

Ra	0.1883	µm

5.11.6.17

Taylor Hobson PRECISION

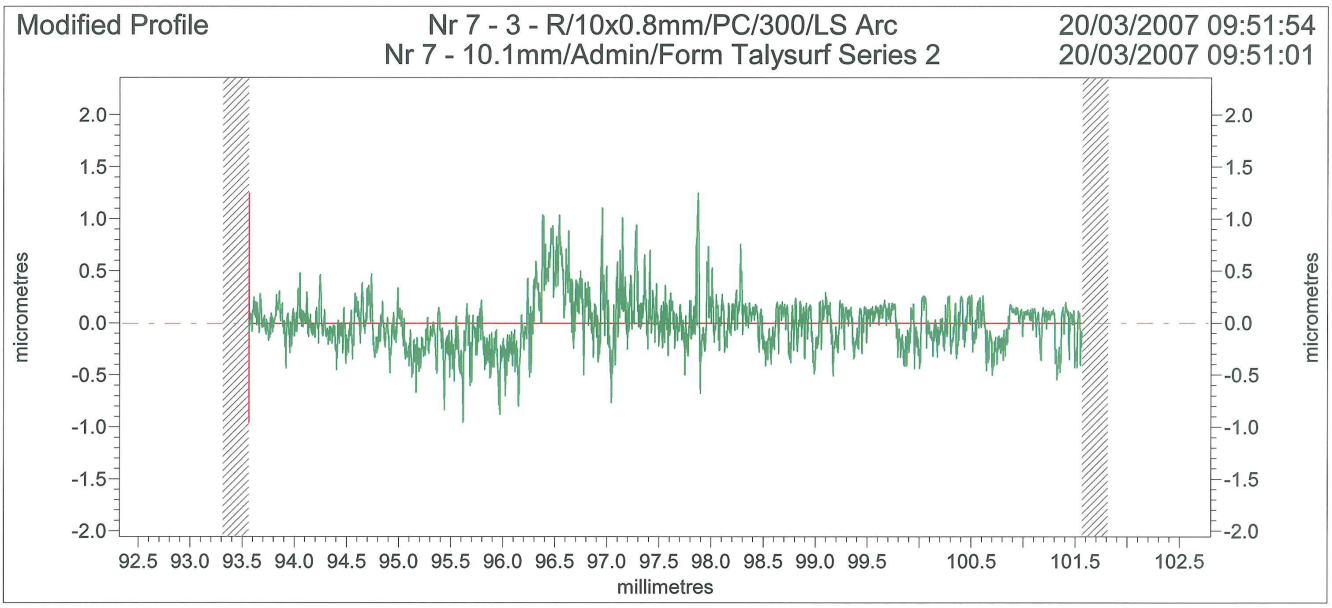

Ra	0.1839	µm

5.11.6.17

Taylor Hobson PRECISION

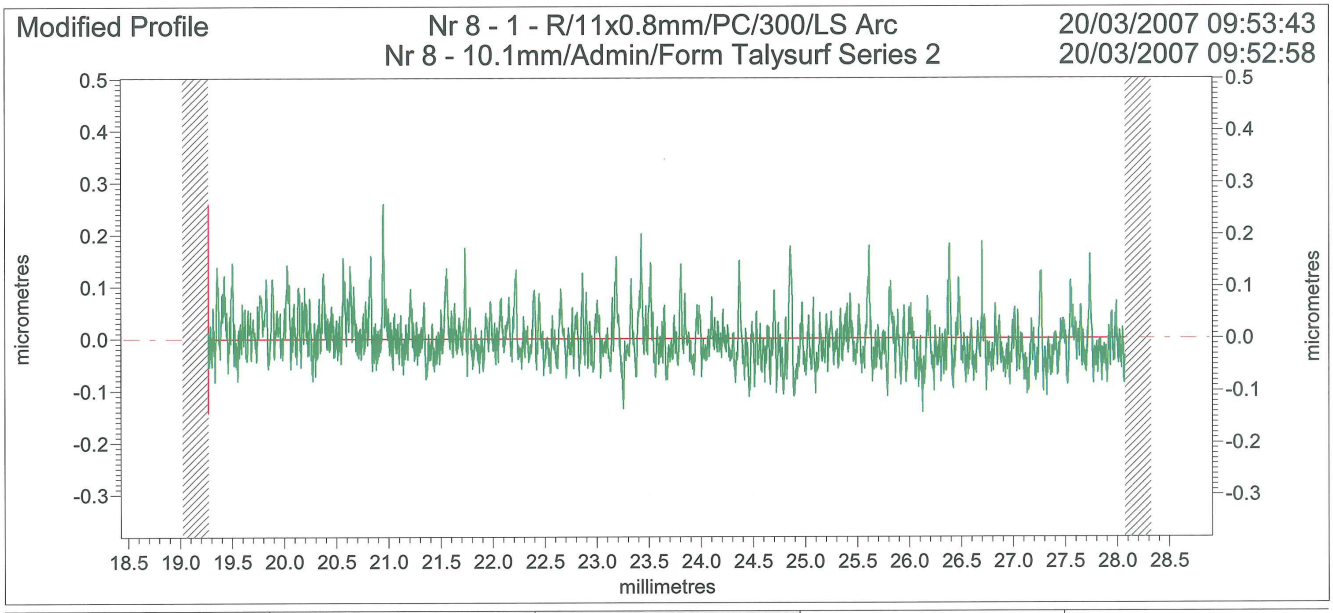

Ra	0.0355	µm

5.11.6.17

Taylor Hobson PRECISION

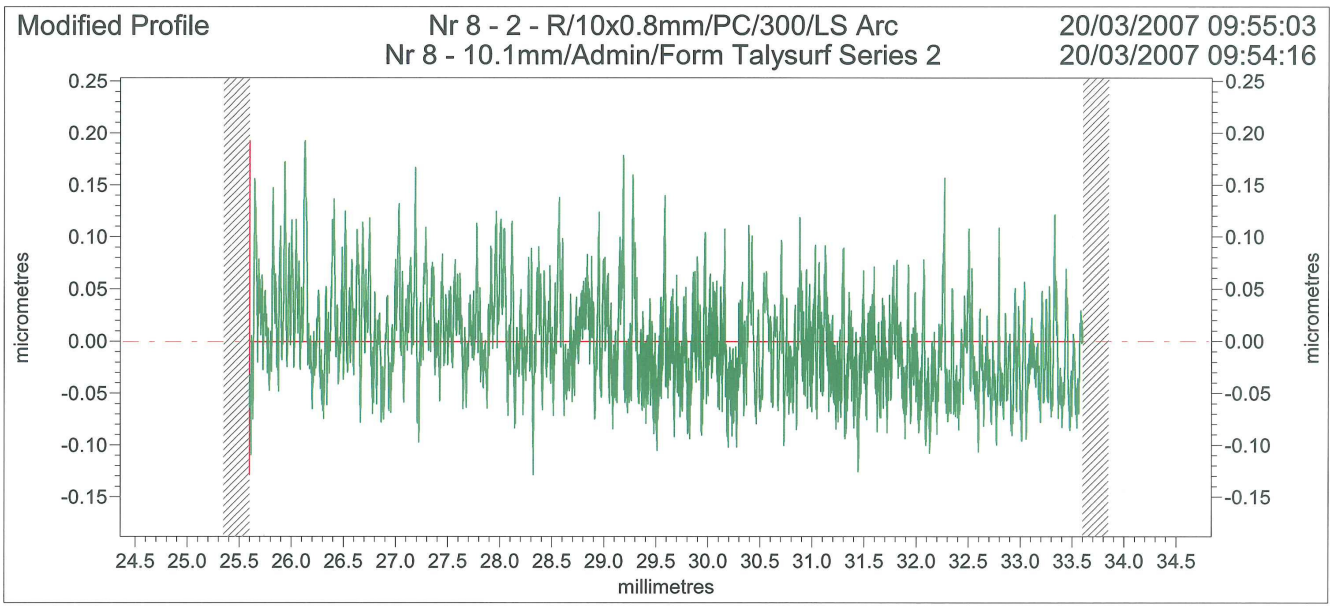

Ra	0.0364	µm

Taylor Hobson PRECISION

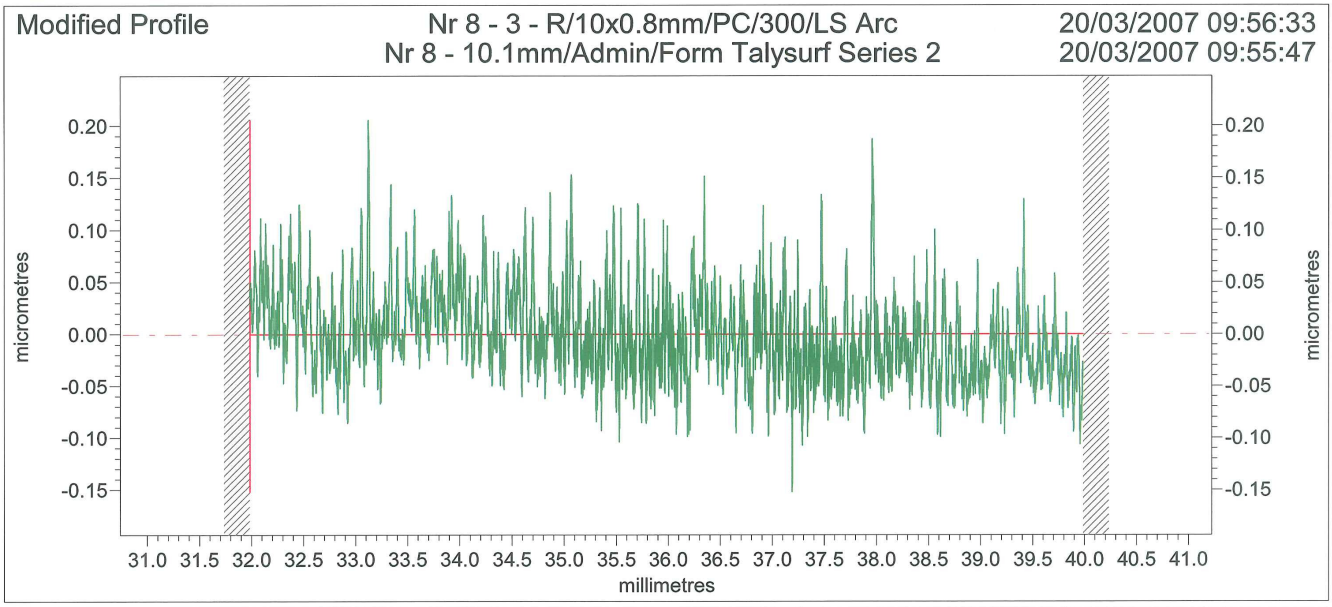

Ra	0.0338	µm

5.11.6.17

Taylor Hobson PRECISION

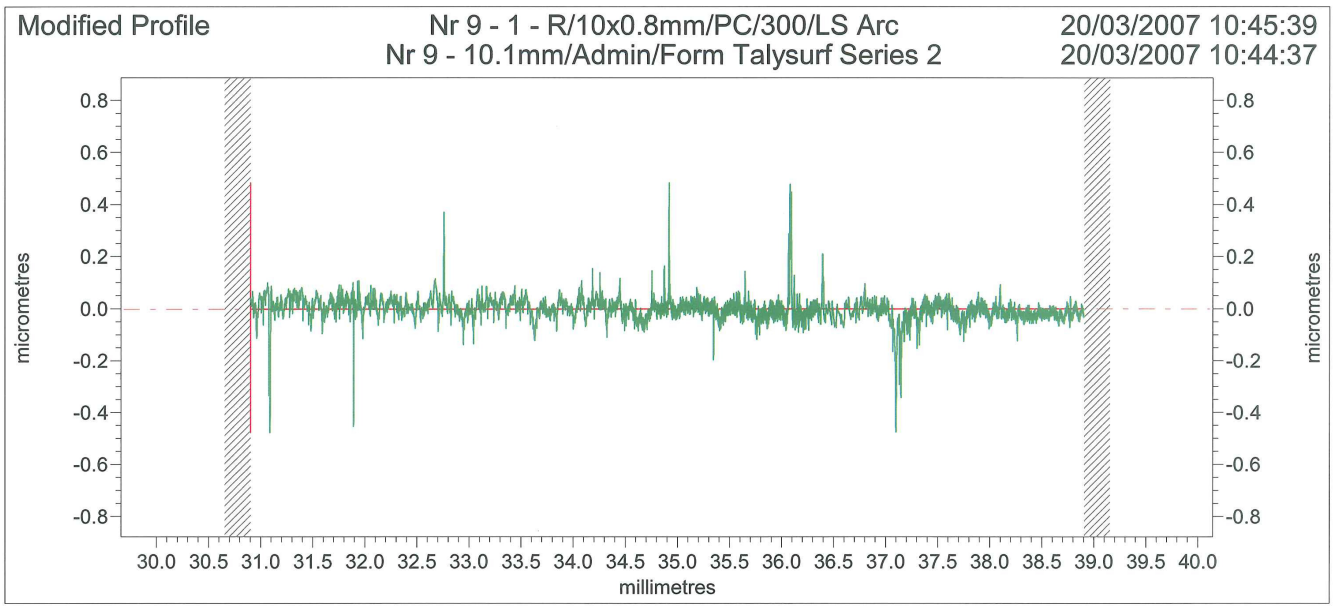

Ra	0.0304	µm

5.11.6.17

Taylor Hobson PRECISION

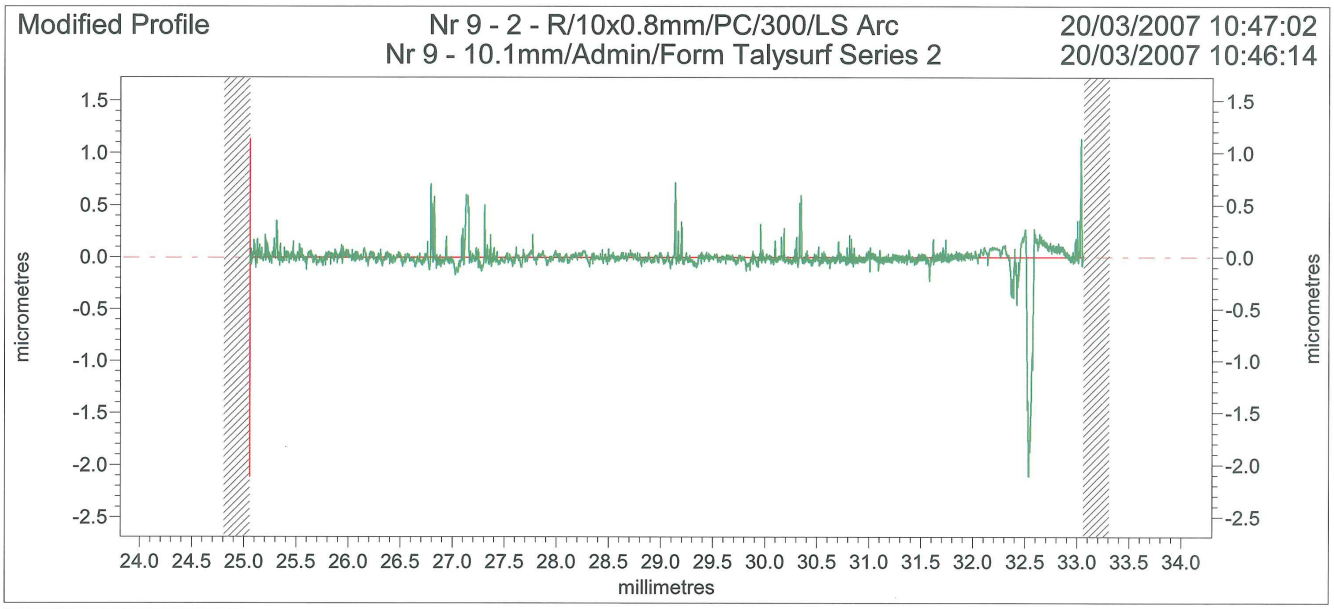

Ra	0.0558	µm

5.11.6.17

Taylor Hobson PRECISION

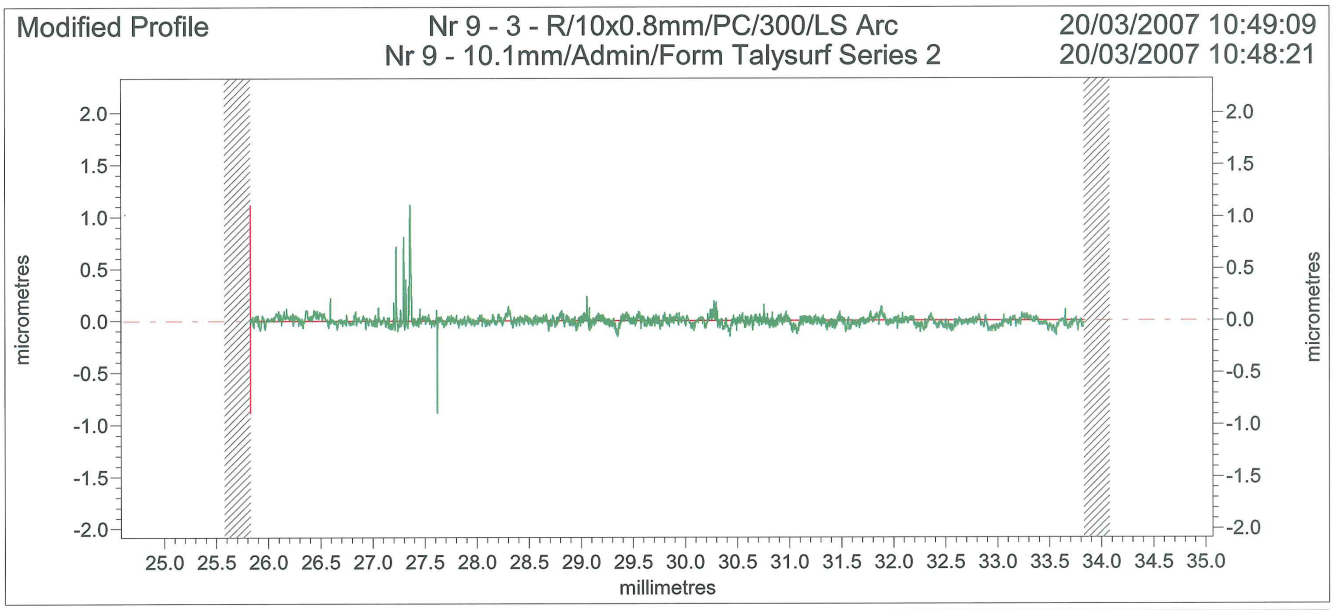

Ra	0.0329	µm

5.11.6.17

Taylor Hobson PRECISION

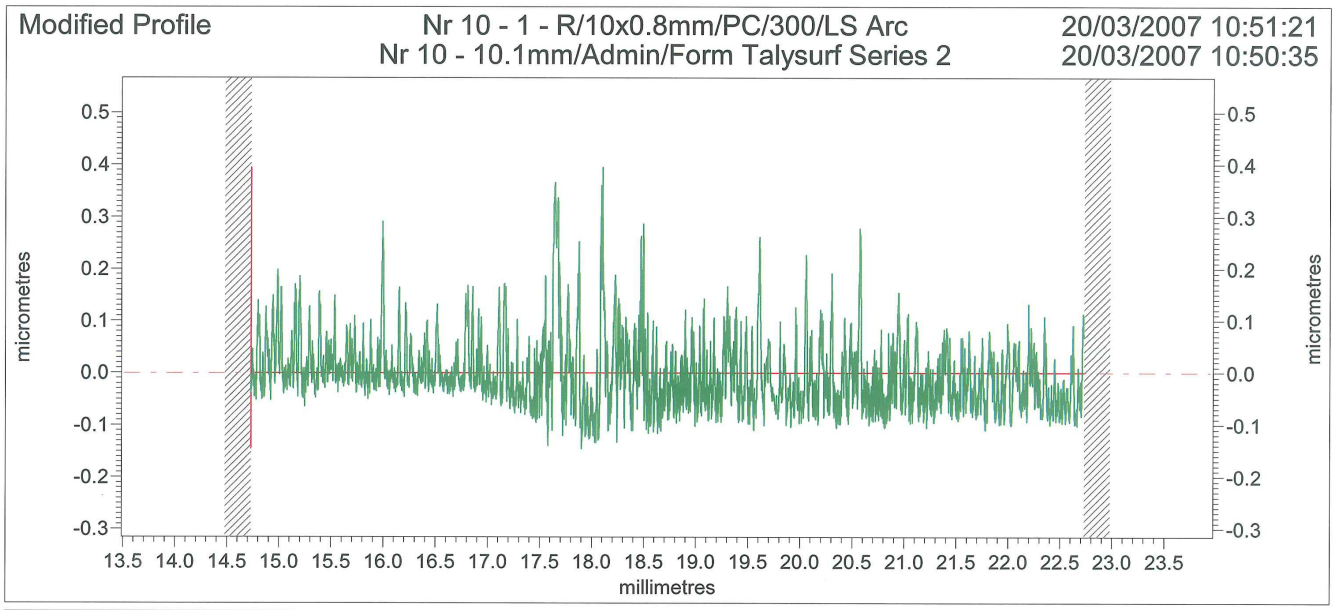

Ra	0.0498	µm

5.11.6.17

Taylor Hobson PRECISION

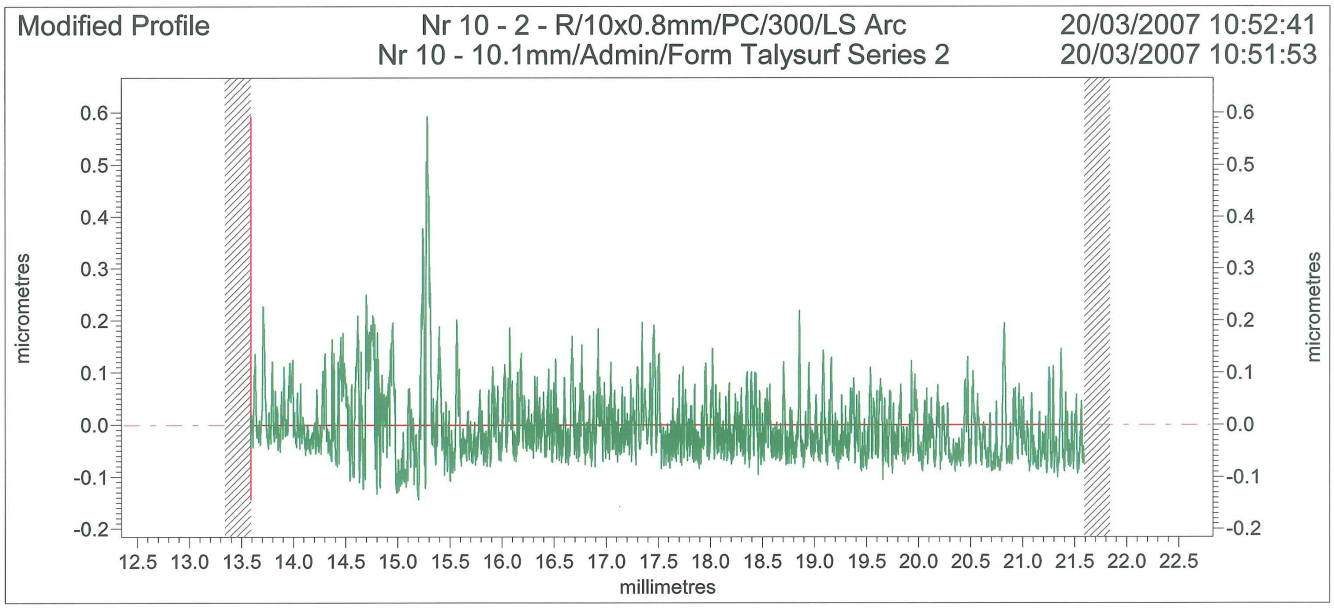

Ra	0.0494	µm

5.11.6.17

Taylor Hobson PRECISION

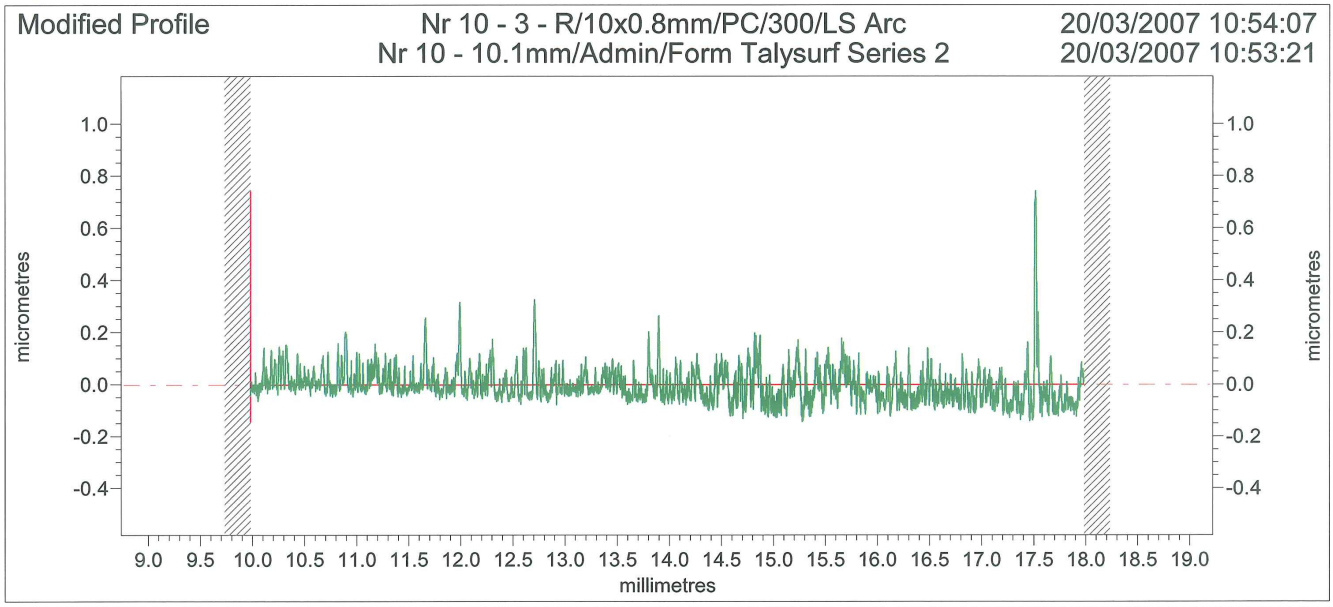

Ra	0.0488	µm

5.11.6.17

Taylor Hobson PRECISION

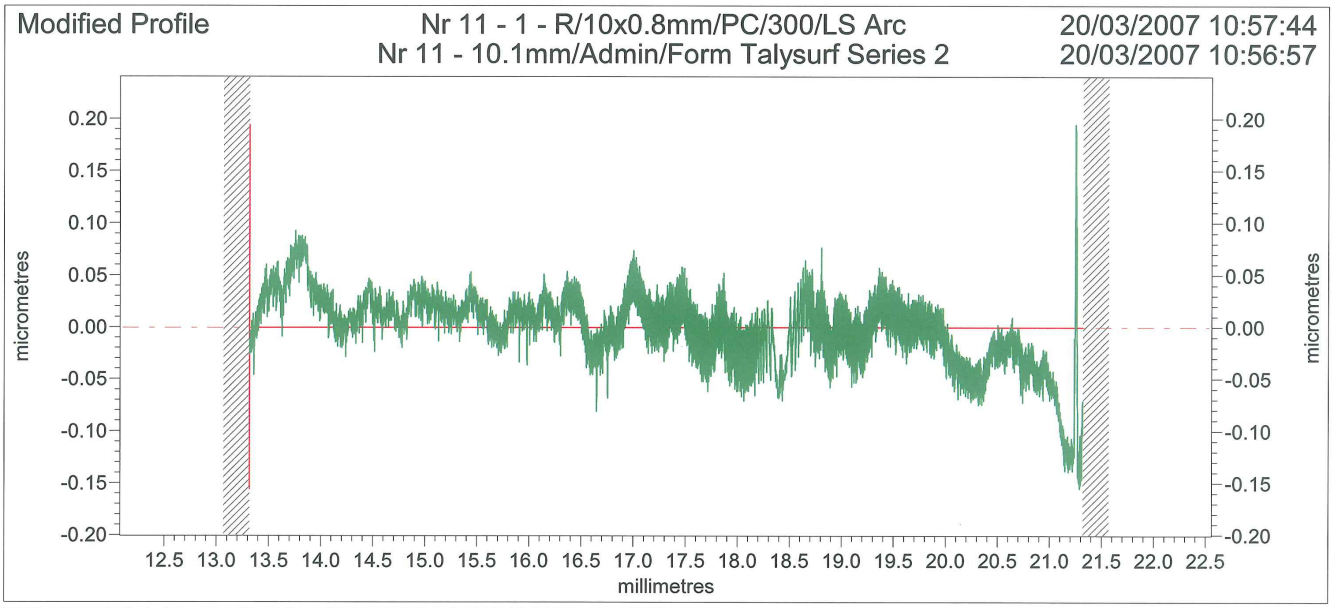

Ra	0.0260	µm

5.11.6.17

Taylor Hobson PRECISION

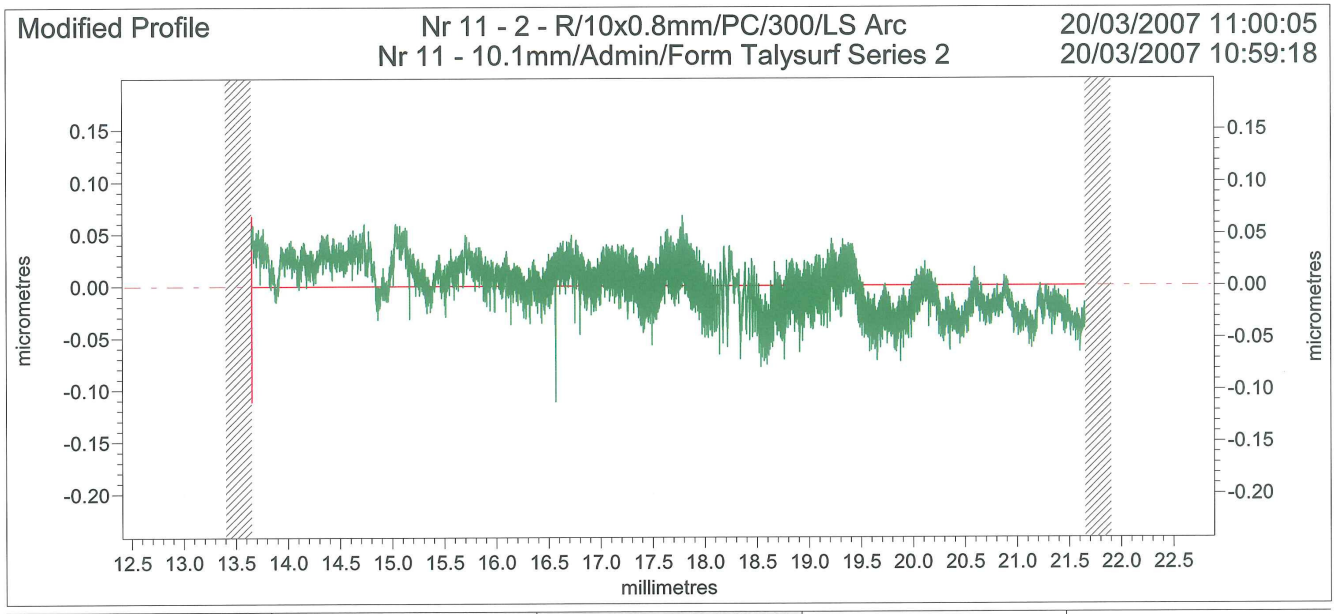

Ra	0.0205	µm

5.11.6.17

Taylor Hobson PRECISION

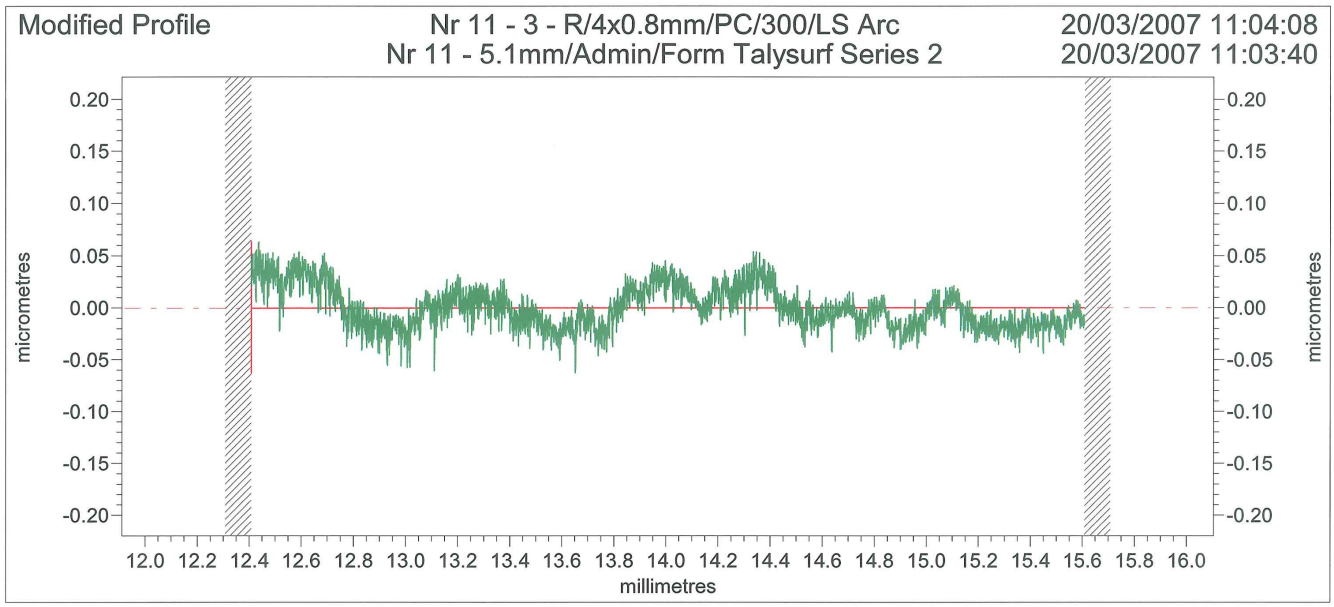

Ra	0.0162	µm

5.11.6.17

Taylor Hobson PRECISION

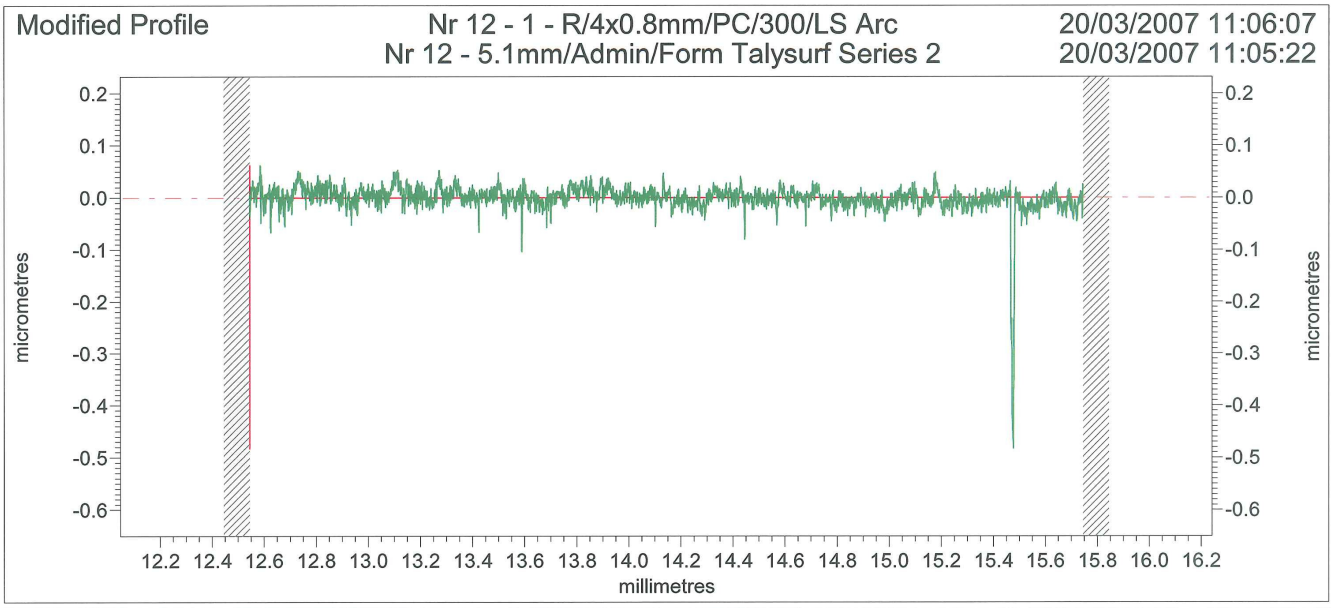

Ra	0.0138	µm

5.11.6.17

Taylor Hobson PRECISION

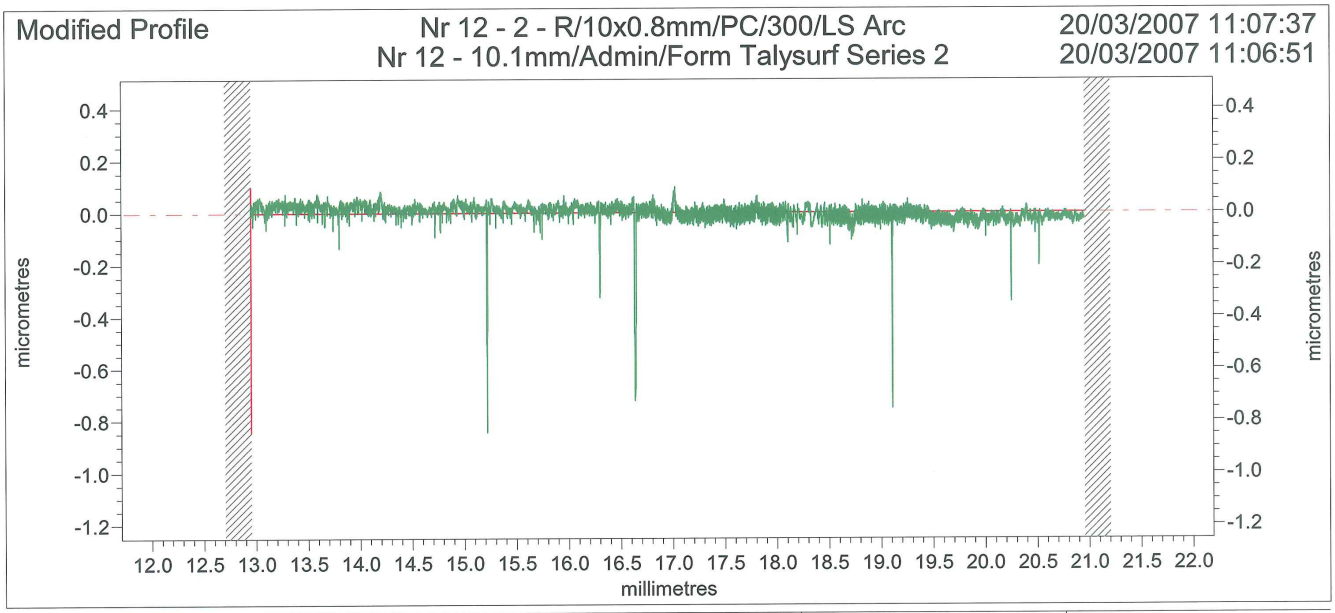

Ra	0.0242	µm

5.11.6.17

Taylor Hobson PRECISION

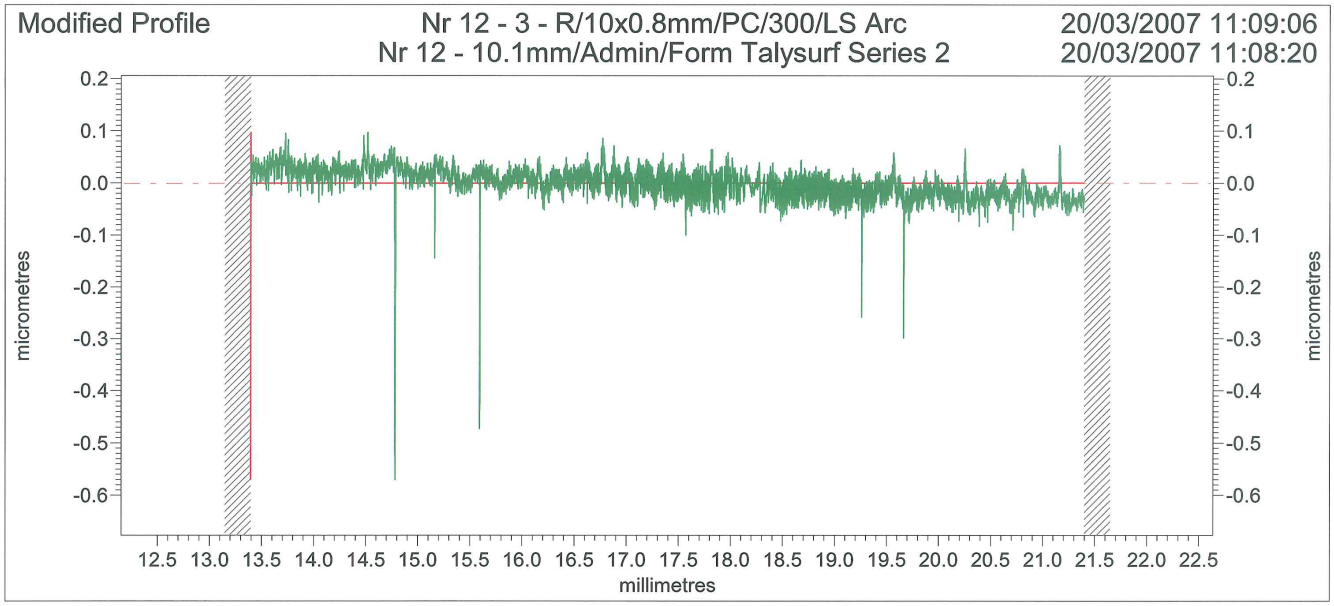

Ra	0.0226	µm

5.11.6.17

Taylor Hobson PRECISION

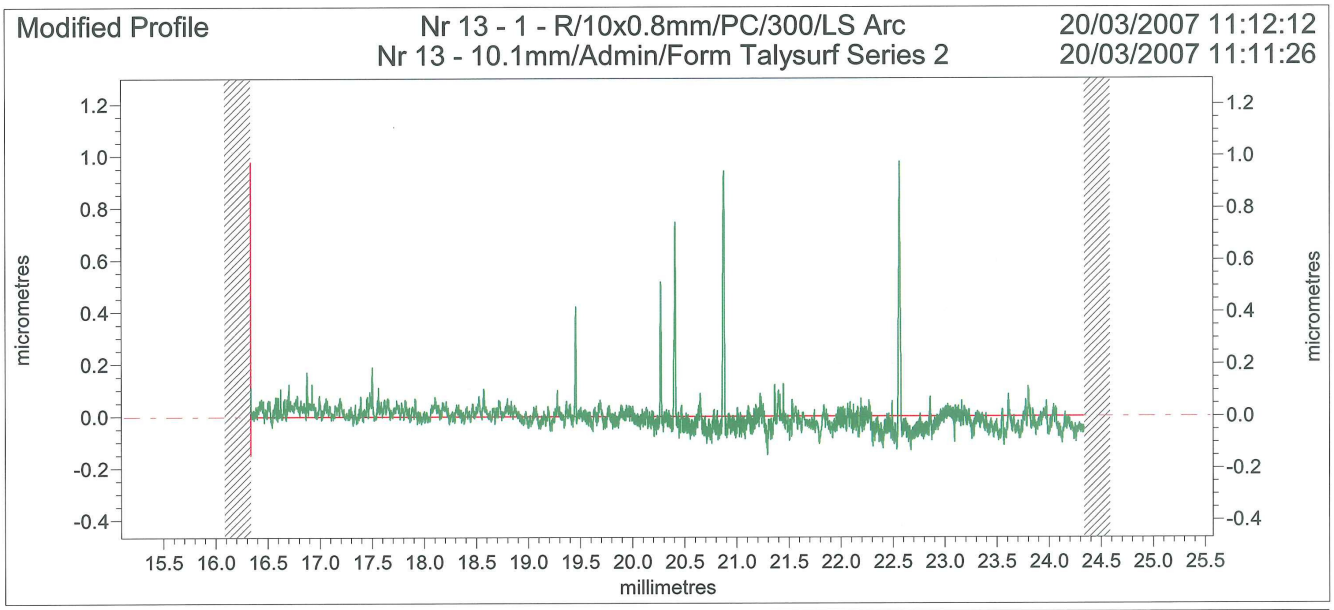

Ra	0.0345	µm

5.11.6.17

Taylor Hobson PRECISION

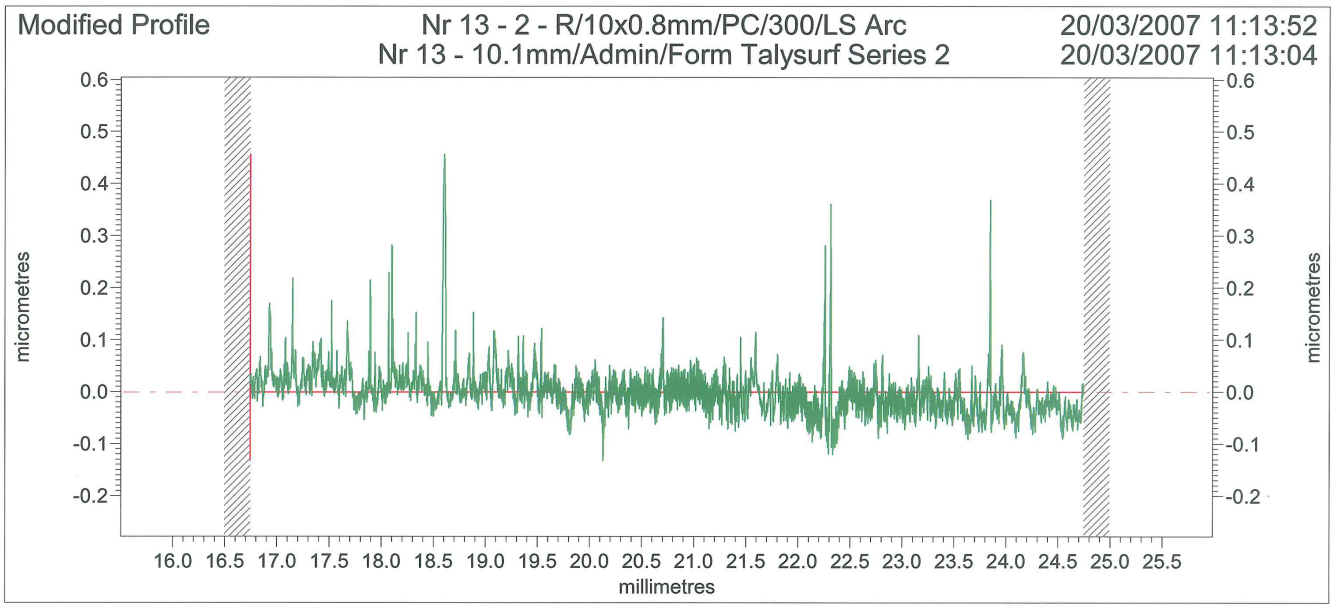

Ra	0.0296	µm

5.11.6.17

Taylor Hobson PRECISION

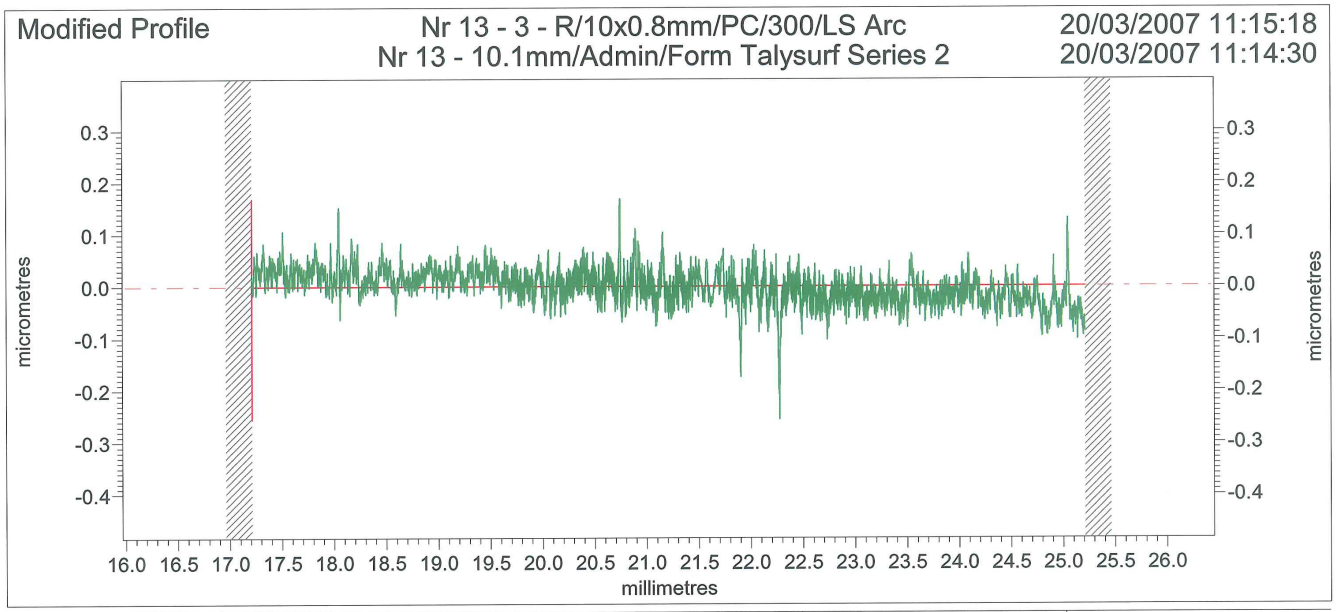

Ra	0.0268	µm

5.11.6.17

Taylor Hobson PRECISION

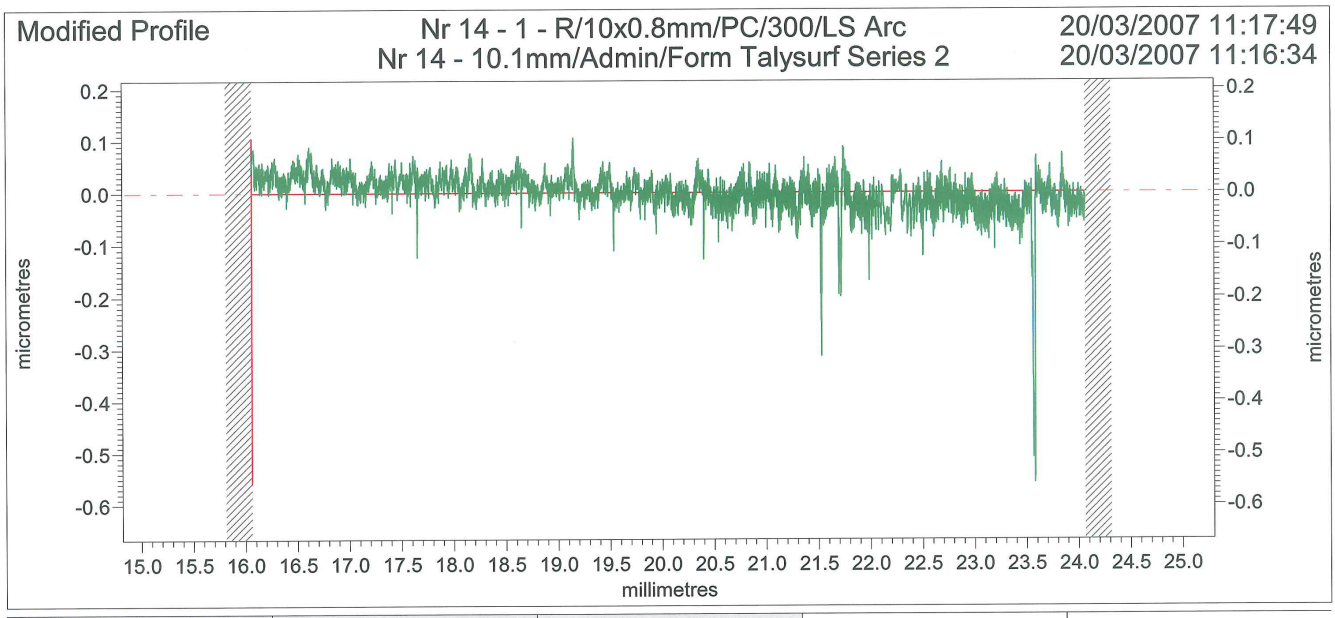

Ra	0.0253	µm

5.11.6.17

Taylor Hobson PRECISION

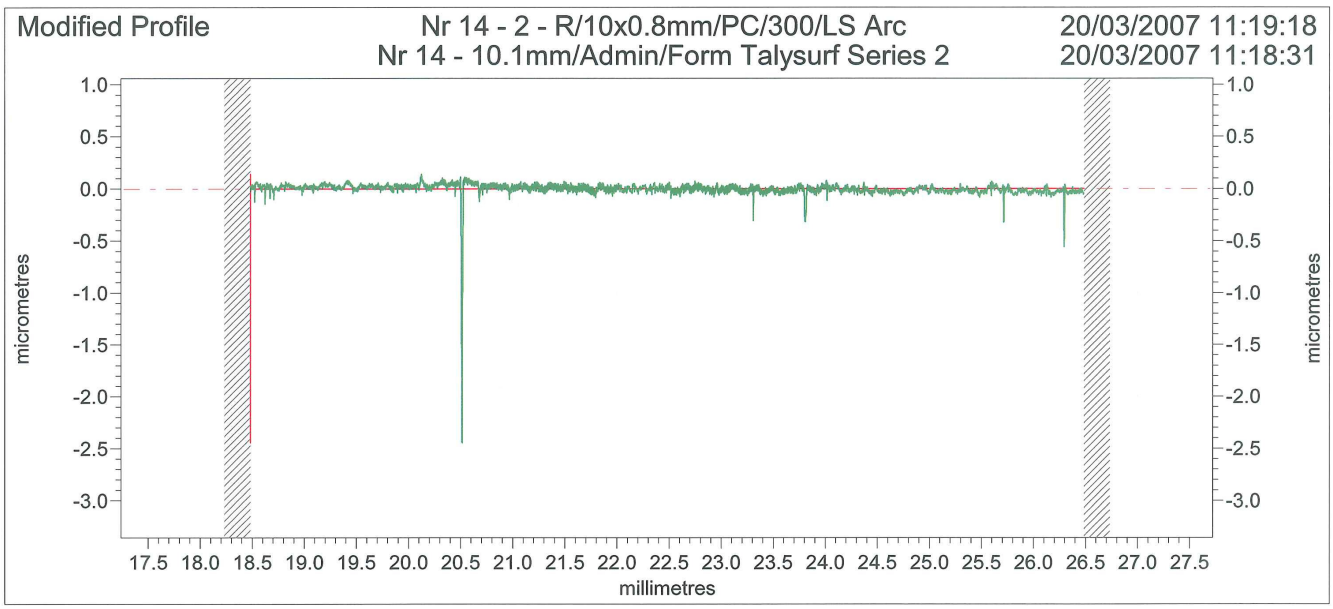

Ra	0.0296	µm

5.11.6.17

Taylor Hobson PRECISION

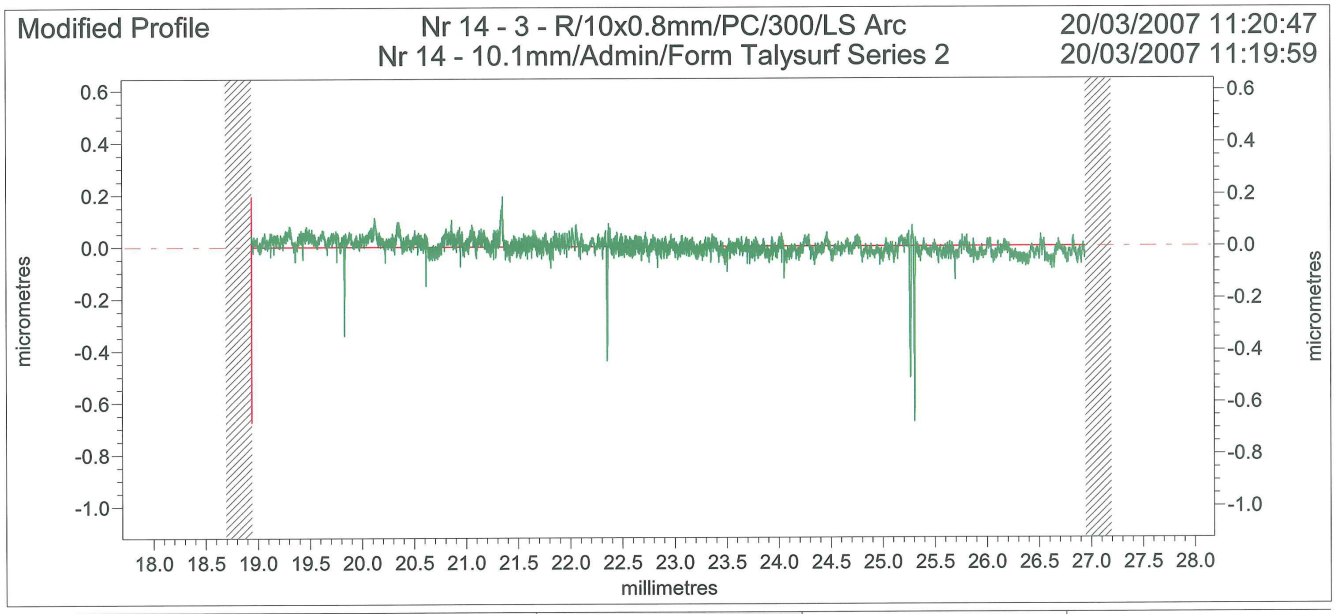

Ra	0.0251	µm

5.11.6.17

Taylor Hobson PRECISION

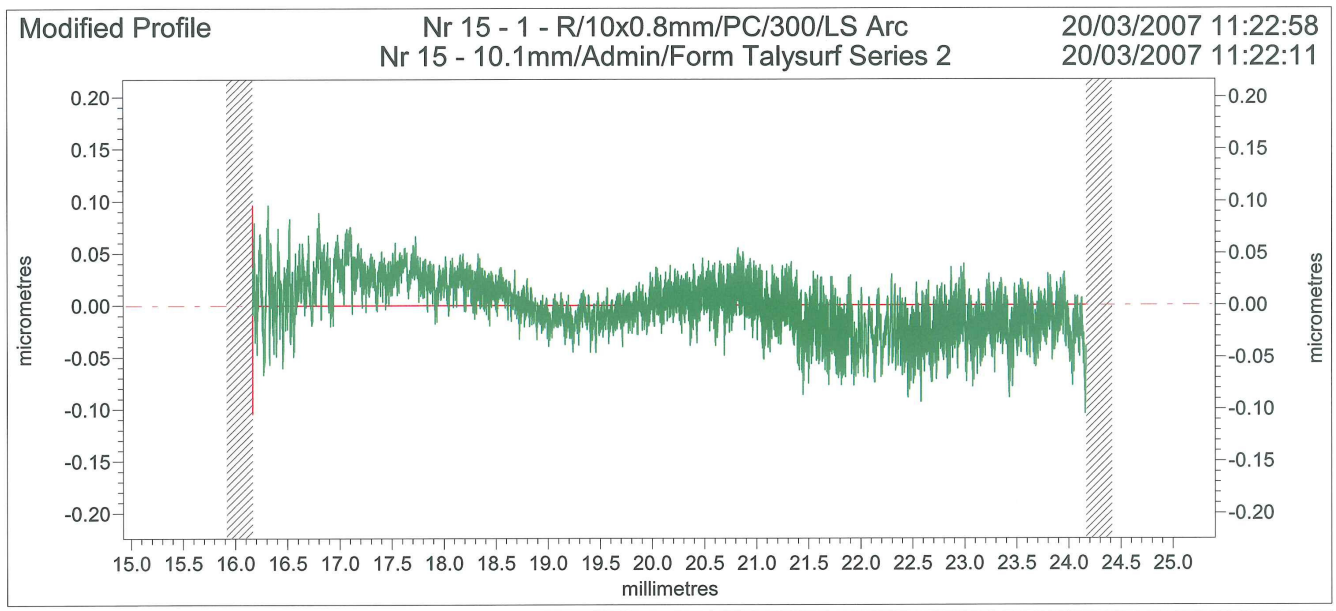

Ra	0.0215	µm

5.11.6.17

Taylor Hobson PRECISION

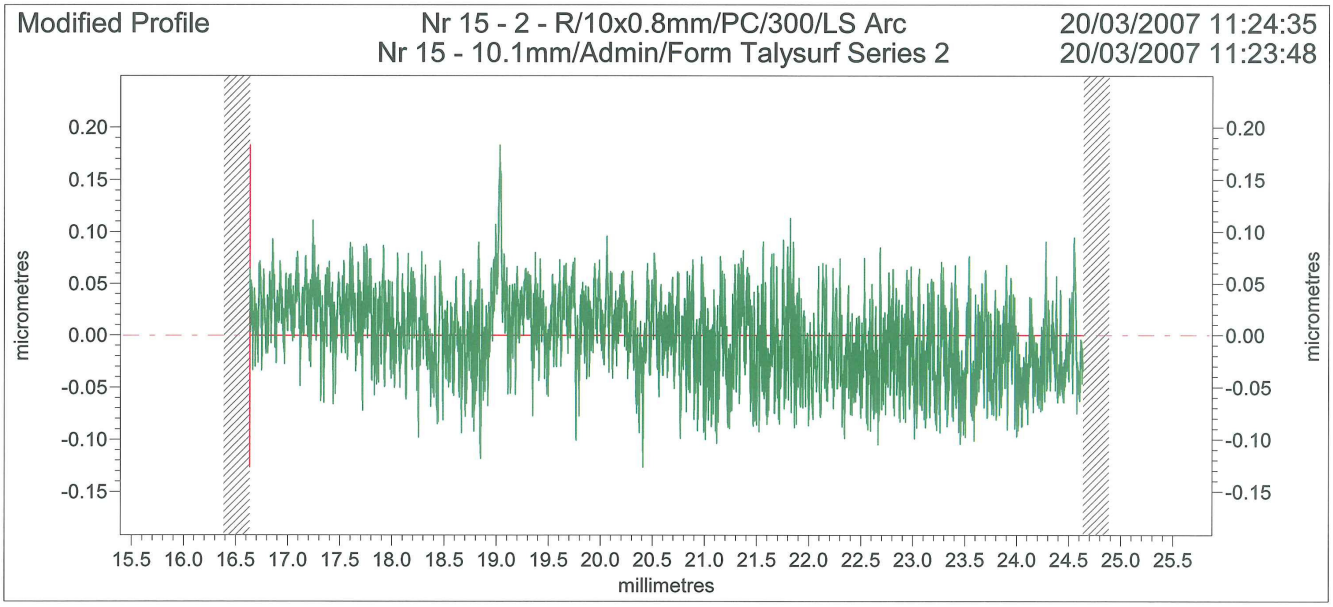

Ra	0.0318	µm

5.11.6.17

Taylor Hobson PRECISION

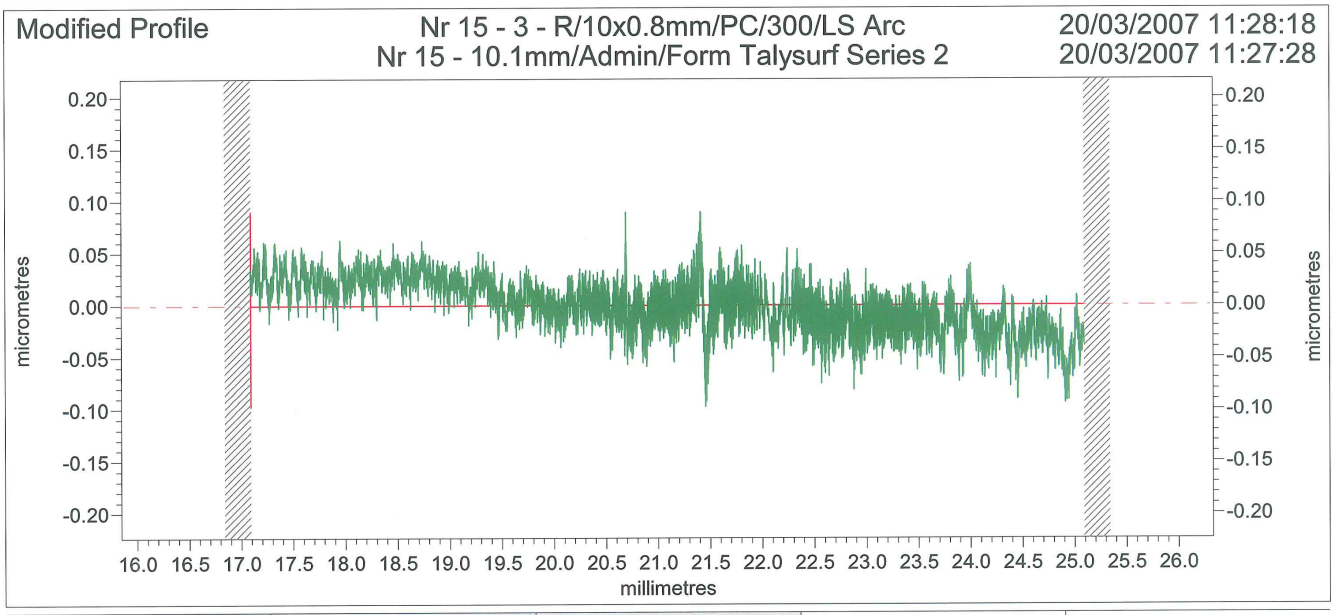

Ra	0.0217	µm

5.11.6.17

Taylor Hobson PRECISION

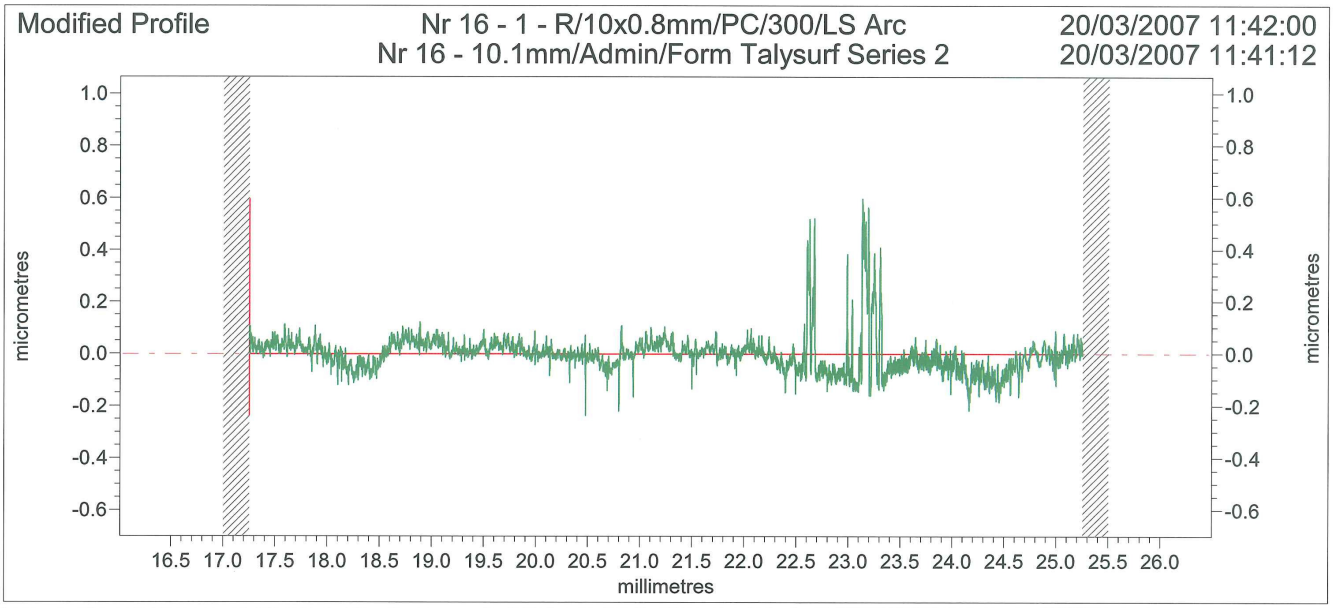

Ra	0.0450	µm

5.11.6.17

Taylor Hobson PRECISION

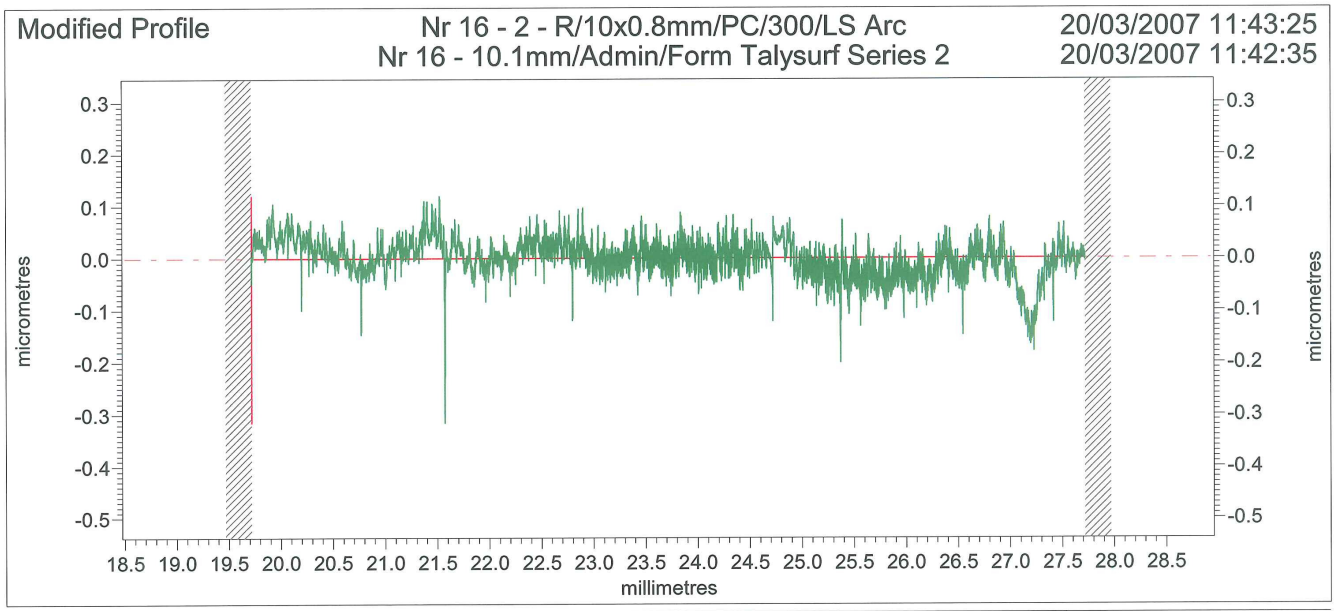

Ra	0.0283	µm

5.11.6.17

Taylor Hobson PRECISION

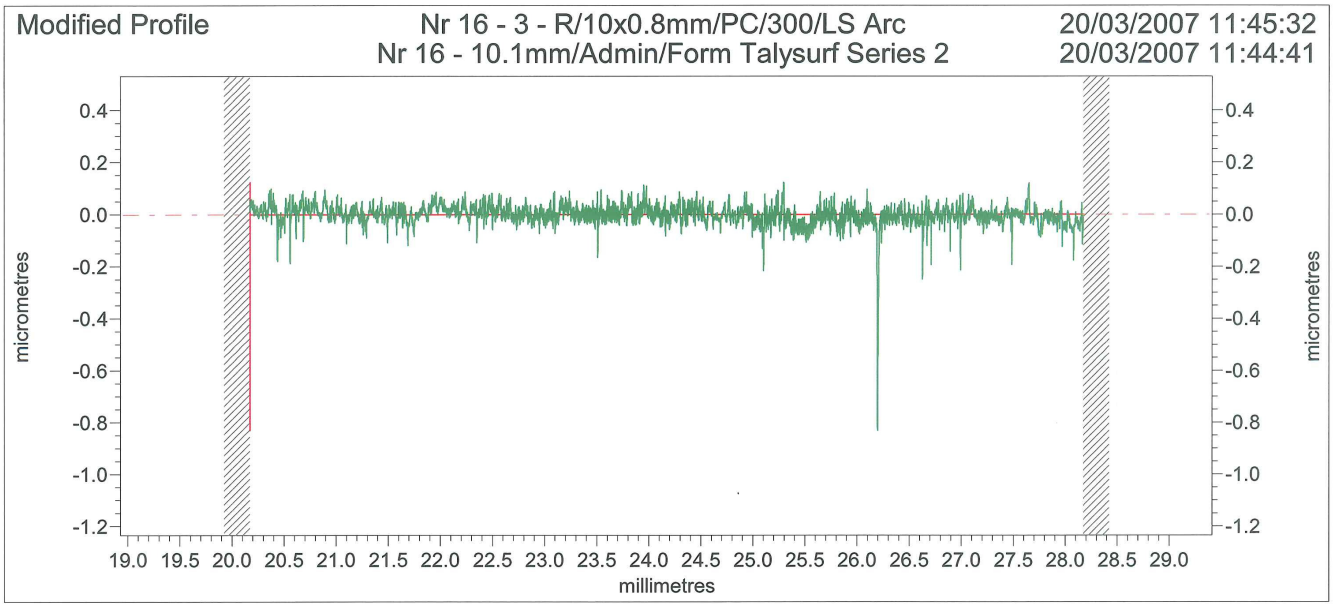

Ra	0.0259	µm

5.11.6.17

Taylor Hobson PRECISION

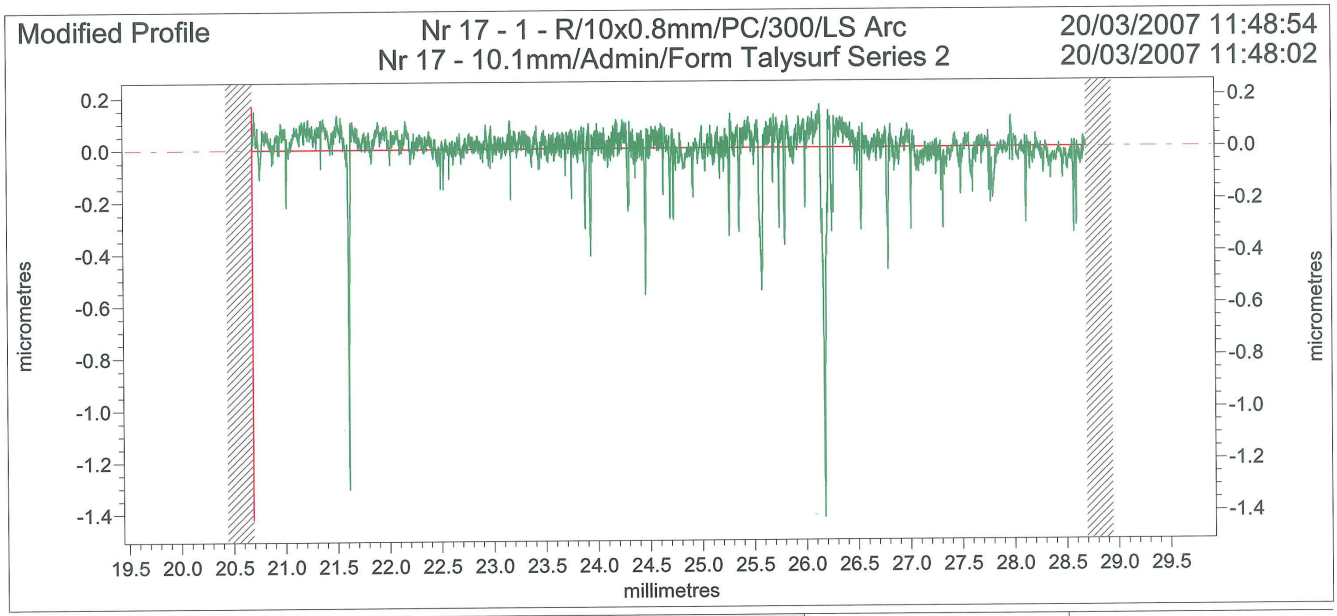

Ra	0.0519	µm

5.11.6.17

Taylor Hobson PRECISION

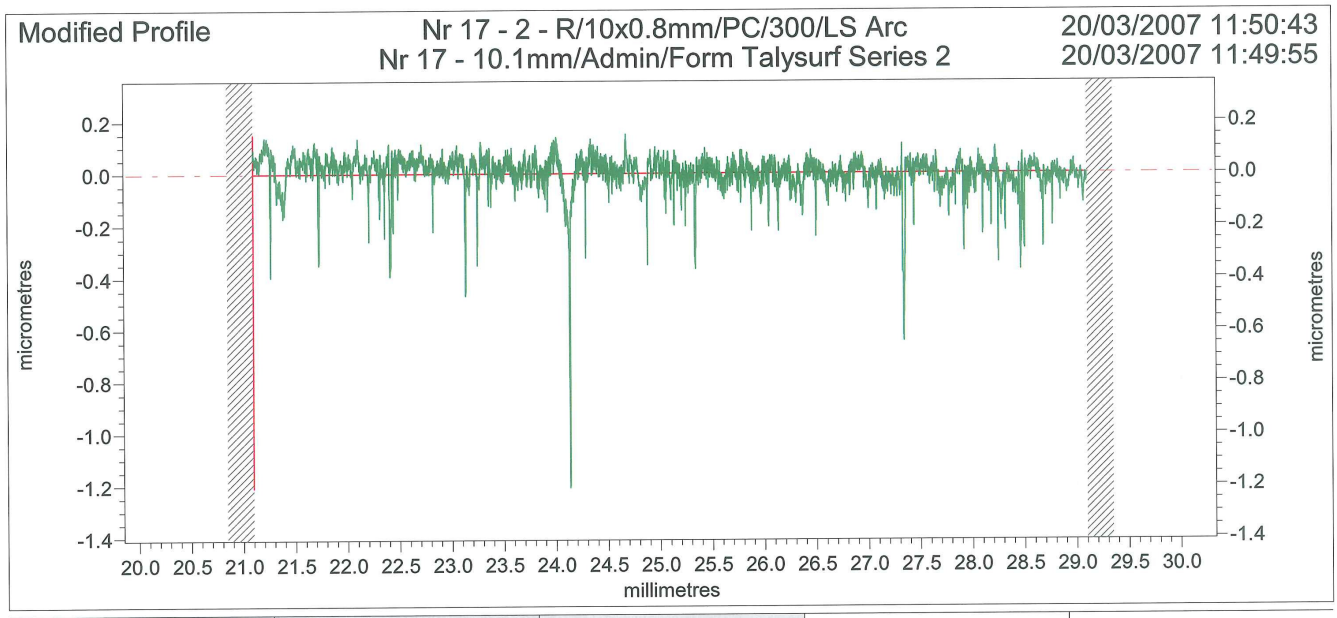

Ra	0.0442	µm

5.11.6.17

Taylor Hobson PRECISION

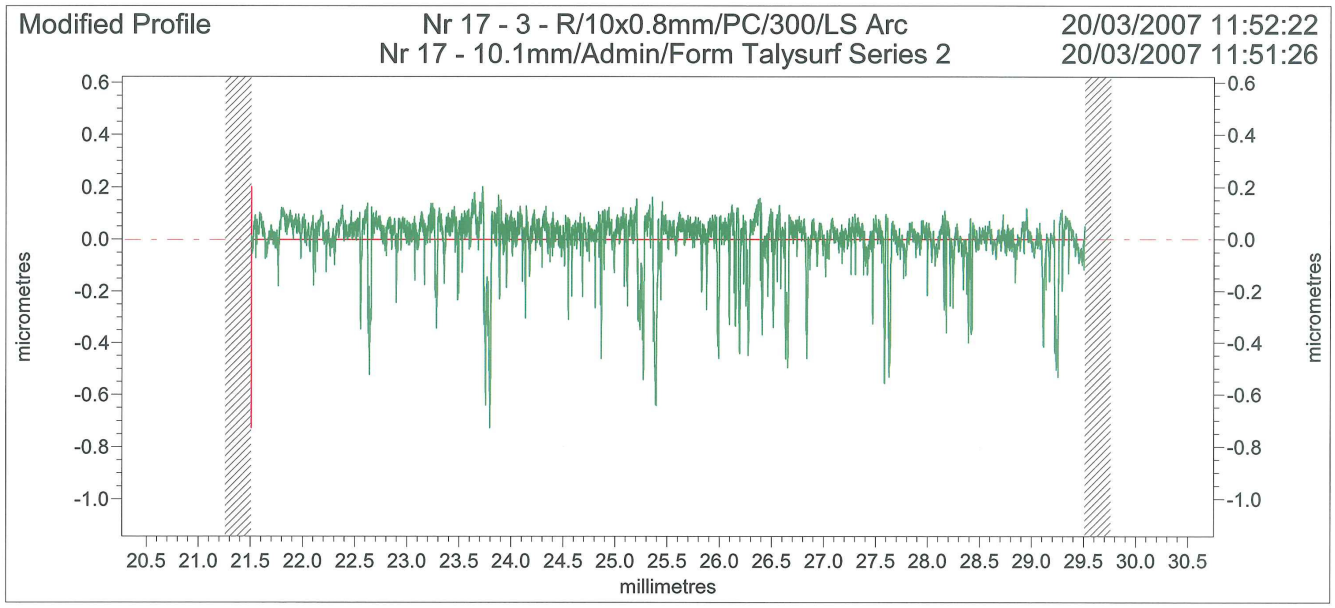

Ra	0.0649	µm

5.11.6.17

Taylor Hobson PRECISION

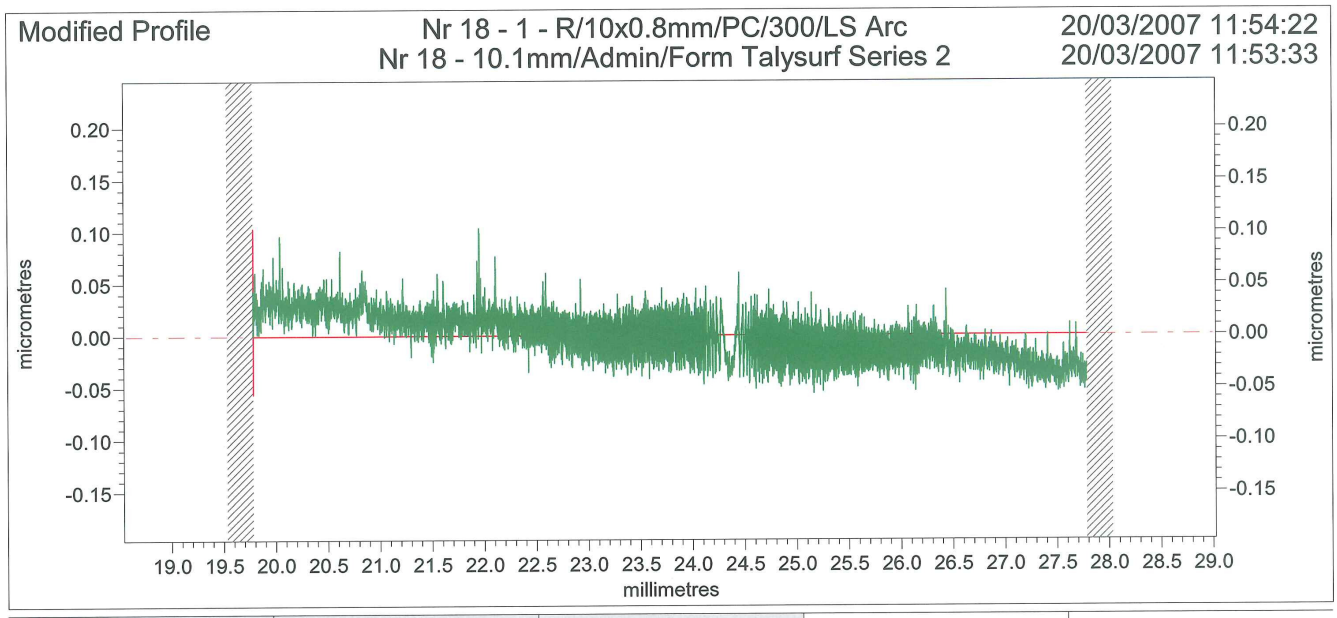

Ra	0.0192	µm

5.11.6.17

Taylor Hobson PRECISION

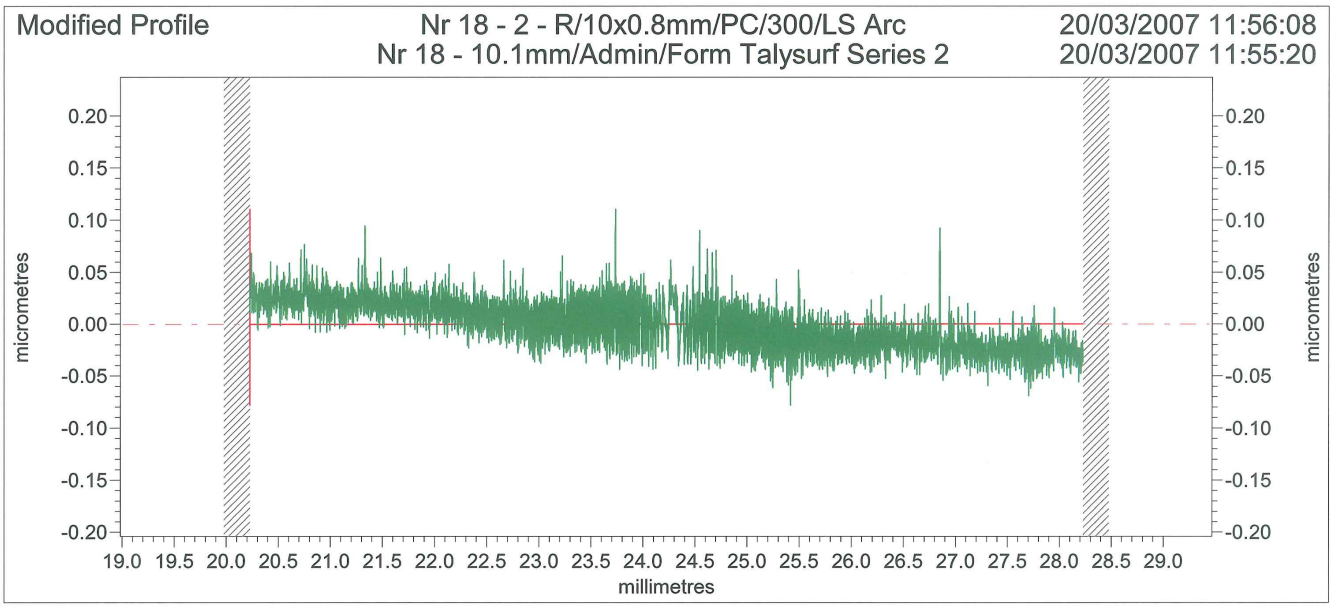

Ra	0.0195	µm

5.11.6.17

Taylor Hobson PRECISION

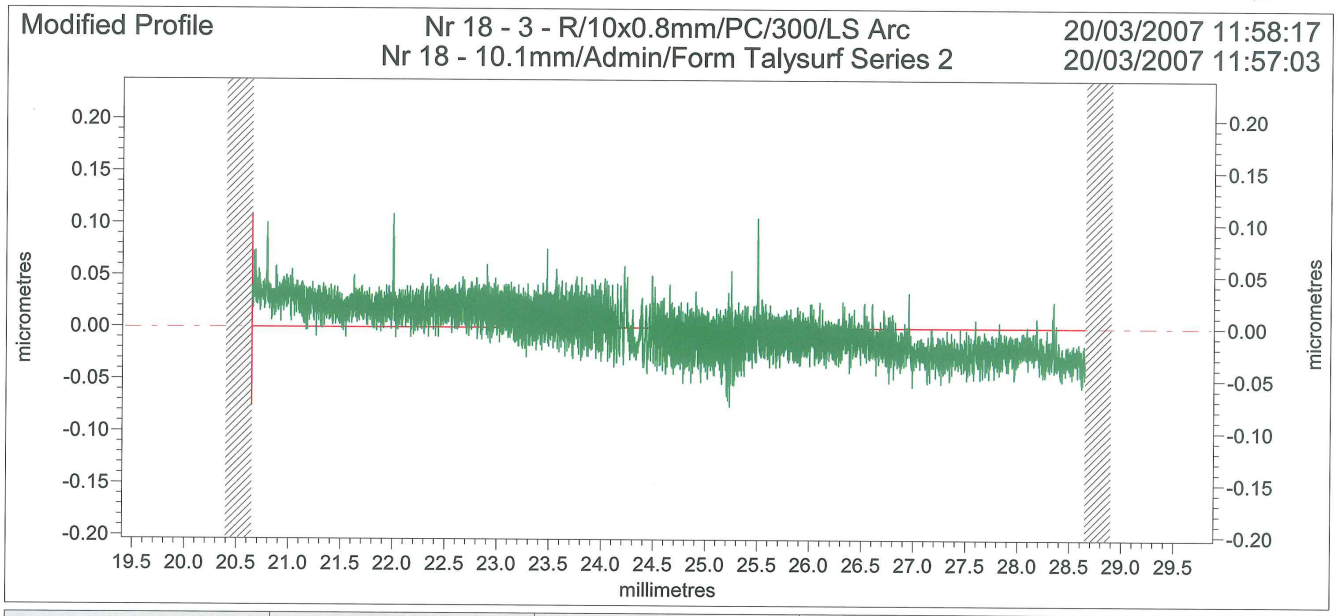

Ra	0.0195	µm

5.11.6.17

Taylor Hobson PRECISION

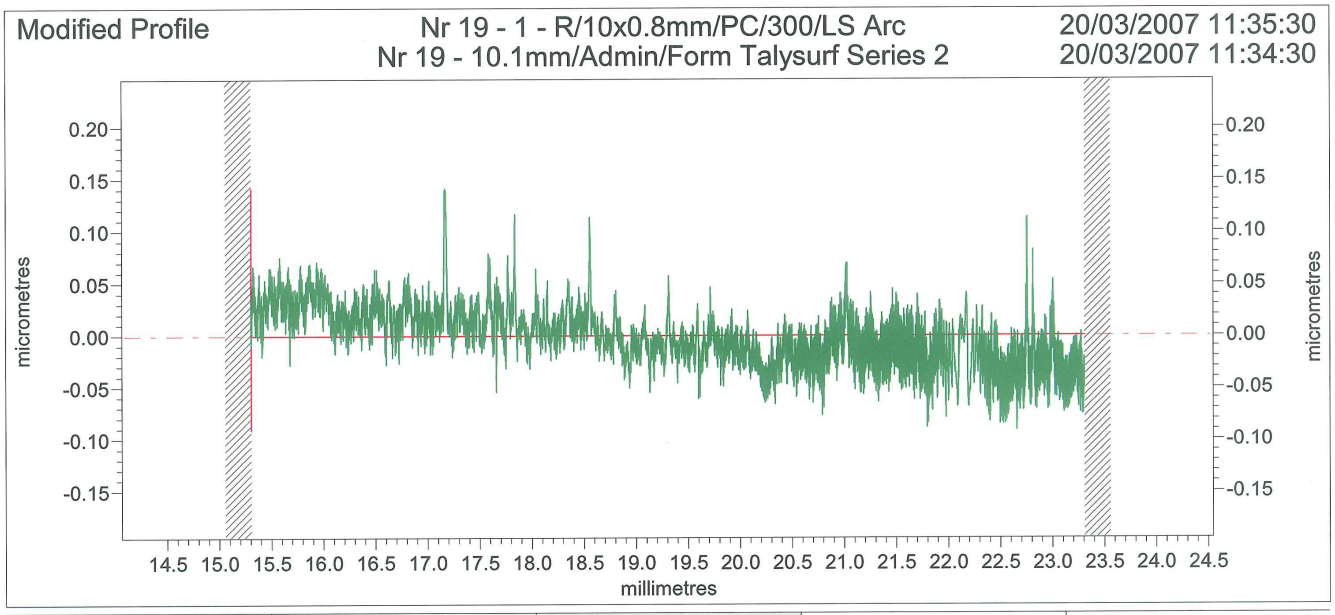

Ra	0.0227	µm

5.11.6.17

Taylor Hobson PRECISION

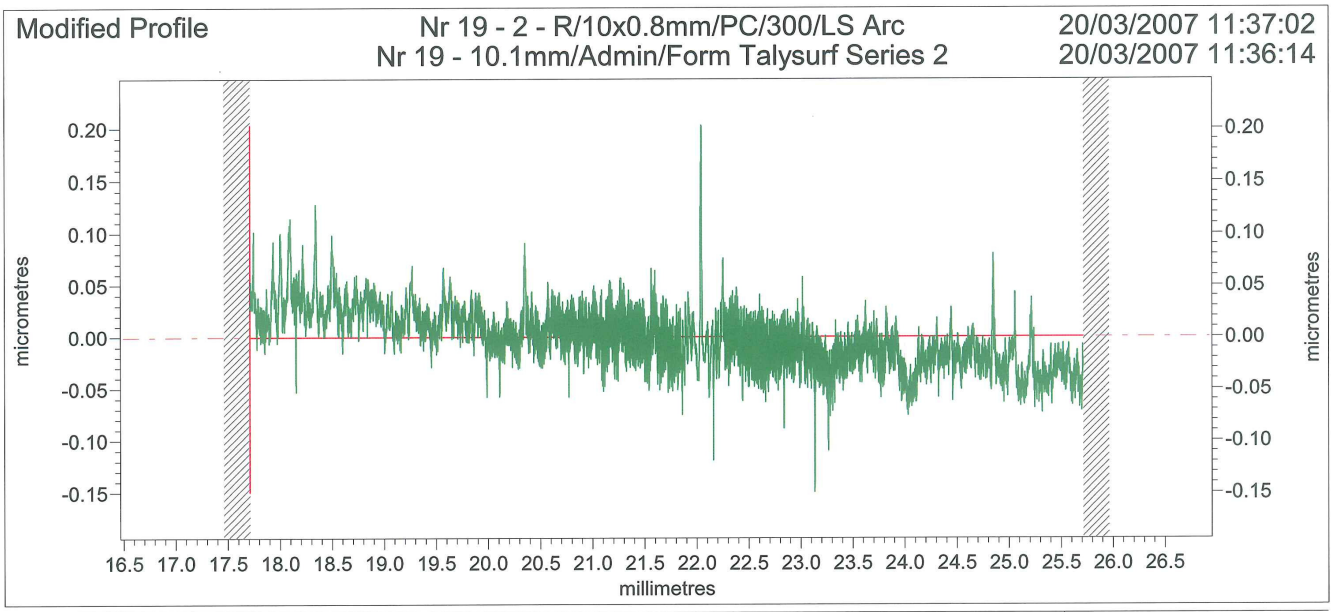

Ra	0.0232	µm

5.11.6.17

Taylor Hobson PRECISION

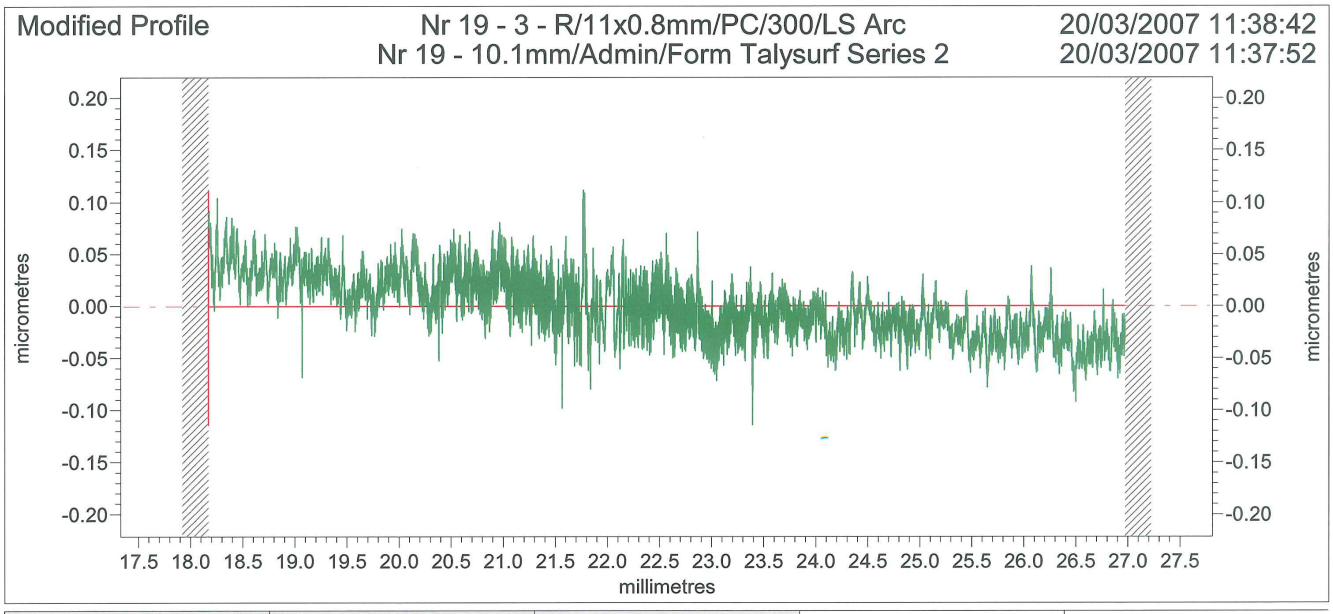

Ra	0.0251	µm

5.11.6.17

Taylor Hobson PRECISION

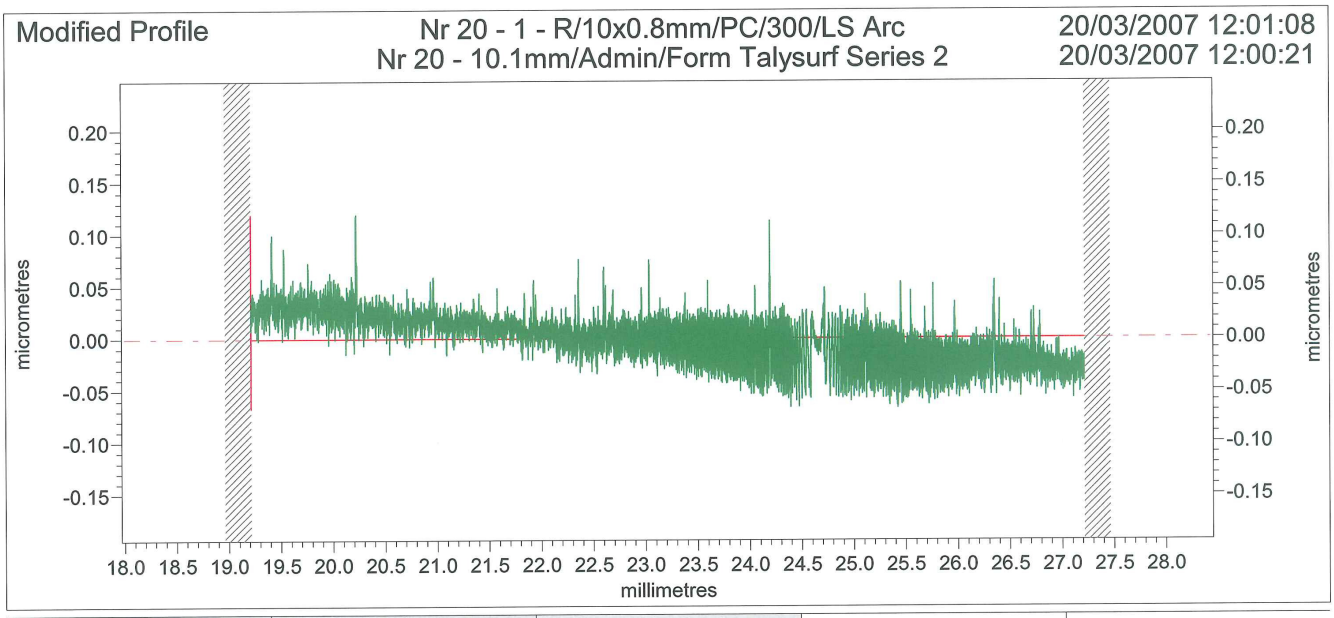

Ra	0.0199	µm

5.11.6.17

Taylor Hobson PRECISION

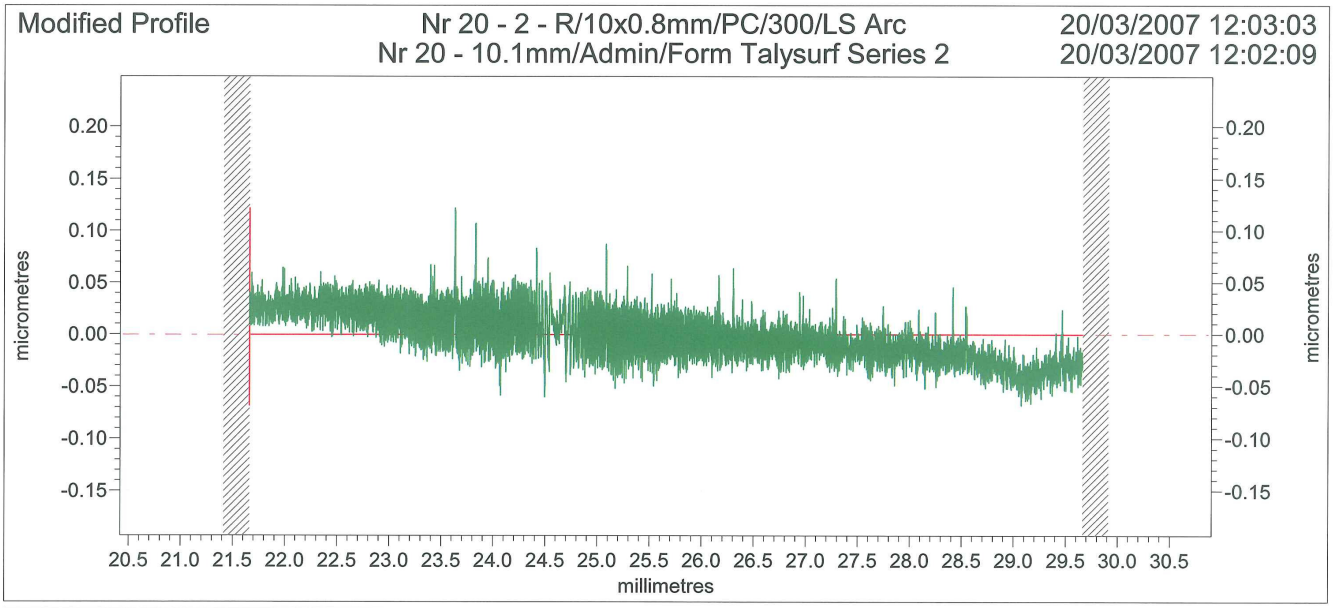

Ra	0.0202	µm

Taylor Hobson PRECISION

Modified Profile

Nr 20 - 3 - R/11x0.8mm/PC/300/LS Arc
Nr 20 - 10.1mm/Admin/Form Talysurf Series 2

20/03/2007 12:04:46
20/03/2007 12:03:52

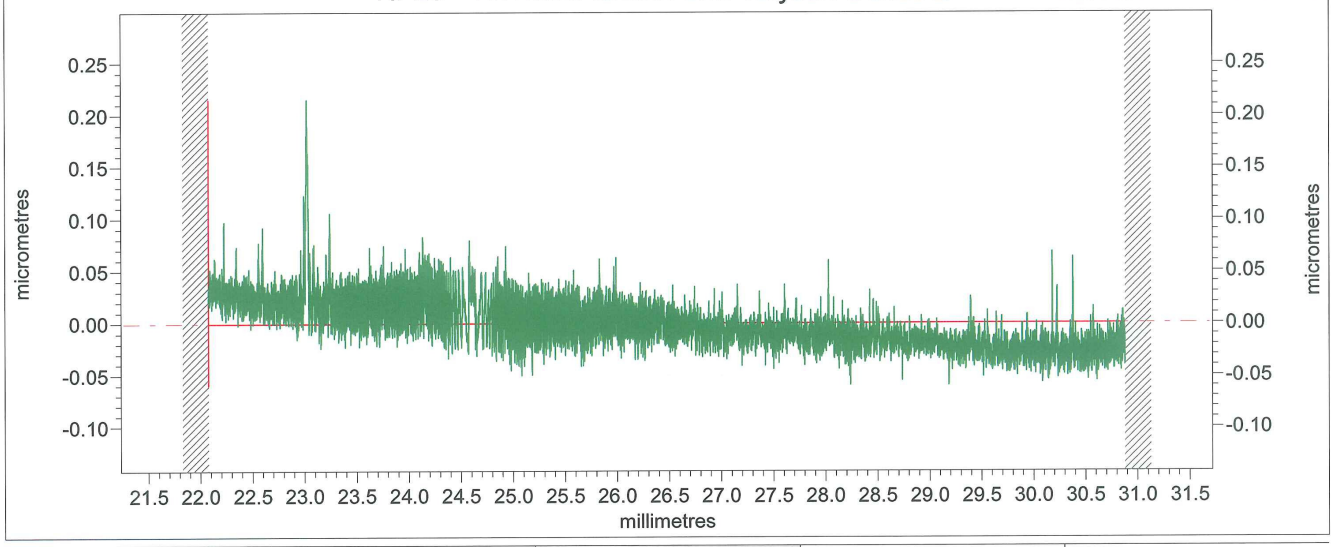

Ra	0.0197	µm

5.11.6.17

Taylor Hobson PRECISION

Modified Profile

Nr 21 - 1 - R/10x0.8mm/PC/300/LS Arc
Nr 21 - 10.1mm/Admin/Form Talysurf Series 2

20/03/2007 12:08:08
20/03/2007 12:06:35

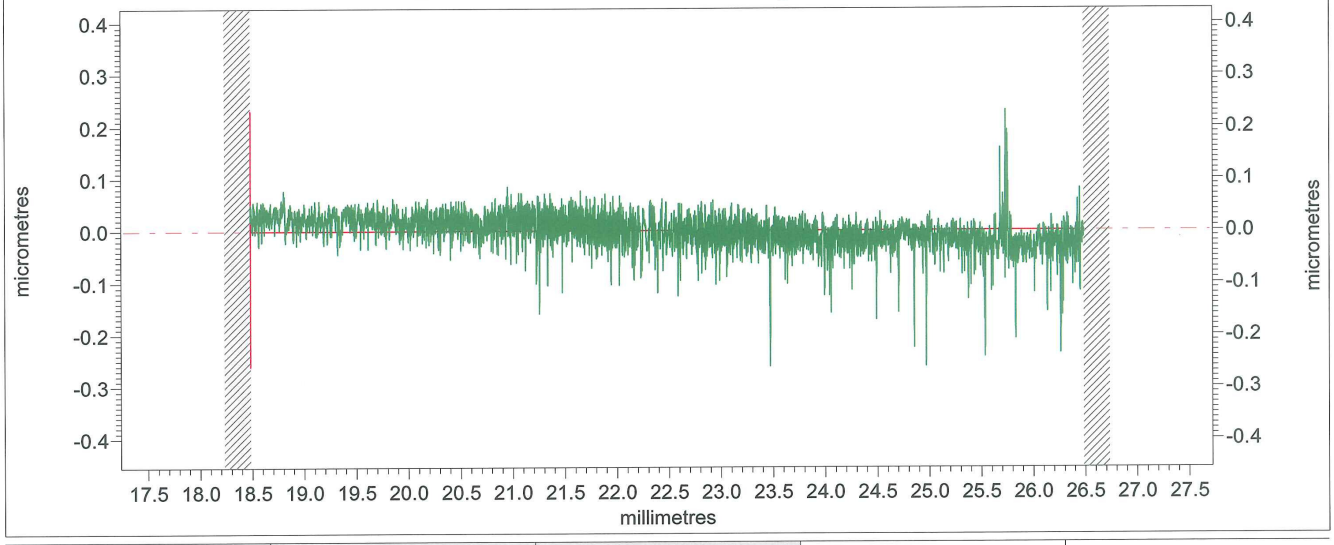

Ra	0.0239	µm

Taylor Hobson PRECISION

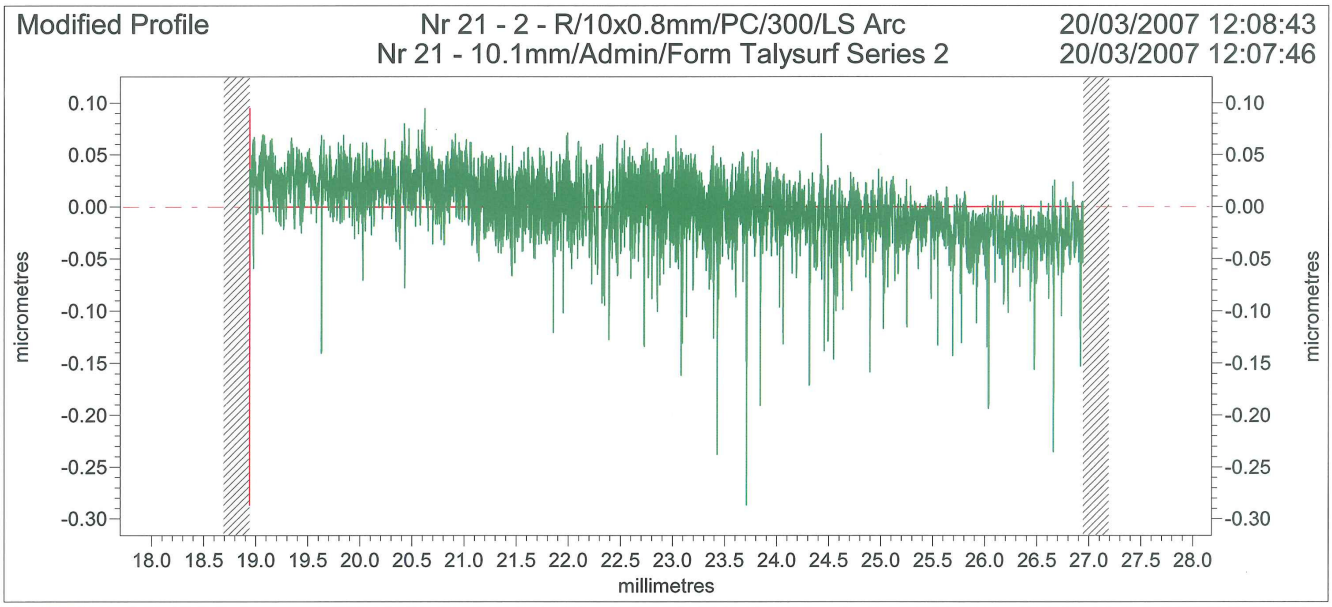

Ra	0.0232	µm

Taylor Hobson PRECISION

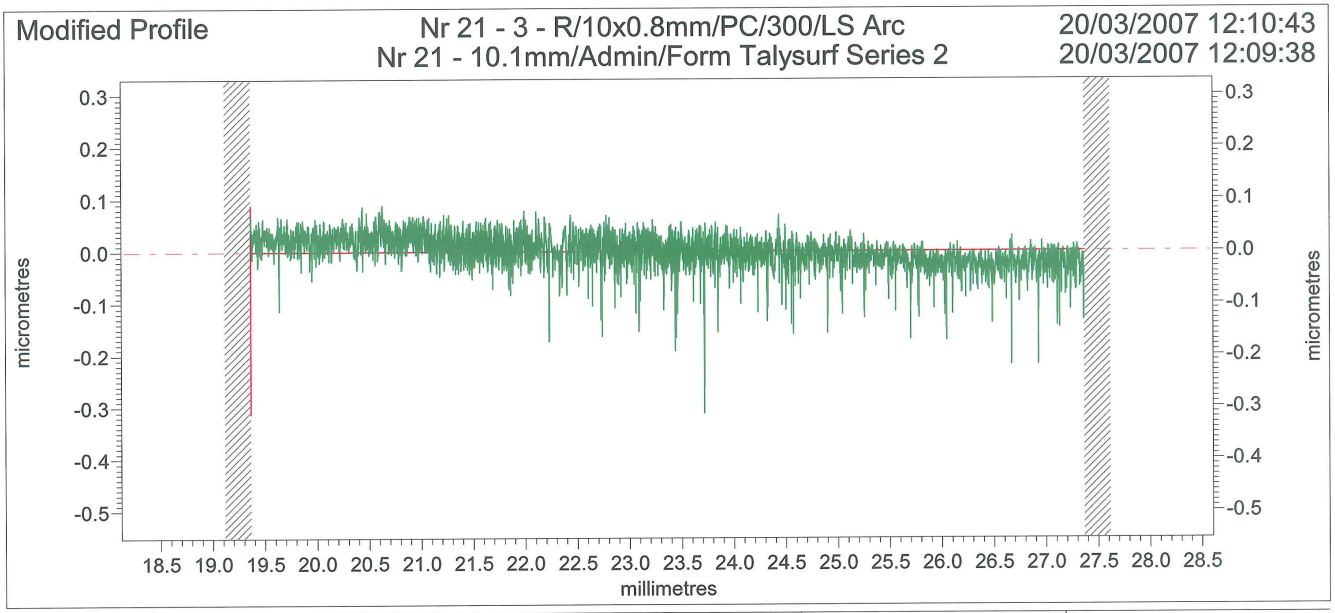

Ra	0.0230	µm

5.11.6.17

Taylor Hobson PRECISION

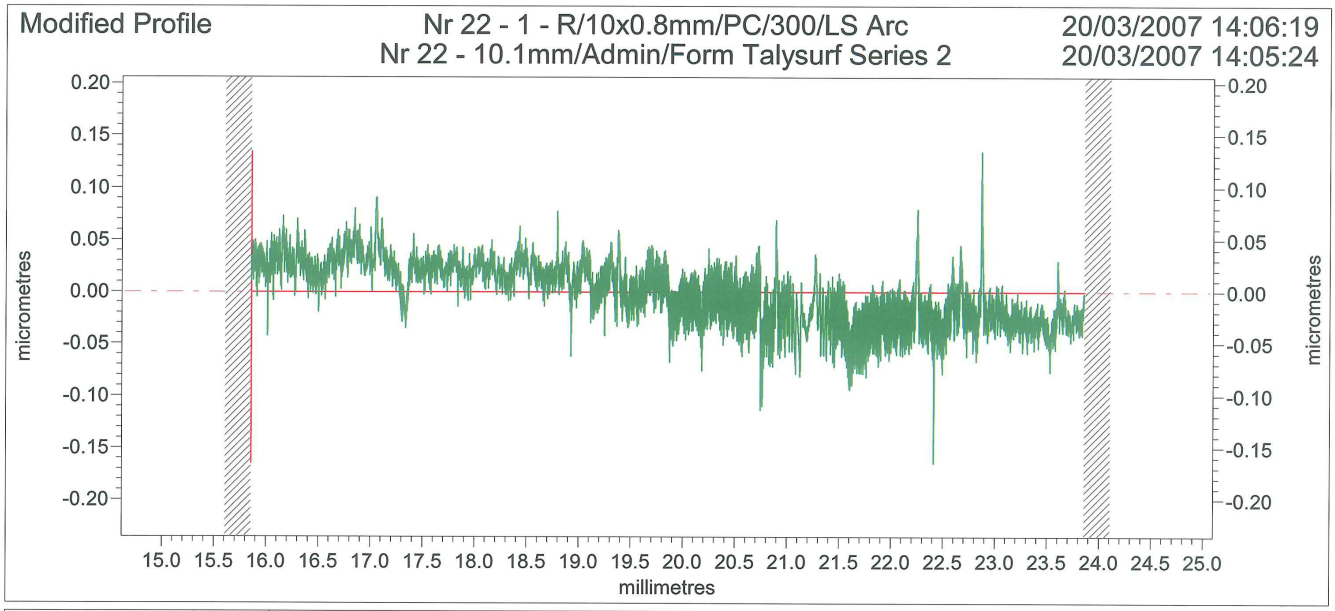

Ra	0.0252	µm

5.11.6.17

Taylor Hobson PRECISION

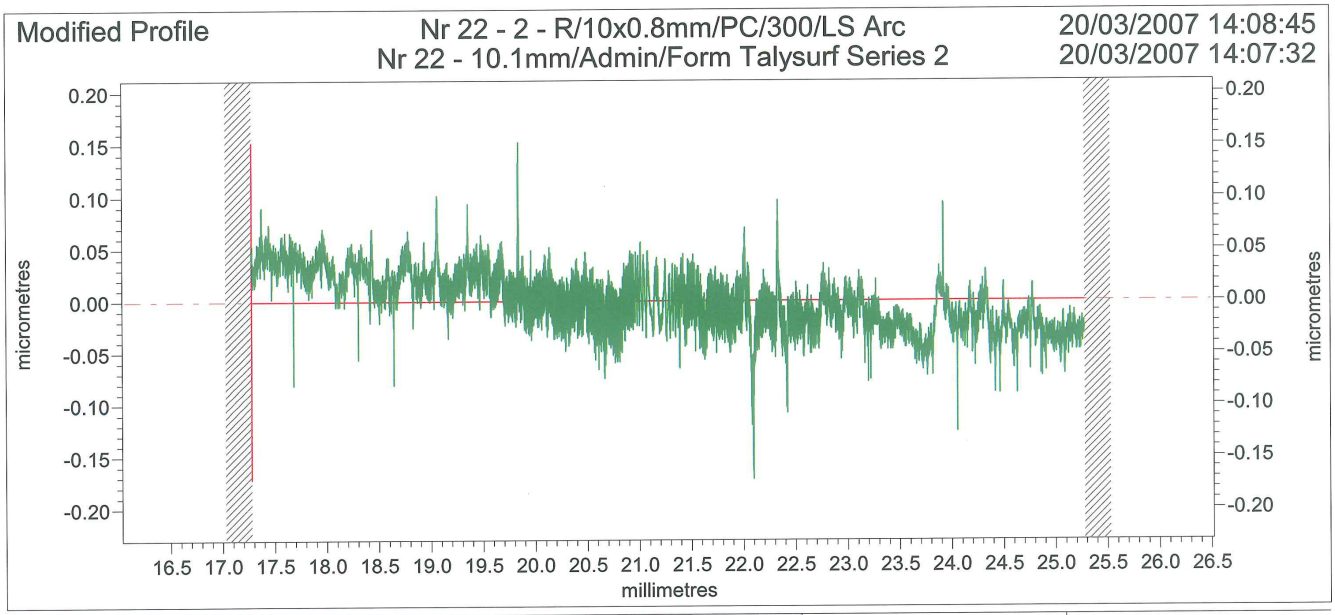

Ra	0.0239	µm

Taylor Hobson PRECISION

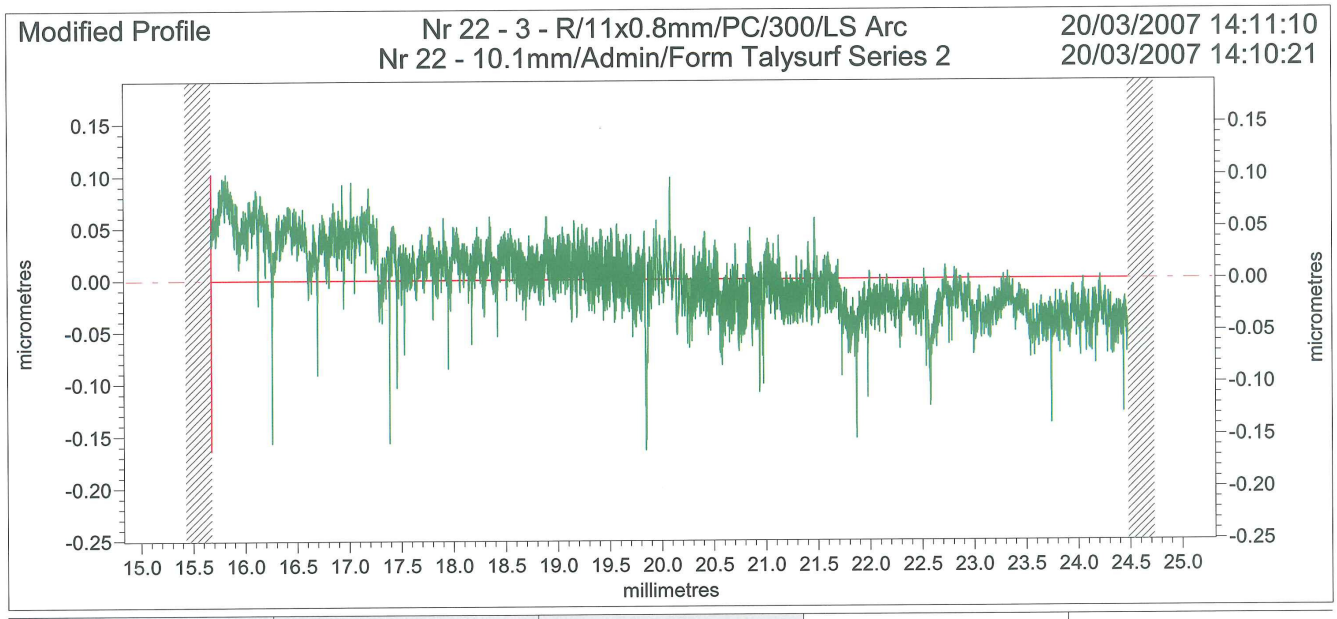

Ra	0.0276	µm

Taylor Hobson PRECISION

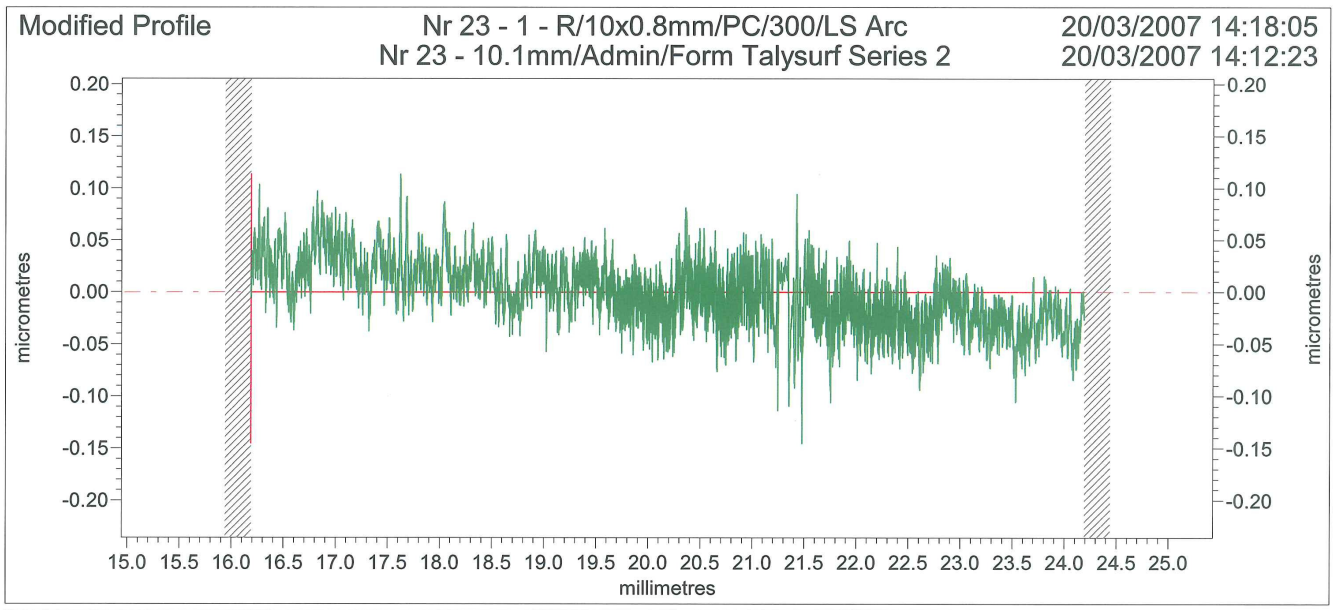

Ra	0.0254	µm

5.11.6.17

Taylor Hobson PRECISION

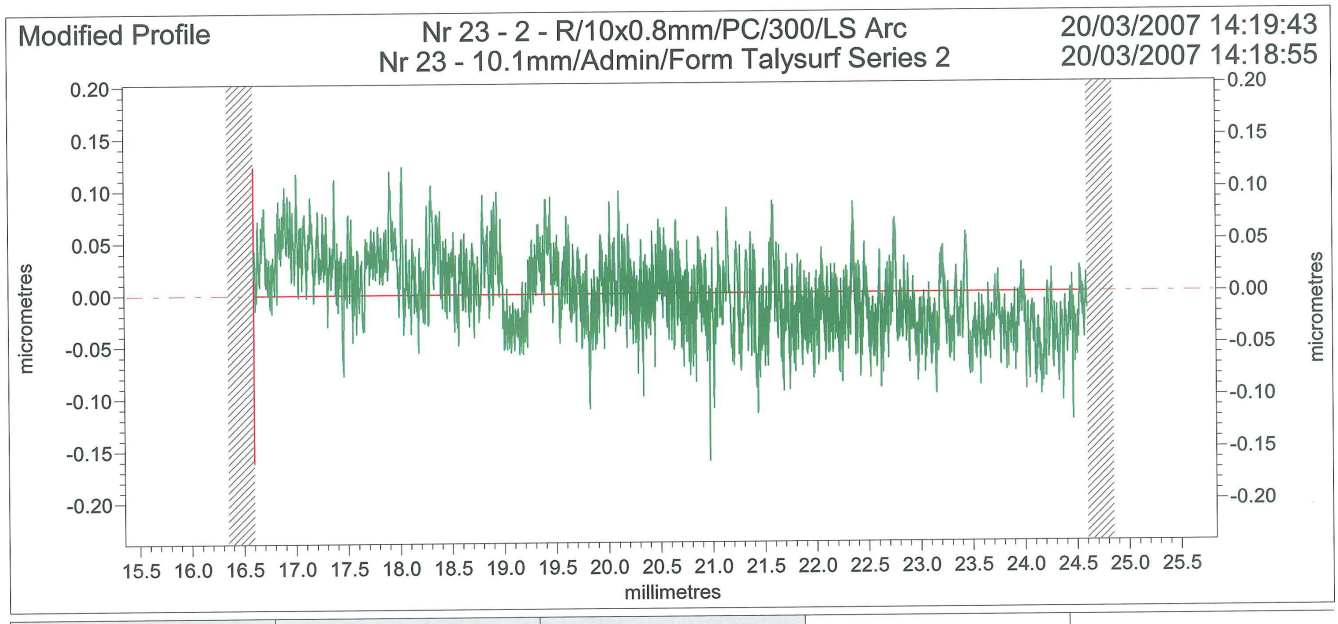

Ra	0.0304	µm

5.11.6.17

Taylor Hobson PRECISION

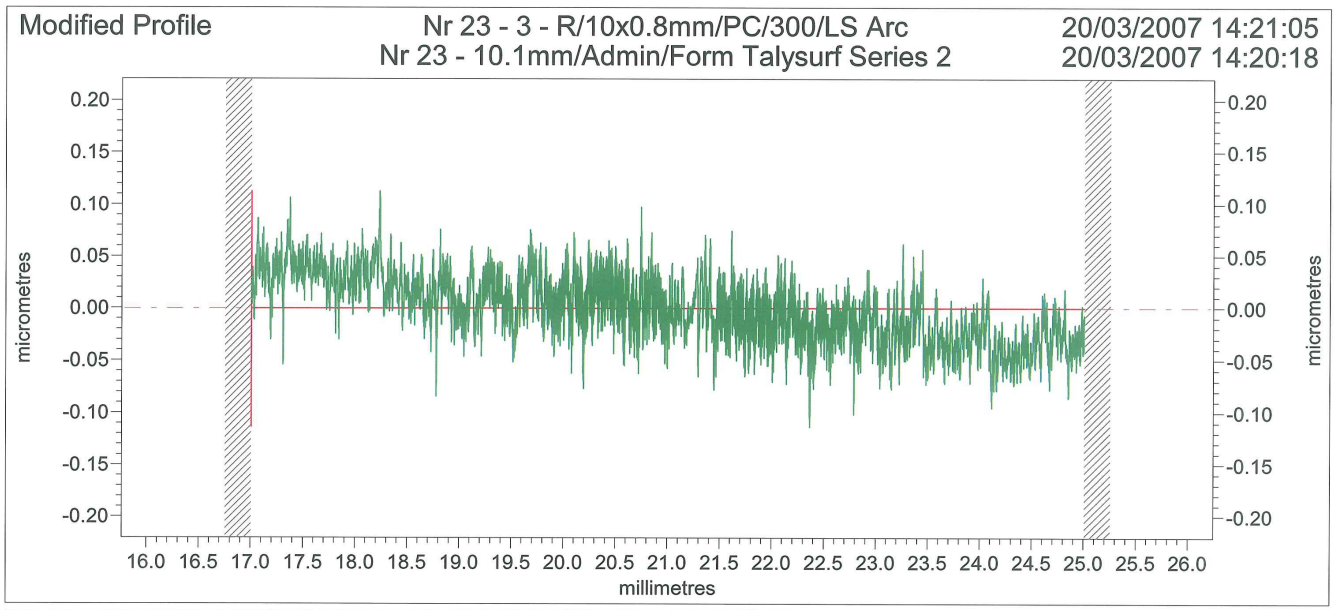

Ra	0.0263	µm

5.11.6.17

Taylor Hobson PRECISION

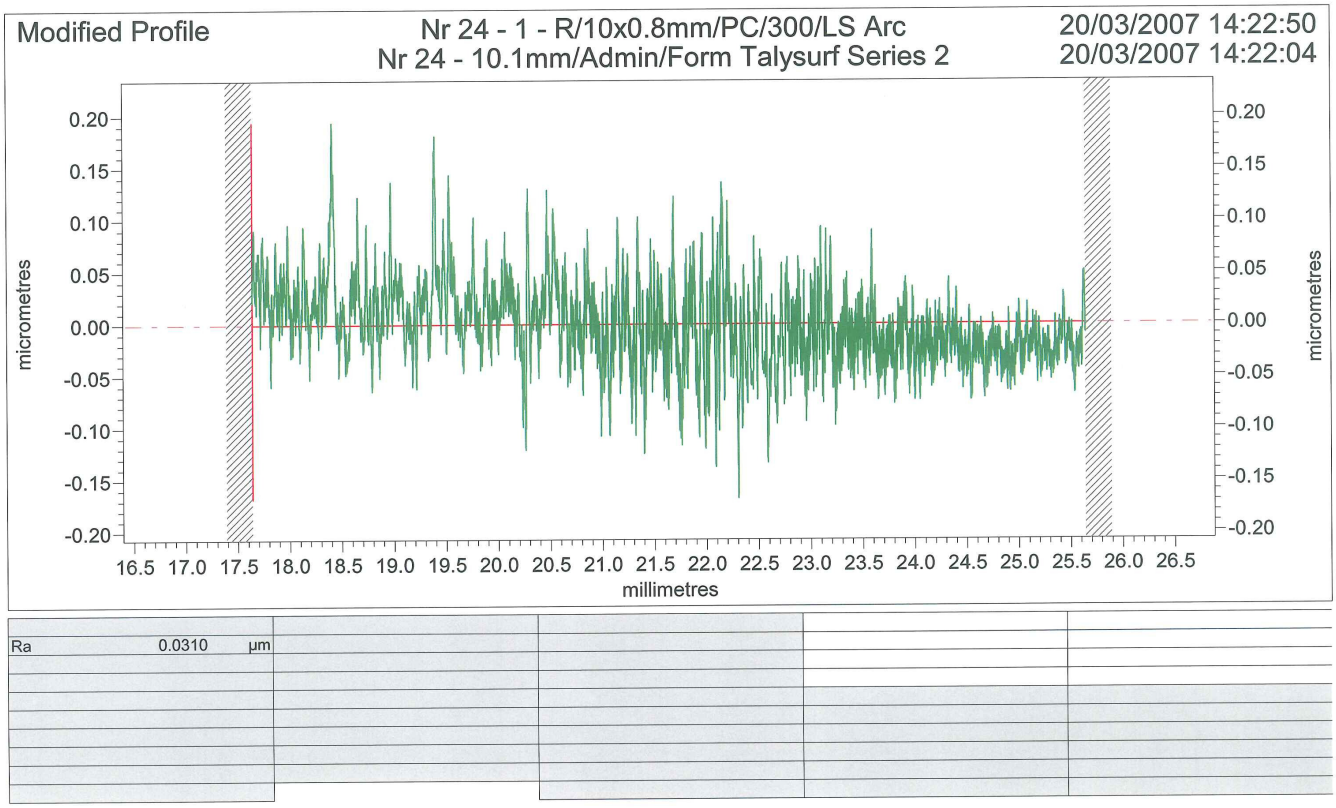

5.11.6.17

Taylor Hobson PRECISION

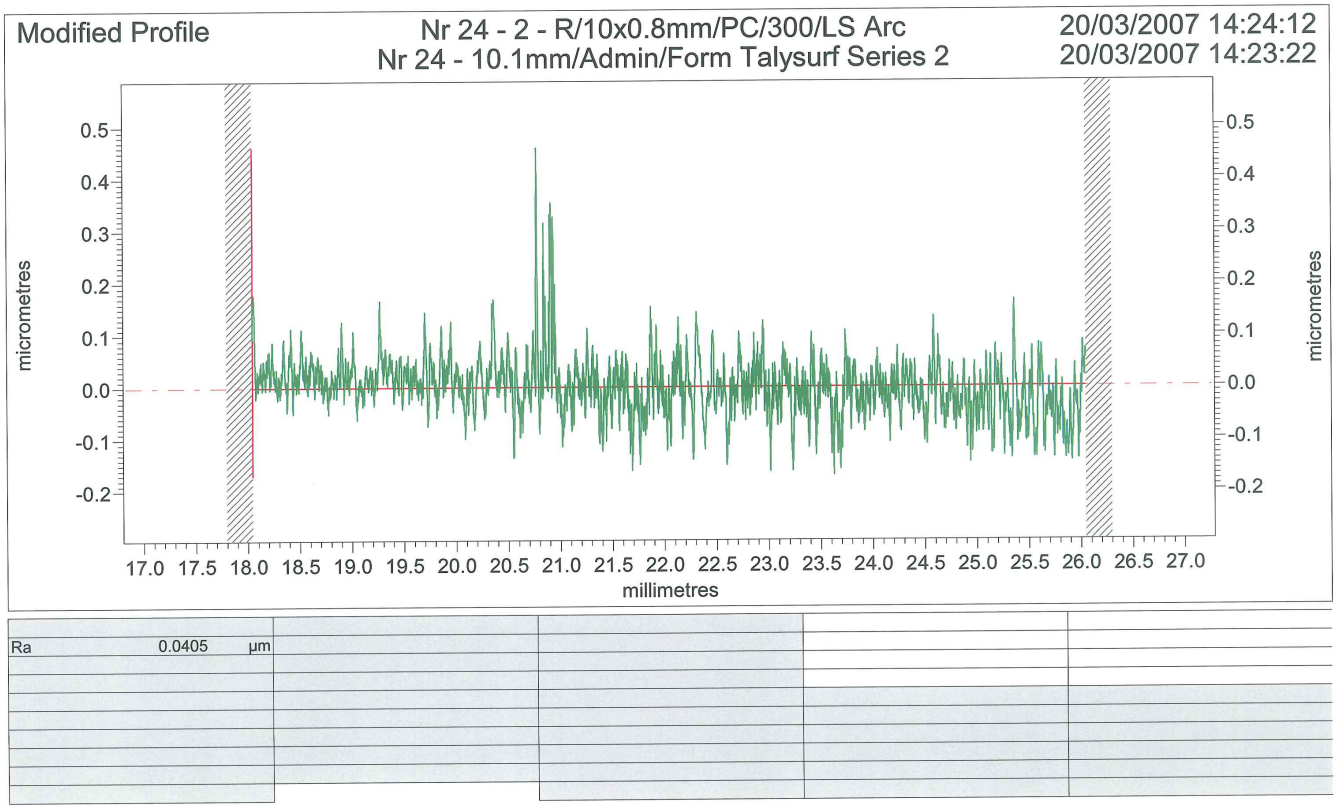

5.11.6.17

Taylor Hobson PRECISION

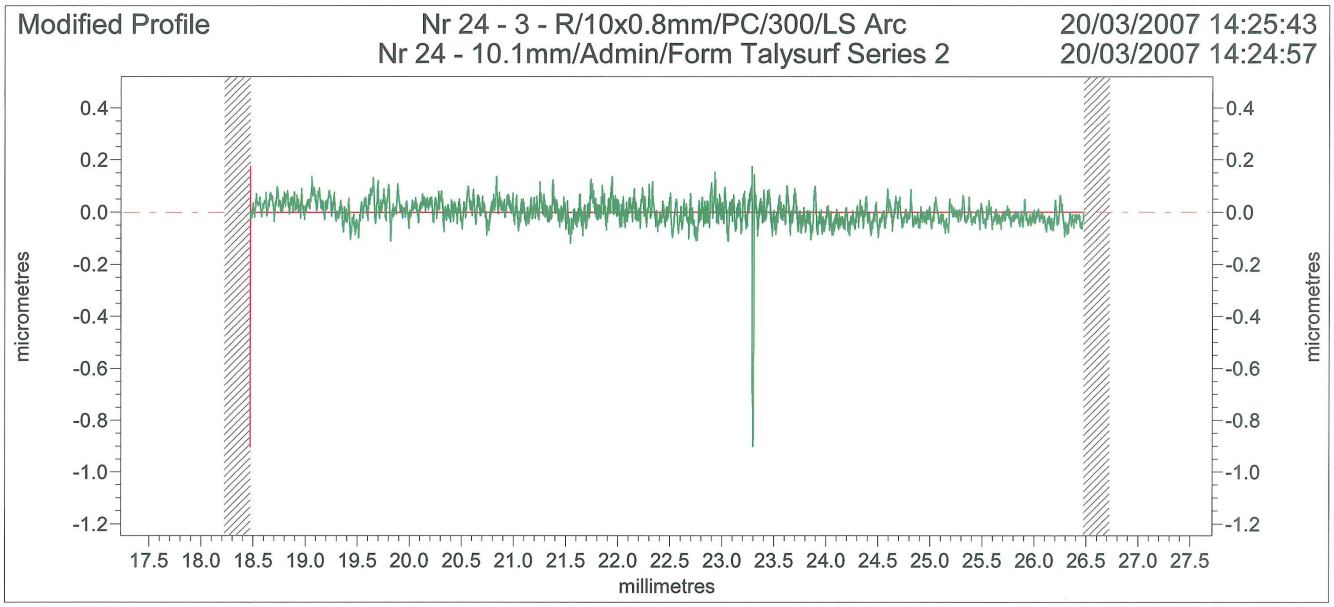

Ra	0.0330	µm

5.11.6.17

Taylor Hobson PRECISION

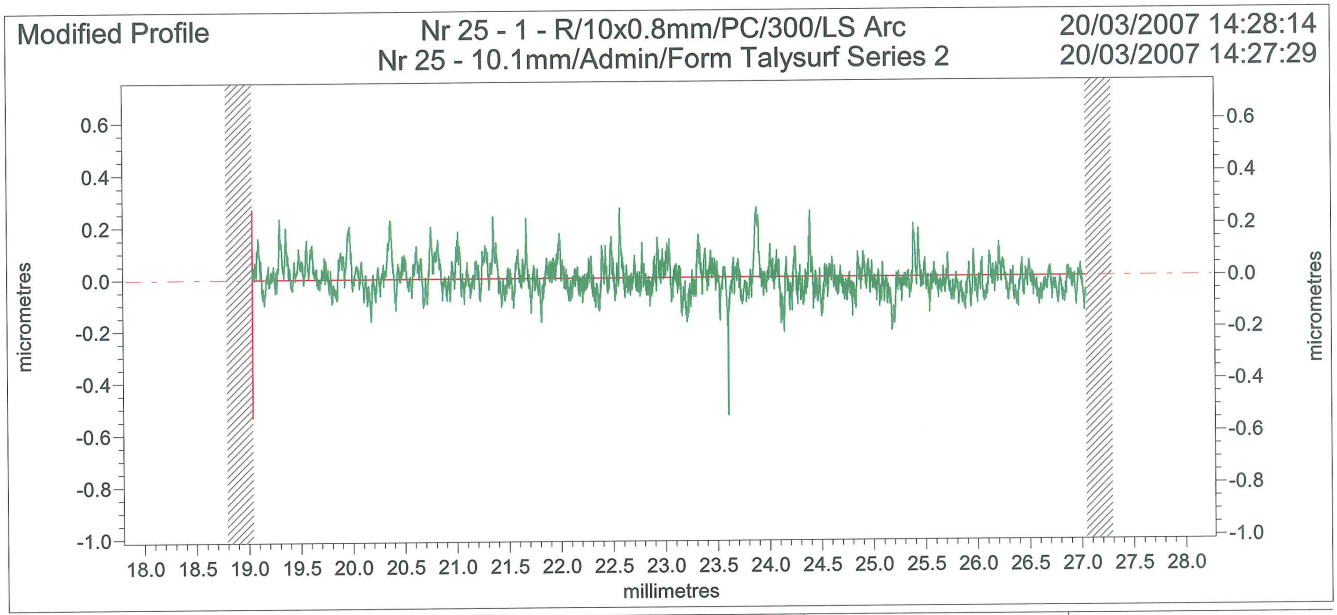

Ra	0.0491	µm

5.11.6.17

Taylor Hobson PRECISION

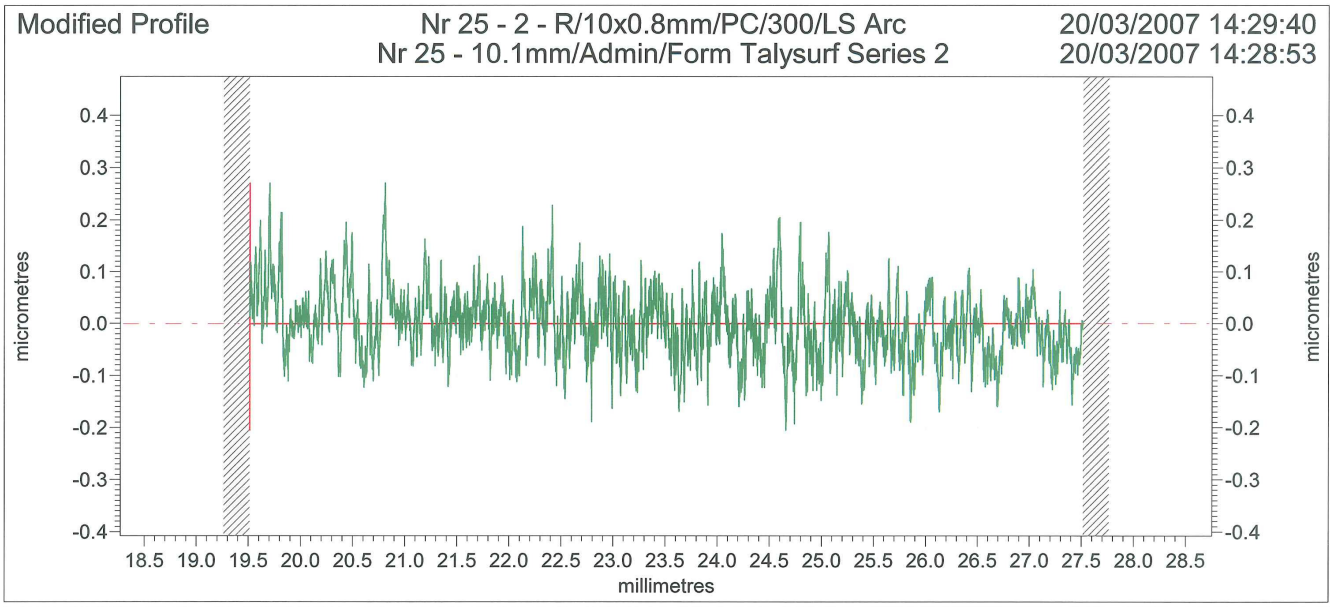

Ra	0.0499	µm

5.11.6.17

Taylor Hobson PRECISION

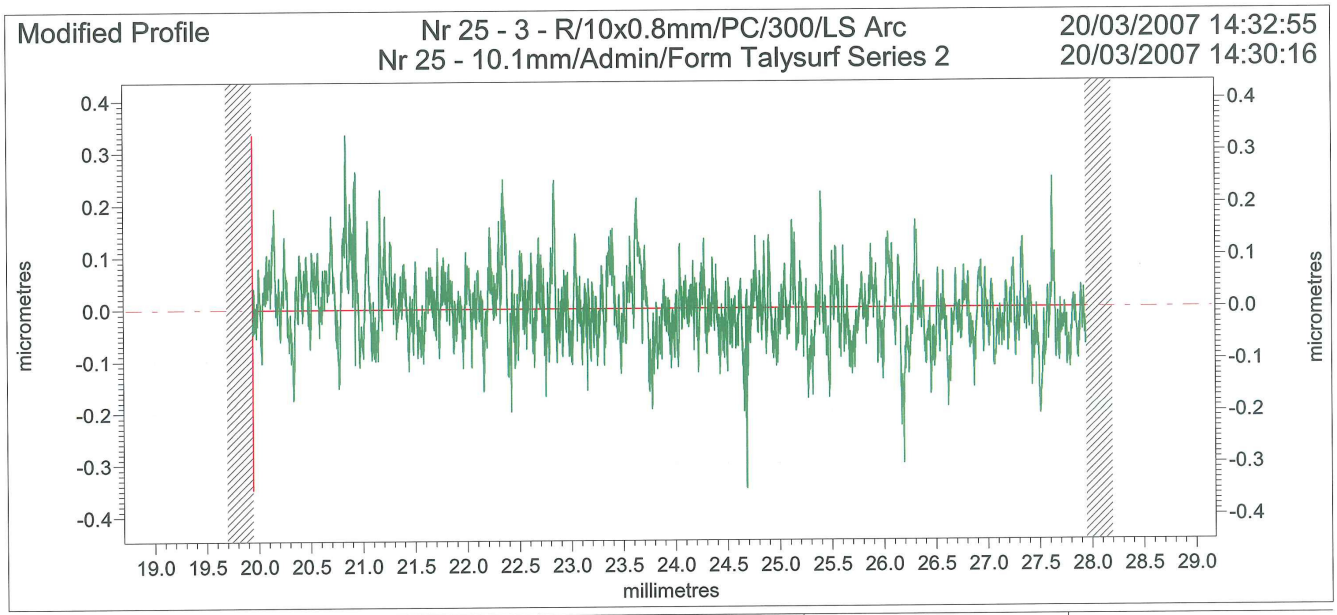

Ra	0.0517	µm

5.11.6.17

Taylor Hobson PRECISION

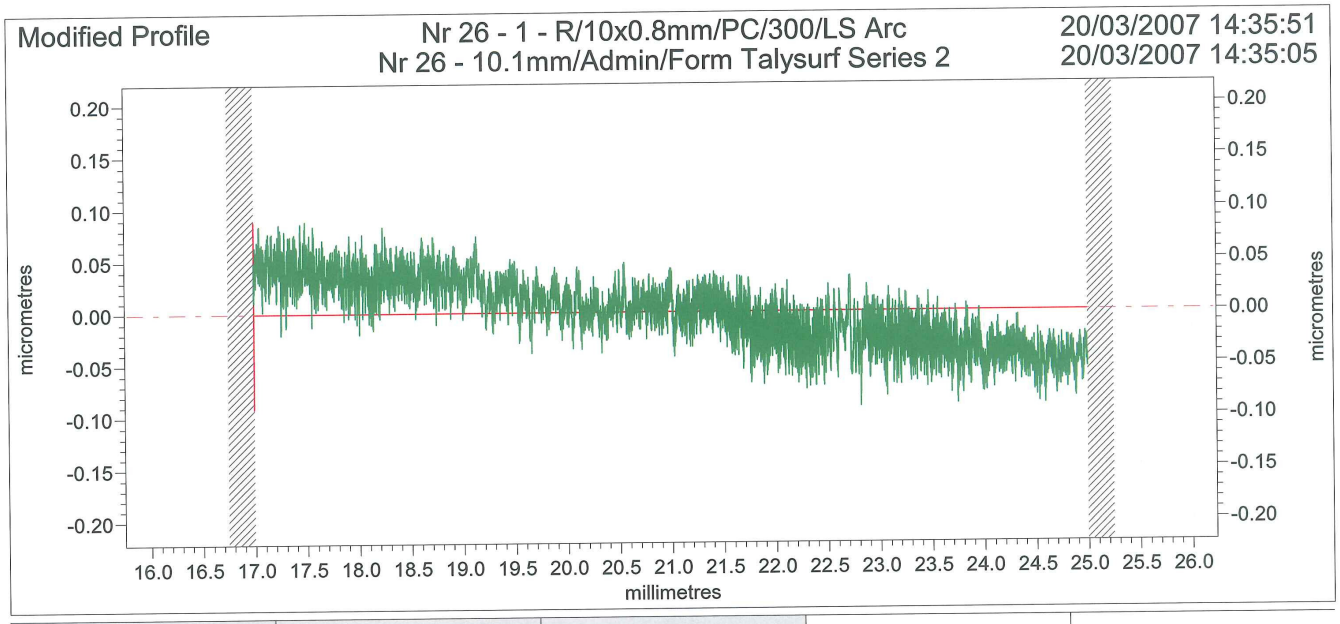

Ra	0.0282	µm

5.11.6.17

Taylor Hobson PRECISION

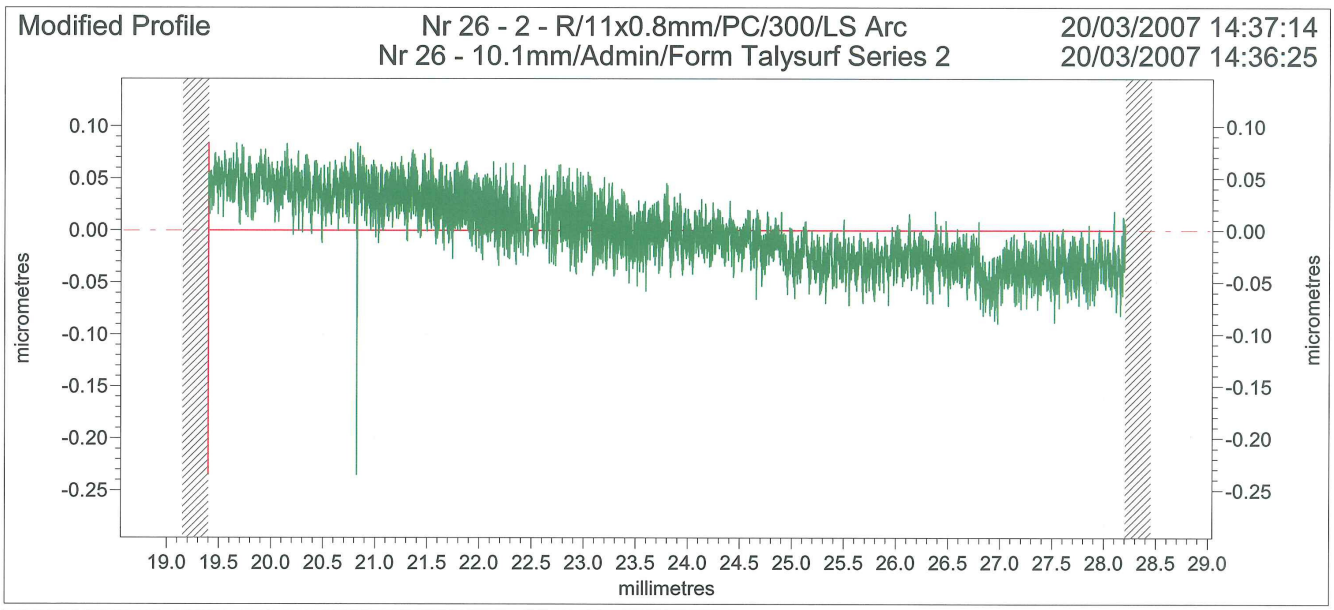

Ra	0.0285	µm

5.11.6.17

Taylor Hobson PRECISION

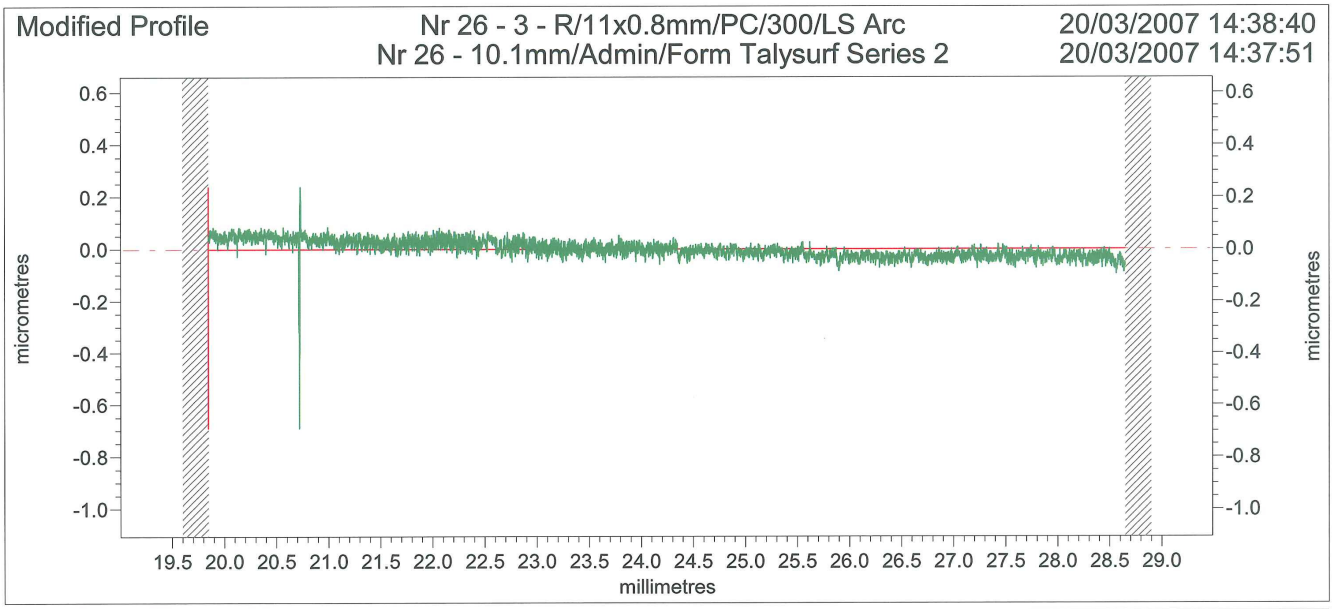

Ra	0.0275	µm

5.11.6.17

Taylor Hobson PRECISION

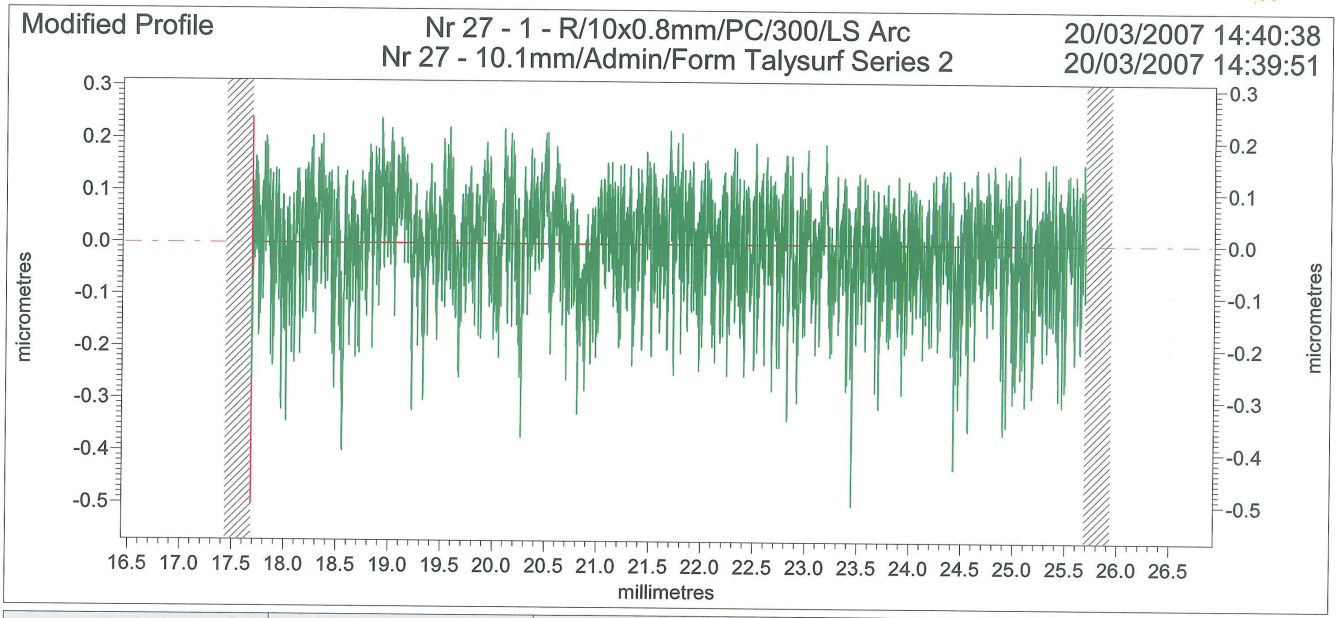

Ra	0.0744	µm

5.11.6.17

Taylor Hobson PRECISION

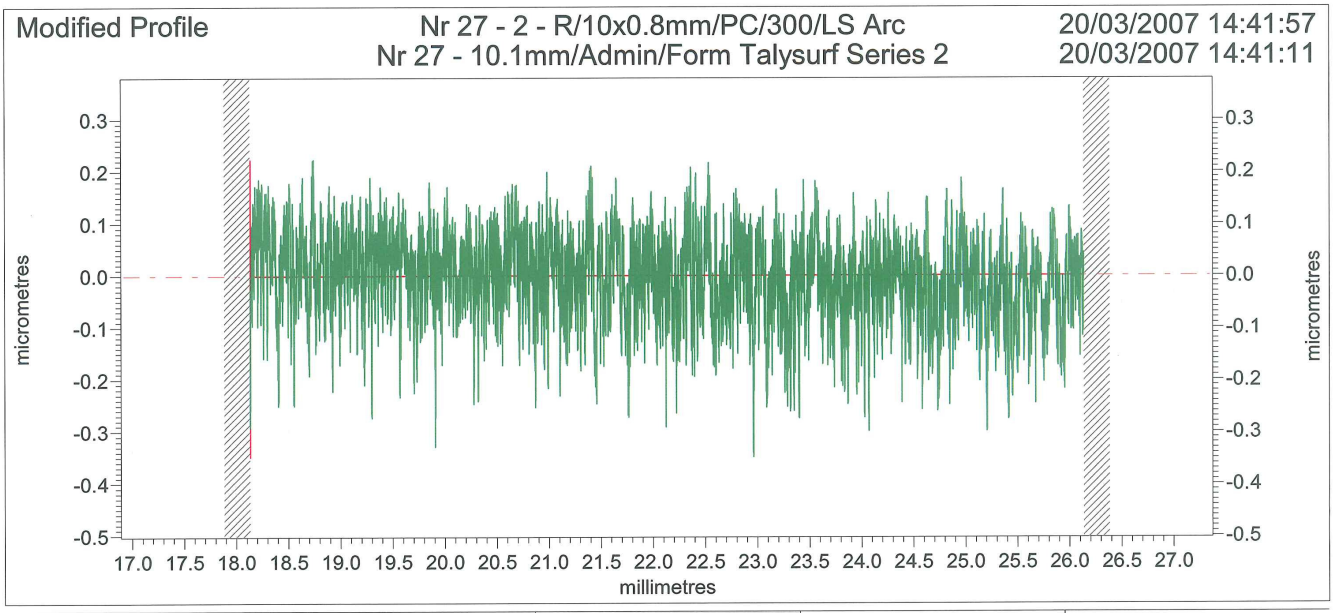

Ra	0.0675	µm

5.11.6.17

Taylor Hobson PRECISION

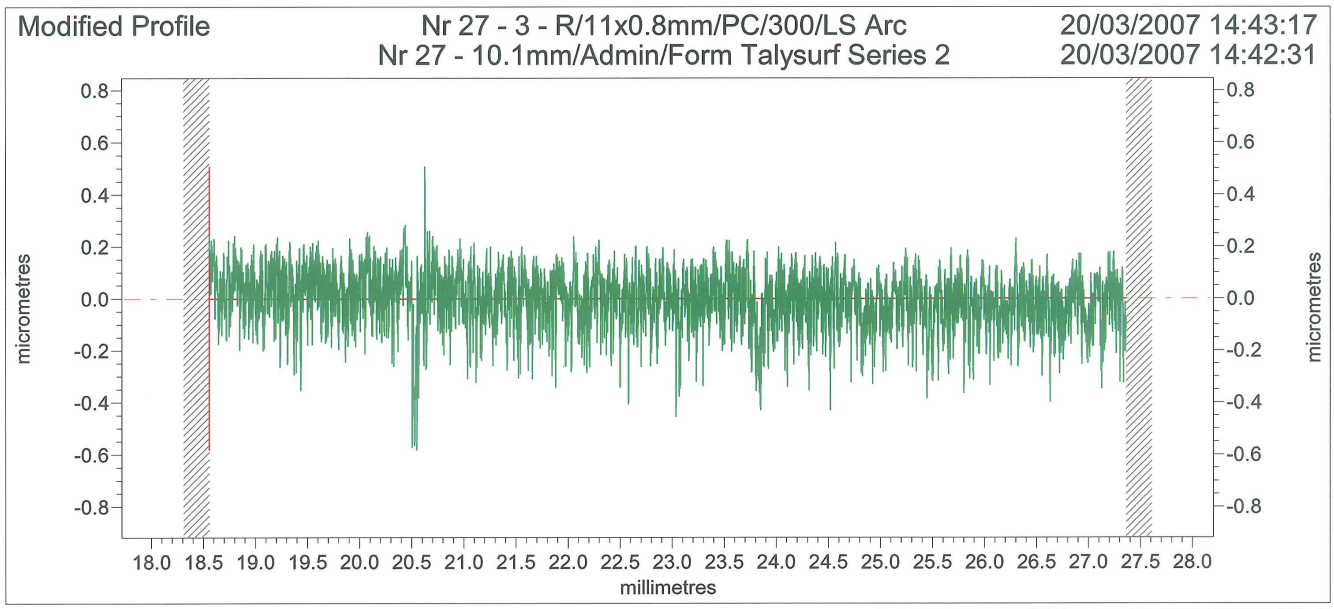

Ra	0.0852	µm

5.11.6.17

Taylor Hobson PRECISION

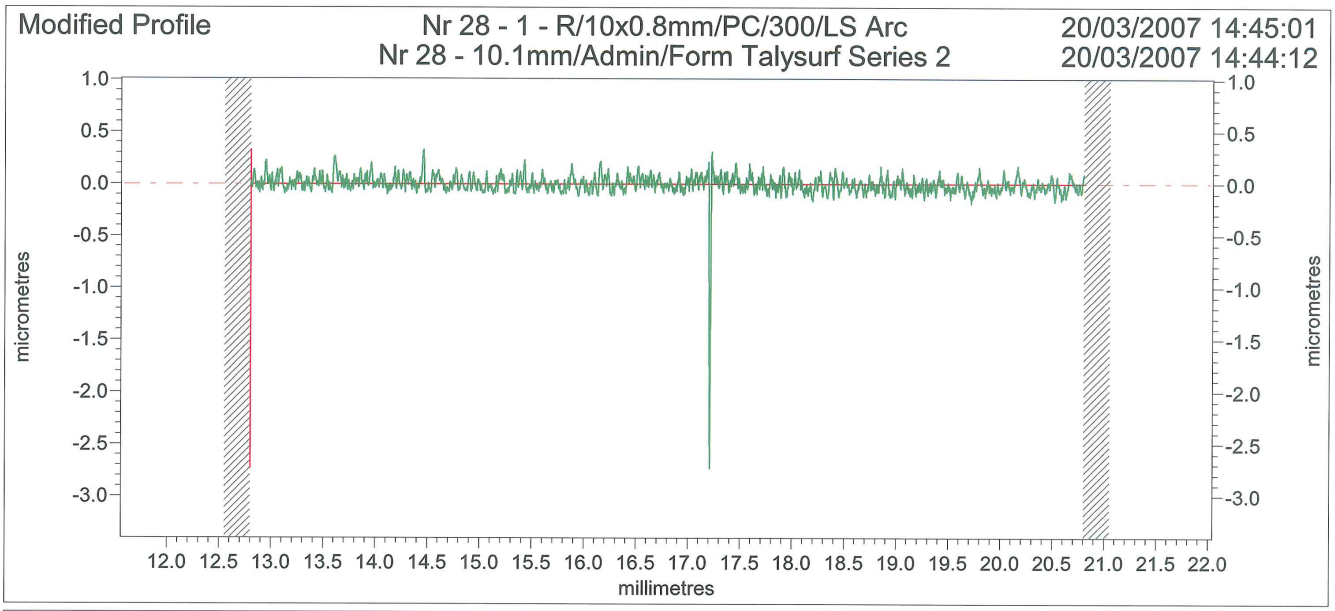

Ra	0.0583	µm

5.11.6.17

Taylor Hobson PRECISION

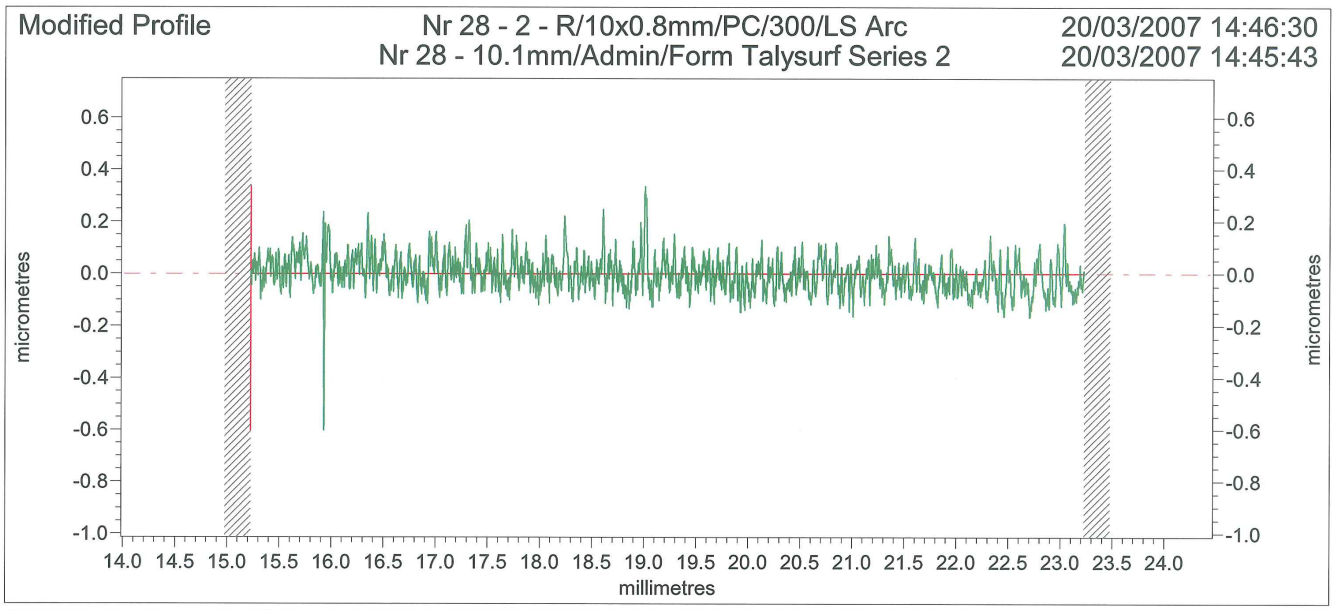

Ra	0.0507	µm

5.11.6.17

Taylor Hobson PRECISION

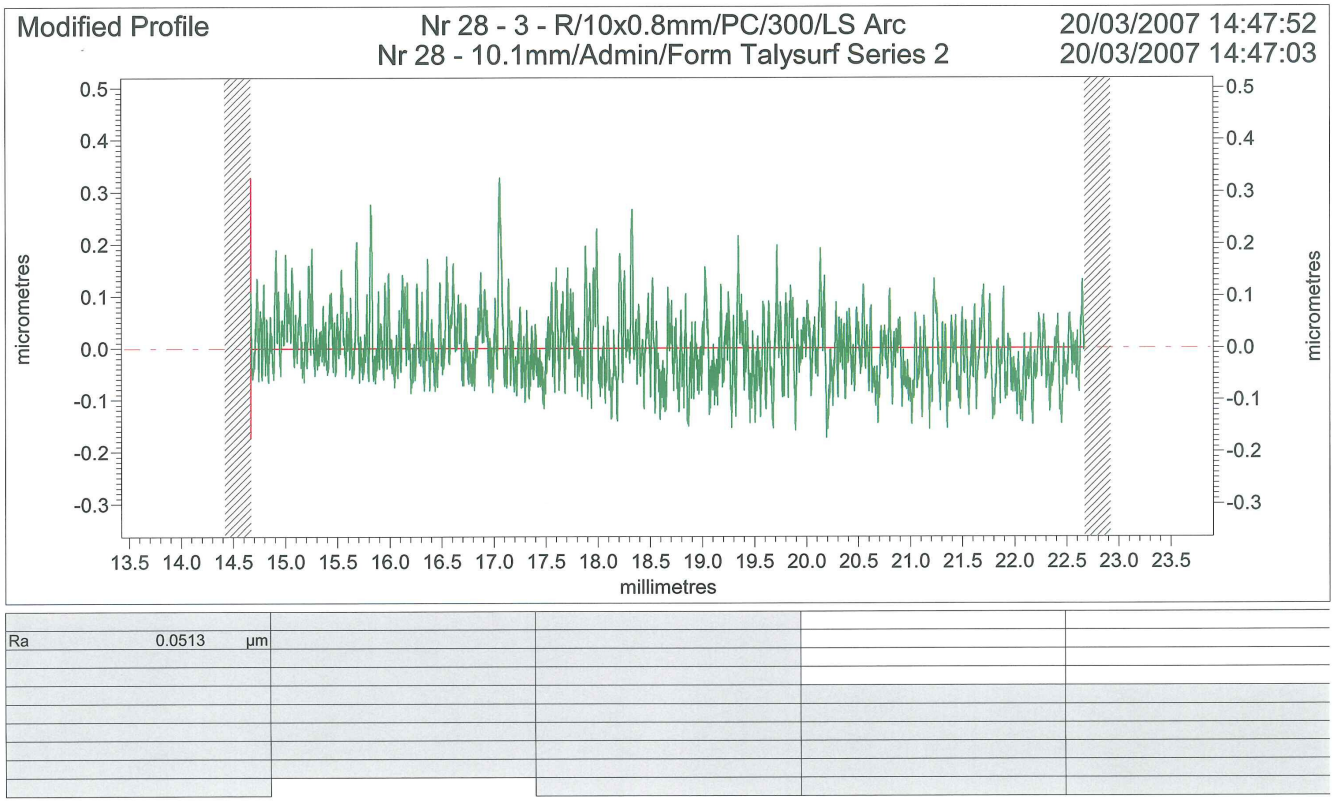

Ra	0.0513	µm

5.11.6.17

Taylor Hobson PRECISION

SAMPLE 29

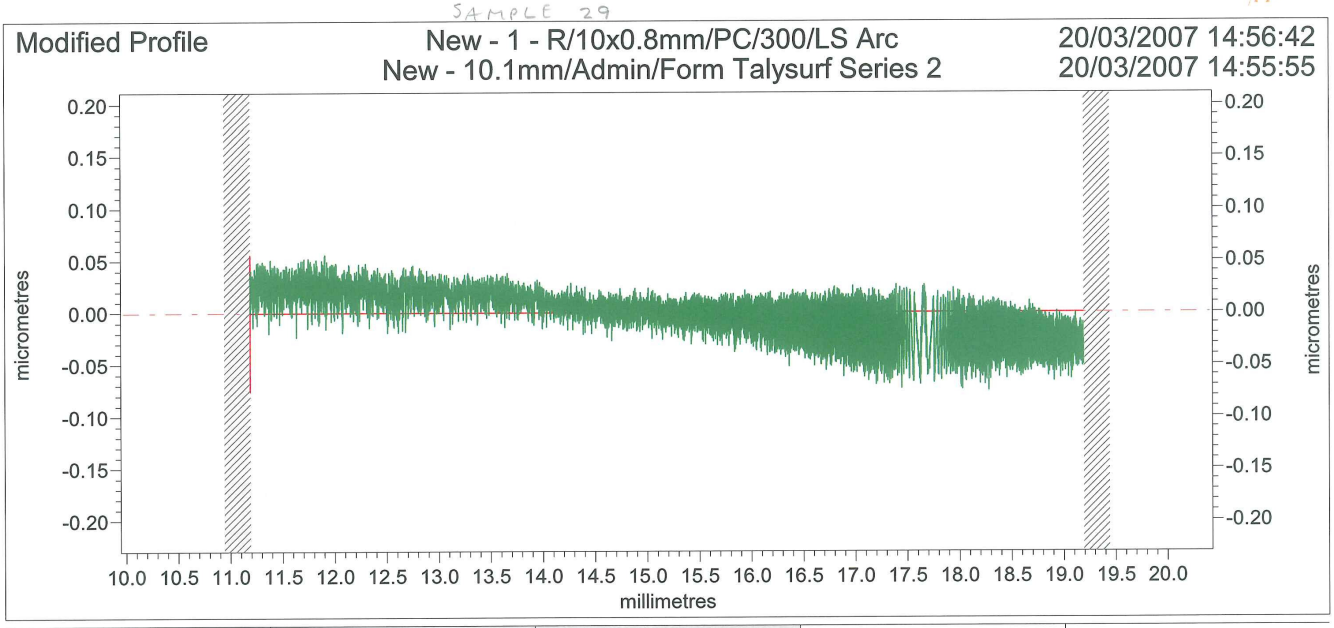

Ra	0.0187	µm

5.11.6.17

Taylor Hobson PRECISION

SAMPLE 30

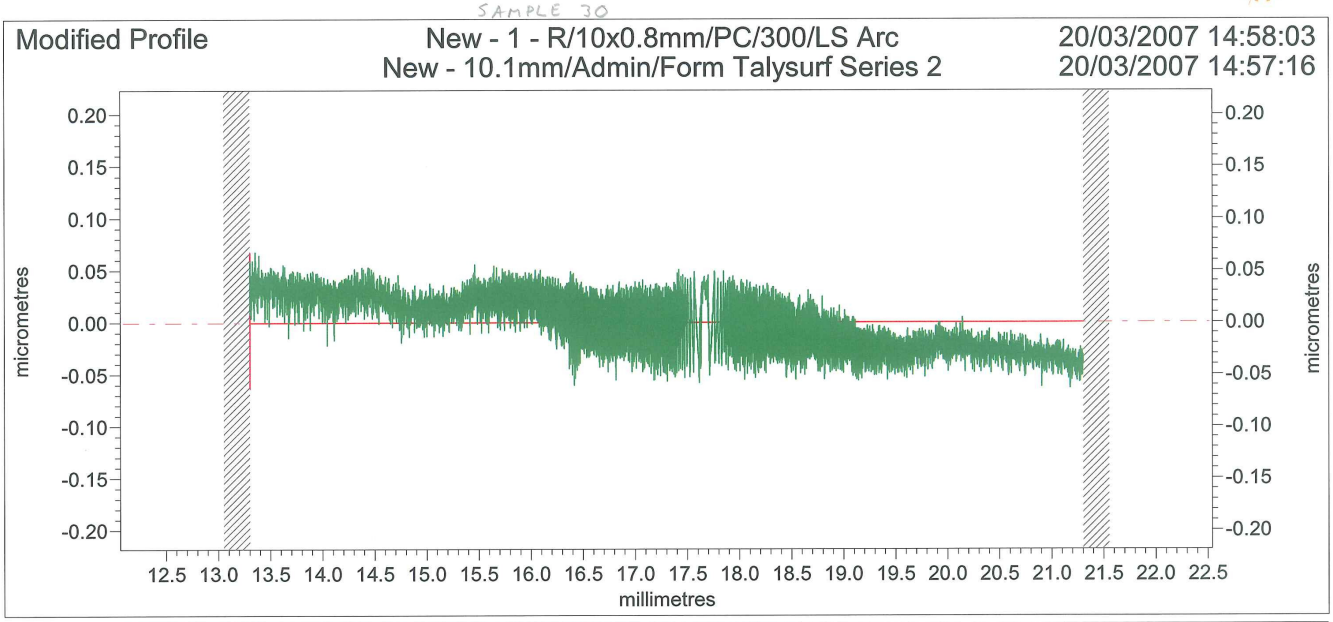

Ra	0.0235	µm

5.11.6.17

Taylor Hobson PRECISION

SAMPLE 31

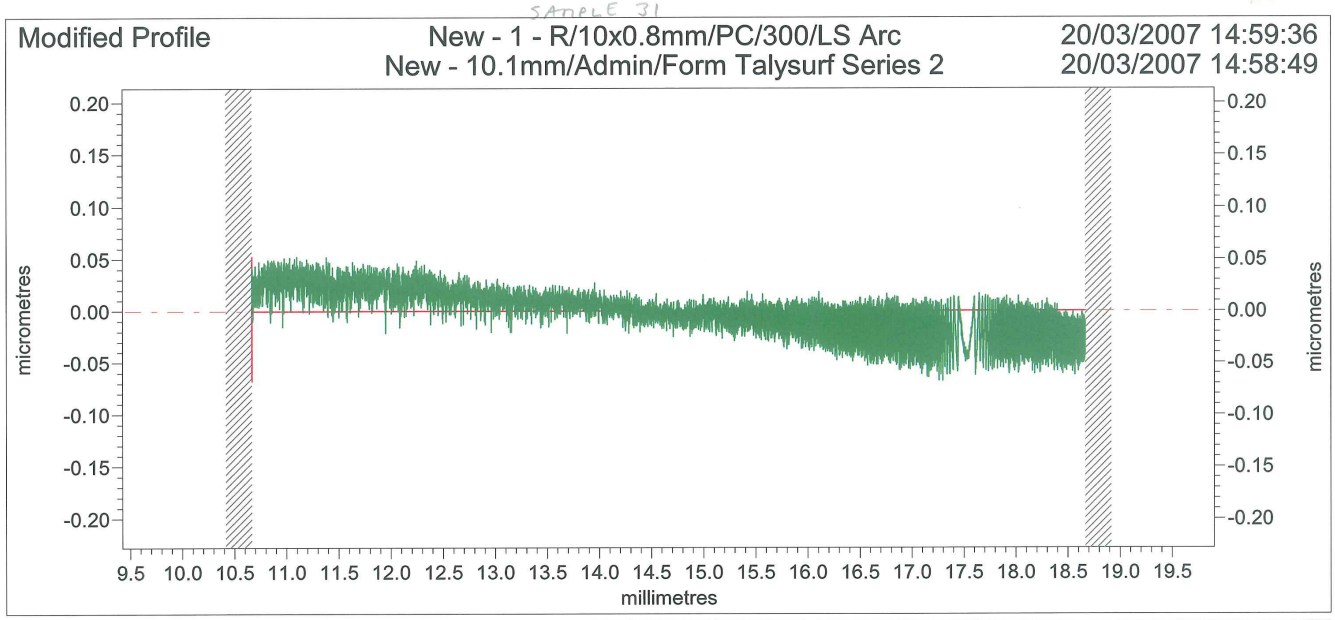

Ra	0.0175	µm